AD-A032 800 SYSTEMS CONTROL INC PALO ALTO CALIF F/G 1/1
IDENTIFICATION OF AIRCRAFT STABILITY AND CONTROL COEFFICIENTS F--ETC(U)
MAR 74 W E HALL, N K GUPTA, R G SMITH N00014-72-C-0328
UNCLASSIFIED TR-2 NL

1 OF 3
AD A032800

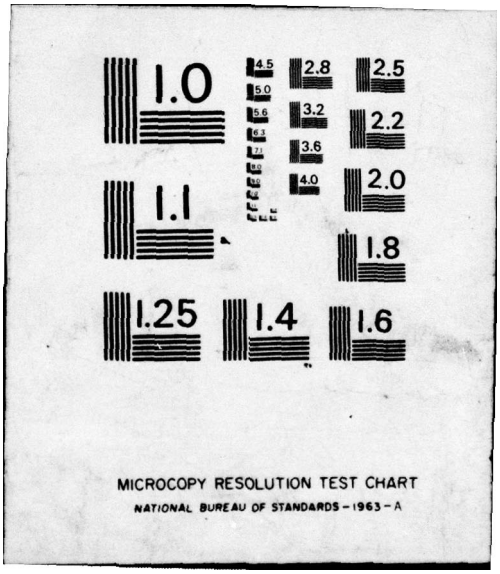
1.0
1.1
1.25
4.5
5.0
5.6
6.3
7.1
8.0
9.0
2.8
3.2
3.6
4.0
1.4
2.5
2.2
2.0
1.8
1.6
MICROCOPY RESOLUTION TEST CHART
NATIONAL BUREAU OF STANDARDS - 1963 - A

SYSTEMS CONTROL, INC.
260 SHERIDAN AVENUE
PALO ALTO, CALIFORNIA 94306

MARCH, 1974

ENGINEERING REPORT

IDENTIFICATION OF AIRCRAFT STABILITY AND CONTROL COEFFICIENTS FOR THE HIGH ANGLE-OF-ATTACK REGIME

TECHNICAL REPORT No. 2

Prepared for

OFFICE OF NAVAL RESEARCH
800 NORTH QUINCY ROAD
ARLINGTON, VIRGINIA 22217

Contract No. N00014-72-C-0328

IDENTIFICATION OF AIRCRAFT STABILITY AND CONTROL COEFFICIENTS FOR THE HIGH ANGLE-OF-ATTACK REGIME

TECHNICAL REPORT No. 2

SYSTEMS CONTROL, INC.
260 SHERIDAN AVENUE
PALO ALTO, CALIFORNIA 94306

Unclassified

SECURITY CLASSIFICATION OF THIS PAGE (When Data Entered)

REPORT DOCUMENTATION PAGE

READ INSTRUCTIONS BEFORE COMPLETING FORM

1. REPORT NUMBER	2. GOVT ACCESSION NO.
3. RECIPIENT'S CATALOG NUMBER	
4. TITLE (and Subtitle) Identification of Aircraft Stability and Control Coefficients for the High Angle-of-Attack Regime.	5. TYPE OF REPORT & PERIOD COVERED Engineering Technical Report 1 Jan 1973 – 31 Dec 1973
	6. PERFORMING ORG. REPORT NUMBER
7. AUTHOR(s) W. E. Hall, Jr., N. K. Gupta, R. G. Smith	8. CONTRACT OR GRANT NUMBER(s) N00014-72-C-0328
9. PERFORMING ORGANIZATION NAME AND ADDRESS Systems Control, Inc. 1801 Page Mill Road Palo Alto, Ca 94304	10. PROGRAM ELEMENT, PROJECT, TASK AREA & WORK UNIT NUMBERS 5984
11. CONTROLLING OFFICE NAME AND ADDRESS Office of Naval Research 800 North Quincy Road Arlington, Va 22217	12. REPORT DATE March 1974
	13. NUMBER OF PAGES 246
14. MONITORING AGENCY NAME & ADDRESS (if different from Controlling Office) Same	15. SECURITY CLASS. (of this report) Unclassified
	15a. DECLASSIFICATION/DOWNGRADING SCHEDULE

16. DISTRIBUTION STATEMENT (of this Report)

Distribution of this document is unlimited.

TR-2

17. DISTRIBUTION STATEMENT (of the abstract entered in Block 20, if different from Report)

18. SUPPLEMENTARY NOTES

19. KEY WORDS (Continue on reverse side if necessary and identify by block number)

Parameter Identification
Model Structure
Input Design
High Angle-of-Attack

20. ABSTRACT (Continue on reverse side if necessary and identify by block number)

A central problem of the stall/post-stall flight regime is the identification of nonlinear aerodynamic coefficients whose adverse characteristics may produce severe handling quality degradation. This identification problem is twofold: determination of the nonlinear aerodynamic models and estimation of the coefficients of these models. An integrated parameter identification procedure based on maximum likelihood methods is presented to resolve these problems with verification results based on a nonlinear six degree-of-freedom digital aircraft simulation.

DD FORM 1 JAN 73 1473 EDITION OF 1 NOV 65 IS OBSOLETE

Unclassified

SECURITY CLASSIFICATION OF THIS PAGE (When Data Entered)

20. The identification procedure consists of the sequential application of a model determination algorithm and a maximum likelihood identification method. Input design and measurement system specification techniques are combined with this application to form the integrated parameter identification process.

The model determination algorithm is based on least squares subset regression techniques. This algorithm determines which coefficients of polynomial expansions of the nonlinear aerodynamic forces and moments can characterize the stall/post-stall flight regime. The procedure not only estimates which nonlinear parameters are significant, but also gives preliminary numerical estimate error values of these parameters. To further define the model structure and parameter estimates, the regression results are used to initialize a maximum likelihood algorithm. This implementation of the maximum likelihood parameter identification method has been previously demonstrated to successfully identify parameters from flight data which is corrupted by gusts and measurement noise. This algorithm not only computes the parameter and noise statistics estimates, but also the confidence intervals for the estimates as a function of angle-of-attack and sideslip angle.

This structure and parameter estimation procedure is applied to the response of an advanced fighter. Results of the application of the identification procedure to these data have shown that the model structure and parameters of the nonlinear regime can be successfully identified, even in the presence of high levels of process and measurement noise. It is further shown that the estimates obtained from a data length with a given input can be used to successfully predict the response of the aircraft to another input in the same flight regime.

The procedures established and verified are highly flexible and may be readily applied to modeling other classes of nonlinear vehicles from test data.

FOREWARD

This report was prepared for the Office of Naval Research, Arlington, Virginia, under Contract N000014-72-C-0328, by Systems Control, Inc.

Mr. David Siegel was the ONR technical monitor for this work which was performed from March 1973 to December 1973.

The project supervisor at Systems Control, Inc. was J. S. Tyler, Jr. The principal investigator was W. E. Hall, Jr. Project engineers were N. I. Gupta, R. G. Smith, and R. Mohr. Analytical and computational support was performed by I. Segall and M. V. Bullock. Report preparation and artwork were done by D. A. Buenz.

Professor Raman Mehra of Harvard University was principal consultant for this work and his contributions to the results, particularly of the input design study, are gratefully acknowledged.

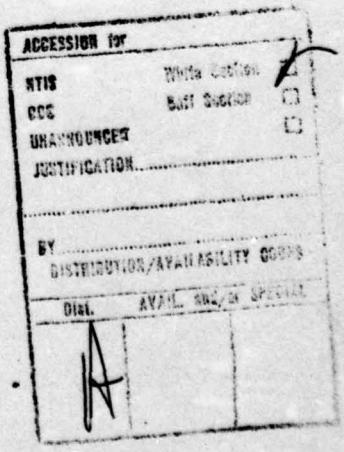

TABLE OF CONTENTS

TABLE OF CONTENTS (Continued)

TABLE OF CONTENTS (Concluded)

LIST OF FIGURES

LIST OF FIGURES (Continued)

LIST OF FIGURES (Concluded)

LIST OF TABLES

I. INTRODUCTION AND SUMMARY

1.1 INTRODUCTION

The stall/post-stall/spin high angle-of-attack operating regime of advanced high performance aircraft is currently recognized as a critical area of the flight envelope which requires more precise definition [1]. The complexity of the dynamic and aerodynamic interactions which characterize such regimes necessitates advanced testing and analysis methods. One of these methods is that of system identification in which flight data from the critical regimes is processed to isolate and quantify the significant aerodynamic contributions.

System identification is emerging as a powerful technology for exploiting test data to significantly improve and increase fundamental knowledge of aircraft dynamics. Such knowledge is essential for more quantitative approaches to handling quality evaluation, aerodynamic modeling for pilot simulators, and verification of analytical and wind tunnel estimates of aerodynamic parameters. In addition, the continuing analytical, computational, and experimental development of system identification promises the realization of on-line application which will reduce flight test time and provide rapid evaluation for aircraft design or control modifications.

As the potential of this method has been realized, however, so also have numerous problem areas associated with limitations of the system identification process itself. Basic approaches to aircraft parameter identification, such as least squares, have, under ideal conditions, demonstrated the fundamental capability to determine estimates of parameters. The deficiencies of such applications become apparent, however, when very high order systems with process and measurement noise errors are considered. When estimates are obtained from such applications (and computation divergence may even prevent such estimates), they are biased. To resolve the deficiencies of such basic techniques, advanced methods have evolved. Of these, one in particular--maximum likelihood--has been widely accepted as a theoretically and practically powerful approach.

There remain implementation problems in the application of this versatile method. The objective of this project has been to address one of the most important of these--identification of the high-order polynomial nonlinear aerodynamic coefficients which are characteristic of the high angle-of-attack stall/post-stall/spin regime. The central problem which has been addressed is the resolution of over-parameterization in specifying the order of the polynomial to be identified. The results of such over-parameterization are excessive computer time, possible computational divergences, and, most importantly, incorrect parameter estimates.

The developments reported here include a method for quickly estimating the required polynomial model to avoid over-parameterization, and an advanced maximum likelihood implementation for identifying the parameters of that polynomial.

The procedure formulated for this project is a further extension of an integrated parameter identification process involving model determination, input design, and maximum likelihood identification algorithms. Previously developed elements of this procedure have been successfully applied to flight test data. The validation of this extended procedure is obtained on a comprehensive digital simulation [1]. The complexity of the high angle-of-attack flight regime requires such "controlled data" for achieving a useful identification program. This is because a fixed set of flight data does not allow the flexibility required to determine specific cause and effect relationships which may degrade identification accuracy.

1.2 PRINCIPAL RESULT

The principal result of this work is a method which quantifies the causes of high angle-of-attack aircraft responses. This method has been formulated by developing advanced tools for determining significant aerodynamic contributions to such responses and estimating numerical estimates of these contributions. The method is very flexible, and is designed to be applicable to a wide range of flight test requirements for aerodynamic coefficient identification.

This method consists of the following algorithms:

1. A model determination procedure using multiple regression techniques: This procedure estimates which aerodynamic parameters adequately describe the input-output data for a given response. This capability is important because it indicates the parameters which should be identified, and thus avoids problems of attempting to identify more parameters than possible from the given data. In particular, this algorithm will indicate whether a linear or nonlinear aerodynamic model is required to be identified. In addition, the procedure provides initial "start-up" estimates for the maximum likelihood algorithm. Such preliminary estimates significantly improve the accuracy of the maximum likelihood algorithm and reduce computational time required to estimate parameters.

2. A flexible maximum likelihood algorithm implementation: This procedure estimates values of the aerodynamic parameters which are generally more accurate than obtainable from the simpler model determination procedure. This algorithm further examines the significance of the aerodynamic contributions by an advanced identifiability criterion (e.g., the rank deficient solution). This model refinement capability, coupled with the robustness of the maximum likelihood algorithm to turbulence and instrumentation errors, results in highly accurate parameter estimates. This implementation is further highly user-oriented with the capabilities to:

    a. Process lateral modes only, longitudinal modes only, or coupled longitudinal and lateral motions. Any subset of equations of these modes may be deleted. These options allow the user to "tailor" the program to specific maneuvers which require only a few equations to model the observed respones. This reduces computation time, produces more accurate estimates, and allows the user to isolate particular parameter effects.

b. Include any combinations of measurements (i.e., measurements may be pitch, roll, yaw accelerations or rates, or both). Various flight test programs have different levels of available instrumentation. Alternately, some instruments may be inoperative over a given flight test record. This program allows the user to specify which measurements are available. (The user must, however, check that the instruments are consistent with the parameters to be estimated.)

c. Identify any coefficient of an arbitrary polynomial up to a maximal order set by the user. This option is used with the model determination procedure which indicates the required linear and nonlinear aerodynamic contributions which should be identified. For reasons of parameter estimate accuracy, the lowest possible polynomial expansion (e.g., Taylor series expansion of the aerodynamic forces and moments) is desirable.

d. Obtain time histories not only of the measurements, but also of the parameters and the estimated covariances of the parameter estimates of the total aerodynamic forces and moments. This aspect of the program indicates the degree of success in estimating the parameters of interest. It is noted that measurement time history "matches" do not guarantee the "correctness" of the parameter estimates, and other tests (described in this report) are necessary.

e. Determine confidence levels for the individual coefficients of polynomial representation of the forces and moment coefficients. This option allows the user to determine confidence levels of various polynomial coefficients (e.g., derivatives) to the total aerodynamic forces and moments.

1.3 ANALYTICAL AND COMPUTATIONAL RESULTS

The development of this method has produced several significant analytical and computational results. These include the following analytical extensions to the application of the maximum likelihood algorithm:

1. A method for adaptively modifying the model structure during the identification computations to reduce the effect of modeling errors on parameter estimate accuracy.

2. An extension of recently developed techniques in the optimal input design for linear system parameter identification. This extension provides a method to select those flight test points which must be used to identify a coefficient which is nonlinear with angle-of-attack.

Computational results have been directed toward verifying the identification method on the simulation data. These results are summarized in the following conclusions:

1. A detailed nonlinear simulation can be used to discover and resolve identification problems in the high angle-of-attack regime. This simulation is sufficiently detailed so that no single model whose parameters are to be identified can correctly describe the simulated response over any regime. This is generally a characteristic of actual aircraft data, particularly in the nonlinear regimes, which must be retained so that modeling errors are realistically simulated. The simulation used for this project is documented in Ref. [1] and reviewed in Chapter II of this report.

2. The model whose parameters are to be identified should be determined from the aircraft response data. The model determination program is a well-defined and repeatable technique for isolating and estimating values of significant linear and nonlinear aircraft model parameters for this objective. This procedure is sufficiently robust to yield reliable results in the presence of high levels of both measurement and process noise.

3. The use of a model determination "pre-identification" filter reduces problems of over-parameterization (more parameters than required to describe the response). Alleviation of such problems produces more statistically reliable estimates and eliminates much extra computation which produces only marginal improvements.

4. The combined model determination and maximum likelihood identification algorithm is generally successful in providing accurate parameter estimates of significant nonlinear coefficients. There are three principal methods to validate the accuracies of these model and parameter estimates:

   a. Measurement time history match between actual and estimated response from the identified model. This is a necessary, but not sufficient, criterion of validation.

   b. Correlation between estimated coefficients and those which are known. For validation on simulation data, this is a paramount test. For similar validation on flight data, a comparison with wind tunnel data, or previous flight test results, may be made, at least where reliable previous data does exist.

   c. Prediction of response capabilities (perhaps the most significant test). This criterion is specified as the ability of the estimated model from one flight test (with a given input) to predict the response of another flight test at roughly the same condition (with a different input).

   The integrated model structure and parameter identification methods developed here are validated by all three of these criteria.

5. Where more accurate estimates of the parameters are required than are obtained from a calculation of parameter estimates from data, input design, estimate information aggregation and data length can be modified to provide improved results on subsequent calculations. This improvement is demonstrated in this report.

6. Input design strategies for polynomial nonlinear systems may be performed as a series of sequential linear designs for those regimes where linear terms predominate. Such regimes do exist even for high angle-of-attack maneuvers and can be verified by the model determination algorithm.

1.4 SUMMARY OF REPORT

The techniques discussed in this report presume familiarity with advanced statistical theory, parameter identification methods, and aerodynamics. To discuss the preliminary assumptions used in this work, Chapter II is devoted to a discussion of the integrated parameter identification procedure, including a review of the details of the simylation. This simulation itself is extensively documented in Ref. [1].

Chapter III discusses the basic ideas of the multiple regression approach and outlines the application of this method to the model determination problem. (Appendix B is adjunct to this chapter and discusses the detailed theory of subset regression.)

Chapter IV summarizes the maximum likelihood algorithm implemented for this development. (Appendix A is complementary to this chapter and presents a unified discussion of maximum likelihood assumptions, equations, and applications.)

Chapter V discusses input design for linear and nonlinear systems. (Appendix C reviews previous advanced developments for input design and new application to nonlinear systems.)

Chapter VI is a review of the significant results produced by applying the integrated identification approach to the nonlinear aerodynamic phenomena of the high angle-of-attack stall/post-stall regime.

Chapter VII presents conclusions and suggestions for further development and flight test data acquisition.

II. THE INTEGRATED PARAMETER IDENTIFICATION PROCESS

2.1 BACKGROUND

Aircraft parameter identification is the process of extracting numerical values for the aerodynamic stability and control coefficients from a set of flight test data (e.g., a time history of the flight control inputs and the resulting aircraft response variables). Although the fundamental theoretical basis of identification has existed for over 75 years, practical application of this technology to aircraft flight testing has been attempted only over the last three decades. Most of this application has been limited only to identification of low-order linear aircraft mathematical models, at low angles-of-attack and Mach number.

There are three principal elements of aircraft parameter identification: (1) the data processing algorithms (identification method), (2) the aircraft instrumentation, and (3) the flight control inputs (Figure 2.1). These elements are highly interactive.

In order to develop a comprehensive identification technology for application to the high angle-of-attack flight regime, a method of approach has been implemented which integrates these interactive elements. As diagrammed in Figure 2.2, this method of approach is composed of two basic phases. Phase 1 is a detailed simulation of a high performance aircraft (as described in ref. [1]). Phase 2 is the application of advanced parameter identification methods to determine the effects of inputs, measurement error, and the algorithms in processing high angle-of-attack data.

2.2 REVIEW OF HIGH ANGLE-OF-ATTACK CHARACTERISTICS AND HIGH ANGLE-OF-ATTACK DATA SIMULATION

An extensive discussion of the dynamic and aerodynamic characteristics of the high angle-of-attack flight regime for high performance aircraft is given in ref. [1]. The principal motivation for the interest in this regime is the nonlinear forces and moments which occur due to the stall of airframe components.

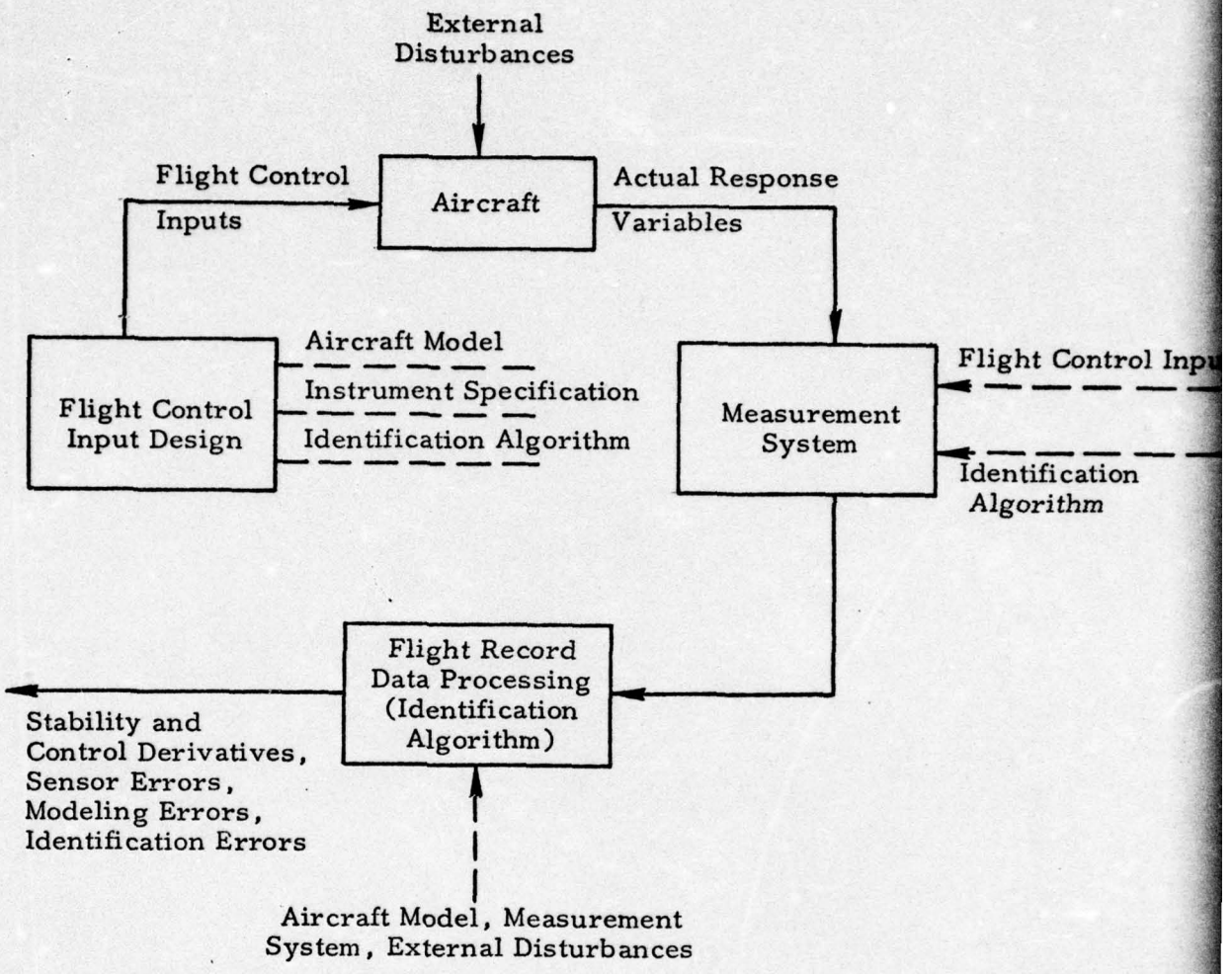

Figure 2.1 The Integrated Aircraft Identification Process

Typical variations of such forces and moments are shown in Figures 2.3 through 2.5 . Such static and dynamic coefficient variation with angle-of-attack play significant roles in determining the stability and control of aircraft in the stall/post-stall regime. The nonlinear C_m versus α of Figure 2.3 leads to the well-known "pitch-up" phenomenon of early century series aircraft. It is still encountered on aircraft, although recent designs have reduced its occurrence. The nonlinear lateral/directional characteristics of Figures 2.4 and 2.5 are indicative of the source of destabilizing forces which may cause inadvertent spin

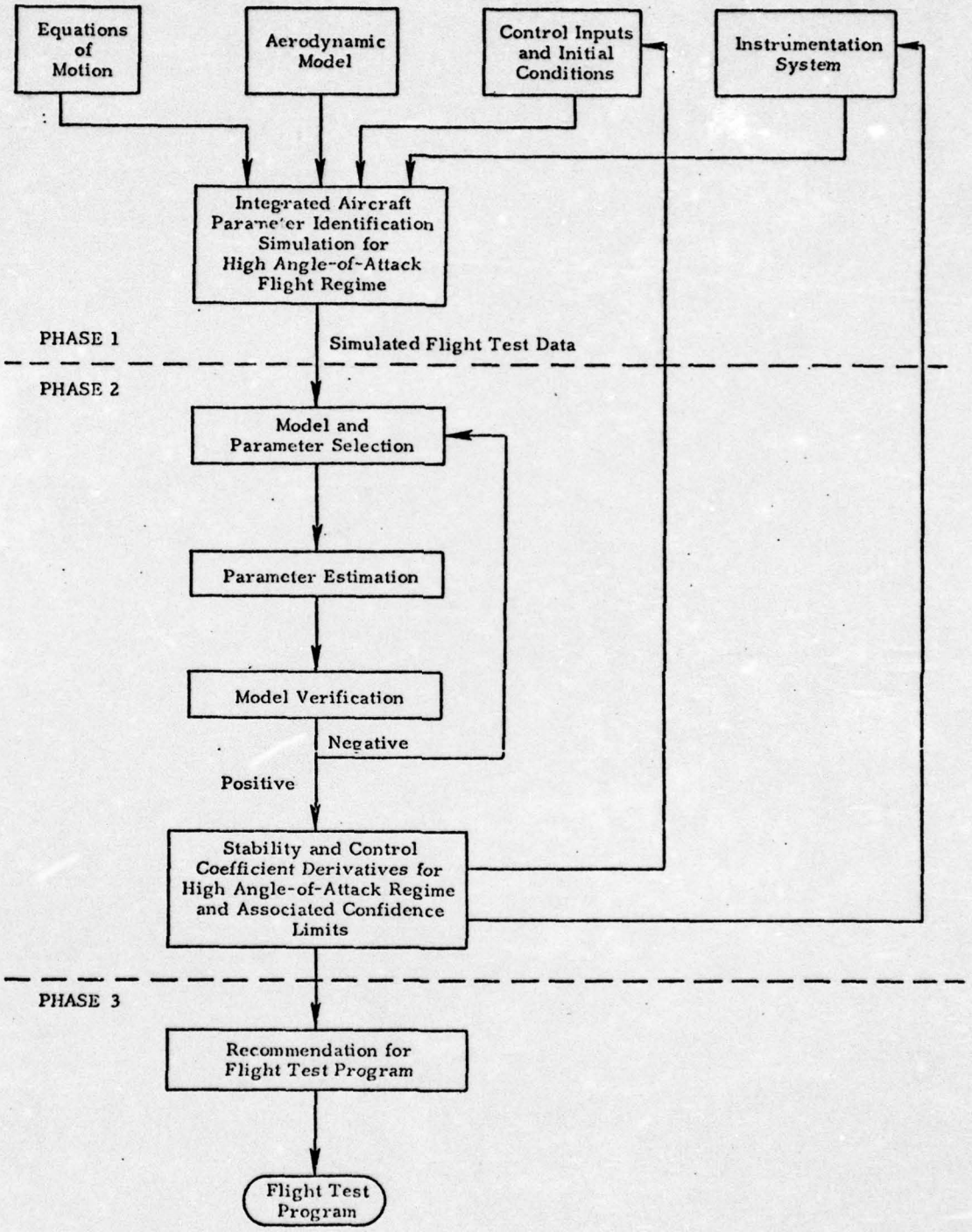

Figure 2.2 Implementation of the Design of an Integrated Parameter Identification Process

of high performance aircraft. Figure 2.6 dramatizes the effect of such nonlinearities on an F-4 aircraft.

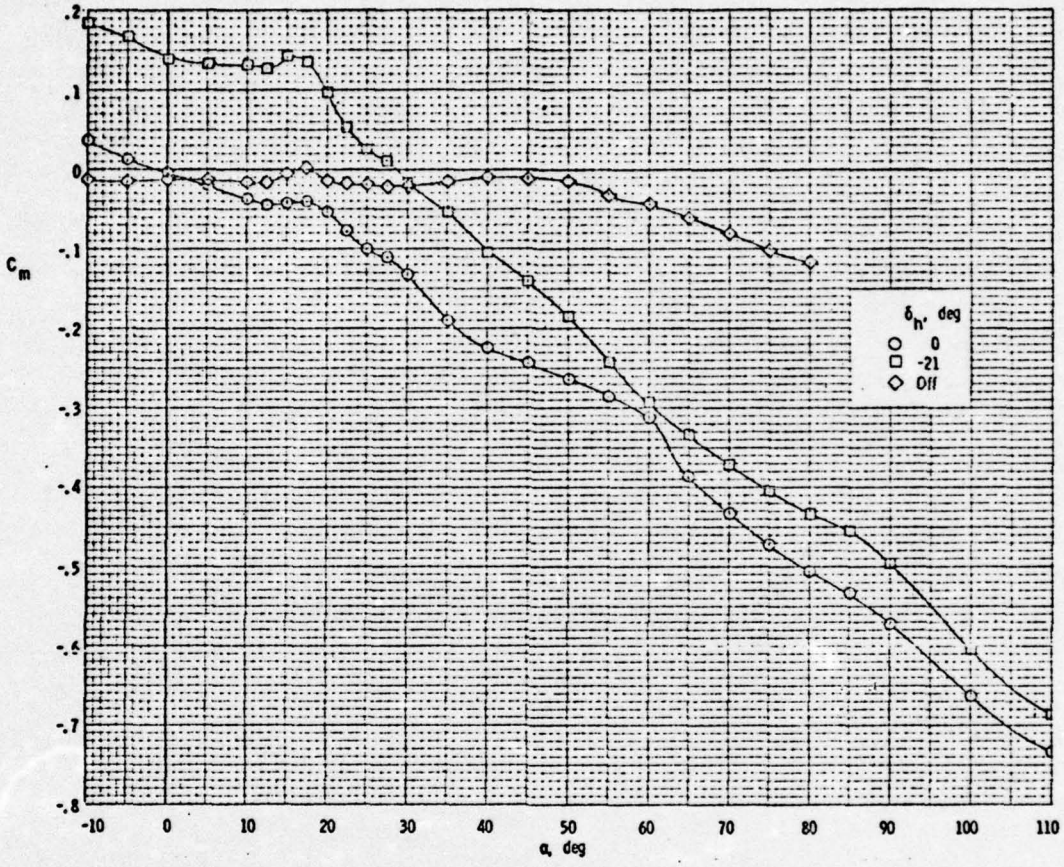

Figure 2.3 Variation of C_m with α as Derived from Wind Tunnel Tests

As demonstrated in ref. [1], responses such as those of Figure 2.6 may be simulated, at least qualitatively, by digital simulation. In particular, responses such as pitch up and yaw departure (due to unstable C_{n_β}) are strongly dependent on wind tunnel measurable static nonlinearities and these critical regions can be predicted for flight conditions simulated by the wind tunnel configuration. Unfortunately, many flight conditions may only be approximated in wind tunnels and, in fact, some aerodynamic (and dynamic) nonlinearities may not

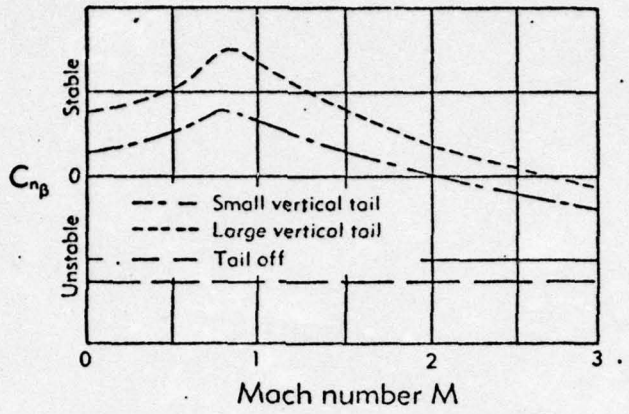

Figure 2.4 Variation of C_{n_β} with Mach Number

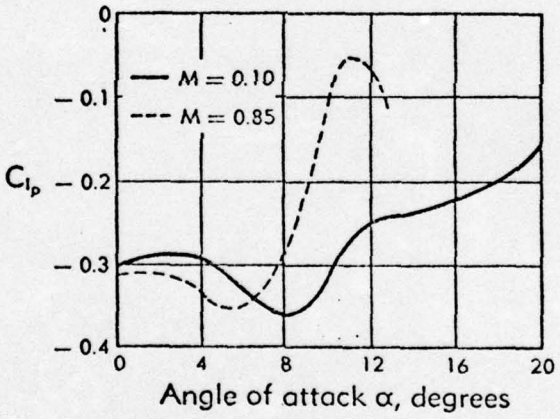

Figure 2.5 Variation of C_{ℓ_p} with Angle-of-Attack in the Subsonic and Transonic Regime

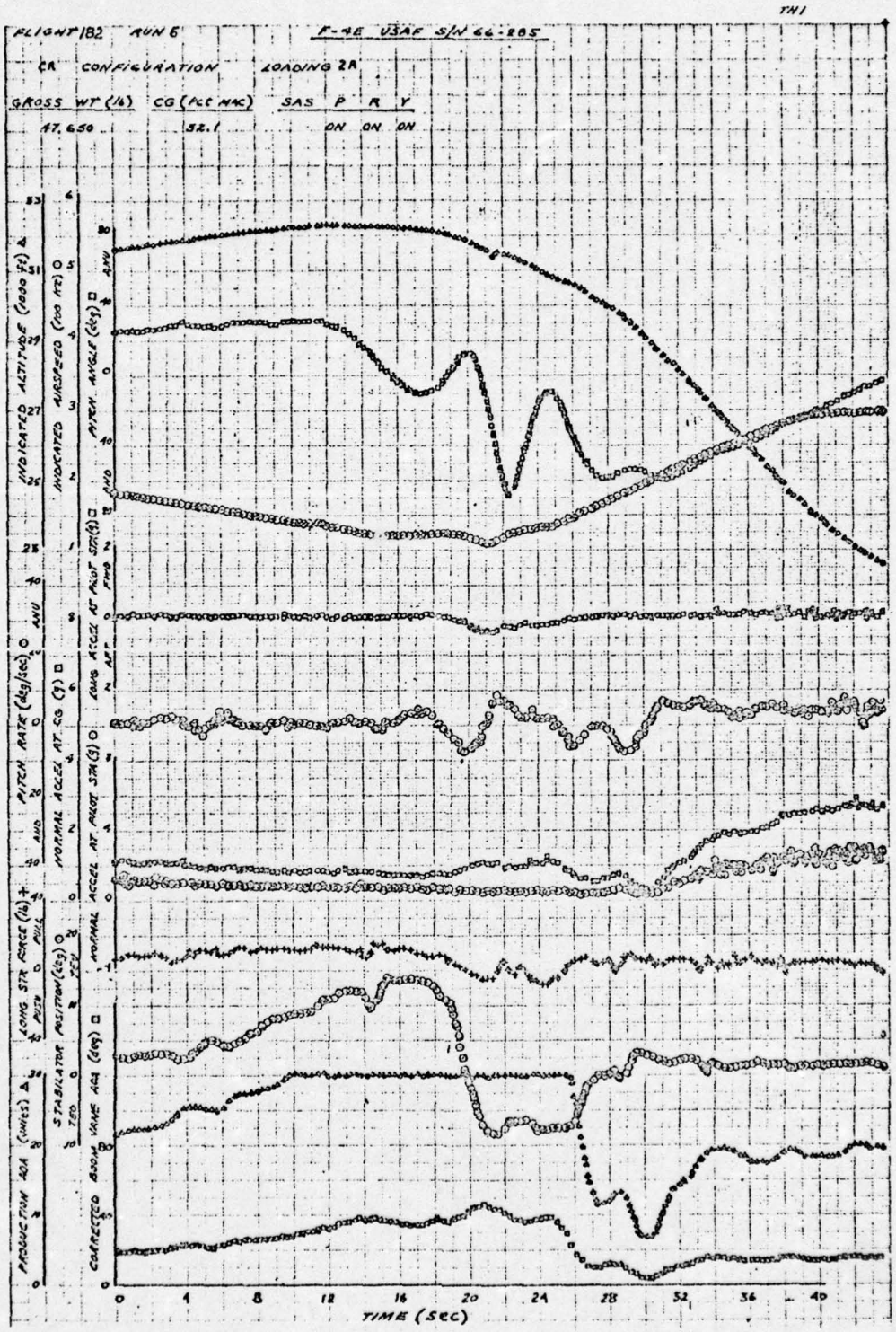

Figure 2.6 Rolling Departure and Recovery Rolls

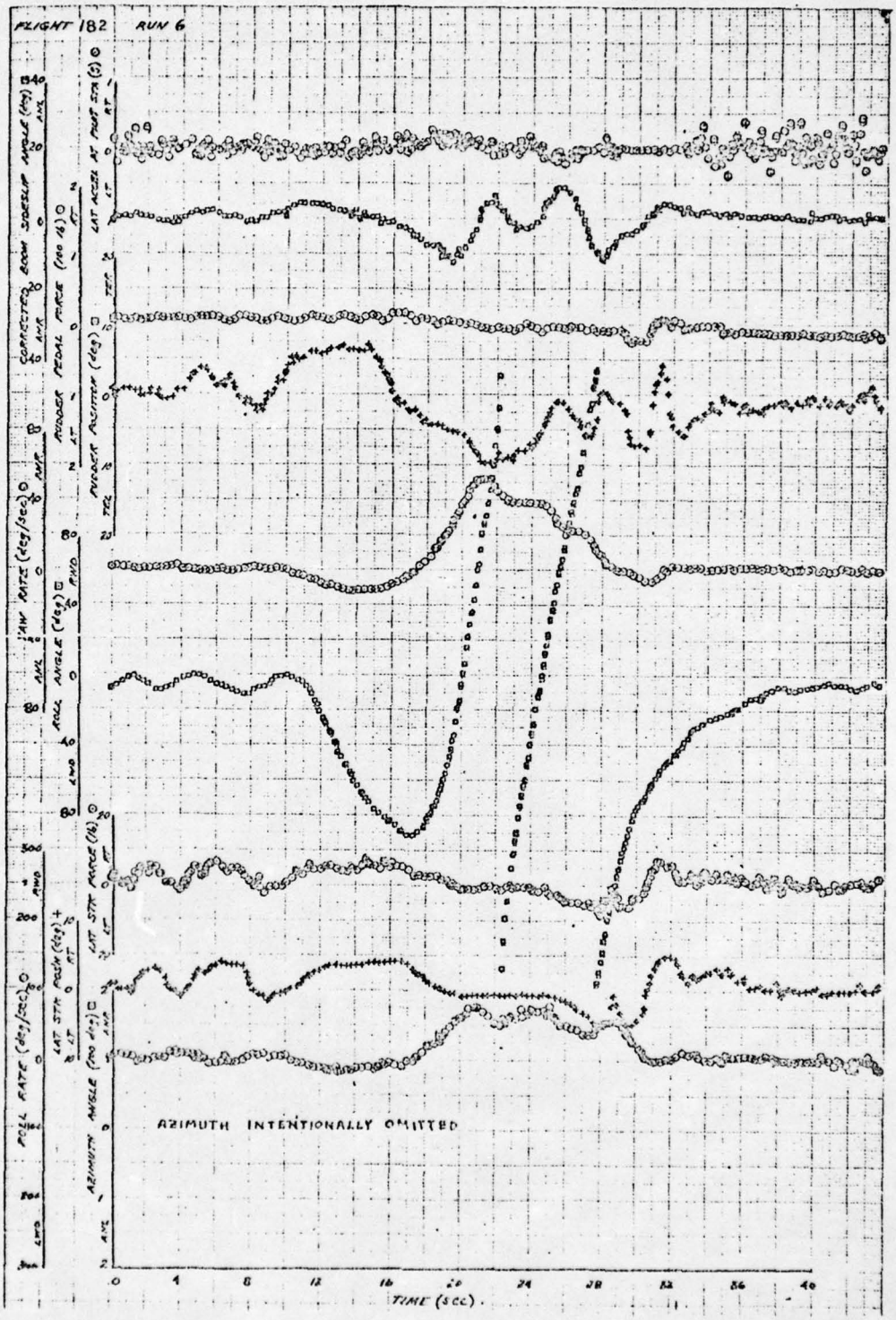

Figure 2.6 (Continued) Rolling Departure and Recovery Rolls

be detected from such tests due to scaling or tunnel model support limitations. In addition, high performance maneuvers will induce complicated interactions between the pilot, the flow fields, and the aircraft which may accentuate destabilizing forces.

The simulation described in ref. [1] was designed as a generator of data which is characteristic of that from the responses of high performance aircraft. The characteristics of this simulation are summarized in Table 2.1.

TABLE 2.1
Characteristics of Aircraft Data Simulation

Dynamic Equations	Six degree-of-freedom coupled nonlinear equations including engine gyroscopic effects, non-symmetric mass loading effects, and asymmetric thrust. Euler angles obtained from integrating direction cosine matrix. [ref. 3,4]
Aerodynamic Data	Tabular data from wind tunnel tests of a model of subject aircraft [ref 5-6]. Data consisted of complete static and dynamic force and moment coefficients for angle-of-attack range ($-10 \leq \alpha \leq 110^{o}$), and sideslip ($-40 \leq \beta \leq 40$). Lagrangian formulae used for interpolation when integrating equations.
Measurement System	Detailed model of position, rate, and acceleration gyros, angle-of-attack and sideslip vanes, accelerometers, and pitot tube. All measurements subjected to random errors--bias error, scale factor error, white noise. [ref. 7]
Control System	Detailed model of the SAS of subject aircraft. [ref. 8] Autopilot used to emulate pilot responses.
Random Disturbances	Random angle-of-attack and sideslip disturbances to simulate gusts. Random variation of normal lift coefficient to simulate buffet.

The simulation was subsequently compared with reported results of the stall/spin tests of an F-4 aircraft [2]. Responses such as pitch-up, yaw departure, and spin were obtained with the simulation. In addition, it was found that wing rock would be simulated, and that the roll, sideslip, and aileron deflection amplitudes and angle-of-attack occurrence were comparable with that recorded in the flight test. However, the frequency of the simulation was 7.5 seconds compared to 4.5 seconds for the actual test. This frequency discrepancy was ascribed to uncertainties in the parameters of the aircraft being tested, the pilot responses of the tests, and the differences between the wind tunnel and actual values of dynamic derivatives such as C_{ℓ_p}. Based on the correlation of the simulated responses with this and other actual responses, the simulation was deemed acceptable as a generator of typical data. Further extensive correlation of the simulation was beyond the scope of the program development.

2.3 SELECTION OF MODELS FOR PARAMETER IDENTIFICATION

2.3.1 Simulation Versus Identification Models

As discussed in ref. [1] and summarized in Section 2.1 of this report, the simulation used to generate data is an extensive and detailed representation of the aircraft and data error sources. Not only the dynamic equations, but also the measurements are nonlinear.

In particular, it is noted that the aerodynamic tables of the simulation are non-analytic functions of angle-of-attack, α, and sideslip angle, β. These data are not globally fitted with polynomials or other analytic functions of α or β in the simulation. There are two reasons for retaining the "table look-up" character of these data. First, such curve fitting could introduce additional error into the simulation as well as increase the development time for the simulation. Secondly, it was anticipated that analytic polynomials would be the basic identification model, and it was desired not to identify the parameters of the model using the same function which generated the data.

This modeling aspect of the efforts reported here is unique in the application of identification algorithms to simulated data. Typical approaches assume a polynomial form for nonlinear parameter variation, generate the time history data with this model, and then attempt to reconstruct the polynomial from the data [9-11]. Such an approach is certainly useful for testing of a program, but may tend to place more confidence in the effectiveness of the algorithm than is justified. This follows because identification of the same functional form which generates the data disregards the modeling error which may occur by approximating the actual function (unknown) by an assumed or a priori function. The approach used in this work is to generate the data by an aerodynamic model which is of higher order than the model which is identified. Hence, the integrated parameter identification process of Figure 2.2 contains the element of modeling error effects explicitly.

2.3.2 Considerations in Selecting Identification Models

2.3.2.1 The Polynomial Assumption

The use of polynomials as the basis of the identification model is itself an assumption about the physics of the aircraft aerodynamics. The assumption is historically based on the dependence between force and moment coefficients and independent variables (α or β, for example) which is observed in wind tunnels (see Figures 2.3 - 2.5). Recent work in England [12] has demonstrated the validity of such approximations with actual aircraft responses in the subsonic regime. Mathematically, polynomial representations result from series expansions about some reference point (e.g., trim) and herein lies the inherent assumption of the polynomial approximation. Specifically, it is assumed that there are continuous derivatives or rates of changes of derivatives (to an arbitrarily high order). In the transonic regime especially, such continuity may be violated forcing discontinuous representations. For this work, continuity is assumed.

2.3.2.2 Axis System Selection Considerations

The simulation used to generate data is written in the body axis coordinate system. The available wind tunnel data was consistent with this representation.

However, it must be noted that this is not the only axis system which can be used, nor is it used by all flight test agencies [13].

Alternate axes systems are the flight stability axis system, the wind tunnel axis system, and the wind axis system [3,4]. These axes systems are defined relative to the aircraft velocity vector. The body axis system, the principal axis system, and the so-called instrumentation axis system are fixed in the aircraft. The stability axis is a hybrid velocity vector-aircraft fixed axis system in that the steady state relative velocity vector defines a body fixed system (x axis along V) for perturbation analysis following a disturbance. A body fixed axis system is usually used for the moment equations (i.e., $\dot{p}$, $\dot{q}$, $\dot{r}$) because the inertias are then constant as would not be the case for the velocity vector systems. The translational equations, however, may be equivalently represented in either a velocity vector system or a body fixed system. In particular, the body axis translational states (u, v, w) are related to the wind axis translational states (α, β, V) by the definitions

$$\alpha = \tan^{-1} \frac{w}{u} \tag{2.1}$$

$$\beta = \sin^{-1} \frac{v}{V} \tag{2.2}$$

For small angle-of-attack, these two systems are simply related by neglecting higher-order terms so that

$$\alpha \sim w/u \tag{2.3}$$

$$\beta \sim v/V \tag{2.4}$$

and the two systems are equivalent, the states of the two systems being (α, β, V) or (u, v, w). The (α, β, V) system is advantageous because all the states are measured directly (e.g., angle-of-attack vane, sideslip vane, pitot tube). The advantage is that the identification model is simply formulated since the states are directly measured. On the other hand, measurements of u, v and w are difficult, at best, and must be found by integrating accelerometer inputs

or by using Eqs. (2.1) - (2.2) to find u, v, and w (since $V^2 = u^2 + v^2 + w^2$) given α and β. These fall into the category of derived measurements of u, v, and w from possibly noisy measurements of α and β.

The advantage of using the (α, β, V) system is offset by the complexity of these equations for high angle-of-attack (or large sideslip angle). Table E.1 of Appendix E shows the (α, β, V) equations for this situation (compare with equations for $\dot{u}$, $\dot{v}$, $\dot{w}$ in Appendix D). It is clear that a signficant increase in equation complexity occurs with this representation. Some of this complexity occurs because of the retention of body fixed forces such as gravity and thrust in the body axis frame. Additional complexity occurs because of coupling of the primary longitudinal and lateral static and dynamic aerodynamic forces (eqs. for $\dot{V}$ and $\dot{\beta}$). An exact formulation in the u, v, w system also causes such coupling, but only through secondary aerodynamic terms such as $C_{y_{\dot{\alpha}}}$, etc. It is also easily shown that the model of the accelerometer is increased in complexity (Table E.2).

In summary, instrumentation is referenced to a body fixed coordinate system, and aerodynamic forces are increasingly being referred to a body fixed frame. It is concluded that the u, v, w equations should serve as the basis of the identification model for high angle-of-attack analysis. Such a representation avoids increased complexity of the equations due to transformations from the body to wind axis frames which is explicit in the α, β, V system.

It must be noted, however, that there is no essential difference between the linear forms of the two representations at low angles-of-attack. The desire to avoid complexities of explicit coordinate transformations for high angle-of-attack is based on the need for an efficient computational structure which avoids excessive multiplications.

2.4 IDENTIFICATION OF MODELS

Having determined an analytical a priori form for the aerodynamic forces and moments, and selected the principal axis systems, the framework is established for estimating the structure and parameters appropriate to a given data length. This system estimation is the central objective of this work. It is within the

a priori structure that a systematic procedure is applied to selection of the identification model (structure and parameters), parameter estimation, and model verification.

For this work, careful distinction between "models" is required. To summarize these, the following clarification is made.

- Simulation Model: This is the complete nonlinear dynamic and aerodynamic simulation discussed in Section 2.1. This model generates the data considered representative of actual flight test data. Changes to this model are made to provide experimental degrees-of-freedom for investigating the performance of the subsequent data processing under various conditions.

- Polynomial Model: This is basically the same system dynamic model as is used in the simulation, with high order polynomials representing the aerodynamic force and moment expansions (as opposed to the discrete wind tunnel data of the simulation model). This will be discussed in detail in Chapter III.

- Identification Model: A lower-order polynomial model, this representation is the model which is actually identified. The parameters so included are a subset of the parameters of the more complete polynomial model. These subset parameters are those which are most significant in determining the response of the system. This identification model parameter solution technique will also be detailed in Chapter III.

The process of arriving at the "identification model" from the data (generated by the simulation or by flight tests) is denoted for this work as the structure identification procedure. The process of determining the coefficients of the "identification" model is denoted as the parameter identification procedure.

2.5 IDENTIFICATION OF PARAMETERS

The extraction of aerodynamic derivatives from flight data has received considerable attention during the last three decades and the most recent efforts

are given in refs. [14-15]. Earlier techniques were mostly manual or analog requiring subjective judgment by operators [16]. These methods are suitable for simple linear systems under very ideal conditions. A large amount of data could not be processed because of lack of techniques which would work for nonlinear system models in the presence of process and measurement noise.

More recently, with the availability of fast digital computing machines and efficient computation algorithms many powerful digital methods have been developed. These methods are usually quicker, do not require subjective judgment of operators, and work under a variety of circumstances. Examples of digital methods are various equation output error methods [17-18], output error methods [19-31], Kalman filter/ smoother approach [10] and maximum likelihood technique [9, 32-34].

Output error methods, which include gradient methods and modified Newton-Raphson, were motivated by earlier curve fitting techniques. These methods may not work well if there is high process noise or if the weighting matrix in the criterion function is improperly chosen. The equation error methods minimize the difference between the left hand side and the right hand side of the state equations. Examples of this method are various forms of least square, correlation methods, and instrumental variable approach. Since these methods do not account for measurement noise, the estimates are biased in the presence of this type of error. In the Kalman filter/smoother approach, the parameters are converted into state variables. The Kalman filter and smoother are developed for this new state vector starting from a priori values of states and parameters and their covariances. This method gives biased estimates even for linear systems and requires a priori knowledge of measurement and process noise covariances.

The maximum likelihood technique solves some of the problems mentioned above. By considering unknown elements of process noise and measurement noise covariances and other instrumentation errors as parameters, it considers these noise sources and also estimates them, if not known a priori. The method determines parameter values which maximize the likelihood function of the parameters, given the measurements and any a priori information. The likelihood function has the same form as the conditional probability of the observations, given the

parameters. The maximum likelihood method maximizes the probability of the observations. It is customary to work with the logarithm of the likelihood function. The method, as applied to parameter identification in nonlinear dynamic systems with measurement and process noise, is a combination of two steps:

1. A Kalman filter for estimates of the state and its covariance.

2. A Gauss-Newton method for parameter estimates, and associated covariances; also unknown noise statistics.

The details of the above steps are given in Appendix A. In addition to estimating the parameters in the state and measurement equations, the maximum likelihood method also determines the covariance of errors in parameter estimates. If the model whose parameters are identified is a true representation of the system in the region of operation and the sampling rate is high, the maximum likelihood method gives unbiased estimates of parameters for long data records. With increasing amounts of data, the estimates converge to their true value almost certainly. It can be shown that the technique extracts all information about the parameters from data; in other words, the method is efficient.

2.6 INPUT DESIGN

Given the structure and parameters of a system, it is possible to design experiments which enhance the accuracy of the parameter estimates. Such enhancement capability is extremely important for design of flight tests either from preflight simulators or from previous flight tests. Analytically, the problem of such input design is one of the most difficult of identification technology.

The basic idea of input design is to find control sequences which provide the highest possible parameter estimate accuracy in the shortest time. Recent advances in the design of such sequences for linear systems are summarized in Appendix C of this report. The advances achieved in linear systems are much more extensive than the advances for nonlinear systems. Nevertheless, the linear techniques may be selectively applied to nonlinear systems for various objectives. (These applications are discussed in Chapter V.)

2.7 SUMMARY

Procedures for validating the structure and parameter estimates are denoted as the model verification process. When combined with instrumentation and input design techniques, the integrated parameter identification method is specified. Application of this procedure to specific problems will require emphasis of some of the method's specific steps and placing less emphasis on others. In general, however, all steps must be included in either a qualitative or quantitative manner.

III. MODEL STRUCTURE DETERMINATION

This chapter discusses the requirement for a method of estimating which significant aerodynamic effects cause high angle-of-attack responses (Section 3.1). This requirement is usually satisfied by basic physical considerations (e.g., the equations of motion) and previous wind tunnel and flight tests. For the complexity of the high angle-of-attack regime, however, a subset regression technique is presented to determine an aerodynamic model from the observed data (Section 3.2). Examples of the application of this technique show that linear models are frequently useful at high angle-of-attack and that there is useful criterion in selecting the required number of parameters when the model is nonlinear (Section 3.3).

3.1 FORMULATION OF AIRCRAFT MODEL

The primary requisite of any parameter identification method is a model whose parameters are to be estimated. Preliminary considerations such as axis system, equations to be included, and type of aerodynamic force and moment representations are discussed in Chapter II. More detailed considerations include specifying the order of polynomials to represent the aerodynamics, the necessity for including terms such as $C_{m_{\dot{\alpha}}}$ and $C_{n_{\dot{\beta}}}$, and the determination of parameters which should be known a priori to achieve the best identification results. The latter aspect is based on the fact that some parameters can only be identified by extreme inputs which are unsatisfactory to man and machine.

3.1.1 Function Representation

The main problem of high angle-of-attack flight data reduction for stability and control coefficients is the reconstruction of nonlinear force and moment equations. In general, this may require estimation of more parameters than is computationally feasible. In addition, the requirement to identify an arbitrarily large set of parameters poses significant problems of identifiability.

In order to reduce the parameter set to be identified, several techniques may be applied. Basic to all of these techniques is the requirement for "engineer-

ing judgment" to postulate a coefficient from and evaluate the results of that assumption. The basic techniques are outlined as follows:

1. Linear: This approach seeks to identify a set of linear aerodynamic derivatives for many flight conditions. The objective is to characterize a nonlinear force or moment variation by identification of function slopes at the selected flight conditions. This method has the advantage of associating the results with classical stability derivatives. Conversely, it does require tests at many points, some of which, particularly in the high angle-of-attack regime, may not be susceptible to establishment of a suitable reference state. Difficulties in achieving a predetermined steady state include problems of controllability and buffet.

2. Quadratic Function: This method is the first degree of complication beyond the linear approach. It is an assumption based on the locally quadratic behavior of airfoil lift characteristics in the stall regime. This representation has been used for at least two decades [35] and is still widely adopted [36,37]. The representation is certainly better in nonlinear regimes than the linear, but, in general, will have greater error at the limits of the independent variable for the function than higher order representations. This results in a problem of matching polynomial segments to "build up" the entire polynomial.

3. Entire Polynomial: This method is a further extension of the quadratic representation which allows high-order polynomials to represent the desired functions. The freedom afforded by this representation is offset by the difficulty of identifiability due to over-parameterization. In addition, this representation poses strict instrumentation accuracy requirements to yield satisfactory reconstruction of high powers of the function independent variable.

For many modern aircraft, there is a comprehensive series of wind tunnel tests which provide the basis for design evaluation and control system design. The data from these tests may also be used to formulate functional forms which may be used as the model for identification from flight data. Because of scaling

and Mach effects, post-wind tunnel design changes, control system modifications, and other similar effects possibly not tunnel tested, these functions may be in error.

The most desirable goal is to use wind tunnel test results (and any other information about the physics of the maneuvers), to define all the possibilities of the functions for the forces and moments. Then, the actual data obtained would be used to specify which of these functions are most probable. Identification techniques would then be applied to these latter functions. The goal is to identify only those polynomial coefficients which are required to reproduce the actual force or moment characteristics. To this end, a fundamental step is implemented for the integrated parameter identification process.

3.1.2 Model Building From Data

The addition to the integrated parameter identification process which has been implemented for high angle-of-attack application is diagrammed in Figure 3.1.

Flight tests are conducted for particular conditions and inputs. The data from these tests is then used as the basis for selecting the functional forms required to reproduce the data. The data is passed through a filter (denoted as the optimal subset regression program). This filter contains suggested variables which might be required to reproduce the force and moment characteristics which generate the data. These variables correspond to the coefficients of powers of the independent variables (say, α or β). In general, the number of terms allowed is dictated by expected significance from a priori considerations. Of these possible required terms, the filter selects the most significant. The model defined by these significant variables is then passed to the identification program (Chapter IV).

The polynomial representations chosen by this approach are not unique. Over a finite data length and range of independent variables, several possible polynomials may fit the functional form adequately. For example, it may be that the two forms

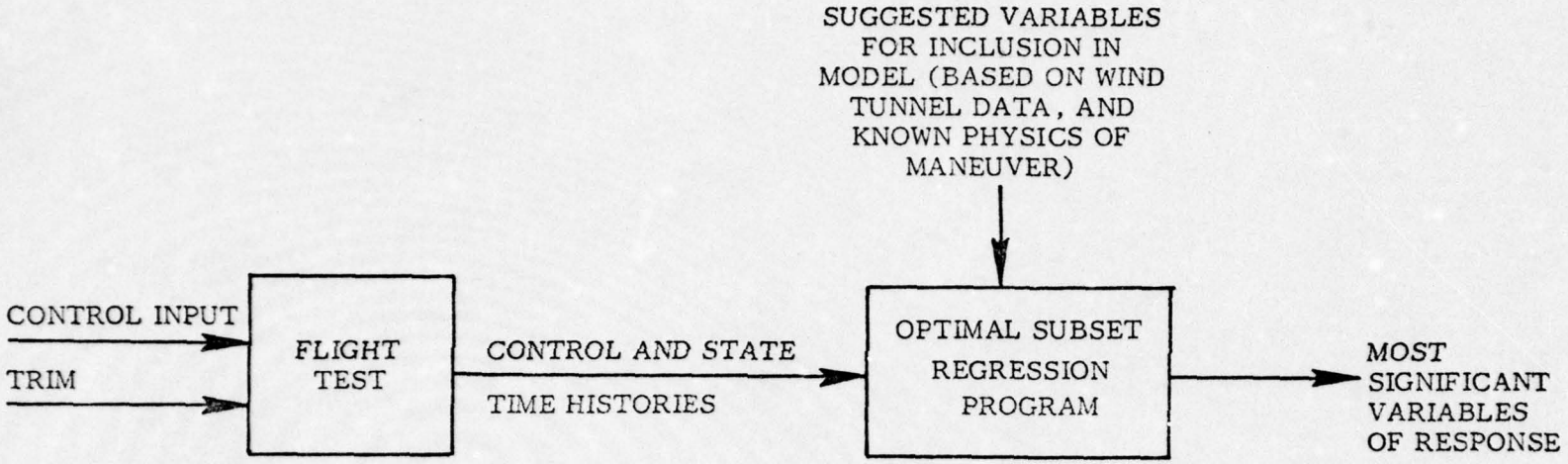

Figure 3.1 Model Determination

(a) $C_m = C_o + C_1\alpha + C_2\alpha^3 + C_3\alpha^4$

(b) $C_m' = C_o + C_1'\alpha + C_2'\alpha^2 + C_3'\alpha^3$

are "equally" good representations of the variation of pitching moment to explain the measurements resulting from a certain input. The optimal subset regression program will not necessarily favor form (a) or (b). The final form may depend on how the parameters are introduced in the regression equation. The coefficients in form (a) and (b) are different and are chosen such that both functional forms are good approximations to the actual variation of pitching moment with angle-of-attack. This point will be discussed further in this and later chapters (e.g., IV and V).

In order to further detail the use and limitations of this program, it is necessary to discuss the basis of the algorithm formulation.

3.2 SUBSET REGRESSION TECHNIQUES

The most fundamental approach to parameter identification is historically through the original least squares theory of Gauss. Extensions of this basic theory include modern optimal control and filter theory, as well as the widely-known Kalman filter (a sequential least squares filter). The extension discussed here is conceptually different from the Kalman filter algorithm.

The theory of subset regression is usually found in advanced texts dealing with statistical inference. The mathematical formulation of the theory is reviewed in Appendix B, and, of necessity, is directed only to the application used for this work. The application of this algorithm to aircraft parameter identification is not known to have been previously reported.

3.2.1 Basic Concept of Subset Regression

Basically, the Kalman filter is a linear sequential least square estimator which provides an updated minimum variance estimate of the state of a dynamic system based on observations of the system output, y. The recursive nature of the algorithm makes

it possible to incorporate the information from the most recent observation without repeating the computations already made.

Subset regression is also a sequential procedure except that, instead of using new data points to reduce estimation error (over time), it iteratively converges on a set of parameters which reduce the least square error over the entire data span. The resulting set of parameters constitutes an optimal subset of all possible parameters which significantly correlate the input and output data.

The principal aspects of the subset regression procedure are based on the decomposition of the observations

$$y = X\theta + \varepsilon \tag{3.1}$$

$$= X_1\theta_1 + X_2\theta_2 + \varepsilon \tag{3.2}$$

where θ is the complete set of parameters and θ_1 and θ_2 are subsets of θ. The first step of the procedure is to estimate θ_1, ignoring θ_2,

$$\hat{\theta}_1 = (X_1^T X_1)^{-1} X_1^T y \tag{3.3}$$

The estimated residuals are

$$\tilde{y} = y - \hat{y} \tag{3.4}$$

$$= y - X_1\hat{\theta}_1 \tag{3.5}$$

$$= \mathcal{M} y \tag{3.6}$$

where $\mathcal{M} = [I - X_1(X_1^T X_1)^{-1} X_1^T]$. The second step is to treat $\tilde{y}$ as a new observation and obtain the least square estimate for θ_2,

$$\hat{\theta}_2 = (X_2^T X_2)^{-1} X_2^T \tilde{y} \tag{3.7}$$

$$= (X_2^T X_2)^{-1} X_2^T \mathcal{M} y \tag{3.8}$$

It may be shown [38] that this technique not only accounts for the influence of X_1 on y, but also X_2 on y, to the extent that X_1 and X_2 are correlated.

The implementation of the algorithm adds and deletes variables to a particular model in an iterative manner. Estimates of previously ignored parameters are incorporated and evaluated by two criteria, as follows:

1. Of all possible variables θ, is θ_i the most highly correlated with y of variables not in the regression?

2. If θ_i is added to the regression, is its contribution to the "fit" significant relative to variables $\theta_{i-1}, \theta_{i-2}, \ldots, \theta_1$ which have already been used? Does the significance of $\theta_{i-1}, \ldots, \theta_1$ diminish because θ_i is included?

These questions are answered within the framework of statistical hypothesis testing (discussed in Appendix B). A generalized flow chart is shown in Figure 3.2. Starting with a list of possible variables, the algorithm enters the variable with the highest correlation (partial) to the observations y. The contribution of this variable to reducing fit error is made, (5), (2), and a new variable entered, (3), Figure 3.2. Subsequent tests add and delete variables to improve the "fit". The final subset of θ which results from the procedure is one which falls within confidence bounds set by the user (for example, 95% or 99%).

In general, the subset, θ_i, of θ is not unique. The particular parameter of the final subset will depend on the order in which they are listed. This occurs because the sum of the squares of the partial correlations of each variable is not equal to the square of the total correlation of all variables on y (ref. Appendix B). This problem may be reduced by using orthogonal variables (which could meet the sum of squares equivalence) or by forcing in variables which are known to be required. In either case, a priori correlations must be introduced which depend on knowledge of the functions sought. The implementation used for the purposes reported here includes ability to force some variables into the regression, but not reformulation in terms of orthogonal variables.

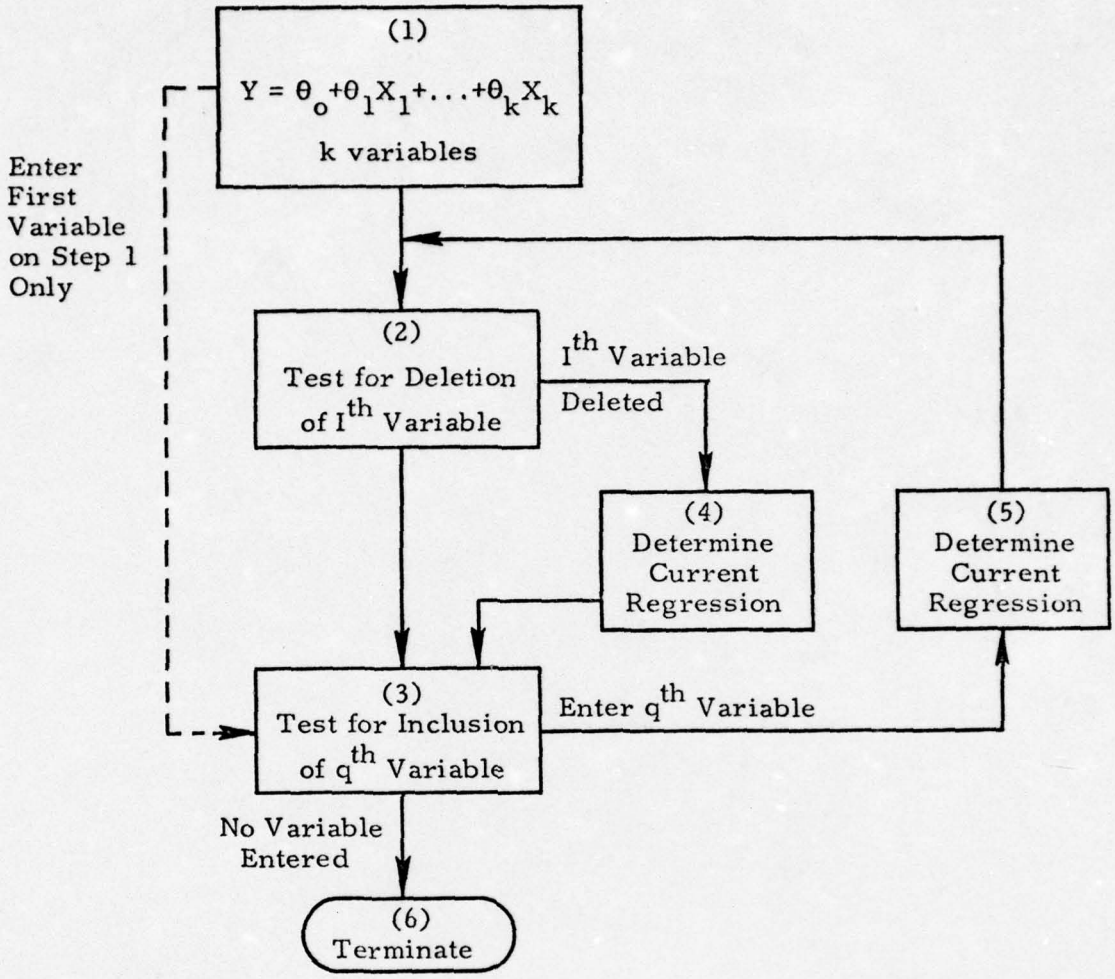

Figure 3.2 Generalized Flow Chart of the Subset Regression Algorithm

The algorithm not only identifies the most significant parameters, but also finds least square estimates of their true values. In general, these estimates will be in error (biased due to measurement noise and high order modeling errors). As such, they may be used for startup values of the maximum likelihood algorithm to reduce computation time and improve convergence, but must not be considered as final estimates themselves.

As an added check on the validity of the determined model, the program computes the residuals, $y-\hat{y}$, on the final pass. This provides an evaluation of the adequacy of the model (whose values yield $\hat{y}$) compared to the "true" process (whose values give y). Ideally, these residuals will be white Gaussian.

3.2.2 Application to Nonlinear Aircraft Modeling

The parameters with which the high angle-of-attack applications are most concerned are the coefficients of polynomial expansions of the aerodynamic force and moments. The reason for this type of expansion is discussed in Chapter II of this report.

3.2.2.1 Assumptions on Regression Model

The following assumptions are made for application of the subset regression algorithm:

a. Mass and inertias of the aircraft are known. This assumption is based on the extensive weight and balance data available for modern aircraft. In actual test conditions, however, there may be marked differences between the current aircraft configuration and the baseline calculations (e.g., unsymmetrical loadings, addition of weapons and instrumentation). This assumption, therefore, requires evaluation of such effects to determine their importance.

b. Aircraft rate (rotary) functions are assumed to vary only with α and β. This assumption limits the model structure to lower Mach numbers and aircraft loadings. Specifically, the terms $C_{m_{\dot{\alpha}}}$, $C_{n_{\dot{\beta}}}$, and $C_{\ell_{\dot{\beta}}}$ are not considered separately from C_{m_q}, C_{n_r}, and C_{ℓ_r}. At extreme conditions, this assumption is questionable. The basic reason for allowing use of this assumption is that the data base [1] does not have the aircraft rate and velocity vector rate terms explicitly separated. In general, extreme inputs would be required to separate these contributions in actual flight tests. It must be

noted that the regression model structure can be easily modified to include terms such as $C_{n_{\dot{\beta}}}$ if required.

c. Aerodynamic coupling effects due to combined angle-of-attack and sideslip angles are limited to second order terms. This assumption limits the cross-coupling terms of the aerodynamic expansions. The expansions in terms of α alone or β alone are unlimited, however.

d. Measurements of aircraft linear and angular accelerations are available. This assumption is the result of the regression procedure. In particular, the method requires measurements of $\dot{p}$, $\dot{q}$, and $\dot{r}$, in addition to the linear accelerometer readings. If not available, equivalent combinations of roll, pitch and yaw rates may be used. For the examples considered in this chapter, the measurements are assumed noiseless. This assumption is dropped in Chapter IV.

3.2.2.2 Specific Expansions

The general expansion for any specific force or moment coefficient is

$$C = C_o(\bar{\alpha},\bar{\beta}) + \sum_i C_{\alpha^{(i)}} \alpha^{(i)} + \sum_i C_{\beta^{(j)}} \beta^{(j)} + \sum_i \sum_j C_{\alpha^{(i)}\beta^{(j)}} \alpha^{(i)}\beta^{(j)}$$

where $\bar{\alpha}$ and $\bar{\beta}$ are reference angle-of-attack and sideslip angle, respectively. The specific coefficients for which such an expansion is used are listed in Table 3.1.

Primary emphasis is placed on the static coefficient structure for the modeling tasks here. All static terms could be minimally expressed as linear combinations of $(C_i\alpha + C_j\beta)^n$, where n=1,2,3. In addition, the coefficients of C_m could be expanded to α^9 and C_n to β^5. Control effectiveness coefficients and dynamic coefficients were generally limited to first order expansions in α only. These expansions were decided upon after initial experimentation with the programs. It was found that higher than first-order terms in α were usually not required on the basis of the regression analysis. In general, these control effect-

TABLE 3.1

Coefficients Which Are Expanded for High Angle-of-Attack Aerodynamic Models

EQUATION	STATIC COEFFICIENT	CONTROL EFFECTIVENESS	DYNAMIC COEFFICIENT
u	$C_x(\alpha,\beta)$	$C_{x_{\delta_s}}$	C_{x_q}
v	$C_y(\alpha,\beta)$	$C_{y_{\delta_a}}$ $C_{y_{\delta_r}}$	C_{y_p}
w	$C_z(\alpha,\beta)$	$C_{z_{\delta_s}}$	C_{z_q}
p	$C_\ell(\alpha,\beta)$	$C_{\ell_{\delta_a}}$ $C_{\ell_{\delta_r}}$	C_{ℓ_p} C_{ℓ_r}
q	$C_m(\alpha,\beta)$	$C_{m_{\delta_a}}$	C_{m_q}
r	$C_n(\alpha,\beta)$	$C_{n_{\delta_a}}$ $C_{n_{\delta_r}}$	C_{n_p} C_{n_r}

iveness and dynamic terms are difficult to identify from acceptable inputs, and first-order α expansions were considered acceptable.

An important aspect of the regression program is that the coefficients are not serial. Thus, if intermediate coefficients were not necessary (e.g., such as $C_{\alpha^2\beta}$), they are not included. (The maximum likelihood program detailed in Chapter IV will automatically eliminate terms not specified by the regression.)

3.2.2.3 Equation Error Formulation of Dynamic Responses

The basic objective of the regression program is to determine the aerodynamic coefficients. Implicit is the requirement that all other variables (in particular, the aircraft states) be known. The general equations of motion (Appendix E) may be written in the form

$$\dot{x} = f(x,u,\theta) + \varepsilon \qquad (3.10)$$

Decomposing f,

$$f(x,u,\theta) = f^I(x) + f^A(x,u) + \varepsilon \tag{3.11}$$

where $f^I(x)$ is a nonlinear function of the aircraft state including products and powers of the state, as well as other nonaerodynamic terms such as gravity and engine moments; and $f^A(x,u)$ is the aerodynamic forces and moments, and is nonlinear in the state x and possibly the control u. $f^A(x,u)$ may be written

$$\begin{aligned} f^A(x,u) &= f(\alpha,\beta,u) \\ &= Fh(\alpha,\beta,u) \end{aligned} \tag{3.12}$$

where F is a matrix of coefficients and $h(\alpha,\beta)$, is a column vector of powers and products of α,β, and u (e.g., δ_s, δ_a, δ_r). A typical j^{th} row of f might be

$$(F)_j = [C_o \quad C_\alpha \quad C_\beta \quad C_{\alpha^2\beta} \quad C_{\delta_s} \quad C_{\alpha\delta_s}]$$

and the corresponding $h(\alpha,\beta)$ would be

$$[1 \quad \alpha \quad \beta \quad \alpha^2\beta \quad \delta_s \quad \alpha\delta_s]^T .$$

Thus, the equation may be written in scalar form as

$$\dot{x}_j - f_j^I(x) = F_j h_j(\alpha,\beta,u) + \varepsilon_j \tag{3.13}$$

Letting $y_j = \dot{x}_j - f_j^I(x)$, Eq. (3.13) may be written, over all j, as

$$y = X\theta + \varepsilon$$

which is precisely the desired form (c.f., Eq. (3.1)).

The subset regression is applied to Eqs. (3.1) equation-by-equation. The left hand sides of Eqs. (3.1) are shown in Table 3.2. Note that the dynamic pressure is included in this left hand side. The variables ILU, ELV, ELW, WLP, ELQ, ELR are calculated from the measured values of the aircraft state, as detailed in Table 3.2. These "pseudo-measurements" are formed from the actual measurements such as p_m, q_m, r_m (the measured values of p, q, r) and accelerometer measurements ($\ddot{x}_m$, $\ddot{y}_m$, $\ddot{z}_m$).

For this application, the terms ELU...,ELR are actually calculated in the simulation program used to generate the data. In actual test data processing, a separate program would have to be used to formulate these terms. It is also required to substitute measured values of α,β, and the control deflections into the program to calculate the observations of "independent" variables ($h(\alpha,\beta)$ of Eq. (3.13)). This latter requirement introduces a modeling error into the estimation scheme.

3.3 EXAMPLE OF SUBSET REGRESSION APPLICATION TO SIMULATED DATA

3.3.1 Lateral-Directional Response Application of the Subset Regression Method

One of the first steps in evaluating the subset regression program was the lateral directional response analysis. This case was considered to be more important and difficult than the longitudinal tests. Most of the reported incidences of degraded stall/post-stall responses occur in roll or sideslip, and multiple nonlinearities characterize the regime.

A number of small perturbation tests were performed for this case. It was determined that severe or complicated control time histories were not warranted for flight tests at high angle-of-attack (due to the basically unstable character of responses in the regime). The fundamental aspect of these examples was to determine the adequacy of a linear model at several angles-of-attack, as opposed to a polynomial model requiring more complicated inputs. These results are shown in Tables 3.3 and 3.4.

TABLE 3.2

Equation Error Model for Subset Regression

$$ELU = \left(\left[\ddot{x}_{c.g.} \right]_m - F_x^e \right) \frac{m}{q_n S}$$

$$ELV = \left(\left[\ddot{y}_{c.g.} \right]_m - F_y^e \right) \frac{m}{q_n S}$$

$$ELW = \left(\left[\ddot{z}_{c.g.} \right]_m - F_z^e \right) \frac{m}{q_n S}$$

$$ELP = \frac{I_x}{q_n S b} \left\{ \dot{p}_m - q_m r_m \left(\frac{I_y - I_z}{I_x} \right) - \left(\dot{r}_m + p_m q_m \right) \frac{I_{xz}}{I_x} \right\}$$

$$ELQ = \frac{I_x}{q_n S \bar{c}} \left\{ \dot{q}_m - p_m r_m \left(\frac{I_z - I_x}{I_y} \right) + \left(p_m^2 - r_m^2 \right) \frac{I_{xz}}{I_y} + r \frac{I_e \Omega_e}{I_y} \right\}$$

$$ELR = \frac{I_z}{q_n S b} \left\{ \dot{r}_m - p_m q_m \left(\frac{I_x - I_y}{I_z} \right) + \left(q_m r_m - \dot{p}_m \right) \frac{I_{xz}}{I_z} - q_m \frac{I_e \Omega_e}{I_z} \right\}$$

where $q_n = \frac{1}{2} \rho_{s.l.} \hat{V}_i^2 \left[1 + \frac{M^2}{4} + \frac{M^4}{40} \right]^{-1}$.

$$\hat{u} = \hat{V}_b \cos \alpha_c \cos \beta_c$$

$$\hat{v} = \hat{V}_b \sin \beta_c$$

$$\hat{w} = \hat{V}_b \sin \alpha_c \cos \beta_c$$

where $\hat{V}_b = \left\{ \frac{\rho_{s.l.}}{\rho} \cdot \frac{\hat{V}_i^2}{1 + \frac{M^2}{4} + \frac{M^4}{40}} \right\}^{\frac{1}{2}}$ and V_i is defined in App. D.2.4.

and $( )_m$ indicates a measured quantity (c.f., Appendix D, E for other nomenclature)

TABLE 3.3

Aileron Doublet ($\pm 5^{o}$ over 2 second period, 10 sec data length)

ANGLE OF ATTACK	MODEL REQUIRED TO EXPLAIN AT LEAST 99% OF C_ℓ VARIATION
5^{o}	$C_\ell = C_{\ell_\beta}\beta + C_{\ell_{\delta_a}}\delta_a + C_{\ell_p}p$
15^{o}	$C_\ell = C_{\ell_\beta}\beta + C_{\ell_{\delta_a}}\delta_a + C_{\ell_{\alpha^2\beta^2}}\alpha^2\beta^2$
25^{o}	$C_\ell = C_{\ell_\beta}\beta + C_{\ell_{\delta_a}}\delta_a + C_{\ell_p}p + C_{\ell_r}r$

TABLE 3.4

Rudder Doublet ($\pm 5^{o}$ over 2 second period, 10 second data length)

ANGLE OF ATTACK	MODEL REQUIRED TO EXPLAIN AT LEAST 99% OF C_n VARIATION
5^{o}	$C_n = C_{n_{\delta_r}}\delta_r + C_{n_\beta}\beta + C_{n_r}r$
15^{o}	$C_n = C_{n_{\delta_r}}\delta_r + C_{n_\beta}\beta + C_{n_r}r + C_{n_p}p$
25^{o}	$C_n = C_{n_{\delta_r}}\delta_r + C_{n_\beta}\beta + C_{n_r}r$

Note that there is roll-pitch coupling at 15° angle-of-attack for the aileron doublet example. This departure from linearity occurs because of the pitch instability at that point. In each case, $C_{\ell_o} = 0$, which indicated zero rolling moment at trim. In addition, the wind tunnel results indicated $C_{\ell_p} \approx 0$ at $\alpha = 15^\circ$ which was substantiated by model structure determination program. At least 98% of the moment variation in each case was explained by using C_{ℓ_β}, $C_{\ell_{\delta_a}}$ and C_{ℓ_o}, with the other terms being much less significant. Again, in each case $C_{n_o} = 0$, indicating a zero yawing moment at trim. The C_{n_β} coefficient, as verified by the known data, changed sign (from positive to negative) between $\alpha = 15^\circ$ and $\alpha = 25^\circ$. As in the aileron doublet case, at least 98% of the yawing moment variation could be explained by using simply $C_{n_{\delta_r}}$, C_{n_β} and C_{n_r}. A linear model seems quite adequate in this case where the critical sign change in C_{n_β} was found by this approach.

The ability of a linear model to explain perturbation input aircraft responses, even in a "nonlinear" regime, has been discussed in Section 3.1.1. The linear model is here shown to indeed be adequate as a point-wise definition of the aerodynamic model. This indicates the possibility of using linear input designs for high angle-of-attack regimes, a subject elaborated on in Chapter V.

This conclusion, however, must be approached with caution. At high angles-of-attack, it may be difficult to hold trim and to conduct even perturbation maneuvers at constant angle-of-attack. Not only inherent instability, but also buffet, may make such inputs difficult at best. The important conclusion which can be attained is that the regression program can be used to delineate those regions where linear or nonlinear aerodynamic modeling is required.

3.3.2 Post-Regression Subset Specification

The subset regression approach is an elegant and efficient means of model structure estimation. As with most data processing aids, however, its use must be moderated with engineering judgment. Extensive use of the technique, as with any analytical approach repeatedly applied to physical problems, allows formula-

tion of certain guidelines which facilitate such judgment. Such guidelines usually have a basis in the theory, but are not easily quantified.

One such guideline is the Akaike final value prediction theorem [39]. This criterion states that, for certain types of systems, there is an optimal number of parameters which describe a model structure. A plot of this criterion function versus the number of parameters has a unique minimum (i.e., in a quadratic sense) which is at the optimal number of parameters [9]. It is also shown that fit error (the residuals of the estimated versus actual output time history) is not satisfactory, since it (as also measured by R^2, the multiple correlation coefficient of Appendix B), as a criterion, does not possess a unique minimum.

Fit error criteria tend to approach an asymptotic value as the number of parameters is increased. The eventual insensitivity of the fit error to an increase in the number of parameters (as parameters are added), is due to the continuing reduction of degrees-of-freedom.* Fundamentally, when the number of data points equals the number of parameters, the regression curve passes exactly through these points. No further improvement is then possible. Noise will, of course, allow more parameters to be entered (since point-by-point fit no longer occurs), but these parameters tend to fit the noise, not the process.

The Akaike criterion is a function of fit error, but also weights this error with the number of degrees of freedom. For the regression, a similar function of fit error is the F-ratio, the ratio of "fit goodness" to fit error, weighted by the degrees-of-freedom. The concept of F-ratio is detailed in Appendix B, and its importance to this work is significant.

That the F-ratio is a measure of the "optimal number" of parameters is shown in Figure 3.3, corresponding to an example to be discussed in more detail in Chapter VI. Its placement here is to emphasize the need, based on a criterion other than fit error, to evaluate model suitability. As shown, R^2 is a monotonically increasing function of the number of parameters. The F-ratio, however, has a maximum with seven parameters (obtained after deleting one variable of small

*Number of observations less number of parameters.

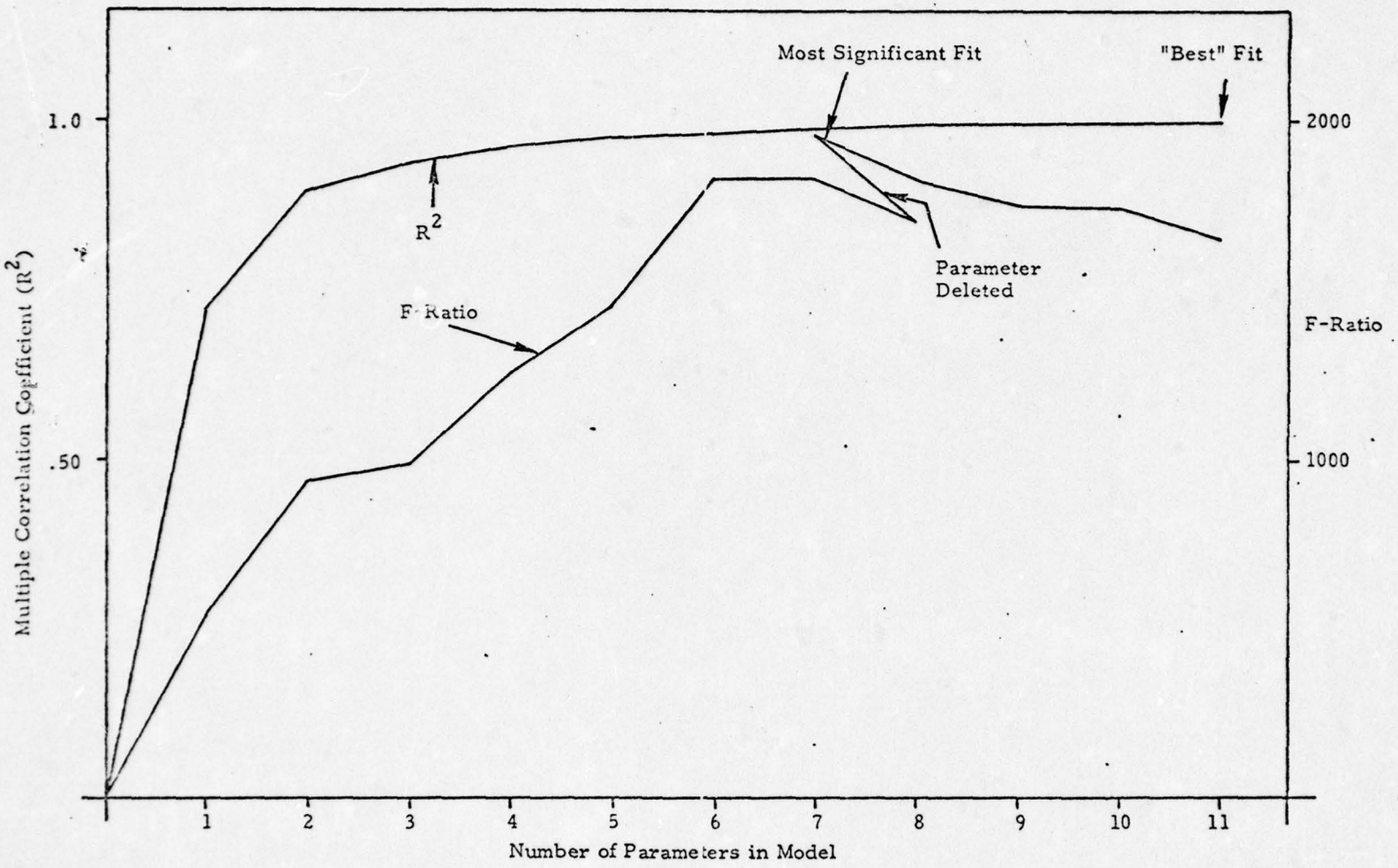

Figure 3.3 Multiple Correlation Coefficient (R^2) and F-Ratio Variation as Parameters are Added to Model (Longitudinal Case)

significance).

In general, it has been found that the subset F-ratio will have local maxima, beyond the first, as parameters are added. This result is shown in Figure 3.4. The first general criterion used for selecting parameters to be identified is to delete all parameters included in the regression past the first maximum.

A second guideline to further optimize the regression subset for maximum likelihood application is to select only parameters whose contribution is a certain percentage of the most significant parameter. This is discussed in Chapter VI.

3.4 SUMMARY OF CAPABILITY OF THE SUBSET REGRESSION PROCEDURE

This chapter has presented the basic idea, implementation details, and example results of the model determination subset regression method. Extensive use of this program will be discussed in more detail in Chapter VI. At this point, a review of the program features will be emphasized.

1. The program gives a set of parameters which approximately describe the input-output relationship. The set of parameters may not be unique, however.

2. The procedure produced biased parameter estimates in the presence of measurement noise. The method is based on a least squares principle, and measurement errors are well-known to produce biased estimates for this technique.

3. The method can be used for input design for nonlinear as well as linear systems.

4. The method is extremely rapid for producing a model structure estimate. This has been found from extensive computation on a UNIVAC 1108.

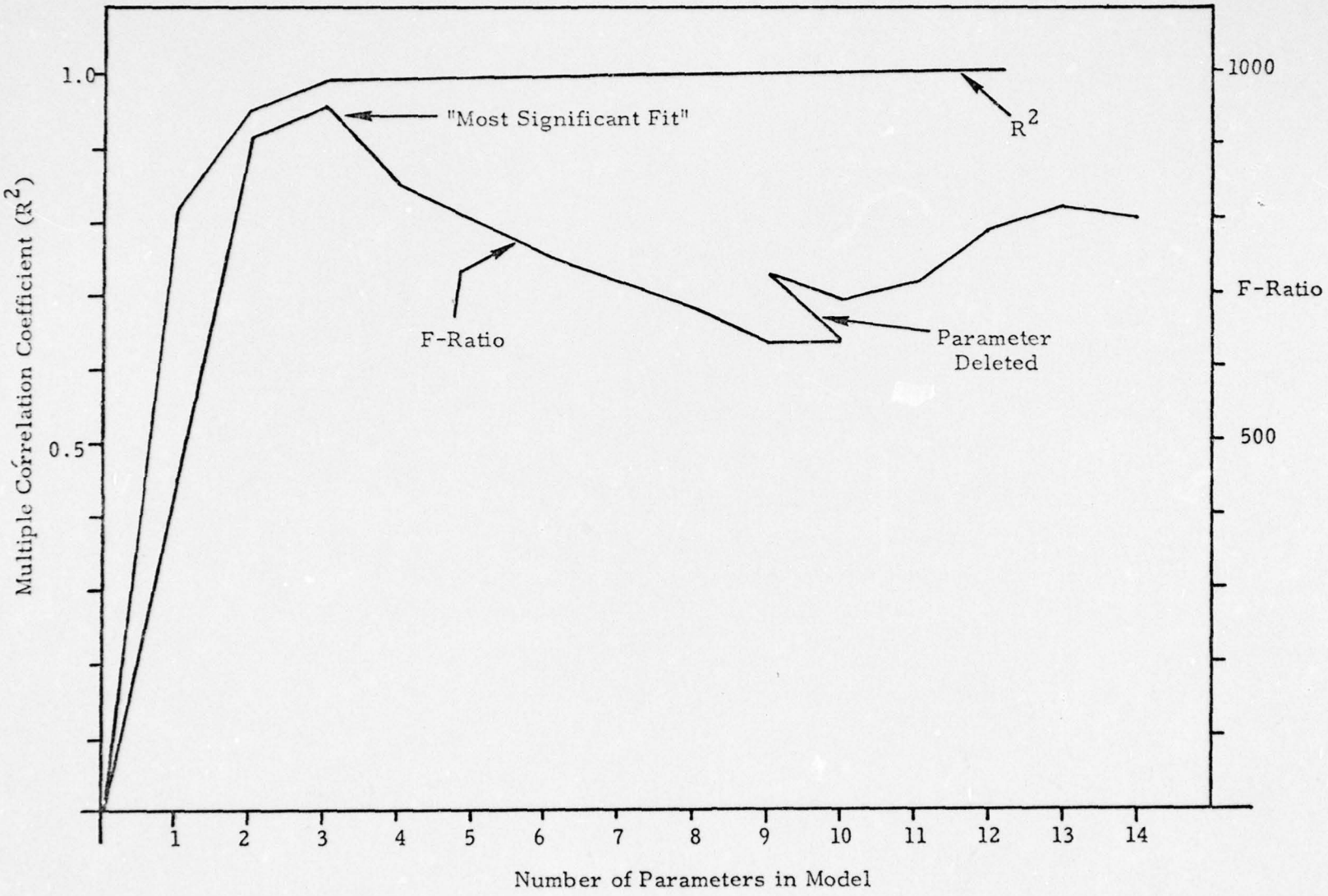

Figure 3.4 Multiple Correlation Coefficient (R^2) and F-Ratio Variation as Parameters are Added to Model (Lateral Case)

5. The method can be used to provide a priori (though biased) estimates of parameters. This follows since the program can basically be interpreted as an equation error start-up procedure.

The robustness of the program to process and measurement noise, and its operational use, are discussed in the following chapter.

This model determination technique is the first step of the method for identifying parameters from flight test data in the high angle-of-attack regime. At this point in the discussion of the method, a procedure has been established for isolating the cause-effect relationships necessary for modeling the aircraft response. Accurate quantification of these models is performed by the second stage of the method--the maximum likelihood procedure.

IV. MAXIMUM LIKELIHOOD METHOD FOR NONLINEAR SYSTEMS

An overall view of the parameter identification process for aircraft stability and control derivative determination was presented in Chapter II. In the high angle-of-attack flight regime, where the aircraft motions are nonlinear, the first step in the identification procedure is the determination of the model structure which adequately describes the relationship between control inputs and measured aircraft response. The subset regression method of Chapter III identifies the model and gives a first pass at the values of unknown parameters in the model. This is computationally simple and quick. The final step is the use of the maximum likelihood method to refine the model structure and to improve parameter estimates so that they are unbiased and have minimum variance, even in the presence of process and measurement noise.

In this chapter, the concept of the maximum likelihood method is reviewed (Section 4.1). The specific maximum likelihood features used for this project are detailed (Section 4.2), and related to the detailed mathematical equations upon which these features rest (Appendix A). Computational considerations are presented (Section 4.3) and an example output is given for illustration (Section 4.4).

4.1 INTRODUCTION

The maximum likelihood method is described in Appendix A and is illustrated in Figure 4.1. Conceptually, this technique can be summarized as follows:

> "Find the probability density functions of the observations for all possible combinations of unknown parameter values. Select the density function whose value is highest among all density functions at the measured values of the observations. The corresponding parameter values are the maximum likelihood estimates."

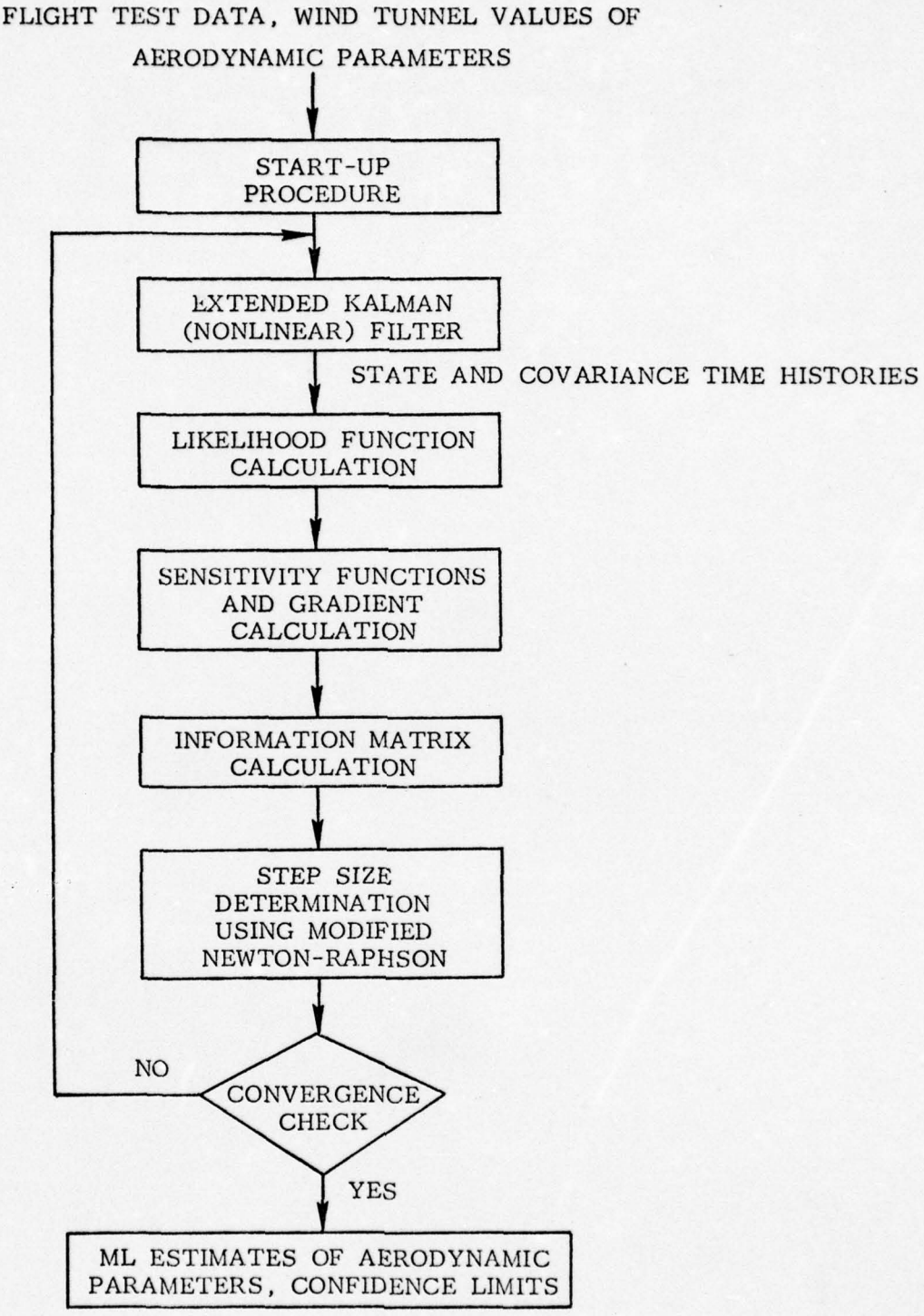

Figure 4.1 Flowchart of Maximum Likelihood Identification Program

Suppose θ can take three possible values: θ_1, θ_2, and θ_3. Let the probability density functions of observations z for these three values of θ be as shown in Figure 4.2. Then, if the actual observation is z, θ_2 is the maximum likelihood estimate of θ. In practice, starting from a priori estimates, the parameters are updated so that the value of the resulting density function at the observations increases monotonically.

The concept implementation is shown in Figure 4.2. An extended Kalman filter is used with fixed parameter values to determine state and covariance time histories. The likelihood function, which has the same form as the density function of the observations, depends on innovations and their covariance. The first and second gradient of the likelihood function are calculated by propagating equations governing the sensitivities of state and covariance called sensitivity equations. Gradient procedures are used to determine step size and update the parameters. This is repeated until convergence occurs.

The most important asset of the maximum likelihood method is its versatility. The next sections describe how this technique is used for estimating parameters in nonlinear aircraft models at high angles-of-attack.

4.2 MAXIMUM LIKELIHOOD TECHNIQUES

The maximum likelihood method is an inherently powerful technique for the study of parameter identification in the high angle-of-attack flight regime. The aircraft motions in this region are highly nonlinear and there is no single model to adequately describe the motions. Here the method is simplified so that more attention is given to the identification and related problems of identifiability of parameters in the model structure determined by techniques of Chapter III. Certain simplifications which are made disregard effects which are only secondary to the above study. These modifications are detailed in the following paragraphs.

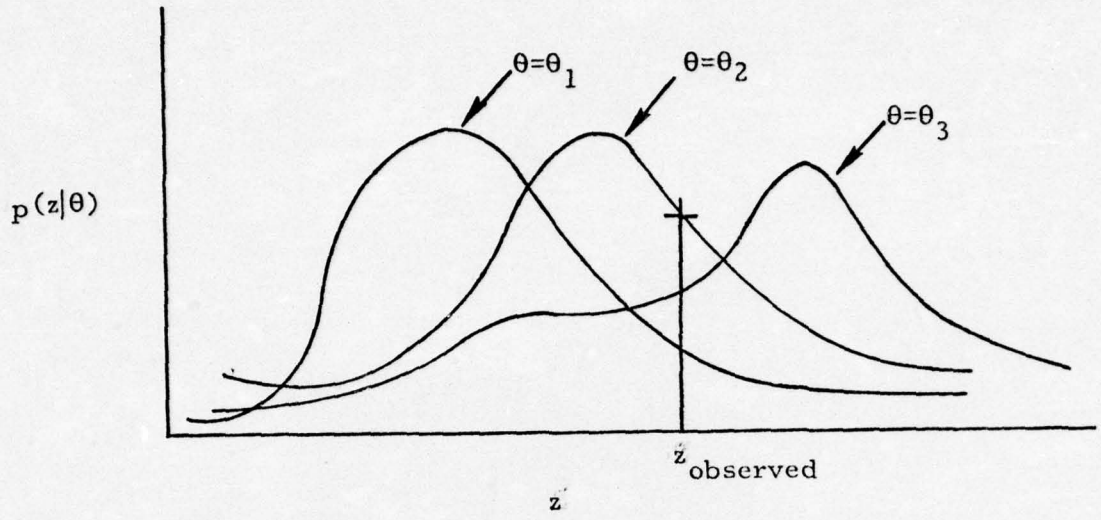

Figure 4.2 Maximum Likelihood Estimates

In the presence of process noise, parameter estimates may be biased unless estimates of the process noise statistics themselves are made. To estimate the process noise statistics, it is necessary not only to propagate the state and sensitivity for all unknown parameters, but also to propagate the covariance of the state estimation error and its sensitivities. This is an increase in computational requirements over the case where process noise statistics are not identified. The ability of the maximum likelihood algorithm to identify process noise statistics has previously been demonstrated [9]. The resolution of the problems of over-parameterization is the central objective of this work. Therefore, the identification of process noise statistics is not included in this implementation of the maximum likelihood algorithm. As will be shown, however, parameter estimates are accurately obtained, even with process noise.

The algorithm equations are detailed in Appendix A of this report. This appendix contains not only the fundamental algorithm, but also the various analytical forms which the algorithm assumes under various simplifications. In particular, the algorithm used for the results of this work is obtained by noting that

$$\hat{x}(t|t_{i-1}) = x(t) \tag{4.1}$$

The implementation of the maximum likelihood method used here is quite sophisticated. Some of the main features of the computer program used to study parameter identification at high angles-of-attack are:

(a) The program incorporates a detailed instrument model. The measurements are assumed to have bias, scale factor errors, and random noise. For example, the measured value of pitch rate is

$$q_m = (1+k_q)q + b_q + w_q \tag{4.2}$$

The scale factor k_q, bias b_q and the spectral density of w_q can be identified or given preassigned values.

(b) In most implementations, the measurement noise covariance matrix is estimated by

$$\hat{R} = \frac{1}{N} \sum_{i=1}^{N} \nu(i)\, \nu^T(i) \tag{4.3}$$

where $\nu(i)$ are innovations. In general, for finite data length, this would give an estimate of the measurement noise covariance matrix with all nonzero elements and no special structure. In other words, Eq. (4.3) assumes that there are $m(m+1)/2$ unknown elements in measurement noise statistics. If the structure of R is known, as is usually the case in aircraft applications, the number of unknown elements in R is fewer than $m(m+1)/2$. For example, if the measurement noise in different channels is independent, only diagonal terms of R need to be estimated. The use of Eq. (4.3) will lead to an over-parameterized model and incorrect parameter estimates. The statistically correct estimate of the measurement noise covariance matrix for independent measurement noise sources is,

$$\hat{R} = \text{diag} \quad \frac{1}{N}\left\{\sum_{i=1}^{N} \nu(i)\, \nu^T(i)\right\} \tag{4.4}$$

(c) In the high angle-of-attack flight regime, the longitudinal and lateral motions, in addition to being nonlinear, are coupled. This requires the solution of nine nonlinear differential equations in u, v, w, p, q, r, φ, θ and ψ. In many instances, one or more equations do not have any unknown parameters. The program is written so that some state equations can be discarded. Since the aircraft is fairly well instrumented, there are measurements of all state variables. The measurements of those states, whose governing equations have been discarded, are used in other equations instead of the value of the states obtained by integrating these equations. This results in a considerable saving in computation time at a slight loss in accuracy. This feature can be used to identify longitudinal and lateral derivatives separately even in regions where these two motions are coupled.

(d) As explained in the last chapter, the aerodynamic derivatives are expressed as polynomial functions of angle-of-attack and sideslip angle. No single expansion with a reasonable number of terms describes most of these derivatives adequately in the entire range under consideration. Therefore, different expansion terms are required in different operating regions. The computer program can handle all possible expansions of aerodynamic coefficients. For example, the equation governing pitch rate, excluding nonlinear dynamic terms, is,

$$\dot{q} = C_{m_q}(\alpha,\beta)q + C_m(\alpha,\beta) + C_{m_{\delta_s}}(\alpha,\beta)\delta_s \tag{4.5}$$

Then, letting c be a parameter,

$$\frac{d}{dt}\frac{\partial q}{\partial c} = \frac{dC_{m_q}(\alpha,\beta)}{dc} q + C_{m_q}(\alpha,\beta)\frac{\partial q}{\partial c} + \frac{dC_m(\alpha,\beta)}{\partial c} + \frac{dC_{m_{\delta s}}(\alpha,\beta)}{dc}\delta_s \tag{4.6}$$

If the expansion for C_m in a particular case is

$$C_m(\alpha,\beta) = \sum_{i=0}^{k}\sum_{j=0}^{\ell} C_{ij}\,\alpha^i\beta^j \tag{4.7}$$

where some C_{ij}'s are zero, then

$$\frac{dC_m(\alpha,\beta)}{dc} = \sum_{i=0}^{k}\sum_{j=0}^{\ell}\left\{\frac{\partial C_{ij}}{\partial c}\alpha^i\beta^i + iC_{ij}\,\alpha^{i-1}\beta^j\frac{\partial\alpha}{\partial c} + jC_{ij}\,\alpha^i\beta^{j-1}\right\} \tag{4.8}$$

and

$$\frac{\partial C_{ij}}{\partial c}\begin{cases} = 1 \text{ if c is } C_{ij} \\ = 0 \text{ otherwise}\end{cases} \tag{4.9}$$

This implementation of the maximum likelihood method can compute the gradient of $C_m(\alpha,\beta)$ and other aerodynamic derivatives with respect to any parameter c for chosen k and ℓ and any C_{ij} zero.

(e) The computer program determines the covariances of estimates of states, measurements and aerodynamic coefficients as a function of time. Let the state and measurement equations be

$$\dot{x} = f(x,u,\theta,t) \tag{4.10}$$

$$y = h(x,u,\theta,t) + v \tag{4.11}$$

The error in state estimate is

$$\tilde{x} = \frac{\partial x}{\partial \theta} \tilde{\theta} \tag{4.12}$$

The covariance of state estimation error is

$$\Sigma_{\tilde{x}} = \frac{\partial x}{\partial \theta} M^{-1} \left(\frac{\partial x}{\partial \theta}\right)^T \tag{4.13}$$

where M is the information matrix, the inverse of which is the Cramer Rao lower bound on parameter error covariances.

The equations for computing state sensitivities are given in Appendix A. The output of the model is

$$\hat{y} = h(\hat{x}, u, \hat{\theta}, t)$$

The covariance of output error is approximately

$$\Sigma_{\tilde{y}} = + \left(\frac{dh}{d\theta}\right) M^{-1} \left(\frac{dh}{d\theta}\right)^T + R \tag{4.14}$$

The correlation between $\tilde{\theta}$, $\tilde{x}$ and v is neglected. The covariance of error in aerodynamic coefficients is computed in a similar fashion.

(f) It is possible to fix any parameter at a preassigned value or constrain it to stay within a region.

The expansion terms, which are identified to be significant for an aerodynamic coefficient during model building, do not completely explain its variation with α and β. Therefore, the model, whose parameters are identified, has residual terms called modeling errors. These modeling errors produce biased parameter

estimates. The bias in the estimates depends on the amount of modeling errors and how changes in parameters can explain this error. Bias also results from inaccurate instrument modeling or fixing parameters at incorrect values. The expected values of these biases do not depend upon the amount of data. On the other hand, the covariance of parameter estimates decreases with increasing data size. In a particular run, it is worthwhile to make simplifications which produce biases in parameters much smaller than the corresponding standard deviations. This could lead to a considerable saving in computation time for an insignificant loss in accuracy. For instance, simplified instrument models may be adequate for short flight testing time.

Information Aggregation

Any available a priori information about parameters can be incorporated into the identification program. This is done by finding the weighted mean of the a priori parameter values and the output of the identification program, the weights varying inversely as the corresponding covariances. This has been done before [9]. A similar approach can be used to combine estimates from different identification runs and thus make full use of available data. These runs give estimates of aerodynamic stability and control derivatives over different ranges of α and β, together with the corresponding covariances. Since these coefficients are approximated by low order polynomials, the coefficients of the polynomial provide a "good" fit over the range of α and β covered by the experiment. It is not possible to use these polynomials for extrapolation. Therefore, the information about the value of an aerodynamic coefficient obtained from all experiments at discrete values of α and β can be combined. Suppose that k different experiments give estimates C_i with variances σ_i for the value of C_m at α_o. Then, the "best" estimate of $C_m(\alpha_o)$ would be

$$\hat{C}_m(\alpha_o) = \frac{\sum_{i=1}^{k} \frac{C_i}{\sigma_i}}{\sum_{i=1}^{k} \frac{1}{\sigma_i}} \qquad (4.15)$$

This can be done at many discrete points to obtain a continuous curve.

4.3 COMPUTATIONAL ASPECTS OF MAXIMUM LIKELIHOOD ESTIMATES

The application of maximum likelihood identification in practice requires accurate computational algorithms to maximize the likelihood function. It is not uncommon to find situations where the likelihood surface has multiple maxima, saddle-points, discontinuities and a singular Hessian in the parameter space. The application of the steepest descent method leads to an extremely slow convergence rate, and the straightforward application of the Newton-Raphson and the Gauss-Newton methods may lead either to no convergence or convergence to wrong stationary points. From a statistical viewpoint, only the absolute maximum of the likelihood function provides an unbiased, consistent, and efficient estimate. Thus, it is important to locate the true maximum of the likelihood function. With the present computation methods of nonlinear programming, in general, this could be an extremely difficult and time-consuming task. In aircraft applications, a priori information about the parameters is used to choose a good starting value and impose physically meaningful constraints on the parameters. This increases the chances of approaching the absolute maxima.

4.3.1 Identifiability Problems and Solutions

Anomalies also occur in the likelihood function due to inadequate model specification and parameterization. Some of the anomalies that lead to numerical difficulties are:

1. Discontinuities and Singularities: There are examples where the likelihood function increases up to a maximum value and then falls immediately to minus infinity. In other cases, the likelihood function may rise suddenly to infinity for some particular parameter values. These problems can often be avoided by either changing the model or changing the parameterization.

2. Singular or Nearly Singular Information Matrix: This is one of the most common problems in parameter identification since it is difficult to determine a priori whether a given sample has adequate information for estimating all the parameters in the model. Generally, the tendency in practical applications is to include all the parameters

about which there is some uncertainty. This leads to overparameterization which in turn produces a singular or a nearly singular information matrix. The likelihood surface in turn has long, curved and narrow ridges along which the convergence rate is extremely slow. Under-parameterization does not really provide the solution since it may lead to spurious local maxima and saddle-points.

The basic iteration in gradient-type nonlinear programming methods is

$$\theta_{i+1} = \theta_i - \rho_i R_i^{-1} g_i \tag{4.16}$$

where θ_i is the parameter vector at the i^{th} iteration, g_i is a vector of gradients of the negative log-likelihood function $J(\theta)$, i.e., the j^{th} component of g_i is given as

$$g_i(j) = \sum_{t=1}^{N} \left\{ \nu^T R^{-1} \frac{\partial \nu}{\partial \theta_i(j)} - \tfrac{1}{2} \nu^T R^{-1} \frac{\partial R}{\partial \theta_i(j)} R^{-1} \nu \right.$$

$$\left. + \tfrac{1}{2} \mathrm{Tr}\left(R^{-1} \frac{\partial R}{\partial \theta_i(j)} \right) \right\} \tag{4.17}$$

R_i is an approximation to the second partial matrix

$$\left. \frac{\partial^2 J}{\partial \theta^2} \right|_{\theta=\theta_i}$$

and ρ_i is a scalar step size parameter chosen to ensure that $J(\theta_{i+1}) < J(\theta_i) - \varepsilon$ where ε is a positive number that can be chosen in a variety of ways. In the Gauss-Newton method used here, the matrix of second partials is approximated by

$$R_i(j,k) = M_i(j,k) \cong \sum_{t=1}^{N} \left\{ \left(\frac{\partial \nu^T}{\partial \theta_i(j)} R^{-1} \frac{\partial \nu}{\partial \theta_i(k)} \right) \right.$$

$$\left. + \tfrac{1}{2} \mathrm{Tr}\left[R^{-1} \frac{\partial R}{\partial \theta_i(j)} R^{-1} \frac{\partial R}{\partial \theta_i(k)} \right] \right\} \tag{4.18}$$

where M is the approximation of R. The first partials of innovations ν and their covariance can be computed by solving linear difference equations (i.e., the sensitivity equations). Notice that in this approximation, computation of second partials of state and covariance is not required.

There are several problems with this method. As long as M_i^{-1} is positive semi-definite, it is possible to find a step which will reduce the cost. As mentioned before, most of the problems arise when the information matrix is almost singular (i.e., the eigenvalues are spread far apart), which is almost always the case in high angle-of-attack problems. This near-singularity of the information matrix manifests itself in several ways:

(a) During the computation of the inverse of the information matrix, the positive-definiteness may be lost because of round-off errors.

(b) The step-size may be very large in those directions which correspond to small eigenvalues of the information matrix. Let

$$M = \sum_{i=1}^{m} \lambda_i v_i v_i^T \tag{4.19}$$

$$M^{-1} = \sum_{i=1}^{m} \frac{1}{\lambda_i} v_i v_i^T \tag{4.20}$$

$$\Delta\theta = -\alpha \sum_{i=1}^{m} \frac{1}{\lambda_i} v_i v_i^T g$$

$$= -\sum_{i=1}^{m} \alpha \frac{\left(v_i^T g\right)}{\lambda_i} v_i \tag{4.21}$$

where λ_i are the eigenvalues and v_i the corresponding eigenvectors of M. Thus, if $v_i^T g$ is not small for small eigenvalues λ_i, the step in the direction of v_i is large. Usually, for small eigenvalues, $v_i^T g$ is also small, but it is the difference of large

and almost equal numbers. Therefore, in most cases, divergence is only a numerical problem. Complications arise from local irregularities in the likelihood function. Several remedies can be used, depending on the problem complexity:

(a) $\Delta\theta = -\alpha M^{-1} g$

Let $\Delta\theta' = M^{-1} g$ (4.22)

then $\Delta\theta = -\alpha\Delta\theta'$ (4.23)

Positive-definiteness of M could be lost during the inversion. This can be avoided through finding $\Delta\theta'$ by solving the following linear equations

$$M\Delta\theta' = g \tag{4.24}$$

The accuracy of Eq. (4.24) also depends on conditioning of M (ratio of maximum and minimum eigenvalues) but will be much superior as compared to Eq. (4.22).

(b) Conditioning of M can be improved. Premultiply both sides of Eq. (4.24) by A^{-1}, where

$$A = \text{diag}\left[\sqrt{M_{11}},\ \sqrt{M_{22}} \cdots \sqrt{M_{mm}}\right] \tag{4.25}$$

to get

$$(A^{-1} M A^{-1})\ (A\Delta\theta') = A^{-1} g$$

or

$$M^*\Delta\theta^* = g^* \tag{4.26}$$

All elements of M* are between -1 and +1. In general, this matrix is much better conditioned than M. Equation (4.26) can be used to solve for $\Delta\theta^*$ and then $\Delta\theta'$ is obtained by rescaling.

(c) The rank deficient inverse of M can also be used. In this procedure, the eigenvalues of the matrix M are arranged in a decreasing order of magnitude and all eigenvalues below a threshold b are neglected in using Eq. (4.20) for the inverse, i.e.,

$$\hat{M}^{-1} = \sum_{i=1}^{k} \frac{1}{\lambda_i} v_i v_i^T \tag{4.27}$$

where

$$\begin{aligned} \lambda_i &\geq b \qquad i \leq k \\ \lambda_i &< b \qquad i > k \end{aligned} \tag{4.28}$$

This is equivalent to searching for the maximum of the likelihood function in the subspace spanned by v_i $(i \leq k)$. If this process is continued until the end, the estimates may never converge to their maximum likelihood values. It should also be noted that since only large eigenvalues are included, step $\Delta\theta$ may be "small".

(d) Instead of neglecting eigenvalues of M, which are smaller than a certain threshold b, these smaller eigenvalues are increased to b. Thus, the inverse of M is approximated as

$$\hat{M}^{-1} = \sum_{i=1}^{k} \frac{1}{\lambda_i} v_i v_i^T + \frac{1}{b} \sum_{i=k+1}^{m} v_i v_i^T \tag{4.29}$$

In this case, when the program converges, the likelihood function will reach a maxima. Convergence may be slow.

(e) This fix of the Gauss-Newton method is a two-step procedure. The first step is taken by finding M^{-1} using Eq. (4.27). Then, another step direction is computed using only the small eigenvalues, i.e.,

$$\Delta\theta_2 = -\alpha \sum_{i=k+1}^{m} \frac{v_i v_i^T g}{\lambda_i} \tag{4.30}$$

Then step size α is chosen by a one dimensional search. As the algorithm approaches the maximum, it may be worthwhile to carry out a one dimensional search in each $v_i (i > k)$ direction.

The last approach, when used with the normalized information matrix M^* of Eq. (4.26), is one of the best and is recommended if the number of unknown parameters is large. In most cases tried, fix (d) was adequate.

4.3.2 Relationship Between Subset-Regression and Rank-Deficient Solutions

The subset-regression method, presented in Chapter III and Appendix B, and the rank deficient solution of Section 4.3, are closely related to each other. In the subset-regression method, an equation error technique is used in conjunction with certain statistical tests to determine the set of parameters which significantly affect the input-output relationship for the given data and the class of models under consideration. In other words, the method determines which parameters are important. Since different models and parameter sets may be adequate for different operating regions, the importance of any parameter depends upon the input and output data.

The rank deficient method uses input-output data and the model structure to determine the information content about linear combinations of parameters in the model. It works in parameter space finding principal directions and information about the linear combination of parameters representing those directions (eigenvectors and eigenvalues of the information matrix). When the rank

deficient inverse of the information matrix is used, the parameter subspace with small information is dropped from consideration. The optimization procedure, then, extremizes the likelihood function over the parameter subspace where enough information is available about parameters from data. This could be used to determine the model structure much in the same way as the subset-regression technique. However, in the rank deficient method, unlike subset regression, significant linear combinations of parameters are obtained. In the numerical computation procedure, the true parameter values are unknown and, therefore, only the conditional information matrix for assumed parameter values is available. This information matrix could be considerably different from the true information matrix at correct parameter values. Thus, dropping a certain parameter subspace in early stages of computation may lead to erroneous conclusions. This factor reduces the applicability of this method in model specification, since the optimal parameter values must be found before the unimportant parameter directions can be determined.

4.4 EXAMPLE OF THE USE OF THE MAXIMUM LIKELIHOOD IDENTIFICATION PROGRAM (HIDENT)

The input to the maximum likelihood program are noisy measurements and the required number of expansion terms in all aerodynamic stability and control derivatives. A priori values of the coefficients in each of these expansion terms, obtained from subset regression subroutine, are also read. This, together with the equations to be propagated and the parameters to be identified, starts the identification subroutine, denoted as HIDENT.

A typical HIDENT output for identifying longitudinal aerodynamic coefficients is presented in Tables 4.1 and 4.2. The states u, w, q, and θ are propagated by integrating the differential equations governing them, while measurements of v, p, r, φ and ψ are assumed to be the values of the corresponding state variables. The measurements of α, u, $\ddot{z}$ and q are used to identify 10 parameters in the longitudinal equations of motion. Many other parameters have nonzero values but are not identified. For example, the parameter $C_{m_{\alpha^2\beta^2}}$ is fixed at -5746 during identification (i.e., is not identified).

TABLE 4.1

HIDENT Output

STATE	NAME	SELECTED USE
1	U	PROPAGATED
2	V	TIME HISTORY
3	W	PROPAGATED
4	P	TIME HISTORY
5	Q	PROPAGATED
6	R	TIME HISTORY
7	PHI	TIME HISTORY
8	THETA	PROPAGATED
9	PSI	TIME HISTORY

MEASUREMENT	NAME	USED
1	ALPHA	1
2	BETA	0
3	XDD	1
4	YDD	0
5	ZDD	1
6	P	0
7	Q	1
8	R	0

Input Parameter Values

PARAMETER	VALUE	IDENTIFIED/FIXED	PARAMETER NUMBER
C_{x_o}	-.03432	Identified	(1)
$C_{x_{\delta s\alpha}}$	1.2078	Identified	(2)
C_{z_o}	-.97113	Identified	(3)
C_{z_α}	-1.5708	Identified	(4)
$C_{z_{\alpha^2}}$	10.219	Identified	(5)
$C_{z_{\delta s}}$	-.4546	Fixed	
C_{z_q}	-11.82	Fixed	
$C_{z_{q\alpha}}$	-287.50	Fixed	
C_{m_o}	-.044415	Identified	(6)
C_{m_α}	-.052864	Fixed	
$C_{m_{\alpha^2}}$	-2.5006	Identified	(7)
$C_{m_{\alpha^3}}$	-33.791	Identified	(8)
$C_{m_{\alpha^9}}$	$.35854 \times 10^7$	Fixed	
$C_{m_{\alpha\beta^2}}$	-144.13	Fixed	
$C_{m_{\alpha^2\beta^2}}$	-5745.7	Fixed	
$C_{m_{\delta s}}$	-.52589	Identified	(9)
C_{m_q}	-7.057	Identified	(10)
$C_{m_{q\alpha}}$	26.3	Fixed	

TABLE 4.2

Typical Hident Iteration Step

```
ITERATION NO.    4

     P      MATRIX       10 ROWS       1 COLUMNS
-3.469352[illegible]-002
 1.230027[illegible]+000
-9.701609[illegible]-001
-1.744871[illegible]+000
 1.048907[illegible]+001
-5.829491[illegible]-002
-1.551145[illegible]+000
-3.013864[illegible]+001
-6.381832[illegible]-001
-1.133604[illegible]+001

     R      MATRIX        4 ROWS        4 COLUMNS
 1.5733119-004  -3.9372577-005  -1.6992635-004   2.1381918-005
-4.5496255-001   4.7601599-005   1.7524455-005   1.9527308-005
-6.0583127-001   1.1358791-001   5.0003628-004  -1.4229570-004
 1.3279364-001   2.2048023-001  -4.9571058-001   1.6478736-004

DETERMINANT R=        .6171114-015

.5*LOG(DET(R))=       -.1751074+002          PREVIOUS=       -.1548979+002

INNOVATIONS PART IN COST=         .1999999+001

TOTAL COST=       -.1551074+002

ABSOLUTE VALUE DELTAJ/J =          .1302931-00

     DJ     MATRIX       10 ROWS       1 COLUMNS
 1.2865773+003
-1.3108753+001
-1.7579831+003
-7.5207525+001
-3.0824417+000
-1.0429641+005
-1.8281260-002
 1.5338981+001
 1.2313684+004
-1.0551891+002

     D2J    MATRIX       10 ROWS       10 COLUMNS
 3.6609977+006   2.5764693+003  -1.9534033+005  -3.8670588+003  -3.6299440+002  -2.9600481+006  -1.0483588+004
    7.8691470+002   3.3117867+005  -1.9231259+003
 2.5764693+003   1.2325340+002  -1.7776911+002   1.7817651+000  -3.8546972-001   6.4333653+003  -2.6718286+000
    1.3855132+000  -7.6431991+002   6.3351449+000
-1.9534033+005  -1.7776911+002   1.8985669+005   1.8966050+002   5.8149559+002   3.5557222+005  -1.1284449+003
    8.1709260+001  -4.5078878+004   5.8452058+002
-3.8670588+003   1.7817651+000   1.8966050+002   8.3725309+002  -2.7077063+001   5.8394003+004   4.0242593+002
   -4.0760202+001  -6.1060769+003   2.2627409+001
-3.6299440+002  -3.8546972-001   5.8149559+002  -2.7077063+001   4.8938310+000   3.1869295+003  -5.7018322+000
    7.6477604-001  -3.8328081+002   2.8723924+000
-2.9600481+006   6.4333653+003   3.5557222+005   5.8394003+004   3.1869295+003   1.1825698+006   3.1027166+005
   -2.5218758+004  -1.3128498+007   6.8635201+004
-1.0483588+004  -2.6718286+000  -1.1284449+003   4.0242593+002  -5.7018322+000   3.1027166+005   1.4130524+003
   -1.2111783+002  -3.5038443+004   2.1740146+002
 7.8691470+002   1.3855132+000   8.1709260+001  -4.0760202+001   7.6477604-001  -2.5218758+004  -1.2111783+002
    1.0935573+001   2.8411067+003  -1.7559418+001
 3.3117867+005  -7.6431991+002  -4.5078878+004  -6.1060769+003  -3.8328081+002  -1.3128498+007  -3.5038443+004
```

TABLE 4.2 (Continued)
Typical Hident Iteration Step

```
    2.8411067+003   1.4647209+006  -8.0189424+003
-1.9231234+003   6.3351449+000   5.8452058+002   2.2627409+001   2.8723924+000   6.8635201+004   2.1740140+002
   -1.7559418+001  -8.0189424+003   6.9495845+001

EIGENVALUES=    .119794+009    .359477+007    .178787+006    .710842+004    .964966+003    .334506+003    .116130+003    .756749+001
                .199770+001    .433615+000

EIGENVECTORS MATRIX

          MATRIX      10 ROWS      10 COLUMNS
 2.5603976-002  -9.9817709-001   5.4598314-002  -8.3801378-004   1.3546932-003  -9.7385835-004   6.3124530-004
   -1.1858809-005   6.2029647-005   4.9878930-005
-5.3504996-005  -7.6458040-004  -2.5455642-004   7.3455212-003  -1.1425048-002   1.0053726-001  -9.9480948-001
   -9.9139927-005  -2.4576654-004  -7.8179061-003
-3.0371711-003   5.4553530-002   9.9792541-001  -3.0246191-002   7.3399114-003  -1.3298216-002  -1.9523327-003
   -1.8343215-004   3.1611379-003   3.5833801-004
-4.9077721-004   6.5586969-004  -7.4537656-004  -5.4922501-002   8.4738012-001   5.2498290-001   4.2892710-002
   -1.3251597-002  -3.5853380-002   4.6090887-003
-2.6876993-005   8.6604344-005   3.1119085-003   1.7200593-003  -2.9274836-002  -2.2267699-002  -1.3403577-003
   -8.6811921-002  -9.9486548-001  -3.6592996-002
-9.9355826-001  -2.5703395-002  -5.0703689-003  -1.0961615-001  -1.1598612-003  -1.0246789-002  -1.7594982-003
    5.4934847-003  -4.0327512-004   2.4443937-004
-2.6078521-003   6.5555707-004  -1.2287577-002   9.7749628-002   5.2713255-001  -8.3419614-001  -9.0351102-002
   -7.0981748-003   6.7678352-004   9.1217832-002
 2.1194538-004  -3.5340420-005   9.2460969-004  -6.9742432-003  -5.3628912-002   7.4190563-002   2.5421698-004
   -1.9837364-002  -3.4957650-002   9.9486459-001
 1.1030707-001   2.0590342-003  -3.1170000-002  -9.8560352-001   5.8210846-003  -1.0988513-001  -1.8473382-002
    5.4476770-002  -4.3378728-003   2.5427079-003
-5.7706801-004   4.7567263-005   2.1125792-003   5.4565910-002   1.1119807-002   6.6624022-003   7.3695599-004
    9.9946777-001  -8.7781909-002   1.7225110-002

NUMBER OF EIGENVALUES ADDED= 10

     MINV  MATRIX      10 ROWS      10 COLUMNS
 3.0973785-007  -6.5327691-006   4.7141337-007  -6.6582152-007  -3.4946973-005   4.4087546-008   1.3195343-005
    1.1310794-004   4.0793120-007  -2.3082136-006
-6.5327691-006   8.5489419-003   5.4459316-006  -2.9167279-004   7.9818985-004   7.2125685-006  -1.1406040-003
   -1.7913103-002   7.5475689-005  -3.1618943-004
 4.7141337-007   5.4459316-006   1.1619042-005  -6.7508013-005  -1.6017001-003   2.9608044-007   1.1480660-004
    7.6407236-004   2.4546488-006  -1.4918536-004
-6.6582152-007  -2.9167279-004  -6.7508013-005   2.2997206-003   1.7557054-002  -1.6677980-005   9.0008053-005
    1.1307544-002  -1.5696322-004   3.6882587-005
-3.4946973-005   7.9818985-004  -1.6017001-003   1.7557054-002   4.9953316-001   1.1789552-004  -7.9129377-003
   -6.6332206-002   1.3279339-003   3.0853775-002
 4.4087546-008   7.2125685-006   2.9608044-007  -1.6677980-005   1.1789552-004   6.2474750-006   7.0891010-005
    5.5143720-004   6.0683783-005   7.4823069-004
 1.3195343-005  -1.1406040-003   1.1480660-004   9.0008053-005  -7.9129377-003   7.0891010-005   2.1634730-002
    2.0909863-001   7.6012749-004   2.6507435-003
 1.1310794-004  -1.7913103-002   7.6407236-004   1.1307544-002  -6.6332206-002   5.5143720-004   2.0909863-001
    2.2837074+000   5.7437936-003   3.8454528-002
 4.0793120-007   7.5475689-005   2.6546488-006  -1.5696322-004   1.3279339-003   6.0683783-005   7.6012749-004
    5.7437936-003   5.9209371-004   7.4395603-003
-2.3082136-006  -3.1618943-004  -1.4918536-004   3.6882587-005   3.0853775-002   7.4823069-004   2.6507435-003
    3.8454528-002   7.4395603-003   1.3521257-001
```

TABLE 4.2 (Concluded)

Typical Hident Iteration Step

```
    NEW  MATRIX       10 ROWS       1 COLUMNS
-3.4409744-002
 1.2107721+000
-9.6797426-001
-1.0325585+000
 9.5956226+000
-5.8329237-002
-2.1959190+000
-3.3387565+001
-6.4526675-001
-9.4133948+000

    STEP  MATRIX       10 ROWS       1 COLUMNS
-3.8377...-004
 9.5956226+000
-5.8329237-002
-2.1959190+000
-3.3387565+001
-6.4526675-001
-9.4133948+000

    STEP  MATRIX       10 ROWS       1 COLUMNS
-2.8377563-004
 1.9255101-002
-2.1866666-003
-1.1231313-001
 8.9345697-001
 3.4326195-005
 6.4477332-001
 3.2487228+000
 7.0835325-003
-1.9226475+000

SQR=  .55654-003  .92460-001  .34086-002  .47955-001  .70677+000  .24994-002  .14708+000  .15111+001  .24352-001  .36771+000

F VAL  .38859+004  .17697+003  .81006+005  .13238+004  .22024+003  .54394+003  .11121+003  .39775+003  .68786+003  .95039+003
```

Table 4.2 is a typical iteration step. The parameters are listed and then the R matrix (average innovations covariance) is given. The upper half, including the diagonal, is the R matrix and the lower half gives the correlation coefficients between different measurements. Since the measurement noise covariance is known to be diagonal, its estimate would be

$$\hat{R} = -\text{diag}[1.48 \times 10^{-6},\ 3.97 \times 10^{-5},\ 5.07 \times 10^{-5},\ 8.58 \times 10^{-6}] \quad (4.31)$$

The total cost for these sets of parameter values is -15.5 and represents a 13% cost decrease from the parameters in the last step. DJ is the first gradient and D2J is the second gradient (information matrix) of the cost with respect to parameters. The eigenvalues and eigenvectors of the information matrix are given. If the range of eigenvalues should exceed a ratio of 10^{10}, one of the remedies suggested in Section 4.3 is used depending on problem complexity. In this case, since the range of eigenvalues is about 10^{8} all eigenvector directions are included in the search. The inverse of the information matrix (i.e., the dispersion matrix), the new parameters and the parameter step are shown next. The terms on the diagonal of the dispersion matrix give parameter error variances, the square root of which are standard deviations of estimates. The F-value is computed as the squared ratio of the parameter estimate to its standard deviation.

Thereafter, we proceed to the next iteration. This process continues until convergence occurs (i.e., the change in cost per iteration falls below a pre-specified tolerance bound).

4.5 SUMMARY

The maximum likelihood technique of parameter identification is the essential second step of a method for quantifying the causes of aircraft responses in the high angle-of-attack flight regime. Combining the two advanced techniques of subset regression and maximum liklihood is, itself, a complicated procedure, but one which is necessary for isolation of the phenomena occurring in these flight regimes. As discussed in Chapter II, however, the identification algorithm is but one part of the entire process. For this effort, the consideration of input design to improve parameter estimates has also been important, and is discussed in the following chapter.

V. INPUT DESIGN

The principal result of this project has been discussed in Chapter III (the model determination phase) and Chapter IV (the maximum likelihood identification phase). Application of this method is detailed in Chapter VI. Because of the importance of control input design in achieving those results, it is necessary to first review various aspects of input specification for the high angle-of-attack flight regime. Requirements for such input designs are summarized (Section 5.1) and present inputs used are reviewed (Section 5.2). Three approaches for high angle-of-attack input design are discussed (Section 5.3). These are: (1) sequential linear designs for locally linear approximations, (2) subset regression evaluation of various inputs, and (3) analytical nonlinear input designs. Examples of procedures (1) and (2) are given (Section 5.4) based on techniques detailed in Appendix C. The third technique, developed analytically in Appendix C, has not been applied usefully due to its excessive computational requirements, but its basis is discussed for completeness.

5.1 INPUT REQUIREMENTS

It has long been realized that the ultimate success of a flight test program depends on the choice of inputs used to excite the desired motions of the aircraft. Good inputs could enhance parameter identifiability and improve confidences on parameter estimates. This is especially true for parameter identification of aircraft models at high angles-of-attack. As explained in Chapter III, the aerodynamic derivatives are expanded as polynomials in angle-of-attack and sideslip angle. This leads to a large number of unknown parameters. Inputs must be chosen carefully to discriminate among different parameters. There are many other considerations for choosing inputs for specific flight tests:

a. Pilot Acceptability: The pilot should be able to safely implement these inputs without incurring dangerous aircraft responses.

b. Instrumentation: The inputs should consider specific instruments available, their dynamic range and accuracy.

V. INPUT DESIGN

The principal result of this project has been discussed in Chapter III (the model determination phase) and Chapter IV (the maximum likelihood identification phase). Application of this method is detailed in Chapter VI. Because of the importance of control input design in achieving those results, it is necessary to first review various aspects of input specification for the high angle-of-attack flight regime. Requirements for such input designs are summarized (Section 5.1) and present inputs used are reviewed (Section 5.2). Three approaches for high angle-of-attack input design are discussed (Section 5.3). These are: (1) sequential linear designs for locally linear approximations, (2) subset regression evaluation of various inputs, and (3) analytical nonlinear input designs. Examples of procedures (1) and (2) are given (Section 5.4) based on techniques detailed in Appendix C. The third technique, developed analytically in Appendix C, has not been applied usefully due to its excessive computational requirements, but its basis is discussed for completeness.

5.1 INPUT REQUIREMENTS

It has long been realized that the ultimate success of a flight test program depends on the choice of inputs used to excite the desired motions of the aircraft. Good inputs could enhance parameter identifiability and improve confidences on parameter estimates. This is especially true for parameter identification of aircraft models at high angles-of-attack. As explained in Chapter III, the aerodynamic derivatives are expanded as polynomials in angle-of-attack and sideslip angle. This leads to a large number of unknown parameters. Inputs must be chosen carefully to discriminate among different parameters. There are many other considerations for choosing inputs for specific flight tests:

a. Pilot Acceptability: The pilot should be able to safely implement these inputs without incurring dangerous aircraft responses.

b. Instrumentation: The inputs should consider specific instruments available, their dynamic range and accuracy.

c. Parameter Identification Procedure: Certain parameter extraction methods require specific inputs. There is, however, no constraint with modern powerful procedures like the maximum liklihood method used with the modified Gauss-Newton optimization technique.

d. Modeling Assumptions: The input should be tailored to the model whose parameters are to be identified. In high angle-of-attack flight regime, the aircraft follows different models for different regions of operation. The input should ensure that the system operates in a region where the model is valid.

e. Objective of Parameter Identification: The inputs must be selected on the basis of the ultimate objective of parameter identification; e.g., regulator design, response prediction, simulator construction.

f. System Integrity Constraints: The aircraft maneuvers produced by the input should not cross the design stresses of various aircraft components.

g. Output Sensitivity: Measured aircraft response resulting from the input should be sensitive to the parameters of interest and insensitive to other unknown parameters.

5.2 CONVENTIONAL INPUTS

In the last few decades, many different inputs have been tried for aircraft parameter identification. Most of these inputs are chosen because of their simplicity and ability to yield responses from which the relatively small number of basic linear derivatives (e.g., C_{m_α}, C_{m_q}, C_{ℓ_p}, C_{n_r}, etc.) may be estimated. The earliest inputs were frequency sweeps, where the aircraft is excited by sinusoidal inputs over a range of frequencies until steady-state is reached at each frequency. This gives the frequency response from which parameters of a suitable linear model can be determined. In addition to being very time consuming, this type of input may require considerable flight test time and can accurately identify parameters of only simple linear systems. Pulse inputs were also used and the frequency

response was obtained by taking the ratio of the Fourier transform of the output and the input at discrete points. This input may also be inaccurate for any but simple, low order linear systems.

More recently, doublets and step inputs are being used to identify aircraft parameters in both linear and nonlinear flight regimes. These inputs can be used with a wide class of models but may lead to poor identifiability of certain parameters. Excessive flight time may be required to obtain good estimates of all parameters.

Recent works of Gupta, Mehra and Hall [51-56] have given considerable insight into the nature of inputs which given good parameter estimates and resolve identifiability problems. A discussion of techniques to determine these inputs is given in Appendix C. Much further work is required in the area of input design for linear as well as nonlinear systems.

5.3 INPUTS FOR HIGH ANGLE-OF-ATTACK FLIGHT REGIME

The aircraft equations of motion are nonlinear at high angles-of-attack. Stall, wing rock and other phenomenon observed in this region cannot be explained by linear models. Under these circumstances, it is possible to consider an aircraft model in which the aerodynamic stability and control coefficients are slowly varying functions of aircraft states, in particular, angle-of-attack α and sideslip angle β. Usually, the form of these functions is not known a priori.

5.3.1 Inputs for Identifying Local Parameter Values

For very small changes in α and β during a maneuver, a model assuming constant values of aerodynamic derivatives is usually adequate, as mentioned in Chapter III. The techniques, described in Appendix C.2, for the design of optimal inputs for linear dynamic systems, can be used to specify inputs for identification of local values of functions representing the stability and control coefficients. It is necessary that there by only small excursions in these states which have maximum effect on parameters being identified.

5.3.2 Inputs to Identify Nonlinear Parameter Variations

Many methods have been suggested to design inputs which would give good identifiability of stability and control coefficients over a range of states. One way could be to carry out flight tests around many angles-of-attack and sideslip angles covering the range of interest. Inputs based on linear models are designed at each of these points, as explained above. This would give an accurate description of each aerodynamic derivative, but may be practically infeasible because:

1. It would require excessive flight testing time and data processing time.

2. It would require carrying out flight tests in regions where the trim condition cannot be reached or the airplane is unstable and/or unsafe.

A better scheme is to approximate the nonlinear aerodynamic derivatives by polynomials (or some other truncated series of complete functions) in independent variables. Each unknown nonlinear function in the equations of motion is thus replaced by a set of parameters. These parameters can be identified in a variety of ways. The aerodynamic derivatives are determined from a knowledge of the coefficients of terms in the polynomial expansions.

For small ranges of α and β, it is possible to determine all the polynomial coefficients in one single experiment. The inputs should have sufficient amplitude so that the motions occur in more or less the entire range of α and β under consideration. The technique for determining the amplitude is given in Appendix C.4.2.1. The amplitude depends on the order of the polynomial, accuracy desired, duration of the experiment and a priori estimate of the polynomial coefficients.

To determine aerodynamic derivatives over a wide range of angle-of-attack ($0 \leq \alpha \leq 30^{\circ}$) and sideslip angle ($-20^{\circ} \leq \beta \leq 20^{\circ}$), it is necessary to perform experiments starting at different α,β trim conditions. The results of these separate experiments are put together to obtain all coefficients in the polynomial. The

algorithm of Appendix C.4.2.2 finds the trim conditions and the duration of the experiment at each trim condition to produce a good estimate of the nonlinear function over the entire range of interest. It is possible to put constraints of an infeasible operation over a region. The technique considers regions where the stability augmentation system (SAS) is required for pilot safety but deteriorates parameter estimates.

A semi-empirical technique is useful in the design of input signals for identifying parameters in complicated systems with known characteristics. As a first step, analytic input designs are based on simplified models, using the techniques of Appendix C. State time histories are generated and inputs are evaluated based on a more accurate but complex model. This would give information about poorly identifiable directions in the parameter space and about poorly excited modes. This is usually done using simple programs which are not necessarily recommended for data reduction from actual flight tests. It is to be noted that input evaluation can be done without generating simulation data and going through the identification process. In the implementation used here, the optimal subset regression program is used to determine identifiable directions resulting from a certain input. A knowledge of the deficiencies in the chosen input, together with known system behavior, is used to modify the input. The process is repeated until an acceptable input is obtained.

Some analytical results for the design of inputs for nonlinear systems are presented in Appendix C. Many of them lead to complicated problems which are difficult, if not impossible, to solve with present computational facilities. They do give an excellent insight into the nature of inputs which could give good identifiability of unknown parameters. If the form of a nonlinear stability or control derivative is now known a priori, it is necessary to operate the system over the entire range of angle-of-attack and sideslip angle of interest. In other words, extrapolation could give misleading results when a nonlinear function is approximated by a finite series of complete functions over a range of the independent variables. Secondly, most input energy should be concentrated over the test regime. If the local variation of C_m with angle-of-attack is to be studied, it is not good to use inputs which give large excursions in angle-of-attack. This will be demonstrated through examples in the next section.

5.4 EXAMPLES OF INPUT DESIGN IN HIGH ANGLE-OF-ATTACK FLIGHT REGIME

5.4.1 Static Pitching Moment Characteristics

One of the most important phenomena of the stall/post-stall regime is "pitch-up". Its principal cause is the positive C_{m_α} which occurs close to stall [1]. Unlike most lateral aerodynamic nonlinearities, the affected mode is the relatively simple short period response which can be conceptually treated as a second order system whose stiffness is controlled by C_{m_α}.

The primary objective is to investigate the following questions:

1. What flight test conditions are required to determine the presence of $C_{m_\alpha} > 0$?

2. What order polynomial is required to represent the C_m versus α characteristic over the test regime?

In order to resolve these issues, several initial conditions and inputs were applied to the F-4 simulation; the subsequent responses were passed through the subset regression program. Since the principal effect of the aerodynamic nonlinearity was known to be on pitch (short period) response, only ELQ, the pitch acceleration regression variable, was used.

Initial conditions and inputs used were the following:

1. Trim at 1^o, 10^o, 20^o angle-of-attack, doublet stabilator 1^o, 2^o, 5^o, respectively.

2. Trim at 10^o angle-of-attack, ramp stabilator (1^o/sec).

3. Trim at 13^o angle-of-attack, sinusoidal stabilator (5^o and 10^o amplitudes).

The results of perturbation inputs in anticipated linear regimes were developed first [1]. These regimes were low angle-of-attack ($\alpha = 1^{o}$), pre-stall ($\alpha = 10^{o}$), and post-stall ($\alpha = 20^{o}$). The data from these maneuvers was passed to the subset regression program. The resulting coefficient model was evaluated on the basis of the quantitative "fit" of the response from the estimated model to the actual simulation response. The results are shown in Table 5.1.

The next series of longitudinal inputs [2] were made with a stabilator ramp of 1^{o}/sec to slowly push the aircraft from the linear regime through the known nonlinear C_m versus α characteristics at about 15^{o} (starting from 10^{o}). In addition, sinusoidal inputs were used (case (3)).

The basic result of these runs was that the C_m versus α nonlinear characteristics required data replication for successful determination. Only the last series of runs, (3), provided this replication. The physical reason for this requirement is based on the negative spring interpretation of the static moment characteristic.

TABLE 5.1

Stabilator Doublet (These results are a compilation of several experiments)

ANGLE OF ATTACK	MODEL
$= 1^{o}$	$\pm 1^{o}$ stabilator doublet, 7 second data length $C_m = C_{m_o} + C_{m_\alpha}\alpha + C_{m_{\delta_s}}\delta_s + C_{m_q} q$ matched (virtually) 100% of pitching moment variation
$= 10^{o}$	$\pm 1^{o}$ stabilator doublet, 7 second data length $C_m = C_{m_o} + C_{m_\alpha}\alpha + C_{m_{\delta_s}}\delta_s + C_{m_q} q$ matched 99.8% of pitching moment variation
$= 20^{o}$	$\pm 5^{o}$ stabilator doublet, 7 second data length $C_m = C_{m_o} + C_{m_\alpha}\alpha + C_{m_{\delta_s}}\delta_s + C_{m_q} q$ matched 99.1% of pitching moment variation

If the initial rates and accelerations with which the aircraft enters the unstable region are too low, the response to a doublet or step would be unstable, forcing the response to a stable region. If the initial accelerations are too high, the aircraft inertia overwhelms the static moment and the data doesn't reflect the nonlinearity. Although several sets of initial conditions and time-varying inputs may exist for isolating the characteristics, no extensive experimentation was performed with other than a sinusoidal stabilator input.

The results for the sine wave inputs are shown in Figures 5.1 through 5.4. Figure 5.1 shows the 10^{o} amplitude sine wave input and the resulting aircraft response (α, q, ELQ). This input was based on a trim angle-of-attack of 13.5^{o}. It is recognized that such a trim may be difficult to establish in a flight test since the aircraft is close to $C_{L_{max}}$.

The data from this run was passed through the regression problem for two maximum allowable polynomials--a fourth order and a ninth order. The results are shown in Figure 5.2. Compared with the (known) simulation C_m versus α, this input did not come acceptably close to the "true" value.

Based on the mechanism discussed above, a new input with half the amplitude and frequency was applied, the response for which is shown in Figure 5.3. This input should provide a more acceptable regression result, which is evident in the new subharmonic response in ELQ. Passing the data of this new input through the regression program (again with two polynomial possibilities) produced the result shown in Figure 5.4. Clearly, a higher order polynomial can be identified (locally) using this input.

5.4.2 Yaw Stiffness Variation with Angle-of-Attack

Yawing moment produced by sideslip angle (C_{n_β}) is an important parameter in determining stability of the lateral modes of the aircraft. A positive C_{n_β} usually implies a stable dutch roll mode and vice versa. C_{n_β} varies with angle-of-attack. Figure 5.5 shows a plot of C_{n_β} as a function of angle-of-attack α at zero sideslip angle. It is generally positive in the low angle-of-attack flight regime and changes

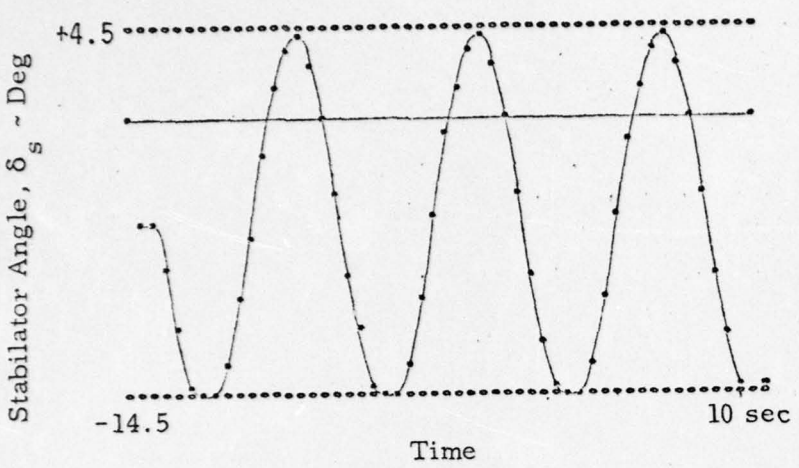

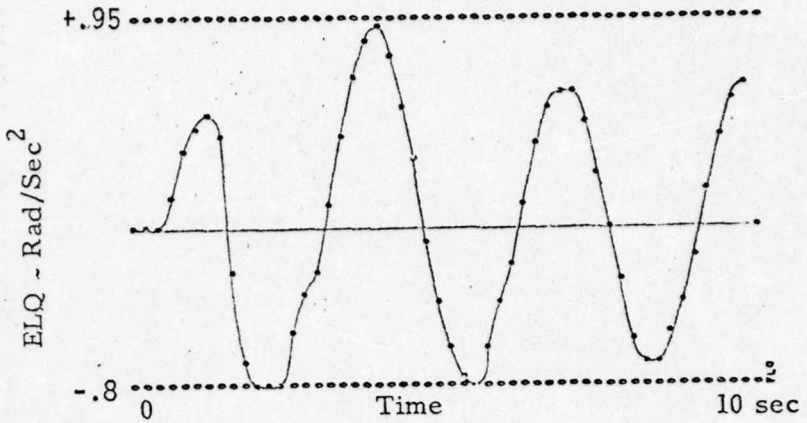

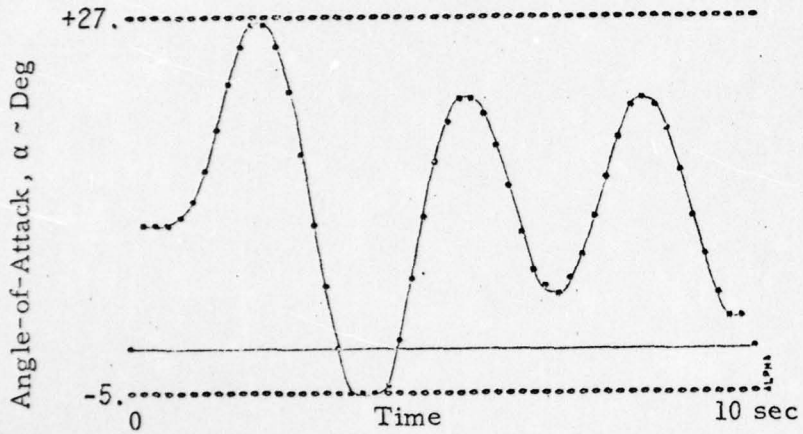

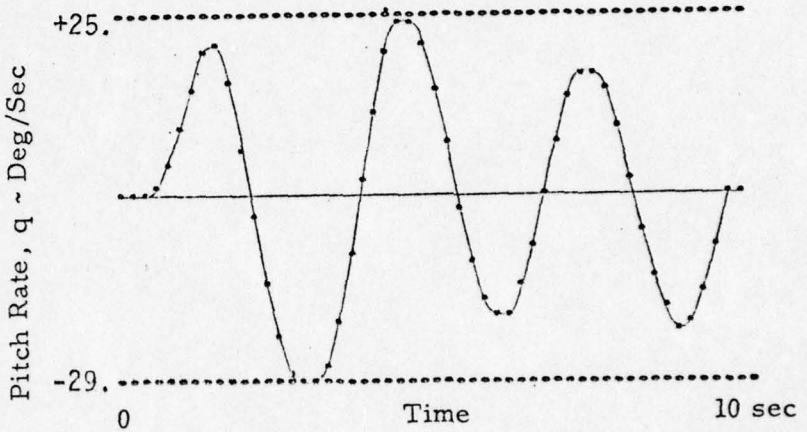

Figure 5.1 Data From Simulation With $\delta_s = -10^o \sin\left(\frac{2\pi t}{3}\right)$

———— Known C_m vs. α for Simulation

— — — $C_m = -5.2(10)^{-3} - 2.51(10)^{-3}\alpha + 1.74(10)^{-4}\alpha^2 - 3.03(10)^{-7}\alpha^4$

—·—·— $C_m = -5.2(10)^{-3} - 2.47(10)^{-3}\alpha + 9.18(10)^{-5}\alpha^2 + 2.74(10)^{-8}\alpha^5$
$-1.23(10)^{-10}\alpha^7 + 1.07(10)^{-13}\alpha^9$

$$\delta_s = -10^o \sin \frac{2\pi t}{3}$$

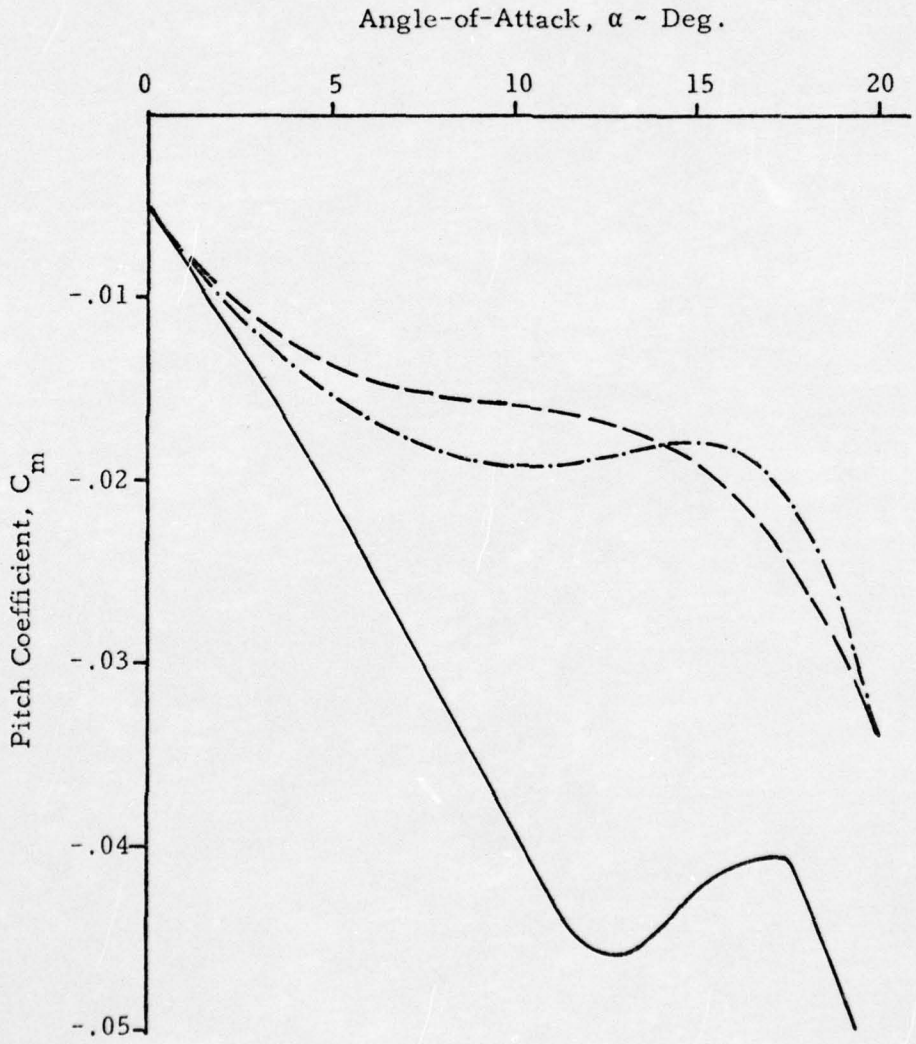

Figure 5.2 Effect of Polynomial Order on C_m Extraction from Simulated Data (10^o δ_s)

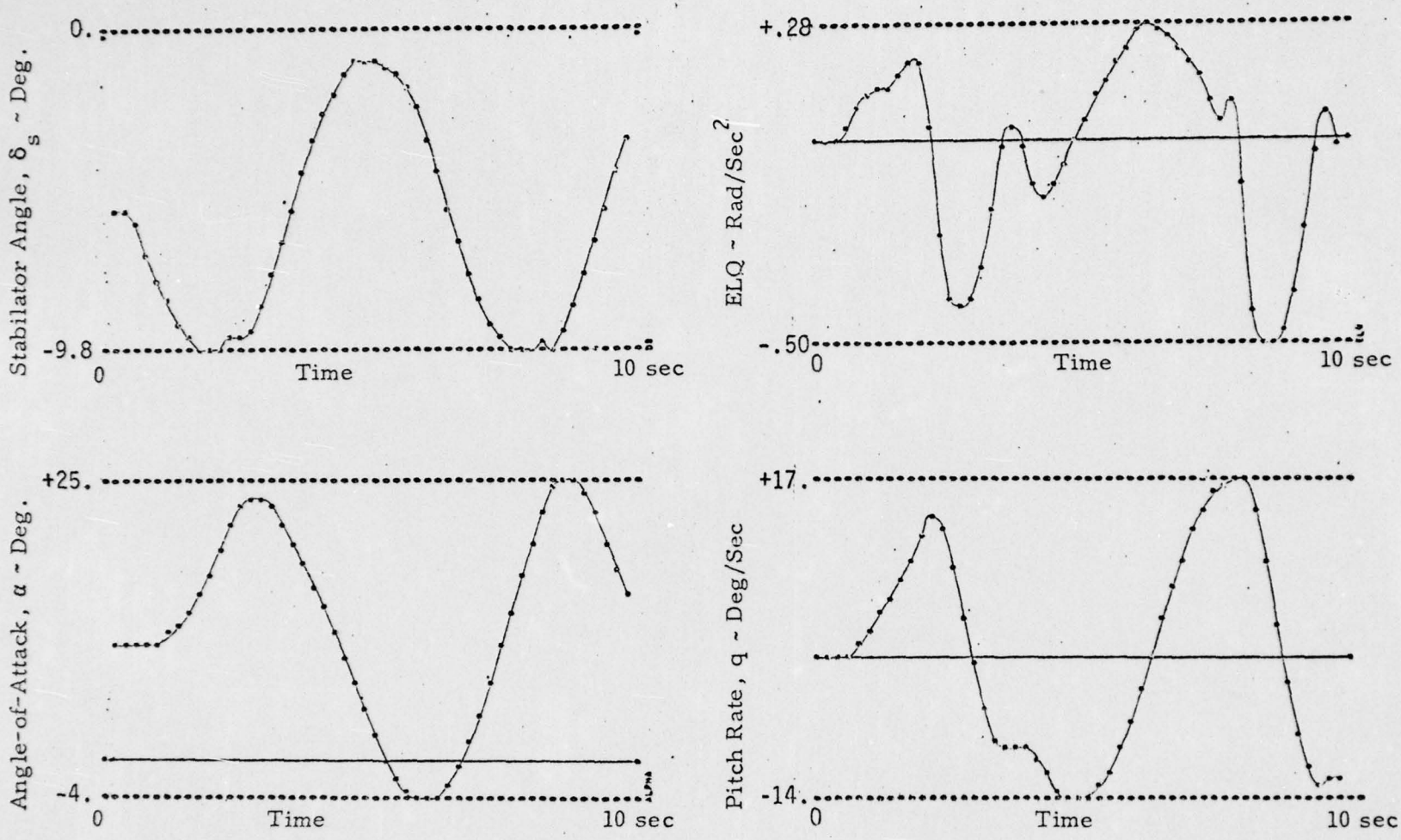

Figure 5.3 Data From Simulation With $\delta_s = -5^\circ \sin\left(\frac{2\pi t}{6}\right)$

———— Known C_m vs. α for Simulation

— — — $C_m = -5.2(10)^{-3} - 3.67(10)^{-3}\alpha + 1.58(10)^{-4}\alpha^2 - 1.21(10)^{-8}\alpha^5$

—·—·— $C_m = -5.2(10)^{-3} - 2.54(10)^{-3}\alpha - 1.42(10)^{-5}\alpha^4 + 1.84(10)^{-6}\alpha^5$
$-9.02(10)^{-9}\alpha^7 + 4.31(10)^{-10}\alpha^8 - 6.07(10)^{-12}\alpha^9$

$$\delta_s = -5^o \sin \frac{2\pi t}{6}$$

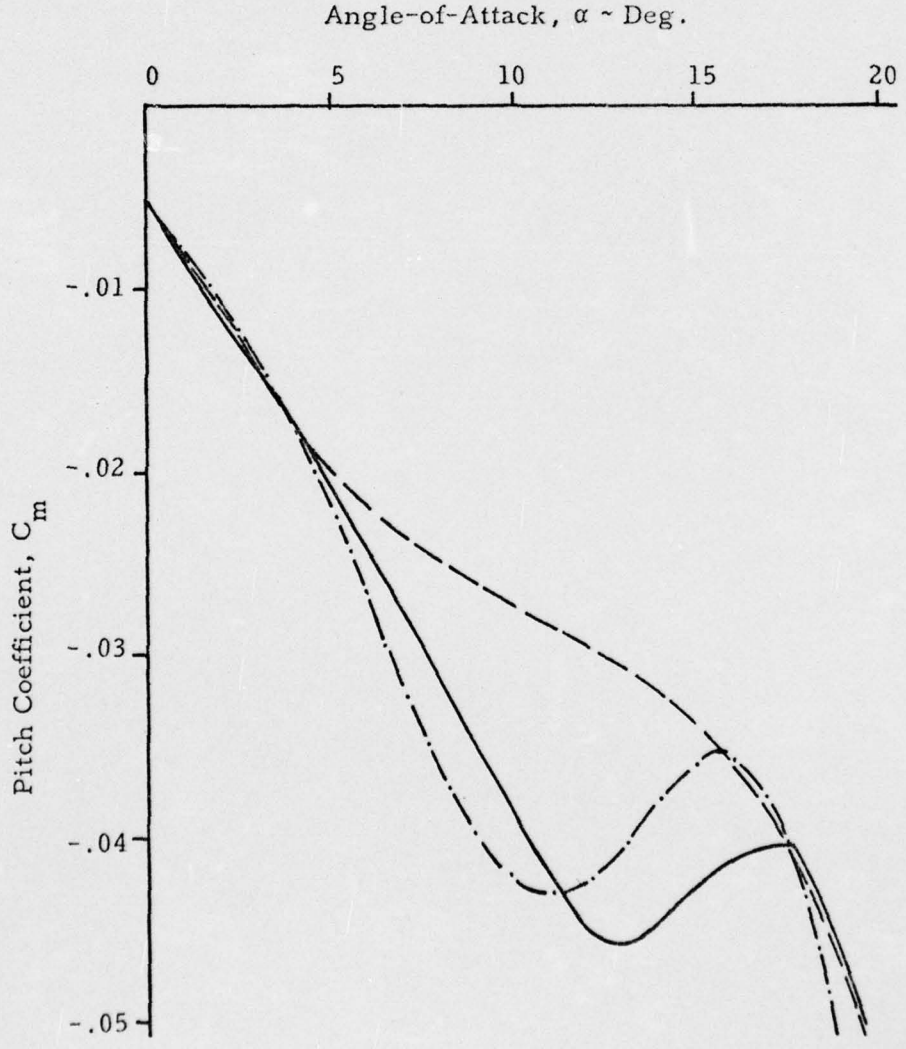

Figure 5.4 *Effect of Polynomial Order on* C_m Extraction from Simulated Data ($5^o \delta_s$)

sign beyond the stall angle. Also shown in Figure 5.5 is a least squares fourth order polynomial fit to the simulation data.

A computer program* has been written to determine the angles-of-attack at which C_{n_β} must be identified locally to give a good estimate of the C_{n_β} curve for $0^o \leq \alpha \leq 30^o$. It is assumed that operation is possible throughout this range of angle-of-attack. If the angle-of-attack is greater than 20^o, however, it is necessary to use the stability augmentation system to make the airplane stable enough. This use of SAS at high angles-of-attack results in poorer parameter estimates for the same duration of the experiment time. The information available about C_{n_β} at any α is assumed to increase linearly with the experiment time around that α. The use of SAS increases the standard deviations by a factor of three for the same experiment time. The information about C_{n_β} for a unit experiment time at different angles-of-attack is shown in Figure 5.6.

To identify coefficients in the polynomial which approximate C_{n_β} as accurately as possible, a 100 sec. long experiment time should be divided as shown in Table 5.2. Many different designs would give the same information matrix for unknown parameters. The design with a minimum number of points where the experiment need be carried out is chosen. Notice that to identify coefficients in an nth-order polynomial, it is necessary to find the value of the polynomial at no less than (n+1) points. Therefore, five is the minimum number of points where the experiment need be carried out.

5.5 SUMMARY

The role of input design for parameter extraction is significant for high angle-of-attack applications. Linear input designs are useful, particularly for local linear flight regimes and for determining flight test schedules that minimize time to obtain estimates with such linear inputs. For highly nonlinear regimes, however, iterative use of the model determination program will aid in specifying required inputs. Analytical design methods for nonlinear regimes can be formulated, but appear to present computational problems which must be resolved by further study.

*This is a modification of a program written by SCI for NASA Edwards Flight Research Center, Edwards, California under Contract NAS 4-2068.

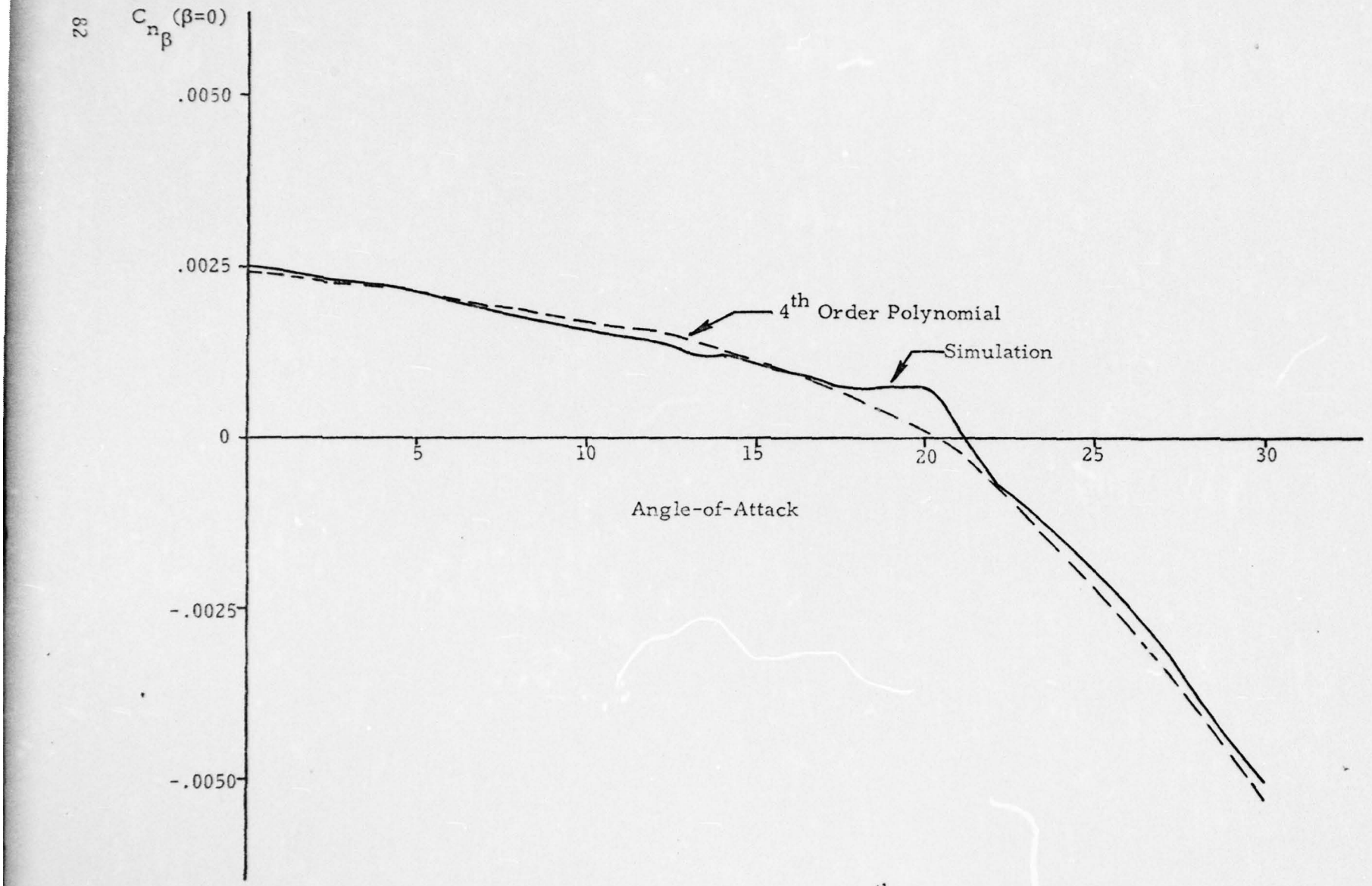

Figure 5.5 C_{n_β} as a Function of α (Simulation and 4th Order Polynomial Fit)

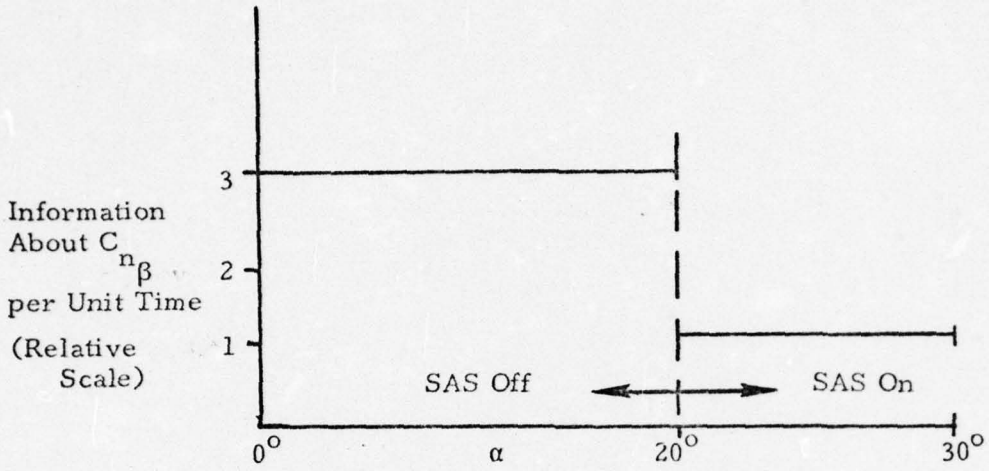

Figure 5.6 Information Function for Local Identification of C_{n_β}

TABLE 5.2

Flight Test Schedule to Identify

$C_{n_\beta}(\alpha)$ $[0^\circ \leq \alpha \leq 30^\circ]$

α	EXPERIMENT DURATION (SEC)
0°	12.5
4.5°	36.1
13°	28.2
20°	15.9
30°	7.3 [SAS on]

VI. IDENTIFICATION IN THE STALL/POST-STALL HIGH ANGLE-OF-ATTACK REGIME

6.1 INTRODUCTION

In this chapter, evaluation of the integrated parameter identification process is carried out using simulated aircraft flight test data. The simulation employed is that of the F-4 aircraft described in ref. [1], Chapter II and Appendix D. State and measurement model equations used in this maximum likelihood procedure are detailed in Appendix E. Nine state equations and eight measurement equations containing thirty-three nonlinear, aerodynamic coefficients compose the identification model. (Each of these coefficients are further expanded as discussed in Chapters III and IV.)

In the identification procedure, the subset regression program is used on the simulated flight test data to identify the model structure and give initial estimates of the selected aerodynamic coefficient polynomial expansion parameters. The maximum likelihood program is then used to refine the parameter estimates obtained from the regression analysis to yield the final parameter estimates and a measure of the confidence associated with those estimates. The detailed flow chart of the entire process is illustrated in Figure 6.1.

In addition to evaluating the identification procedure on a variety of simulated flight test experiments, investigations are also carried out to assess the effects of the following:

a. Different levels of measurement noise
b. Process noise
c. Control input variations
d. Identified parameter set size
e. Data length

The first two items illustrate the robustness of the procedure to corrupting influences. In general, increased noise levels degrade both the final estimates of parameters and the ability of the regression to identify model structure. The last three items show the intrinsic limitations imposed on parameter estimates

INTEGRATED PARAMETER IDENTIFICATION PROCEDURE

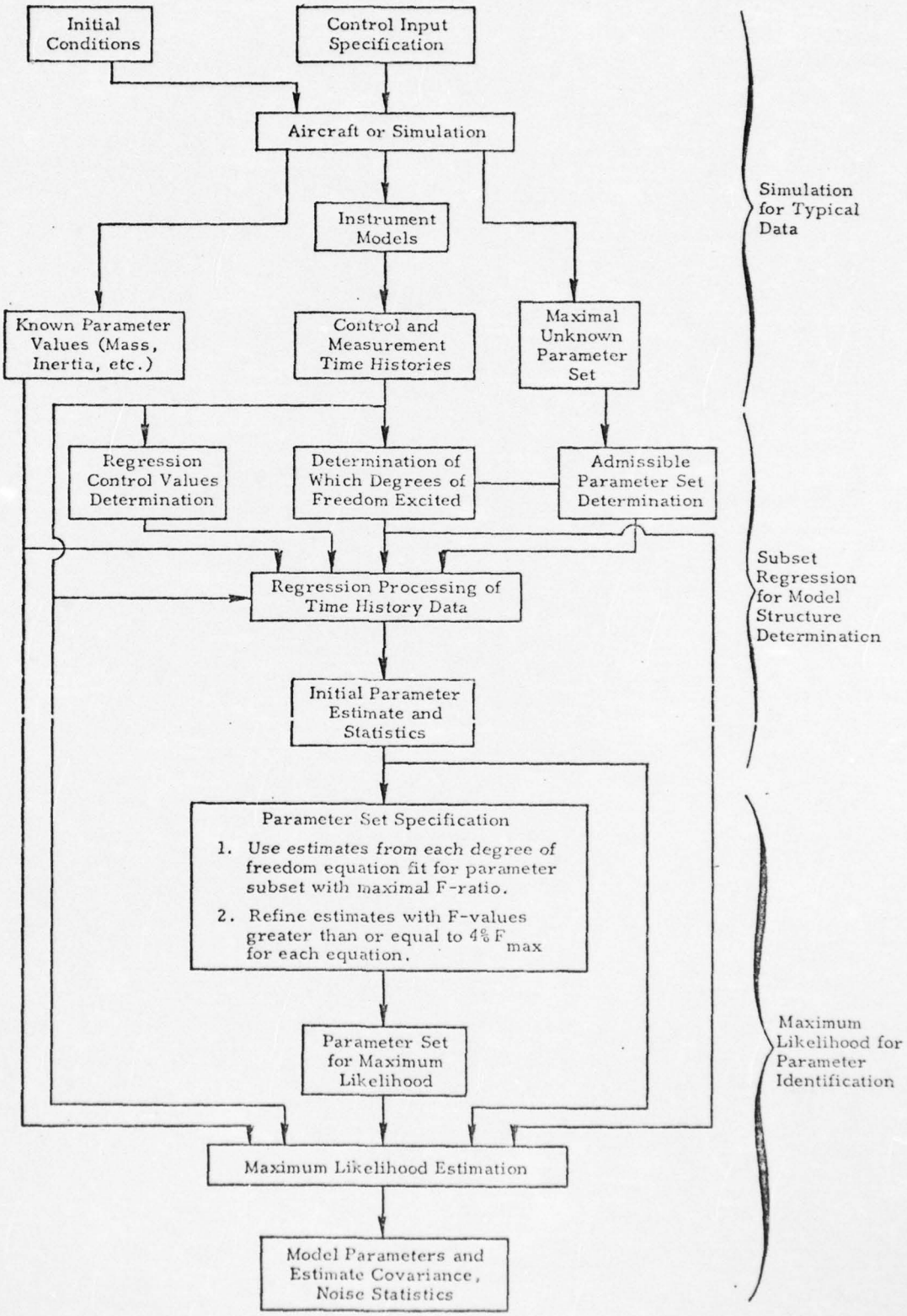

Figure 6.1 Operational Flow Chart of Integrated Parameter Identification Process

by the information content of the data. Increasing the information content by appropriate input design and/or increasing the amount of data in time or numbers of measurements will increase the number of parameters that can be identified with a significant level of confidence.

6.2 EVALUATION OF THE INTEGRATED IDENTIFICATION PROCESS

The objective of the integrated parameter identification procedure is to determine values for unknown or poorly known parameters of a mathematical model of a process by matching data from the real process with the model's predicted results. For the process considered in this work, the parameters are the polynomial expansion terms in α and β of the aerodynamic coefficients in the aircraft rigid body dynamics model. Aircraft dynamic data is obtained by means of a simulation using a much more detailed model.

6.2.1 Selection of Test Conditions

The identifiability of the stall/post-stall regime is the prime objective of the applications conducted for the identification process. This angle-of-attack regime (10° to 25° and beyond) is characterized by multiple nonlinearities in the pitch, roll, and yaw moments and forces. The central objective of this application is that resolution of the identifiability problems for this range is the prime requisite for any high angle-of-attack identification procedure.

The evaluation procedure which has been determined is based on the following considerations:

1. Selection of Inputs: Not all inputs will sufficiently excite the aircraft to induce nonlinear forces and moments. These results were noted in Chapter III. A standard set of inputs is selected for this purpose.

2. Selection of Data Length: In general, the longer the data length, the better will be the identification accuracy of those parameters which can be identified. At high angles-of-attack, however, the amplitude of responses may prohibit extensive time at a particular

AD-A032 800 SYSTEMS CONTROL INC PALO ALTO CALIF F/G 1/1
IDENTIFICATION OF AIRCRAFT STABILITY AND CONTROL COEFFICIENTS F--ETC(U)
MAR 74 W E HALL, N K GUPTA, R G SMITH N00014-72-C-0328
UNCLASSIFIED TR-2 NL

2 OF 3
AD A032800

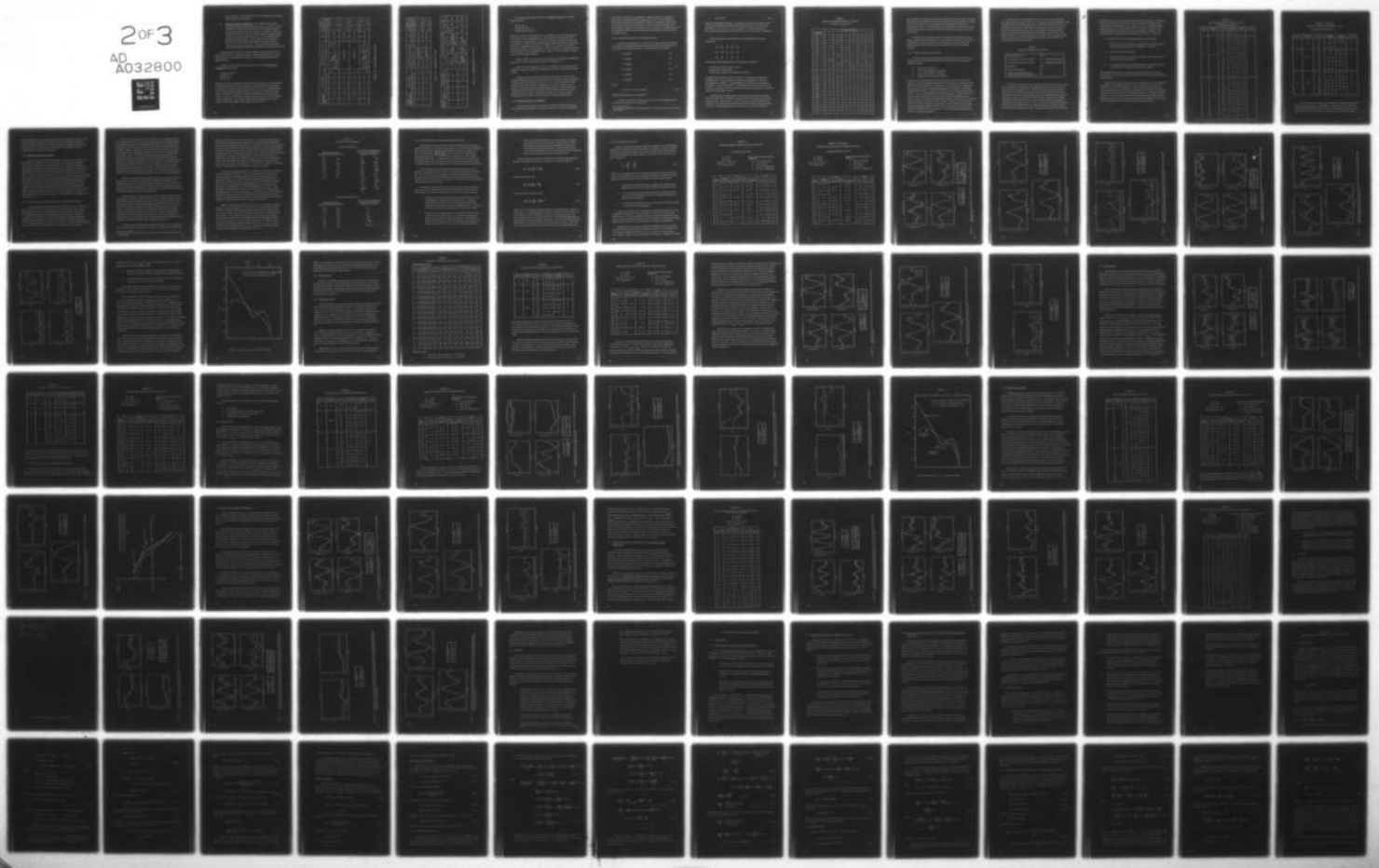

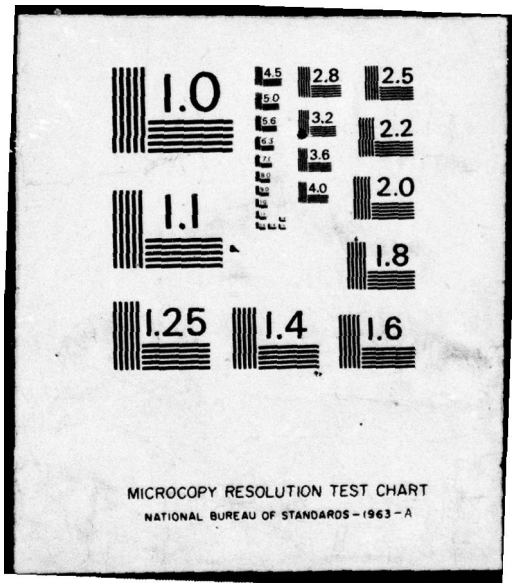
1.0
1.1
1.25
1.4
1.6
1.8
2.0
2.2
2.5
2.8
3.2
3.6
4.0
4.5
5.0
5.6
MICROCOPY RESOLUTION TEST CHART
NATIONAL BUREAU OF STANDARDS - 1963 - A

flight condition. This consideration led to a data length of 10 seconds, with a sample rate of 10/second.

3. Selection of Primary Coefficients: The coefficients which affect aircraft response may be classified as primary or secondary. Primary coefficients are those which most affect aircraft response and which are of greatest interest to the test engineers. Secondary coefficients are those which have, in general, smaller effects on aircraft response, but which, for certain requirements (e.g., SAS or handling quality studies), may be of interest. For the applications discussed here, the static force and moment coefficients are considered primary (e.g., C_x, C_y, C_z, C_m, C_n, C_ℓ). The subset regression program is the essential step in the definition of primary or secondary coefficients.

Tabular summaries of the selected test conditions, inputs and noise levels are given in Figure 6.2. Three basic classes of test condition are given--lateral mode excitation, longitudinal mode excitation, and coupled longitudinal-lateral mode excitation.

In the first class, control inputs are chosen to excite the lateral directional modes of the aircraft:

- Lateral velocity, v
- Roll rate, p
- Yaw rate, r

Applied controls are a half period sine wave pulse in rudder, δ_r, of 10^o amplitude and period duration of 2.5 seconds followed by a full period sine wave doublet in ailerons of 7^o amplitude and period duration of 2.5 seconds. Total data length is 10 seconds real time, sampled every 0.1 seconds to give 100 points for each measured variable. Initial flight conditions are specified in Figure 6.2 under Case 1. Cases 2 and 3 use the same control sequence as Case 1, but with different noise characteristics. Case 4 adds a simultaneously applied stabilator input to force the aircraft through a larger range of angle-of-attack.

LATERAL RESPONSE CASE	DATA LENGTH, SEC	INITIAL CONDITIONS					CONTROL INPUTS (from initial conditions)				NOISE		RESULTS	
													α, deg	β, deg
		α, deg	β, deg	V, ft/sec	θ, deg		δ_r, deg	δ_a, deg	$\Delta\delta_s$, deg	SAS	Meas.	Process	Mean / Std. Dev.	Mean / Std. Dev.
1	10	17.5	0	445	17.5	p = 0 q = 0 r = 0 φ = 0 ψ = 0	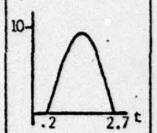	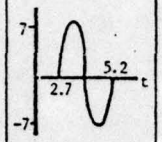	NONE	t < 7.5 off t > 7.5 on	BASE	NONE	18.0 / 1.81	-.607 / 3.90
2	10	17.5	0	445	17.5		SAME AS CASE 1				HIGH	NONE	18.8 / 1.83	-.595 / 3.90
3	10	17.5	0	445	17.5		SAME AS CASE 1				BASE	YES	17.4 / 2.45	-.207 / 3.52
4	10	17.5	0	445	17.5		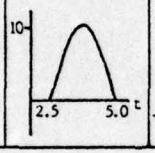	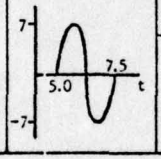		NONE	BASE	NONE	20.6 / 1.5	-.696 / 4.45

Figure 6.2a Lateral Response Test Cases

LONGITUDINAL RESPONSE CASE	DATA LENGTH, SEC	INITIAL CONDITIONS					CONTROL INPUTS (from initial conditions)				NOISE		RESULTS	
		α, deg	β, deg	V, ft/sec	θ, deg		δ_r, deg	δ_a, deg	$\Delta\delta_s$, deg	SAS	Meas.	Process	α, deg (Mean / Std Dev)	β, deg (Mean / Std Dev)
1	10	10	0	550	10	p = 0 q = 0 r = 0 φ = 0 ψ = 0	NONE	NONE	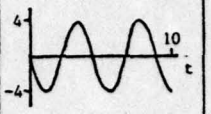	NONE	BASE	NONE	11.55 / 5.85	-.069 / .118
2	10	10	0	550	10		NONE	NONE	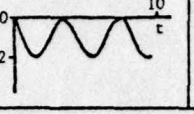	NONE	BASE	NONE	15.8 / 3.19	-.0014 / .0425

Figure 6.2b Longitudinal Test Cases

LONG/LAT RESPONSE CASE	DATA LENGTH, SEC	INITIAL CONDITIONS					CONTROL INPUTS (from initial conditions)				NOISE	
		α, deg	β, deg	V, ft/sec	θ, deg		δ_r, deg	δ_a, deg	$\Delta\delta_s$, deg	SAS	Meas.	Process
1	15	15	0	464	15	p = 0 q = 0 r = 0 φ = 0 ψ = 0	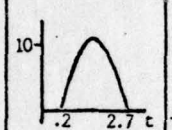	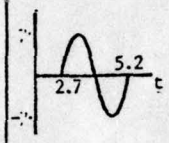	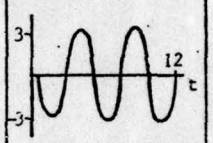	$t \leq 10$ off $t > 10$ on	BASE	NONE
2	10	15	0	464	15		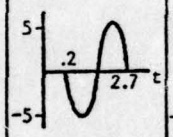	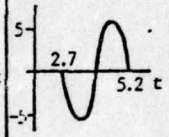	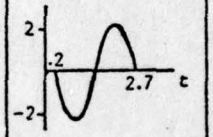	NONE	BASE	NONE

Figure 6.2c Longitudinal/Lateral Test Cases

The second class primarily involves the longitudinal mode with an input chosen to excite:

- Pitch rate, q
- Vertical velocity, w
- Longitudinal velocity, u

Stabilator (elevator) input (Figure 6.2b) is a continuous sine wave superimposed on the initial constant stabilator angle. With a period of 4 seconds, the input is designed to be approximately at the short period mode frequency of the aircraft and, therefore, yield the most possible information about the parameters governing that mode. Amplitude of the input is -4^{o}. Again, the data length is 10 seconds real time and there are 100 sample points. Table 6.2 contains a complete description of this experiment under longitudinal case 1. Case 2 is also a sinusoidal stabilator input, but with smaller amplitude.

Finally, inputs to excite more coupled responses are specified as longitudinal-lateral cases 1 and 2. These inputs are shown in Figure 6.2c.

Lateral case 1 and longitudinal case 1 are "baseline" cases which are evaluated first to establish a reference for comparison with input, noise and data length effects.

These tests are performed in the stall/post-stall regime so that nonlinear α and β expansion terms in some of the aerodynamic coefficients should be required for large enough excursions in α and β. To assure coefficient α and β variation, relatively large control inputs are necessary. An important point is that it is difficult to accurately identify parameters affecting specific aircraft motion and characteristics if the data do not contain enough information about those motions and characteristics. Hence, the nonlinear regimes must be entered (which usually implies large control inputs) in order to identify nonlinear effects.

6.2.2 Application of Subset Regression

Univariate subset regression is used with the simulated data in the parameter identification procedure to develop a reduced set of significant parameters

from the full set allowed for identification. Initial estimates of the significant parameters, although biased due to measurement noise, are also determined. The regression formulates an identification model by assigning estimated values of zero to parameters which have little or no effect in matching the given data. As discussed in Chapter III, subset regression is, therefore, essentially equivalent to a rank deficient least squares equation error identification procedure applied to a single equation.

6.2.2.1 Independent-Dependent Variable Determination

For aircraft identification, the regression program is applied successively to each of the six differential equations described in Chapter III modeling motion in each of the six degrees of freedom. Those equations are of the form:

$$\dot{u} = f_1(\underline{x}, \underline{\theta}) \qquad \text{(a)}$$

$$\dot{v} = f_2(\underline{x}, \underline{\theta}) \qquad \text{(b)}$$

$$\dot{w} = f_3(\underline{x}, \underline{\theta}) \qquad \text{(c)}$$

$$\dot{p} = f_4(\underline{x}, \underline{\theta}) \qquad \text{(d)} \qquad (6.1)$$

$$\dot{q} = f_5(\underline{x}, \underline{\theta}) \qquad \text{(e)}$$

$$\dot{r} = f_6(\underline{x}, \underline{\theta}) \qquad \text{(f)}$$

where

$$\underline{x} = \text{col}\{u, v, w, p, q, r, \varphi, \theta, \psi\} * \qquad (6.2)$$

and the Euler angles given in Appendix E.

In order to calculate the unknown parameters, $\underline{\theta}$, using regression, Eqs. (6.1) and (6.2) must be put into the form

*Note that $\underline{\theta}$ is the vector of unknown parameters, while the scalar θ is the aircraft pitch angle.

$$y_i = \underline{\theta}\,\underline{\xi} + \theta_c \qquad (6.3)$$

where the independent variables y_i are modified versions of $\dot{x}_i$, and $\underline{\xi}$ is a vector of linear and nonlinear dependent variables composed from the state variable, $\underline{x}$, subset u, v, w, p, q, and r. θ_c is an unknown but constant parameter. The transformations to produce the variables in Eq. (6.4) are given in Chapter III.

The measurements available from the simulated flight data are (ref. Appendix D):

$$\alpha_m \quad \varphi_m \quad p_m \quad \dot{p}_m \quad \ddot{x}_m$$

$$\beta_m \quad \theta_m \quad q_m \quad \dot{q}_m \quad \ddot{y}_m$$

$$V_m \quad \psi_m \quad r_m \quad \dot{r}_m \quad \ddot{z}_m$$

These measurements coupled with the assumed known values for

- aircraft mass and moments of inertia,
- engine thrust and moments,
- aerodynamic constants, air density and velocity,

are sufficient to calculate measured values for all independent and dependent variables in Eq. (6.2) according to the equations of Appendix E. There are six independent variables y corresponding to six left hand side variables of the model (c.f. eqs. of Chapter III). The dependent variable list has 30 elements. As Table 6.1 indicates, however, not all 30 variables are admissable for regression against each independent variable.

The dependent variables involving α and β are transformed to variables $(\alpha-\bar{\alpha})$ and $(\beta-\bar{\beta})$, where $\bar{\alpha}$ and $\bar{\beta}$ are average values for the particular experiment being evaluated. This procedure "centers" the data for α and β variations and is helpful in reducing correlations between dependent variables that are functions of α and β. High correlations between dependent variables make it difficult

TABLE 6.1

Regression Independent/Dependent Variables

x = allowed in regression fit

INDEPENDENT VARIABLES	DEPENDENT VARIABLES					
	$\dot{\hat{u}}$	$\dot{\hat{v}}$	$\dot{\hat{w}}$	$\dot{\hat{p}}$	$\dot{\hat{q}}$	$\dot{\hat{r}}$
δ_r		X		X	X	X
$\alpha\delta_r$		X		X	X	X
δ_a		X		X	X	X
$\alpha\delta_a$		X		X	X	X
δ_s	X		X			
$\alpha\delta_s$	X		X			
$\alpha^2\delta_s$					X	
p		X		X	X	X
αp		X		X	X	X
q	X		X			
αq	X		X			
r		X		X	X	X
αr		X		X	X	X
α	X	X	X	X	X	X
β	X	X	X	X	X	X
α^2	X	X	X	X	X	X
β^2	X	X	X	X	X	X
$\alpha\beta$	X	X	X	X	X	X
α^3	X	X	X	X	X	X
β^3	X	X	X	X	X	X
$\alpha^2\beta$	X	X	X	X	X	X
$\alpha\beta^2$	X	X	X	X	X	X
α^4	X	X	X	X	X	X
β^4	X	X	X	X	X	X
$\alpha^2\beta^2$	X	X	X	X	X	X
α^5	X	X	X	X	X	X
β^5	X	X	X	X	X	X
α^6	X	X	X	X	X	X
α^7	X	X	X	X	X	X
α^8	X	X	X	X	X	X
α^9	X	X	X	X	X	X

for the regression to distinguish significant differences between dependent variables. The result is, for variables that are powers of α and/or β, that high power variables may be substituted for low power variables for statistically small differences in significance levels. Such a situation is undesirable since the low power variable is usually preferable for reasons such as the increased error of high power terms due to noise.

The stall/post-stall regime, however, may require such high order terms simply to describe the nonlinearities. It is the tradeoff between the need to account for high order nonlinear contributions, and the desire to use the lowest order terms possible, which constitutes a major problem with any model estimation technique.

6.2.2.2 Evaluation of Regression Results

Univariate subset regression provides several statistical controls for determination of the most significant variables for inclusion in the fit of a particular dependent variable:

a. Error test on overall fit
b. F-value for inclusion of a variable
c. F-value for deletion of a variable
d. Tolerance or correlation of variables

The error test is a measure of fit that varies from 0 for worst to 1.0 for best fit. F-value is a statistic calculated for each variable's correlation coefficients to determine the relative significance and confidence of a coefficient value. Specifically, the F-value is the ratio of a numerical parameter mean divided by the standard deviation of that estimate. A high F-value implies a low coefficient standard deviation and, hence, good confidence in the coefficient estimate. Tables of F-distributions are used to choose a critical F-value for a particular confidence level to include or delete a variable in the fit given the number of data points to be regressed and the number of admissible variables. Finally, tolerance is a measure of the maximal correlation of variables not included in the fit variables or combinations of variables already included in the fit. Tolerance levels vary between 1.0 for perfect correlation to 0 for no correlation. A more detailed explanation of these statistics is given in Appendix B.

For the test conditions described in Section 6.2, the various regression control parameters are given in Table 6.2. The regression procedure adds variables to the fit one at a time in decreasing order of significance until either the F value or tolerance of unincluded variables is below the preset values, or until the fit error test is above another preset value. The purpose is to identify as many significant aerodynamic parameters as possible and not to merely match a time history. Hence, this error test criteria is set very high in order that all variables will be included which meet the 99% coefficient confidence level implicit in the $\bar{F}$ value limit and the tolerance criteria.

TABLE 6.2

Regression Statistical Control Values

Error Test Criteria		0.999	
F-value for inclusion of a variable		3.0	(99% confidence level)
F-value for deletion of a variable		3.0	(99% confidence level)
Tolerance		0.01	
Number of data points		100	
Number of admissible dependent variables	Lateral	26	
	Longitudinal	22	

The desire to determine as many significant variable coefficients as possible must be tempered to some extent in that addition of the last few variables may only contribute marginally to the fit. Statistically these marginal fit improvements may not be significant, and, hence, the variable should not be included. The justification for this is that although the fit to the available data is improved, the number of degrees-of-freedom in the fit relative to the degrees-of-freedom in the data is increased and, therefore, the confidence bands for predictions to match new data could be reduced. The F-ratio for the overall fit (see Appendix B) measures this tradeoff between fit quality and degrees-of-freedom in the fit versus degrees-of-freedom in the data. Therefore, in selecting the best variable

set from the regression for use in the maximum likelihood procedure, the maximal F-ratio value determines which of the sequential fit attempts produced by the regression should ultimately be used. Figures 3.4 and 3.5 of Chapter III show the cutoff criterion for selecting parameters to be identified. In general, all parameters added to the regression up to and including the maximum F-value are identified by the maximum likelihood algorithm (c.f. Figs. 3.4 and 3.5).

In summation, the criteria for using the stepwise regression are:

1. Set F-level limit for variable inclusion/deletion to the 99% confidence level based on available data and admissible variable set.

2. Set tolerance limit at about 0.01.

3. Set error test criteria such that the regression steps terminate only on F-level or tolerance criteria.

4. From among the regression steps performed, use results from that step which has the maximal F-ratio for the overall fit.

The coefficient values for the regression variables obtained according to the above criteria are then used as a priori parameter estimates in the maximum likelihood procedure.

Regression results for lateral case 1 and longitudinal case 1 are summarized in Table 6.3. In the longitudinal case, note the relatively few variables and their low F-values in the $\dot{u}$ equation fit. The low confidence is a result of the low information present in the data interval which is short relative to the phugoid mode time constants. By contrast, in the lateral example, the $\dot{v}$ equation fit also has only a few variables, but the high F-value indicates good confidence in the coefficient values. The conclusion is that the motion in the data is well described by just the few linear terms selected by the regression procedure.

TABLE 6.3

Regression Results for Demonstration Cases

Lateral Response Case 1

EQUATION	OVERALL FIT F-RATIO	PARAMETER	PARAMETER ESTIMATE	PARAMETER F-VALUE	$F \geq 4\% F_{max}$
$\dot{v}$	1320.4	C_{y_β}	-5.06×10^{-1}	1.32×10^{3}	X
		C_{y_o}	3.69×10^{-4}	-----	
$\dot{p}$	2221.8	C_{ℓ_β}	-6.97×10^{-2}	3.24×10^{3}	X
		$C_{\ell_{\delta_a}}$	-3.01×10^{-2}	3.29×10^{2}	X
		$C_{\ell_{r_\alpha}}$	2.45×10^{1}	1.49×10^{2}	X
		C_{ℓ_α}	1.05×10^{-1}	1.27×10^{2}	
		$C_{\ell_{\alpha^2\beta}}$	-1.69×10^{1}	9.54×10^{1}	
		C_{ℓ_r}	4.95×10^{-1}	8.70×10^{1}	
		$C_{\ell_{\alpha^2}}$	1.51	5.56×10^{1}	
		$C_{\ell_{\beta^2}}$	-2.47×10^{-1}	4.14×10^{1}	
		$C_{\ell_{\alpha\beta}}$	2.79×10^{-1}	4.12×10^{1}	
		$C_{\ell_{\beta^4}}$	1.41×10^{1}	3.01×10^{1}	
		$C_{\ell_{\delta_r}}$	3.56×10^{-3}	1.78×10^{1}	
		$C_{\ell_{\alpha\beta^2}}$	-3.28	1.55×10^{1}	
		C_{ℓ_r}	-2.52×10^{-2}	7.14	
		C_{ℓ_o}	2.02×10^{-3}	-----	
$\dot{r}$	721.0	$C_{n_{\delta_r}}$	-4.18×10^{-2}	1.36×10^{3}	X
		C_{n_β}	4.64×10^{-2}	1.56×10^{2}	X
		$C_{n_{\delta_a}}$	1.26×10^{-2}	7.34×10^{1}	X
		$C_{n_{\beta^3}}$	2.47	6.20×10^{1}	X
		$C_{n_{\alpha\beta}}$	-4.80×10^{-1}	5.15×10^{1}	
		$C_{n_{\beta^2}}$	4.19×10^{-1}	5.06×10^{1}	
		$C_{n_{\beta^4}}$	-2.60×10^{1}	4.71×10^{1}	
		$C_{n_{\alpha^2\beta}}$	-2.66×10^{1}	4.67×10^{1}	
		C_{n_α}	-3.31×10^{-2}	4.29×10^{1}	
		$C_{n_{\delta_r}}$	1.35×10^{1}	3.33×10^{1}	
		$C_{n_{\alpha^2\beta^2}}$	-2.82×10^{2}	3.25×10^{1}	
		C_{n_r}	-1.77×10^{-1}	1.43×10^{1}	
		$C_{n_{\alpha\beta^2}}$	2.82	5.95	
		C_{n_o}	-4.04×10^{-4}	-----	

TABLE 6.3 (Continued)

Regression Results for Demonstration Cases

Longitudinal Response Case 1

EQUATION	OVERALL FIT F-RATIO	PARAMETER	PARAMETER ESTIMATE	PARAMETER F-VALUE	$F \geq 4\% F_{max}$
$\dot{u}$	314.5	$C_{x_{\alpha^2}}$	-1.12	5.56×10^{2}	X
		$C_{x_{\delta_s}}$	8.56×10^{-2}	8.60×10^{1}	X
		C_{x_o}	-1.49×10^{-2}	----	
$\dot{z}$	18305.0	C_{z_α}	2.82	1.71×10^{4}	X
		$C_{z_{\alpha^2}}$	4.57	2.75×10^{3}	X
		$C_{z_{q_\alpha}}$	-9.56×10^{1}	4.24×10^{2}	
		$C_{z_{\alpha^3}}$	2.01×10^{1}	4.01×10^{2}	
		$C_{z_{\delta_s}}$	-2.13×10^{-1}	7.44×10^{1}	
		C_{z_o}	-7.60×10^{-1}	----	
$\dot{q}$	1967.4	$C_{m_{\delta_s}}$	-4.53×10^{-1}	8.50×10^{2}	X
		C_{m_q}	-5.52	3.59×10^{2}	X
		$C_{m_{\alpha^6}}$	-8.40×10^{2}	1.58×10^{2}	X
		$C_{m_{\alpha^5}}$	-8.49×10^{1}	1.02×10^{2}	X
		C_{m_α}	-5.06×10^{-2}	5.20×10^{1}	X
		$C_{m_{\alpha^2\beta^2}}$	-1.48×10^{2}	1.87×10^{1}	
		C_{m_o}	-4.42×10^{-1}	----	

The other equation fits contain more variables, including several nonlinear polynomial expansion terms. High confidence coefficient estimates, however, are primarily associated with linear variables, indicating that even for the fairly large α, β excursions (see Figure 6.2) encountered in these examples, linear

effects predominate. It is expected that if the operating range is reduced enough, the aircraft motion should be described quite well by the linearized versions of the aerodynamic coefficients in the model equations. Nonlinear effects should basically be second- and lower-order type effects superimposed on the basic model linearized about the operating point.

6.2.3 Maximum Likelihood Application

Parameter estimation by the maximum likelihood method in the output error formulation (see Chapter IV) is the final step in the identification procedure used. Maximum likelihood estimation provides refined, unbiased estimates of the parameter set defined by the regression results. Actually, the maximum likelihood portion of the procedure could be applied without the regression, provided reasonable a priori estimates of the parameters could be obtained from another source, such as from wind tunnel data. Even if such a priori estimates are available, however, there is a penalty in terms of required computation. Because a priori knowledge of the subset of significant parameters for the data being evaluated is not available, estimates must be attempted for the full parameter set. Since computation to obtain parameter estimates by the maximum likelihood function optimization is more lengthy than for the regression, it is more efficient to develop initial, albeit biased and less confident, estimates and significance ranking by the regressions and then use the results as a starting point for the maximum likelihood procedure.

6.2.3.1 Parameter Set Decomposition for Maximum Likelihood Identification

As discussed above, the computational requirements of maximum likelihood make it very desirable to concentrate as much as possible on estimates of only those parameters which can be estimated well from the available data. Since the computation requirements are roughly proportional to both the number of parameters and the number of model states propagated, estimating parameters which are ill-specified by the data materially increases computation with only, at best, marginal increases in useful results. In fact, as Section 6.4 will illustrate, over-parameterization can actually decrease the quality of all the estimates.

First of all, many parameters can be isolated by examination of the data. If it is apparent that there is only minor excitation and, hence, little information corresponding to a particular identification model state, the state equation for that model and its associated parameters can be removed from the identification procedure. Either a constant or a measured time history of that state can then be substituted in the remaining state equations where there is cross-coupling to the removed state. This technique can be applied in much parameter estimation work involving aircraft where the longitudinal and lateral degrees of freedom can frequently be decoupled for inputs confined to one plane or the other. The two example experiments, lateral case 1 and lateral case 2, illustrate this state equation elimination, where in place of the original nine state equations for the complete identification model, only four equations are required in the longitudinal experiment and five in the lateral. The cross-coupling to eliminated states is satisfied by using measured time histories of the states not propogated.

Isolation of a reduced set of significant parameters by equation elimination can generally be applied before using subset regression on the data. After regressing the data, if the results for a particular equation reveal a low F-ratio for the overall fit (below approximately 100) or if all the included variable coefficients have F-values below 100,* that equation also can reasonably be eliminated in the maximum likelihood optimization procedure.

Further development of the parameter subset for maximum likelihood estimation based on regression estimate F-values is also desirable. Experimentation reveals that both less computation and better estimates result if maximum likelihood is used to refine estimates of only those parameters whose F-value is more than 4% of the maximum parameter F-value for a particular equation. The 4% cutoff corresponds to parameter estimate confidence five times less than those of the "best" parameter estimate (c.f. Table 6.3). Attempts to identify more parameters with the maximum likelihood procedure may over-parameterize the fit to the given data, resulting in poorer overall estimates of the parameters when compared to the estimates obtained with a smaller parameter set.

If the parameters remaining after insignificant modes have been eliminated, the regression subset is decomposed into two parts. The first part is those terms

*An F-value of 100 corresponds to a 95% parameter estimate confidence (2 sigma) of about $\pm 20\%$.

which are "significant" by the various F-tests. The regression estimated values of these terms are defined more precisely by the maximum likelihood algorithm. The second part consists of terms which are "insignificant", but for which numerical values have been estimated. Because these latter estimates do constitute additional information about the system, they are used as fixed values in the maximum likelihood algorithm. Hence, all regression estimates are used for the maximum likelihood identification; one subset as a priori start-up values and the other subset as fixed values. The reason for including the non-zero values of the "insignificant" subset is that these regression estimates, though not perfect, should be closer to the actual value than an estimate of zero. The estimates of "identified" parameters improve if the estimates of "non-identified" parameters are better.

Overall, the intent of emphasizing reduction of the parameter set for maximum likelihood estimation is twofold. First, and most importantly, the problem of over-parameterization and the attendant risk of poorer general quality of all parameter estimates. This difficulty arises largely because with a finite set of noisy data, the addition of more parameters to obtain a better model fit to the data will eventually result in the model attempting to fit the noise process at the expense of knowledge of the actual underlying process of interest. Thus, the attempt to identify large numbers of parameters merely for the sake of the accomplishment may be counter-productive. The second reason is that of efficiency. Diminishing returns result in terms of estimate confidences by increasing the parameter set identified from a fixed data set, but the computation effort required continues to increase at least as fast as the parameter set size.

Table 6.4 presents the parameter sets for the two demonstration examples, lateral case 1 and longitudinal case 2. Included in the sets used for maximum likelihood estimation in addition to the parameters selected by statistical means are the constant terms for each state equation and the bias on sideslip angle, β, measurement. These additional parameters do not have the F-value statistic for significance ranking, but are nevertheless felt to be potentially important enough to be included. In the case of the constant terms, the value is that of the primary aerodynamic coefficient values (C_ℓ, C_m, C_w, C_x, C_y, C_z) at the mean α and β for the experiment data. Thus, the final rule in determining the parameter set should always be the judgment of the user.

TABLE 6.4

Parameter Set Decomposition

Lateral Response Case 1

Parameter Estimates Refined by Maximum Likelihood		Other Non-Zero Regression Parameter Estimates Used in Maximum Likelihood	
C_{y_β}	$C_{n_{\delta_r}}$	C_{ℓ_α}	$C_{n_{\alpha\beta}}$
C_{y_o}	C_{n_β}	$C_{\ell_{\alpha^2\beta}}$	$C_{n_{\beta^2}}$
C_{ℓ_β}	$C_{n_{\delta_a}}$	C_{ℓ_r}	$C_{n_{\beta^4}}$
$C_{\ell_{\delta_a}}$	$C_{n_{\beta^3}}$	$C_{\ell_{\alpha^2}}$	$C_{n_{\alpha^2\beta}}$
$C_{\ell_{r_\alpha}}$	C_{n_o}	$C_{\ell_{\beta^2}}$	C_{n_α}
C_{ℓ_o}	b_β	$C_{\ell_{\alpha_\beta}}$	$C_{n_{\alpha r}}$
		$C_{\ell_{\beta^4}}$	$C_{n_{\alpha^2\beta^2}}$
		$C_{\ell_{\delta_r}}$	C_{n_r}
		$C_{\ell_{\alpha^2\beta^2}}$	$C_{n_{\alpha\beta^2}}$
		C_{ℓ_p}	

Longitudinal Response Case 1

Parameter Estimates Refined by Maximum Likelihood		Other Non-Zero Regression Parameter Estimates Used in Maximum Likelihood
$C_{x_{\alpha^2}}$	$C_{m_{\delta_s}}$	$C_{z_{q\alpha}}$
$C_{x_{\delta_s}}$	C_{m_q}	$C_{z_{\alpha^3}}$
C_{x_o}	$C_{m_{\alpha^6}}$	$C_{z_{\delta_s}}$
C_{z_α}	$C_{m_{\alpha^5}}$	$C_{m_{\alpha^2\beta^2}}$
$C_{z_{\alpha^2}}$	C_{m_α}	$C_{m_{\delta s\alpha^2}}$
C_{z_o}	C_{m_o}	

6.2.3.2 Evaluating Results of Maximum Likelihood Estimation

In addition to the actual parameter estimates obtained using the maximum likelihood procedure, covariances of the estimates are available from the information matrix (see Appendix A) using the sensitivities (of the other variables) in the model to the parameters $\left(\frac{\partial \hat{y}}{\partial \theta}, \frac{\partial x}{\partial \theta}, \frac{\partial c}{\partial \theta}\right)$, covariances as well as time histories can also be propagated for estimates of states, measurements, and nonlinear aerodynamic coefficients. When plotted with actual time histories available from the simulated data, the estimated time histories and associated covariances form an excellent method for evaluating the results of the entire identification procedure.

Plots of only the actual and estimated time histories are useful, but the addition of covariances for the estimates is helpful in examining poor time history fits. Especially in the case of aerodynamic coefficients composed of several parameters, high covariances resulting from low information content in the data should still bracket most of the actual variation in a coefficient, even if the estimated value does not conform very well.

Some latitude must be allowed in the covariance time histories, however, since the available covariances are also only estimates of the actual covariances. The estimated covariances will, in general, be too small for several reasons:

1. Covariances are generated based on the information matrix for only the parameters in the maximum likelihood search. Inclusion of less significant parameters in the information matrix calculation would tend to increase the covariances of all parameters. The amount of the increase depends on significance of the parameters added.

2. Uncertainty in other fixed constants not estimated in the model such as mass, inertias, engine thrusts, and instrument misalignments are not accounted for in the information matrix. Inaccuracies inherent in these estimates as well as uncertainty in the states incorporated as time histories will also increase covariance estimates.

3. Finally, estimated covariances are linearized estimates which presumes all model parameters are at their "actual" values. In fact, the modeling process itself involves simplifications which make it impossible for the model parameters to always equal the "real" values. These modeling errors are manifested both as biased parameter estimates and conservatively small covariance estimates.

For the output error form of the maximum likelihood estimation procedure, linearized covariance estimates for the aerodynamic coefficients, $\underline{\sigma}_c^2$, are,

$$\underline{\sigma}_c^2 = \text{diag} \; \frac{dc}{d\theta} \; \underline{M}^{-1} \; \frac{dc}{d\theta} \tag{6.4}$$

for the state estimates, $\underline{\sigma}_x^2$,

$$\underline{\sigma}_x^2 = \text{diag} \; \frac{dx}{d\theta} \; \underline{M}^{-1} \; \frac{dx}{d\theta} \tag{6.5}$$

and the measurement estimates, $\underline{\sigma}_y^2$,

$$\underline{\sigma}_y^2 = \text{diag} \; \frac{dy}{d\theta} \; \underline{M}^{-1} \; \frac{dy}{d\theta} + R \tag{6.6}$$

In Eq. (6.6), the covariances due to estimates of measurement noise, implicit in the $\underline{R}$ matrix, are incorporated additively to the covariance due to the other parameter estimates. This formulation is a result of assuming the elements of $\underline{R}$ are uncorrelated with other parameter estimates. These simplifying assumptions considerably reduce the computational demands of the maximum likelihood function optimization while leaving unaffected the final parameter estimates. Not making this assumption will result in lower covariance estimates on predicted outputs.

6.2.3.3 Demonstration Examples

Table 6.5 lists a priori maximum likelihood parameter values (obtained from the regression algorithm results), final parameter estimates, parameter F-values, and other optimization results for the two example cases. The F-value presented for maximum likelihood parameter estimates is calculated in the same way as it is for the regression:

$$F_{\theta_i} = \frac{\theta_i^2}{\sigma^2_{\theta_i}} = \frac{\theta_i^2}{M_{ii}^{-1}} \tag{6.7}$$

The F-value associated with the a priori parameter estimate is given for both the regression and zeroth iteration of the maximum likelihood for comparison purposes. Comparison of these tabular results reveals the following important points:

a. Final maximum likelihood F-values are higher than a priori values, indicating improvement in estimate quality over regression results.

b. F-value ordering indicates relative parameter significance remains close to regression, lending confidence to using the regression for parameter set specification.

c. F-values from the regression and a priori maximum likelihood results are of the same order of magnitude.

Figures 6.3 through 6.8 are time history plots of measurements and various aerodynamic coefficients showing actual values and estimated values with $\pm 2\sigma$ confidence limits. The most prominent characteristic of both demonstration cases is the excellent measurement estimate fits to the actual data. Estimate 2σ confidence limits bracket the measurement noise induced variations of the actual data.

Estimate fits to the nonlinear aerodynamic coefficients reveal a range from excellent estimates to fairly significant biased estimates. For the lateral motion case, the major coefficient estimates, C_ℓ, C_n, and C_y are very good; again, with confidence limits bracketing actual data most of the time. Estimates of control

TABLE 6.5

Maximum Likelihood Results for Demonstration Cases

Lateral Response Case 1

$J_o = 15.036$

$J_f = 18.543$

$J_f - J_{f-1}/J_f = 2.125 \times 10^{-7}$

No. of Iterations = 5

Measurement Noise Covariance Estimates:

β	3.38×10^{-3}	radians
$\ddot{y}$	9.40×10^{-3}	g
p	7.05×10^{-3}	radians/sec
r	5.32×10^{-3}	radians/sec

PARA-METER	A PRIORI			FINAL	
	ESTIMATE (FROM REGRESSION)	F-VALUE		ESTIMATE	F-VALUE
		REGRESSION	MAX. LIKELIHOOD		
C_{ℓ_β}	-6.97×10^{-2}	3.24×10^{3}	7.10×10^{3}	-6.73×10^{-2}	6.77×10^{4}
$C_{n_{\delta_r}}$	-4.18×10^{-2}	1.36×10^{3}	3.26×10^{2}	-4.95×10^{-2}	5.61×10^{3}
$C_{\ell_{\delta_a}}$	-3.01×10^{-2}	3.29×10^{2}	3.57×10^{3}	-2.68×10^{-2}	3.12×10^{3}
C_{ℓ_o}	2.02×10^{-3}	----	3.65×10^{2}	1.42×10^{-3}	1.85×10^{3}
$C_{\ell_{r_\alpha}}$	2.45×10^{1}	1.49×10^{2}	2.92×10^{2}	2.25×10^{1}	1.76×10^{3}
C_{y_β}	-5.06×10^{-1}	1.32×10^{3}	1.28×10^{3}	-5.36×10^{-1}	1.54×10^{3}
C_{n_β}	4.64×10^{-2}	1.56×10^{2}	5.67×10^{1}	5.88×10^{-2}	4.04×10^{2}
b_β	0.0	----	0.0	6.89×10^{-3}	1.66×10^{2}
$C_{n_{\delta_a}}$	1.26×10^{-2}	7.34×10^{1}	2.02×10^{1}	6.87×10^{-3}	9.38×10^{1}
C_{n_o}	-4.04×10^{-4}	----	5.67	3.29×10^{-4}	7.65×10^{1}
$C_{n_{\beta^3}}$	2.47	6.20×10^{1}	2.7×10^{1}	1.09	1.55×10^{1}
C_{y_o}	3.69×10^{-4}	----	9.36×10^{-2}	-3.40×10^{-3}	1.16×10^{1}

TABLE 6.5 (Continued)

Maximum Likelihood Results for Demonstration Cases

Longitudinal Response Case 1

$J_o = 14.965$

$J_f = 18.397$

$J_f - J_{f-1} / J_f = 5.476 \times 10^{-7}$

No. of Iterations = 7

Measurement Noise Covariance Estimates:

α	1.94×10^{-3}	radians
$\ddot{x}$	6.05×10^{-3}	g
$\ddot{z}$	1.01×10^{-2}	g
q	1.17×10^{-2}	radians/sec

PARAMETER	A PRIORI			FINAL	
	ESTIMATE (FROM REGRESSION)	F-VALUE		ESTIMATE	F-VALUE
		REGRESSION	MAX. LIKELIHOOD		
C_{z_o}	-7.60×10^{-1}	----	3.10×10^{3}	-7.62×10^{-1}	3.27×10^{5}
C_{z_α}	-2.82	1.71×10^{4}	7.26×10^{2}	-2.86	1.19×10^{5}
$C_{m_{\delta_s}}$	-4.53×10^{-1}	8.50×10^{2}	1.01×10^{3}	-4.64×10^{-1}	1.76×10^{4}
C_{m_o}	-4.42×10^{-2}	----	7.30×10^{2}	-4.04×10^{-2}	9.50×10^{3}
C_{m_q}	5.52	3.59×10^{2}	2.01×10^{2}	-5.79	6.87×10^{3}
$C_{z_{\alpha^2}}$	4.57	2.75×10^{3}	2.53×10^{1}	4.45	2.89×10^{3}
$C_{m_{\alpha^6}}$	-8.40×10^{2}	1.58×10^{2}	2.89	-6.11×10^{2}	8.61×10^{2}
C_{m_α}	-5.06×10^{-2}	5.20×10^{1}	6.45	-7.80×10^{-2}	8.45×10^{2}
$C_{x_{\alpha^2}}$	-1.12	5.56×10^{2}	1.22×10^{2}	-1.12	5.46×10^{2}
$C_{m_{\alpha^5}}$	-8.49×10^{1}	1.02×10^{2}	1.62	-6.73×10^{1}	3.99×10^{2}
C_{x_o}	-1.49×10^{-2}	----	4.23×10^{1}	-1.43×10^{-2}	1.42×10^{2}
$C_{x_{\delta_s}}$	8.56×10^{-2}	8.60×10^{1}	1.69×10^{1}	8.86×10^{-2}	9.00×10^{1}

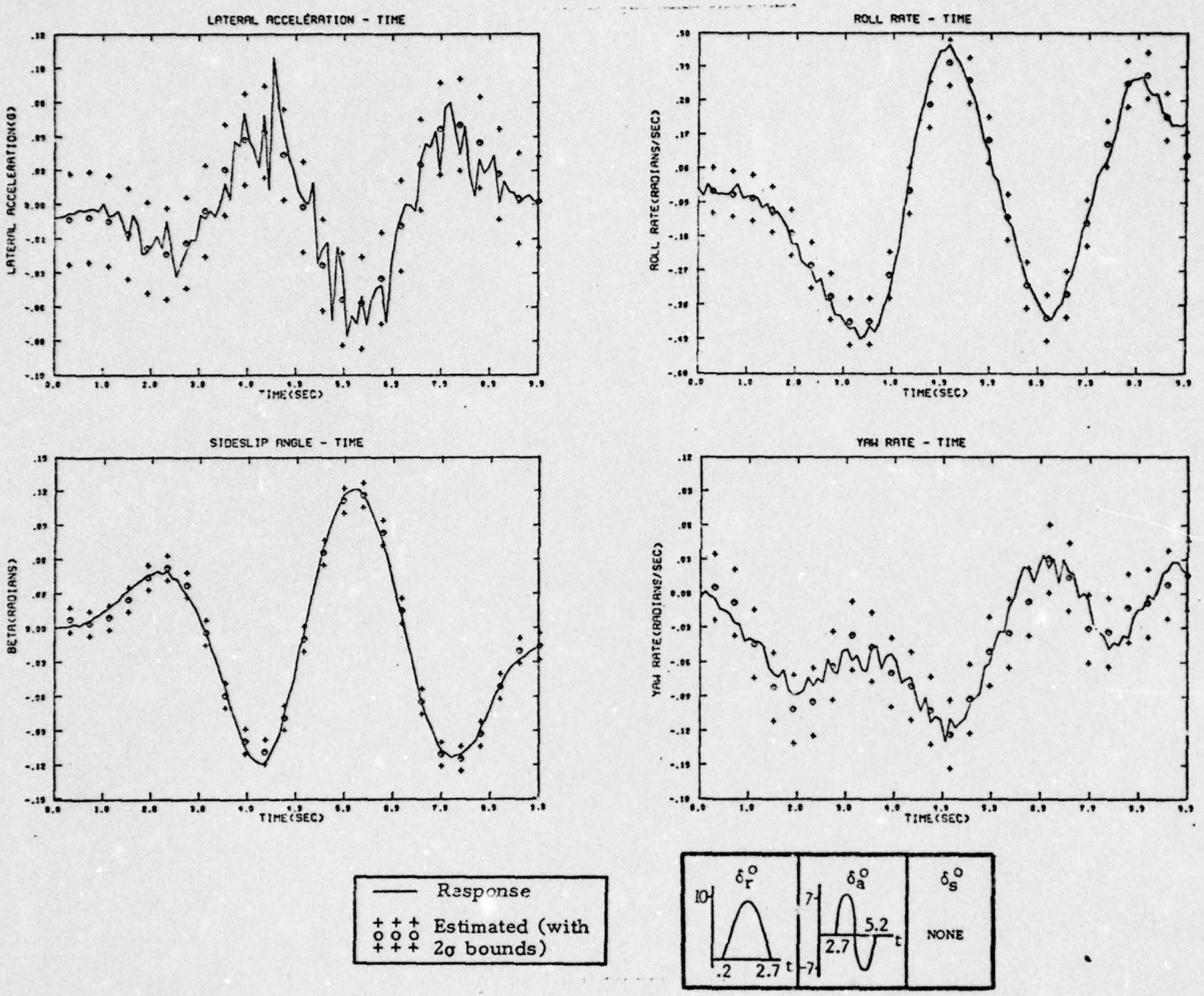

Figure 6.3 Lateral Measured and Estimated Response to Combined Aileron/Rudder Input (Lateral Case 1, Ref. Fig. 6.2a).

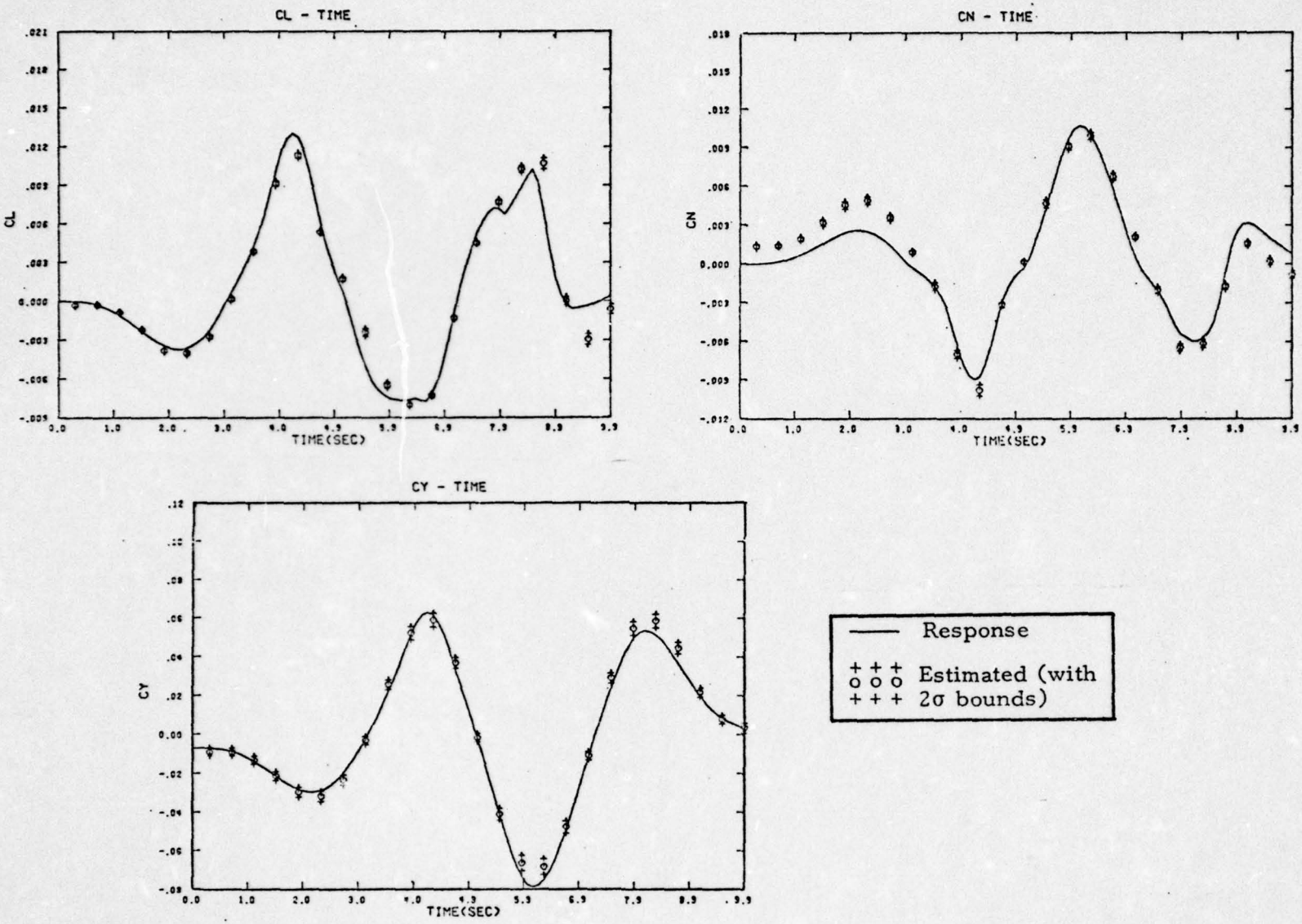

Figure 6.4 Lateral Static Coefficient Response (Simulated or Estimated) to Combined Aileron/Rudder Input (Lateral Response Case 1, Ref. Fig. 6.2a).

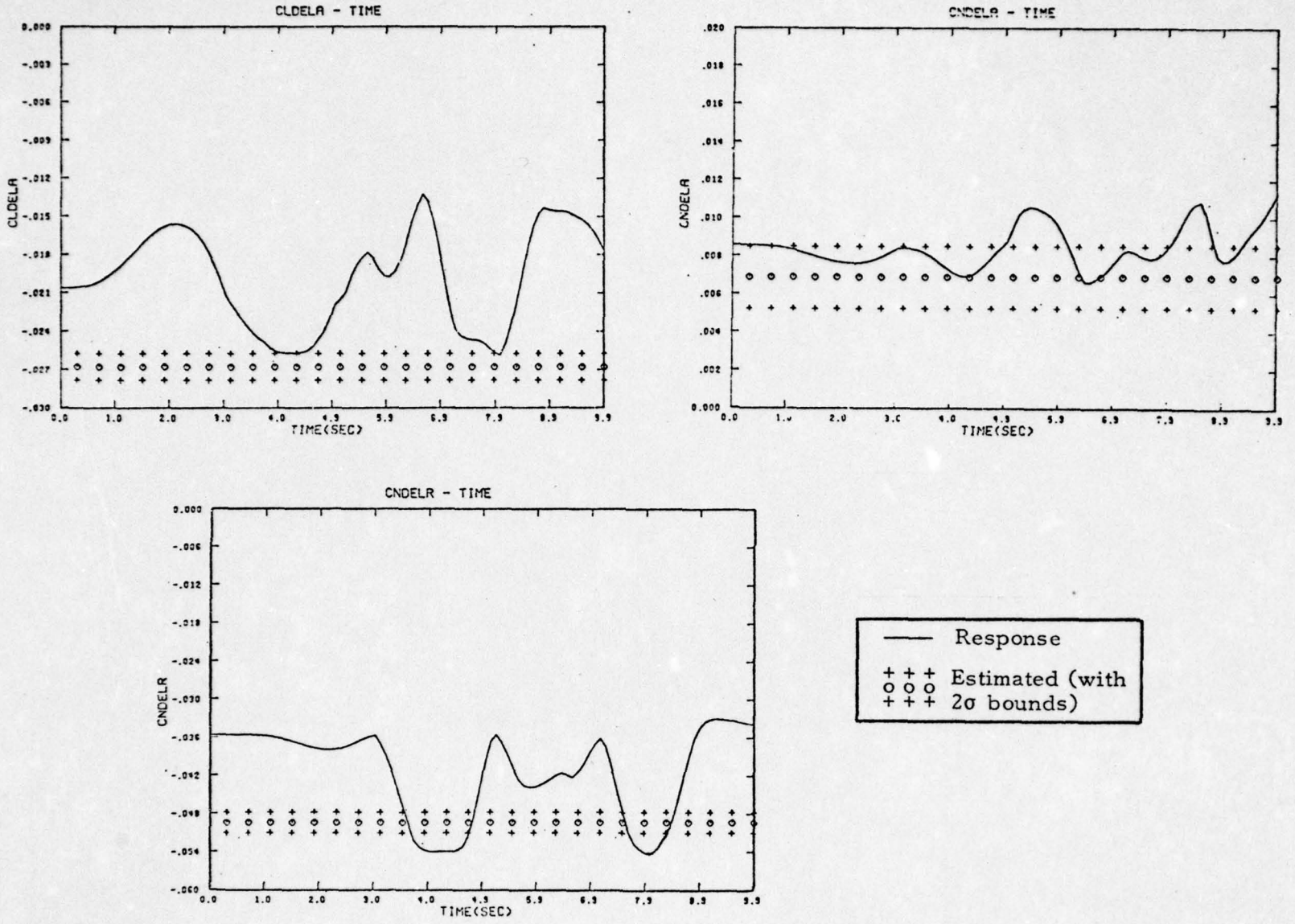

Figure 6.5 Lateral Control Effectiveness Coefficient Response (Simulated or Estimated) to Combined Aileron/Rudder Input (Lateral Response Case 1, Ref. Fig. 6.2a).

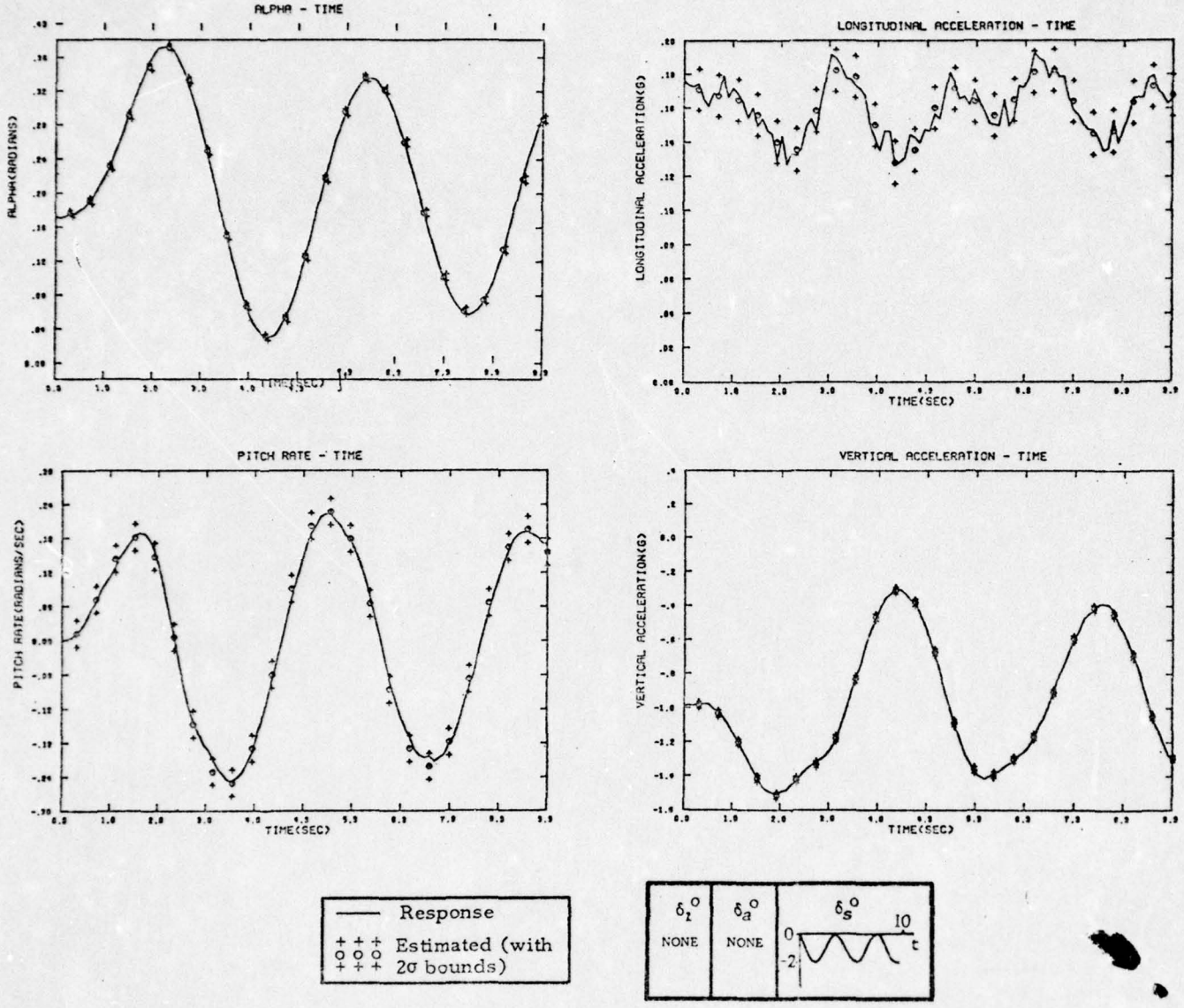

Figure 6.6 Longitudinal Measurement Response (Simulated and Estimated) to Sinusoidal Stabilator Input (Longitudinal Case 1, Ref. Fig. 6.2c).

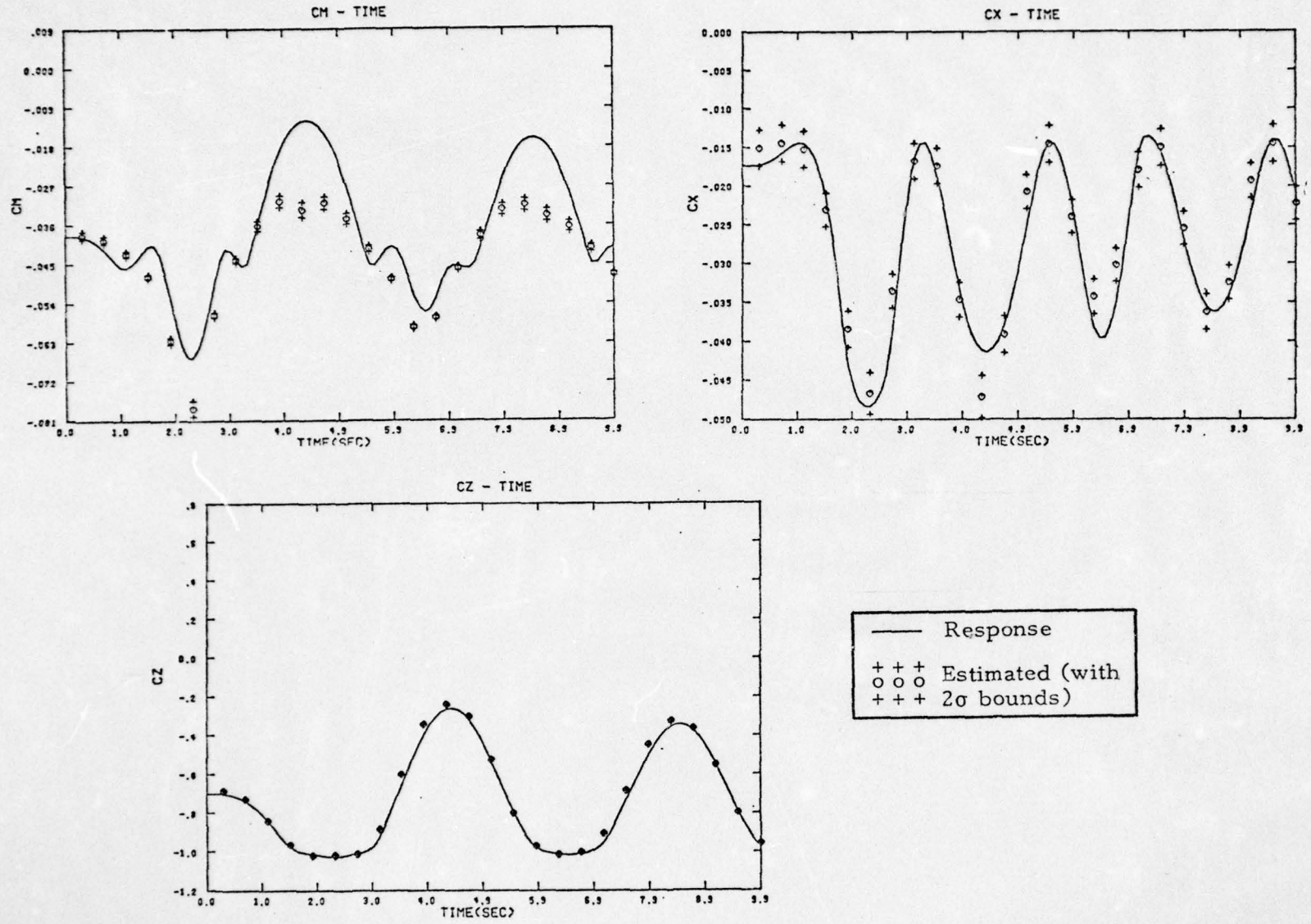

Figure 6.7 Longitudinal Static Coefficient Response (Simulated and Estimated) to Sinusoidal Stabilator Input (Longitudinal Case 1, Ref. Fig. 6.2c).

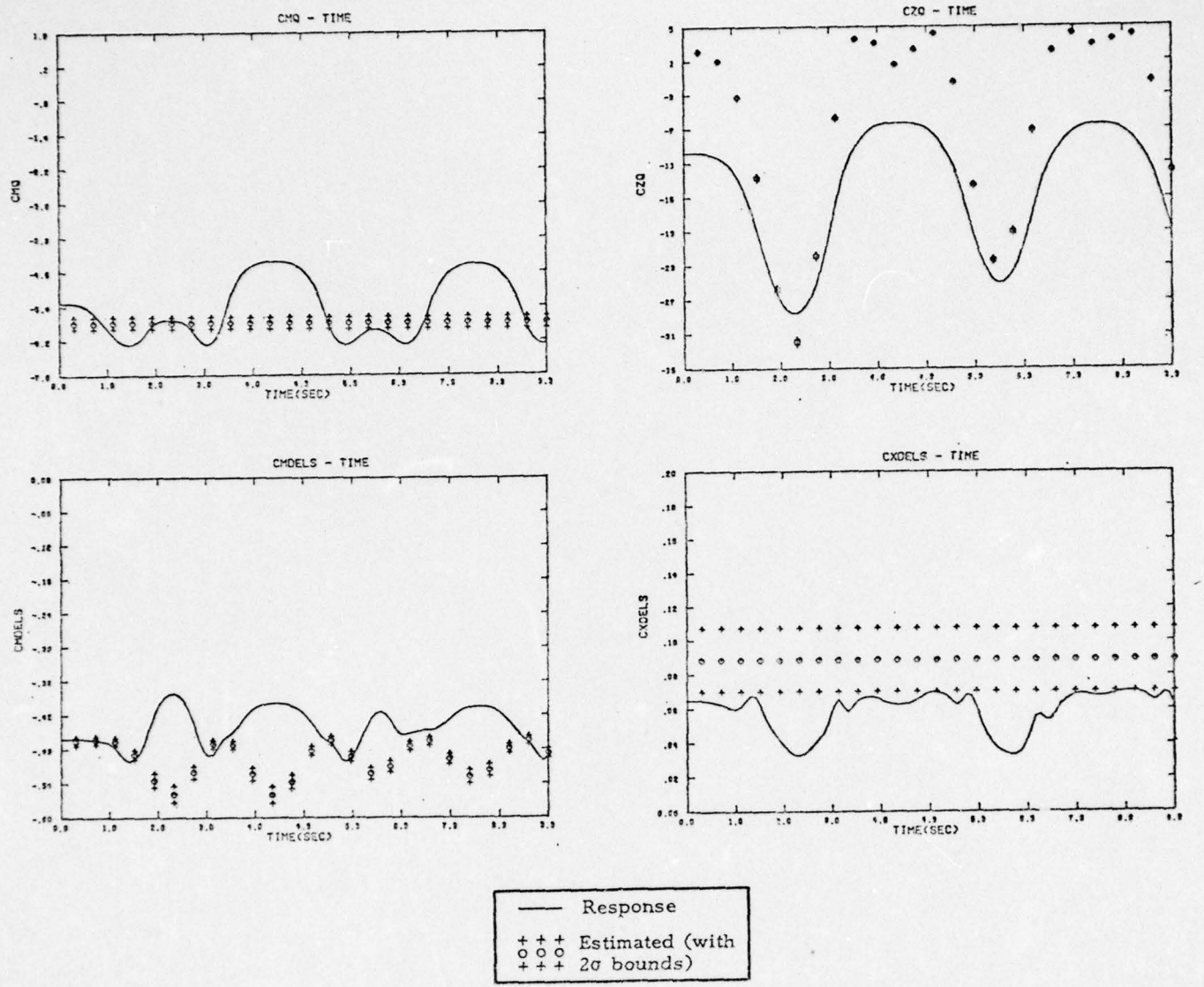

Figure 6.8 Longitudinal Dynamic and Control Effectiveness Coefficient Response (Simulated and Estimated) to a Sinusoidal Stabilator Input (Longitudinal Case 1, Ref. Fig. 6.2c).

derivatives such as $C_{n_{\delta r}}$, $C_{n_{\delta a}}$ and $C_{\ell_{\delta a}}$ tend to be biased, however. The two prime reasons for the biased estimates are:

a. Modeling errors due to higher order variation of actual coefficients with α and β than allowed for in coefficient model polynomial expansion.

b. A small amount of information about control derivatives is available as a result of the short time of control application.

In the longitudinal case, very good estimates of C_X and C_Z are produced, but C_m is in error, especially at the extremes of its variation. Also, the biases in the other coefficients are again evident.

The reason for the degraded estimates of both C_m and $C_{m_{\delta s}}$ is primarily due to lack of information about the highly nonlinear portion of the C_m vs. α curve over which the experiment is centered (see Fig. (6.9)). Information about C_m is small with the high level sinusoidal variation of stabilator force throughout the experiment. The errors in the C_m estimates, in turn, detract from the $C_{m_{\delta s}}$ estimate since an incorrect estimate of C_m will be compensated for by an altered $C_{m_{\delta s}}$ estimate so that measurement time histories will still match. This situation requires data with better information to improve estimates of, and thereby distinguish between, the two coefficients, as is shown in Section 6.4. Input design is thus seen to be extremely important in generating the maximum information for estimating all important parameters simultaneously, since parameter estimate interdependence results in the poor estimate of one parameter causing poor estimates for other parameters.

The basic features and implementation of the overall parameter estimation procedure are demonstrated. Excellent reproduction of measurement time histories are achievable; and within the limitations of discussed of modeling and available information in the data, linear and nonlinear aerodynamic coefficients can be identified extremely well. In the following sections, further exploration of the capabilities of the identification procedure are demonstrated. Included are the effects of measurement noise levels, process noise, input variation, and data length.

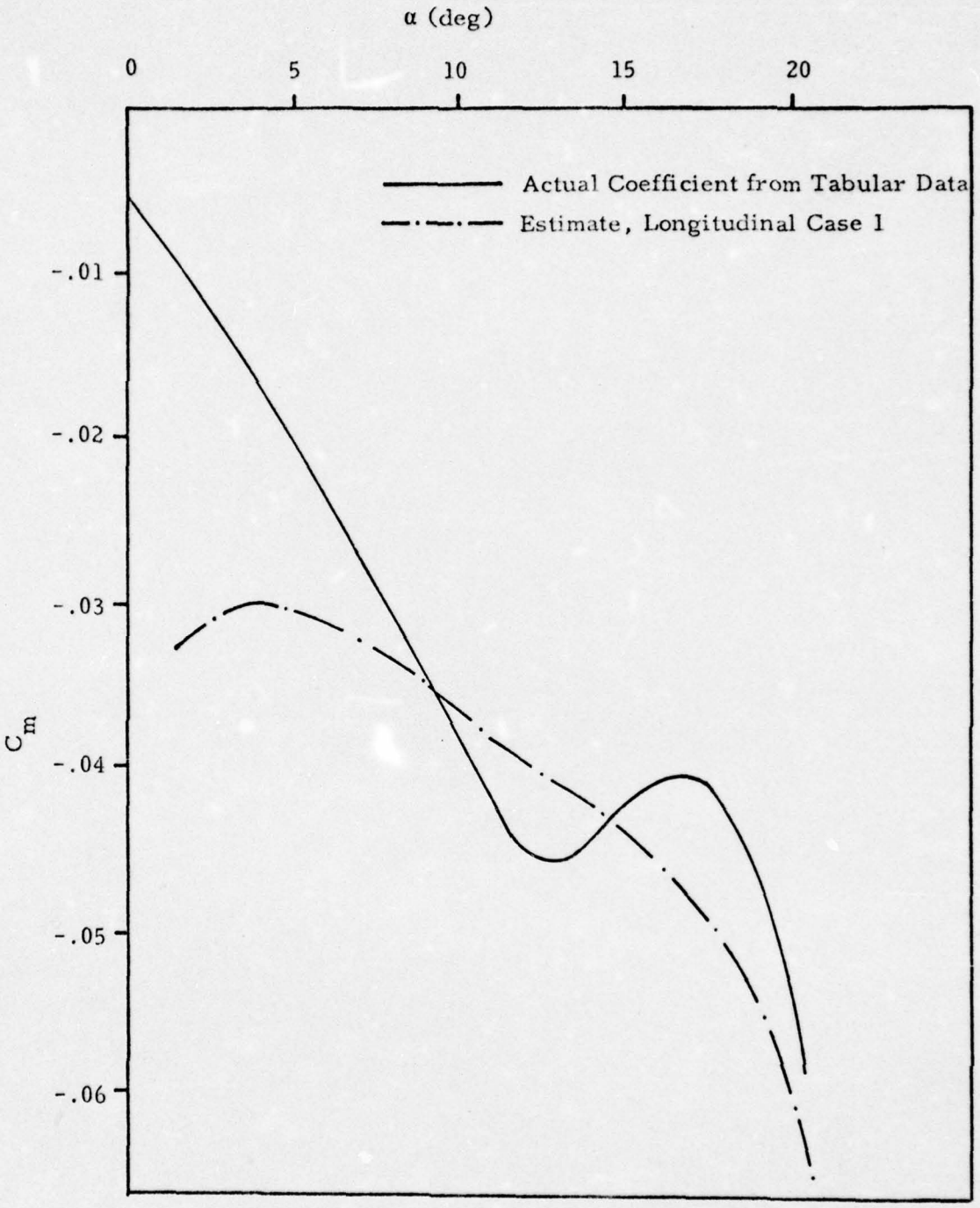

Figure 6.9 Estimate of C_m vs. α for Different Inputs

Finally, a comprehensive, full six degrees-of-freedom, 31 parameters, 15 second data length case is presented. In the truest test of an estimation procedure, the estimated parameters from this final case are used to successfully predict time histories for entirely different control inputs.

6.3 NOISE EFFECTS

In general, the effect of increased noise, whether process or measurement, on parameter estimation is to decrease confidence in the estimates. This section describes experiments to illustrate the impact of noise on the integrated parameter identification procedure. Results show that even for quite high levels of measurement and process noise, the identification procedure is still viable and yields reliable parameter estimates.

6.3.1 Measurement Noise

The base demonstration cases of Section 6.1 employ simulated data in which there is instrumentation measurement noise present. A median level for those noises is used based on information in ref. [1]. Comparison response data, exactly the same as the lateral motion response case 1 except for higher measurement noise levels, is generated by simulation in order to assess the effect of measurement noise. The experiment, lateral response case 2, is described in Figure 6.2, and values are given in Table 6.6 for both base and high measurement noise parameters from the instrumentation simulation equations of Appendix D.

Table 6.7 compares regression results for the high measurement noise case to those obtained previously for base measurement noise. As expected, there is a substantial decrease in included parameters due to the higher coefficient covariances (lower F-values) that result from the increased noise. For what otherwise is the same data, the addition of more measurement noise reduces the amount of useful information for identifying parameters.

Significantly, however, the parameters that the regression does identify in the high measurment noise case are exactly the same as the most important

TABLE 6.6

Measurement and Process Noise Statistics

•MEASUREMENT NOISE

MEASUREMENT	BASE NOISE LEVEL VALUE			HIGH NOISE LEVEL VALUE								
	INSTRUMENT ERRORS, 1σ			ALIGNMENT ERRORS, 1σ						ALIGNMENT ERRORS, MEAN		
	SCALE	BIAS	NOISE	x, ft	y, ft	z, ft	φ, deg	θ, deg	ψ, deg	x, ft	y, ft	z, ft
a	.02 / .02	.05° / .2°	.05° / .2°	.5 / 1.0	.5 / 1.0	.5 / 1.0				34. / 34.	.5 / .5	.2 / .2
β	.02 / .02	.05° / .05°	.05° / .05°	.5 / 1.0	.5 / 1.0	.5 / 1.0				34. / 34.	.5 / .5	.2 / .2
V	.01 / .01	5.0 f/s² / 6.25	5.0 f/s² / 6.25									
ẍ	.005 / .005	.005 f/s² / .005	.005 f/s² / .005	.5 / 1.0	.5 / 1.0	.5 / 1.0		.6° / .9°	.6° / .9°			
ÿ	.005 / .005	.0005f/s² / .001	.0005 f/s² / .001	.5 / 1.0	.5 / 1.0	.5 / 1.0	.6° / .9°		.6° / .9°			
z̈	.005 / .005	.005 f/s² / .025	.005 f/s² / .025	.5 / 1.0	.5 / 1.0	.5 / 1.0	.6° / .9°	.6° / .9°				
ṗ	.005 / .005	.1°/s² / .3°	.1°/s² / .3°					.6° / .9°	.6° / .9°			
p	.005 / .005	.1°/s² / .75°	.1°/s² / .75°					.6° / .9°	.6° / .9°			
q̇	.005 / .005	.1°/s² / .3°	.1°/s² / .3°				.6° / .9°		.6° / .9°			
q	.005 / .005	.1°/s / .3°	.1°/s / .3°				.6° / .9°		.6° / .9°			
ṙ	.005 / .005	.1°/s² / .3°	.1°/s² / .3°				.6° / .9°	.6° / .9°				
r	.005 / .005	.1°/s / .3°	.1°/s / .3°				.6° / .9°	.6° / .9°				
φ	.005 / .005	.5° / .9°	.5° / .9°									
θ	.005 / .005	.15° / .45°	.15° / .45°									
ψ	.005 / .005	.15° / .45°	.15° / .45°									

•PROCESS NOISE

u - zero mean, white, Gaussian σ_u = 21.2 ft/sec

v - zero mean, white, Gaussian σ_v = 21.2 ft/sec

TABLE 6.7

Regression Results for High Measurement Noise Case

EQUATION	OVERALL FIT F-RATIO	PARAMETER	PARAMETER ESTIMATE	PARAMETER F-VALUE	$F \geq 4\% F_{max}$
$\dot{v}$	445.9	C_{y_β}	-4.83×10^{-1}	4.46×10^{2}	X
		C_{y_o}	1.20×10^{-3}	----	
$\dot{p}$	962.7	C_{ℓ_β}	-8.11×10^{-2}	2.32×10^{3}	X
		$C_{\ell_{\delta_a}}$	-3.16×10^{-2}	1.89×10^{2}	X
		$C_{\ell_{\alpha^5}}$	-1.11×10^{3}	5.48×10^{1}	
		C_{ℓ_o}	9.41×10^{-4}	----	
$\dot{r}$	473.9	$C_{n_{\delta_r}}$	-4.11×10^{-2}	3.97×10^{2}	X
		C_{n_β}	4.07×10^{-2}	8.10×10^{1}	X
		$C_{n_{\delta_a}}$	1.77×10^{-2}	5.66×10^{1}	X
		$C_{n_{\beta^3}}$	2.14	2.84×10^{1}	X
		C_{n_o}	1.40×10^{-3}	----	

parameters isolated by the regression for the base measurement noise case. This, despite the fact that there is measurement noise in this formulation of the regression, tends to bias parameter estimates. The example thus reinforces confidence in the regression's primary purpose of isolating the most important parameters from the full admissible set, even in the presence of severe instrumentation errors.

Maximum likelihood refined parameter estimates for the high measurement noise case are given in Table 6.8. Note that the final F-values are approximately an order of magnitude below those for the bias measurement noise case. Also, the final F-value ordering is considerably changed from the a priori ordering, indicating severe estimate biases from the regression.

TABLE 6.8

Maximum Likelihood Results for High Measurement Noise Case

$J_o = 11.693$

$J_f = 15.016$

$J_f - J_{f-1} / J_f = 4.729 \times 10^{-7}$

No. of Iterations = 7

Measurement Noise Covariance Estimates:

β	5.24×10^{-3}	radians
$\ddot{y}$	1.45×10^{-2}	g
p	3.64×10^{-2}	radians/sec
r	1.47×10^{-2}	radians/sec

PARAMETER	A PRIORI			FINAL		
	ESTIMATE	F-VALUE		ESTIMATE	F-VALUE	2σ CONFIDENCE
		REGRESSION	MAX. LIKELIHOOD			
C_{ℓ_β}	-8.11×10^{-2}	2.32×10^{3}	9.01×10^{3}	-7.98×10^{-2}	8.03×10^{3}	$\pm.18 \times 10^{-2}$
C_{n_o}	1.40×10^{-3}	----	1.53×10^{1}	1.97×10^{-3}	2.55×10^{3}	$\pm.08 \times 10^{-3}$
$C_{n_{\delta_r}}$	-4.11×10^{-2}	3.97×10^{2}	1.10×10^{2}	-6.93×10^{-2}	2.39×10^{3}	$\pm.28 \times 10^{-2}$
C_{n_β}	4.07×10^{-2}	8.10×10^{1}	2.53	1.67×10^{-1}	7.11×10^{2}	$\pm.13 \times 10^{-1}$
C_{y_β}	-4.83×10^{-1}	4.46×10^{2}	2.51×10^{2}	-5.07×10^{-1}	5.43×10^{2}	$\pm.44 \times 10^{-1}$
$C_{n_{\beta^3}}$	2.14	2.84×10^{1}	5.47×10^{-1}	-1.05×10^{1}	2.58×10^{2}	$\pm.13 \times 10^{1}$
$C_{\ell_{\delta_a}}$	-3.16×10^{-2}	1.89×10^{2}	6.07×10^{1}	-2.18×10^{-2}	2.03×10^{2}	$\pm.31 \times 10^{-2}$
b_β	0.0	----	0.0	8.53×10^{-3}	6.60×10^{1}	$\pm2.1 \times 10^{-3}$
C_{ℓ_o}	-9.41×10^{-4}	----	4.16	1.69×10^{-4}	6.10	$\pm1.4 \times 10^{-4}$
$C_{h_{\delta_a}}$	1.77×10^{-2}	5.66×10^{1}	1.03×10^{1}	6.11×10^{-3}	5.45	$\pm5.3 \times 10^{-3}$
C_{y_o}	-1.20×10^{-3}	----	2.22×10^{-1}	-2.56×10^{-3}	2.59	$\pm3.2 \times 10^{-3}$

Comparison of the parameter estimates from bias and high measurement noise cases on a one-for-one basis does not indicate very close correspondence in most cases. Only C_{y_β}, b_β, $C_{n_{\delta a}}$, and C_y for the high measurement noise case have estimates within 2σ of the base measurement noise estimates. However, because the two parameter sets are not completely analogous, it is only legitimate

to compare the net nonlinear aerodynamic coefficients composed of several parameters since nearly similar fits can be obtained with different parameter sets. Figures 6.10 through 6.12 are the time history comparisons for the high measurement noise case, including the aerodynamic coefficient traces. Of all the coefficient estimate time histories, only that of C_n is seriously different from the actual time history. Thus, despite the large variations in specific parameter estimates between high and base measurement noise cases, the variation estimates of the total coefficients are not comparatively in error. In fact, the primary difference is the expected increase in covariances for the high noise case.

Time histories for measurement estimates again exhibit excellent fit to the actual data. These consistently good fits of estimated and actual measurements are indicative of the basic principle that for a sufficiently generalized model (such as the one used here) and enough independent parameters (degrees-of-freedom) almost any measurement data can be matched very closely. The difficulty is that too close a measurement match will result in decreased relevence of the parameter values to the characteristic they are supposed to model. This can be seen in the yaw rate time history and the C_n coefficient. Close inspection of the yaw rate estimate reveals tracking of the actual yaw rate value to the point of following some of the noise variations. This effect has been discussed in Section 3.3.2 where it is noted that one effect of choosing more parameters than actually required is to allow the estimates to "track the noise". For this data, with the high noise present masking to a large extent higher order variations in C_n, the attempt to estimate both $C_{n_{\beta^3}}$ and C_{n_β} is probably over-parameterization.

The parameter set specification described in Section 6.1.2 eliminates a great deal of the risk of over-parameterization. In some cases, the regression technique will tend to select higher order polynomial terms when lower order terms would be satisfactory, especially when high noise levels are present. The regression technique has an option for forcing in lower order terms which is used in such cases. Such "forcing in" does not necessarily require that the terms be included, only that they not be deleted unless found highly insignificant relative to other terms.

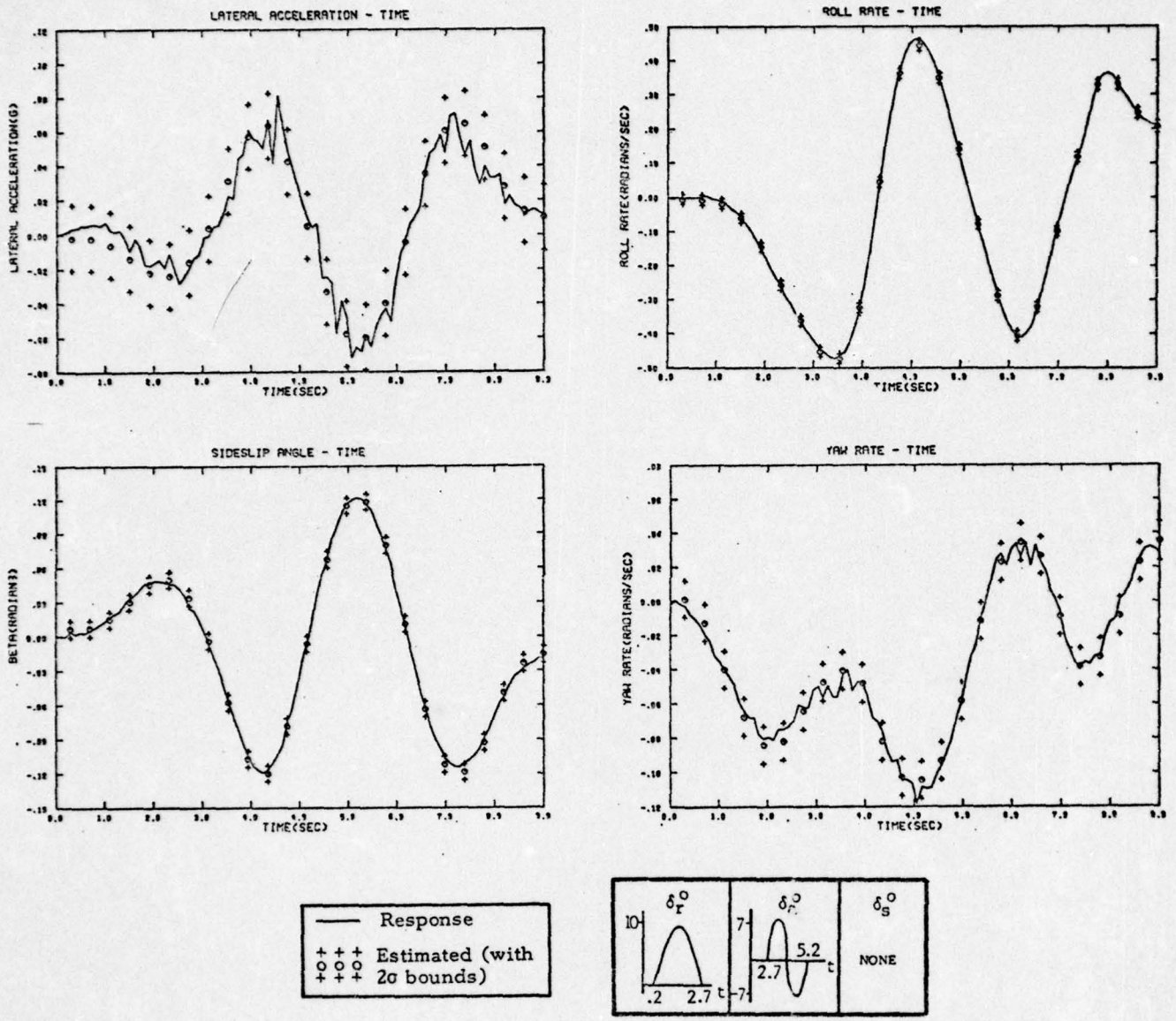

Figure 6.10 Lateral Measured and Estimated Response with Increased Instrument Noise (Lateral Case 2, Ref. Fig. 6.2a).

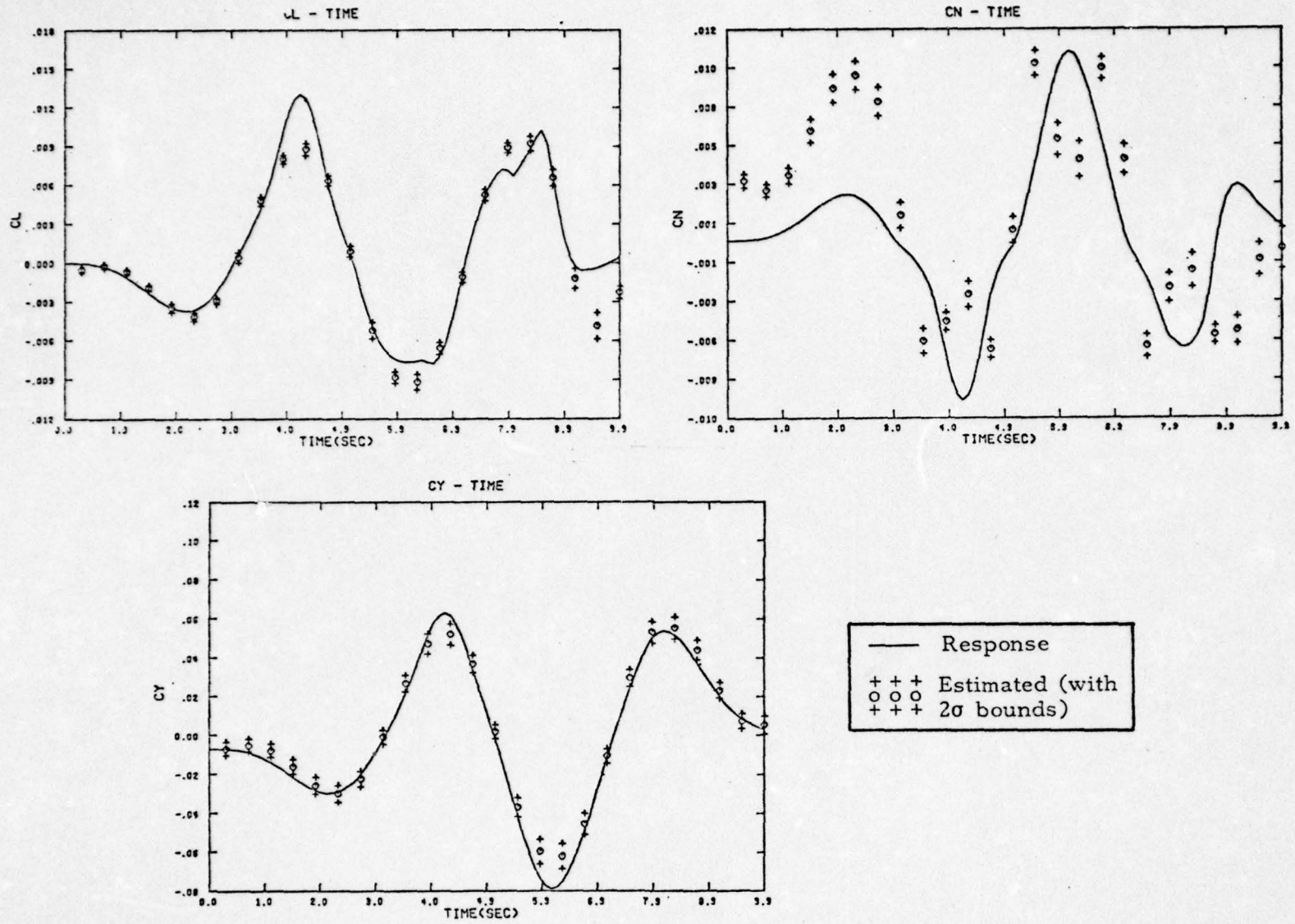

Figure 6.11 Lateral Static Coefficient Response (Simulated and Estimated) for Measurements with Increased Instrument Noise (Lateral Case 2, Ref. Fig. 6.2a).

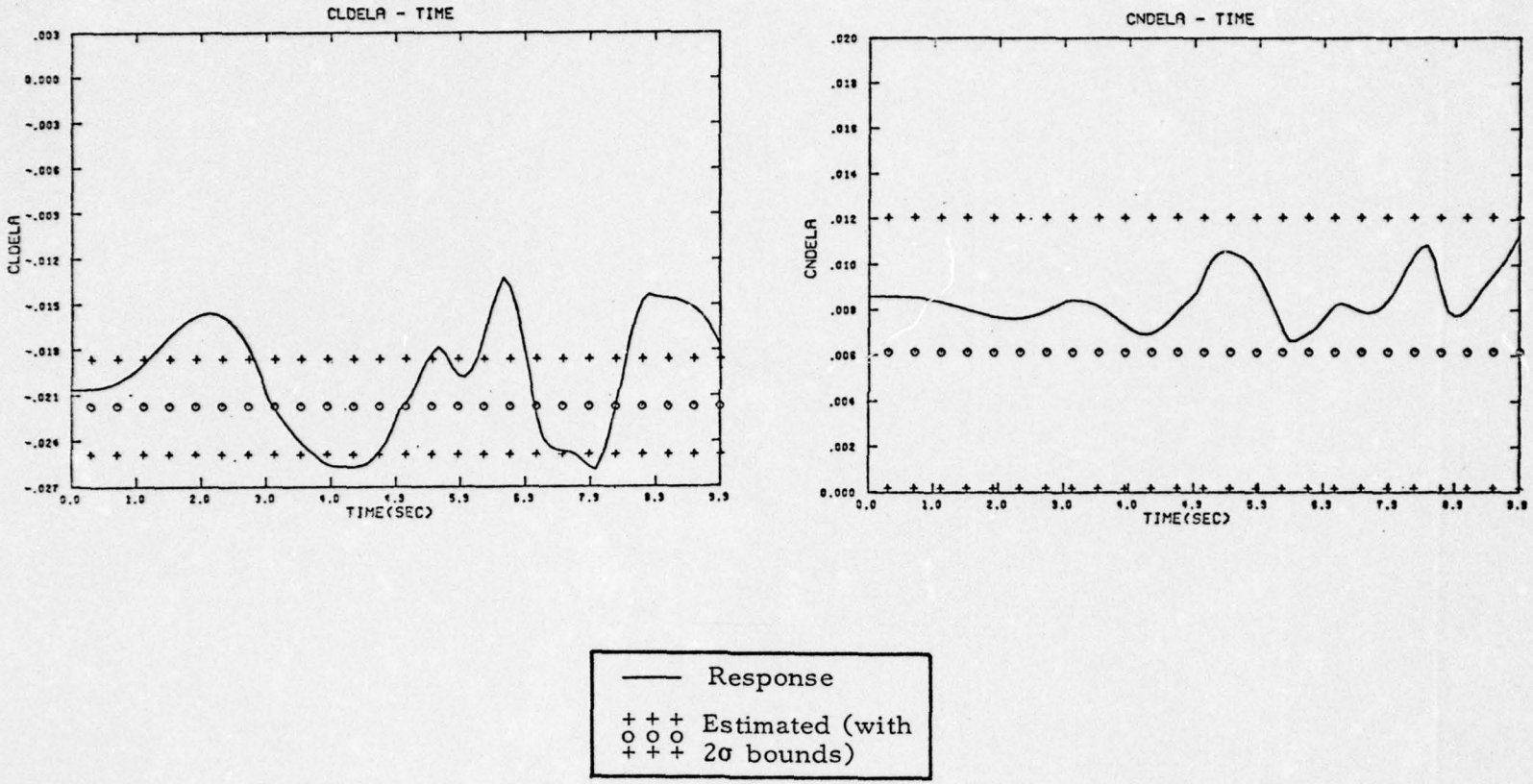

Figure 6.12 Lateral Control Effectiveness Coefficient Response (Simulated and Estimated) for Measurements with Increased Instrument Noise (Lateral Case 2, Ref. Fig. 6.2a).

6.3.2 Process Noise

The formulation of the maximum likelihood estimation procedure used is the output error form which does not identify the process noise in the experiment data. The chief advantage of this formulation is a large reduction in the computations needed to carry out the nonlinear estimation process. Unless gusts are specifically to be estimated, such computational increases may not be necessary. In addition, properties of the regression program reduce the effect of such noise on the estimate.

Even when no process noise is assumed, some process noise type effects always exist as a result of modeling errors. In order to evaluate the identification procedure's robustness to a more significant level of process noise, an experiment is simulated in which moderate levels of white wind gust turbulence are added to vertical and horizontal aircraft velocities for the lateral mode demonstration case (base measurement noise is also present). Figures 6.13 through 6.14 show the measurement and coefficient time histories. Table 6.8 gives the process noise parameter values, and the experiment is described under lateral response case 3 in Figure 6.2.

Regression results are given in Table 6.9 and maximum likelihood estimates in Table 6.10. C_y, C_{ℓ_β}, $C_{n_{\delta r}}$, and C_{n_β} are once again isolated by the regression as the most significant parameters for the three equation fits (as in the base and high measurement noise cases). Beyond those four, only $C_{n_\beta}{}^3$ corresponds with significant sets for those other cases. That leaves five different parameters picked in the process noise case. The aerodynamic coefficient estimates appear, as well as can be determined with the high level of noise in the actual data, excellent, with the possible exception of $C_{n_{\delta r}}$. The 2σ covariance estimates on the aerodynamic coefficients are, however, considerably less than the apparent noise in the actual data. This is because the maximum likelihood output error's structure does not account for the process noise responsible for the random variation in coefficients. Instead, the process noise is similar in effect to additional measurement noise, as can be seen in the measurement estimate covariances which bracket the actual measurement variations due to both measurement and process noise. The increased uncertainty in the net measurements

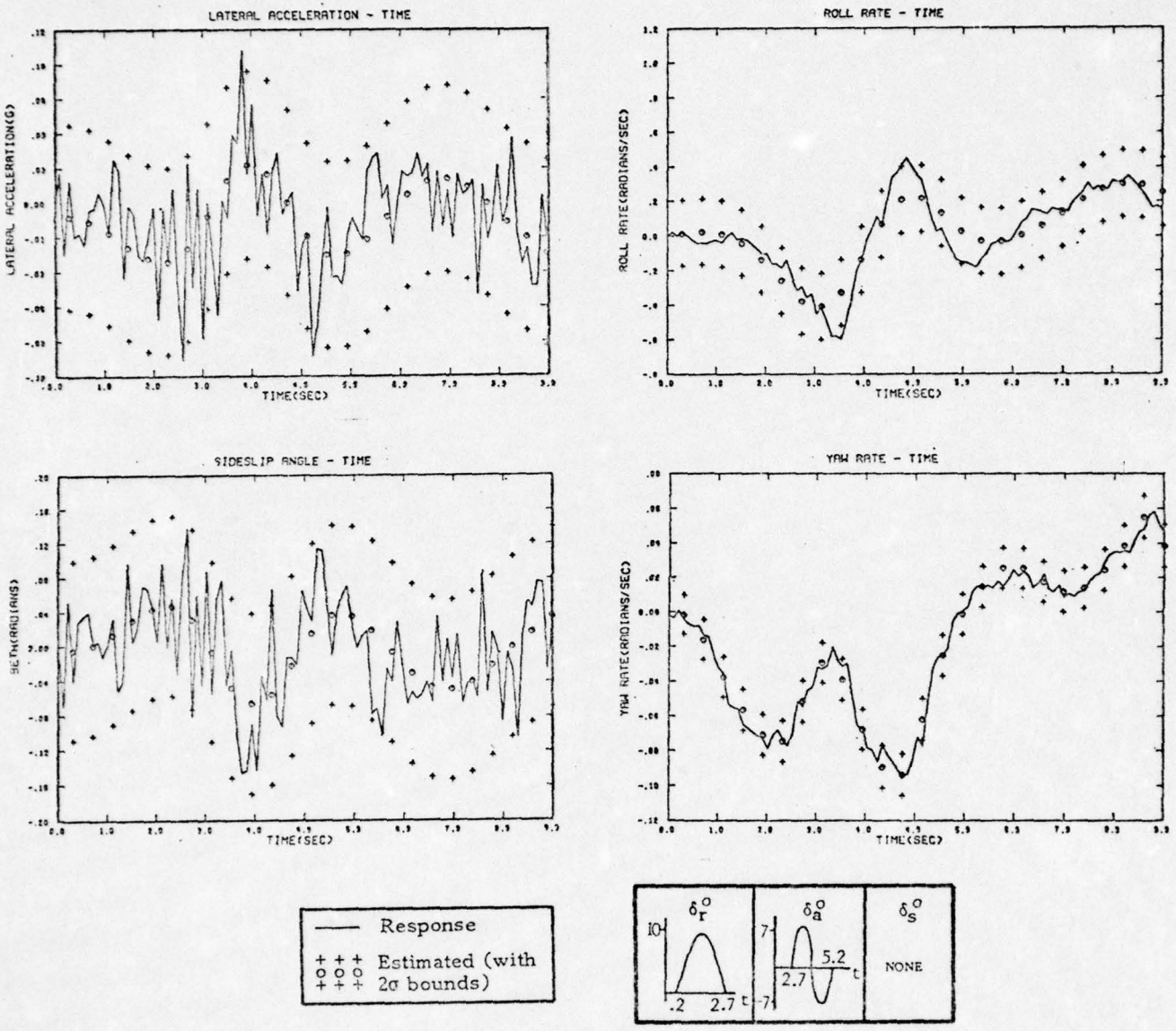

Figure 6.13 Lateral Measurement Response with Simulated Increased Gusts (Lateral Case 3, Ref. Fig. 6.2a).

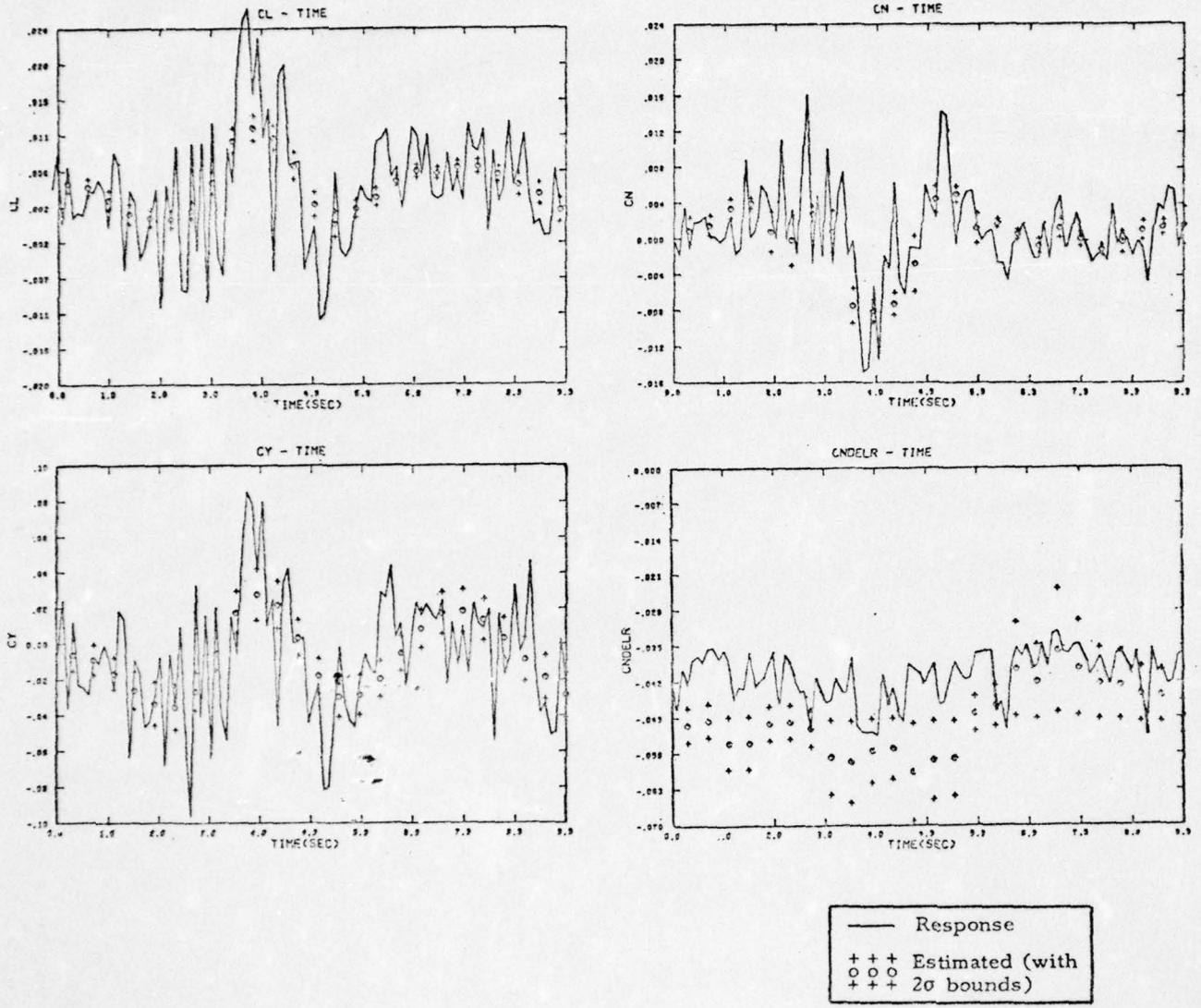

Figure 6.14 Lateral Static Coefficient Response with Simulated Increased Gusts (Lateral Case 3, Ref. Fig. 6.2a).

TABLE 6.9

Regression Results for Process Noise Case

EQUATION	OVERALL FIT F-RATIO	PARAMETER	PARAMETER ESTIMATE	PARAMETER F-VALUE	$F \geq 4\% F_{max}$
$\dot{v}$	967.3	C_{y_β}	-5.25×10^{-1}	9.68×10^{2}	X
		C_{y_o}	-6.43×10^{-3}	----	
$\dot{p}$	477.6	C_{ℓ_β}	4.07×10^{-3}	6.26×10^{2}	X
		$C_{\ell_{\alpha_\beta}}$	9.83×10^{-2}	8.39×10^{1}	X
		C_{ℓ_o}	4.60×10^{-4}	----	
$\dot{r}$	330.9	$C_{n_{\delta_r}}$	-3.71×10^{-2}	4.60×10^{2}	X
		C_{n_β}	4.66×10^{-2}	2.26×10^{2}	X
		$C_{n_{\alpha_\beta}}$	-5.57×10^{-1}	1.29×10^{2}	X
		$C_{n_{\beta^3}}$	2.10	4.90×10^{1}	X
		C_{n_r}	-1.85×10^{-2}	4.35×10^{1}	X
		$C_{n_{\delta_{r_\alpha}}}$	2.63×10^{-1}	3.12×10^{1}	X
		$C_{n_{\beta^2}}$	1.23×10^{-1}	2.61×10^{1}	X
		C_{n_o}	3.66×10^{-4}	----	

is reflected in aerodynamic coefficient covariances higher than for both of the measurement noise cases. The covariances are not as large, however, as would be the case if process noise was taken directly into account. Nevertheless, the actual coefficient estimates themselves are still very good.

6.4 METHODS FOR IMPROVING PARAMETER ESTIMATES

The ultimate limit of the accuracy of any parameter estimate, compared to its "true" value, is set by the relative effect the parameter has on the response data. This is determined by the overall information content of the data. In general,

TABLE 6.10

Maximum Likelihood Results for Process Noise Case

$J_o = 10.659$

$J_f = 12.028$

$J_f - J_{f-1}/J_f = 7.657 \times 10^{-5}$

No. of Iterations = 7

"Measurement" Noise Covariance Estimates

β 5.16×10^{-2} radians

$\ddot{y}$ 2.92×10^{-2}

p 9.49×10^{-2} radians/sec

r 5.64×10^{-3} radians/sec

PARAMETER	A PRIORI			FINAL		
	ESTIMATE	F-VALUE		ESTIMATE	F-VALUE	2σ CONFIDENCE
		REGRESSION	MAX. LIKELIHOOD			
C_{ℓ_β}	-1.02×10^{-1}	6.26×10^{2}	9.68×10^{2}	-8.60×10^{-2}	1.66×10^{3}	$\pm.42 \times 10^{-2}$
$C_{n_{\delta_r}}$	-3.71×10^{-2}	4.60×10^{2}	1.41×10^{2}	-4.99×10^{-2}	9.45×10^{2}	$\pm.32 \times 10^{-2}$
C_{n_r}	-4.26×10^{-1}	4.35×10^{1}	1.02×10^{1}	-1.26	2.25×10^{2}	$\pm.17$
$C_{n_{\alpha_\beta}}$	-5.57×10^{-1}	1.29×10^{2}	6.92	-1.50	1.50×10^{2}	$\pm.24$
C_{n_β}	4.66×10^{-2}	2.26×10^{2}	8.89	1.25×10^{-1}	1.01×10^{2}	$\pm.24 \times 10^{-1}$
$C_{\ell_{\alpha_\beta}}$	9.00×10^{-1}	8.39×10^{1}	1.47×10^{2}	6.71×10^{-1}	8.95×10^{1}	$\pm1.4 \times 10^{-1}$
C_{y_β}	-5.25×10^{-1}	9.68×10^{2}	4.98×10^{1}	-5.59×10^{-1}	3.95×10^{1}	$\pm1.8 \times 10^{-1}$
C_{ℓ_o}	4.60×10^{-4}	----	1.68	9.22×10^{-4}	1.91×10^{1}	$\pm4.2 \times 10^{-4}$
$C_{y_{\beta^2}}$	1.23×10^{-1}	2.61×10^{1}	1.67×10^{-1}	-9.56×10^{-1}	1.58×10^{1}	$\pm4.8 \times 10^{-1}$
$C_{n_{\beta^3}}$	2.10	4.90×10^{1}	2.16×10^{-1}	-2.72×10^{1}	1.45×10^{1}	$\pm1.4 \times 10^{1}$
$C_{n_{\delta_{r_\alpha}}}$	2.63×10^{-1}	3.12×10^{1}	5.18	1.48×10^{-1}	5.34	$\pm1.2 \times 10^{-1}$
C_{n_o}	3.66×10^{-4}	----	7.84×10^{-1}	5.00×10^{-4}	3.55	$\pm5.3 \times 10^{-4}$
C_{y_o}	-6.43×10^{-3}	----	2.75	-4.53×10^{-3}	1.83	$\pm6.7 \times 10^{-3}$
b_β	0.0		0.0	-4.62×10^{-3}	6.32×10^{-1}	$\pm12.0 \times 10^{-3}$

parameter estimates can be only as "good" as this data information content. As shown in Section 6.3, increasing noise in the data reduces the quantity of useful information available for parameter identification. This section discusses practical means for improving the useful information and thus providing more accurate estimates.

The following methods are considered for this improved identifiability objective:

a. Input design
b. Data aggregation (use of a priori information)
c. Data length increase (use of more data)
d. Addition of more parameters

6.4.1 Input Design

In the discussion of the longitudinal motion demonstration example results, the importance of the input is pointed out with regard to identifying all significant parameters well. If, as in the case with C_m, one parameter is poorly estimated as a result of information unavailable due to an inappropriate input, other parameter estimates, $C_{m_{\delta s}}$, may also be adversely affected.

In an attempt to correct the deficiencies of that first longitudinal motion case, another case, identical in all respects except for the input, is performed. For this example, detailed under longitudinal case 2 in Figure 6.2, the stabilator input amplitude is reduced to 2^o in an attempt to allow the influence of the C_m nonlinearity to have more impact on aircraft motion and thereby increase information in the data about C_m.

Results of this case are contained in Tables 6.11 and 6.12, and Figures 6.15 through 6.18. For this modified input, the C_m estimate time history has a much better fit to the variations in the actual C_m curve, but there is some bias. The bias is caused by the biased estimate of $C_{m_{\delta s}}$ apparent in Figure 6.16. The stabilator input selected for this case is too low in amplitude to satisfactorily estimate $C_{m_{\delta s}}$. Aircraft motion is primarily affected by the nonlinearity in C_m.

TABLE 6.11

Regression Results for Longitudinal Motion Case 2

EQUATION	OVERALL FIT F-RATIO	PARAMETER	PARAMETER ESTIMATE	PARAMETER F-VALUE	$F \geq 4\% F_{max}$
$\dot{x}$	253.6	$C_{x_{\alpha\delta_s}}$	1.27	2.54×10^{2}	X
		C_{x_o}	-3.41×10^{-2}	----	
$\dot{z}$	7105.4	C_{z_α}	-1.51	1.02×10^{4}	X
		$C_{z_{\alpha^2}}$	1.03×10^{1}	2.20×10^{3}	X
		$C_{z_{q_\alpha}}$	-2.89×10^{2}	1.19×10^{2}	
		C_{z_q}	-1.18×10^{1}	8.43×10^{1}	
		$C_{z_{\delta_s}}$	-4.55×10^{-1}	5.14×10^{1}	
		C_{z_o}	-9.65×10^{-1}	----	
$\dot{q}$	1873.7	$C_{m_{\alpha^2}}$	-2.41	4.35×10^{3}	X
		$C_{m_{\delta_s}}$	-5.00×10^{-1}	4.19×10^{3}	X
		C_{m_q}	-6.19	1.91×10^{3}	X
		$C_{m_{\alpha^3}}$	-3.33×10^{1}	1.29×10^{3}	X
		C_{m_α}	5.29×10^{-2}	1.12×10^{2}	
		$C_{m_{\alpha^2\beta^2}}$	-5.75×10^{-2}	5.36×10^{1}	
		$C_{m_{q_\alpha}}$	2.63×10^{1}	5.36×10^{1}	
		$C_{m_{\alpha^9}}$	3.59×10^{6}	2.72×10^{1}	
		$C_{m_{\alpha\beta^2}}$	-1.44×10^{2}	1.93×10^{1}	
		C_{m_o}	-4.70×10^{-2}	----	

TABLE 6.12

Maximum Likelihood Results for Longitudinal Case 2

$J_o = -9.7847$

$J_f = -20.556$

$J_f - J_{f-1} / J_f = 2.915 \times 10^{-4}$

No. of Iterations = 7

Measurement Noise Covariance Estimates:

α	1.21×10^{-3}	radians
$\ddot{x}$	6.30×10^{-3}	g
$\ddot{z}$	7.10×10^{-3}	g
q	2.94×10^{-3}	radians/sec

PARAMETER	A PRIORI			FINAL	
	ESTIMATE	F-VALUE		ESTIMATE	F-VALUE
		REGRESSION	MAX. LIKELIHOOD		
C_{z_o}	-9.65×10^{-1}	----	8.10×10^{4}	-9.71×10^{-1}	7.10×10^{5}
$C_{m_{\dot{\alpha}^3}}$	-3.33×10^{1}	1.29×10^{3}	3.98×10^{2}	-3.37×10^{1}	1.56×10^{4}
C_{z_α}	-1.51	1.02×10^{4}	1.32×10^{3}	-1.57	1.52×10^{4}
$C_{m_{\delta_s}}$	-5.00×10^{-1}	4.19×10^{3}	6.88×10^{2}	-5.29×10^{-1}	1.12×10^{4}
C_{m_q}	-6.19	1.91×10^{3}	9.50×10^{2}	-7.11	8.18×10^{3}
C_{m_o}	4.70×10^{-2}	----	5.44×10^{2}	-4.47×10^{-2}	7.20×10^{3}
$C_{m_{\alpha^2}}$	-2.41	4.35×10^{3}	1.11×10^{2}	-2.49	6.25×10^{3}
C_{x_o}	3.41×10^{-2}	----	3.89×10^{3}	-3.43×10^{-2}	4.97×10^{3}
$C_{z_{\alpha^2}}$	1.03×10^{1}	2.20×10^{3}	2.20×10^{2}	1.02×10^{1}	1.96×10^{3}
$C_{x_{\alpha\delta_s}}$	1.27	2.54×10^{2}	1.77×10^{2}	1.21	2.58×10^{3}

Figure 6.19 compares estimates of C_m for the longitudinal cases 1 and 2. In case 1, the fit is poor, but there is less bias than is present in the better nonlinear convolution fit of case 2. If the information available from both experiments could be combined, a much better net fit would result.

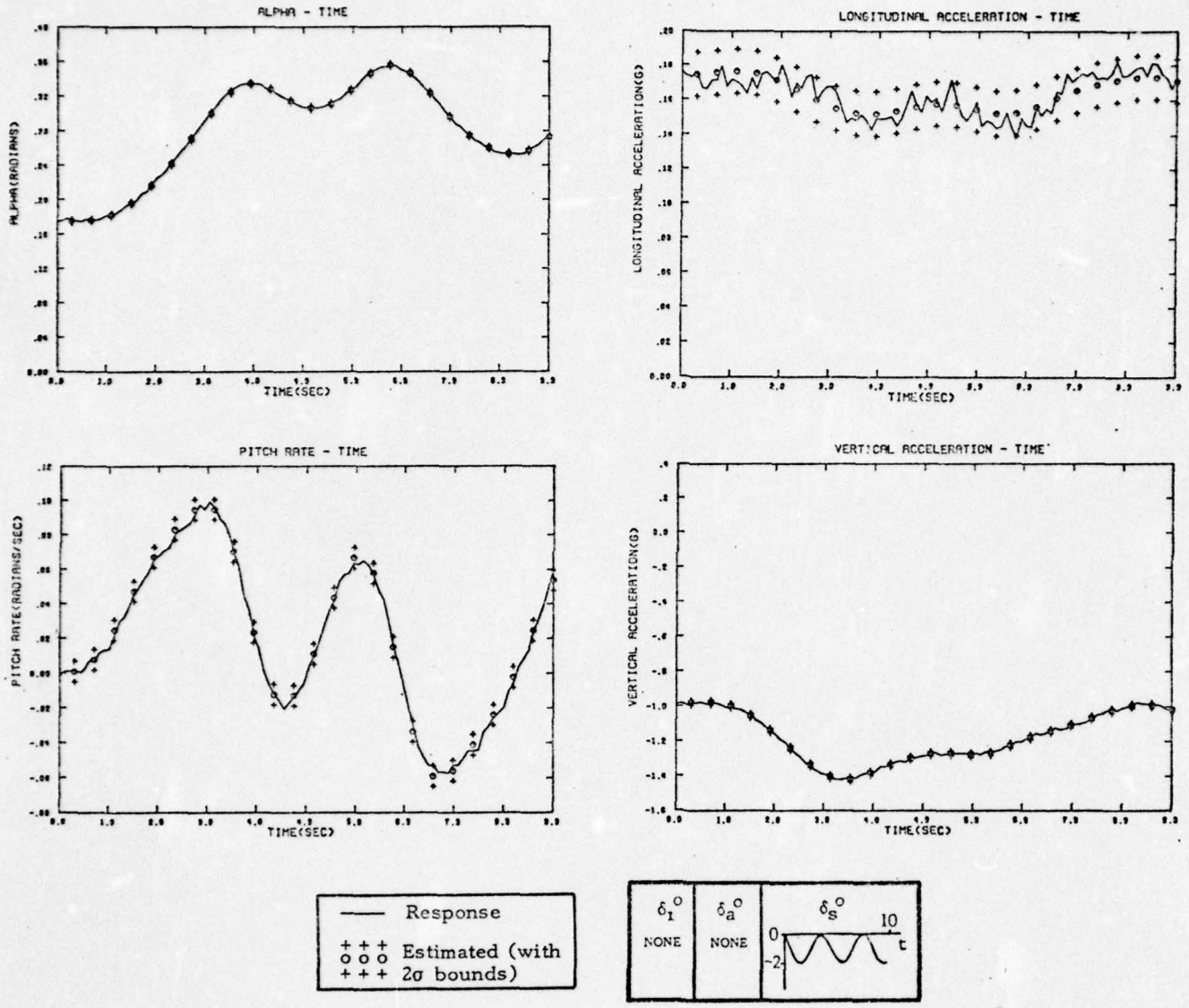

Figure 6.15 Longitudinal Measured and Estimated Response to Reduced Amplitude Sinusoidal Stabilator Input (Longitudinal Case 2, Ref. Fig. 6.2b).

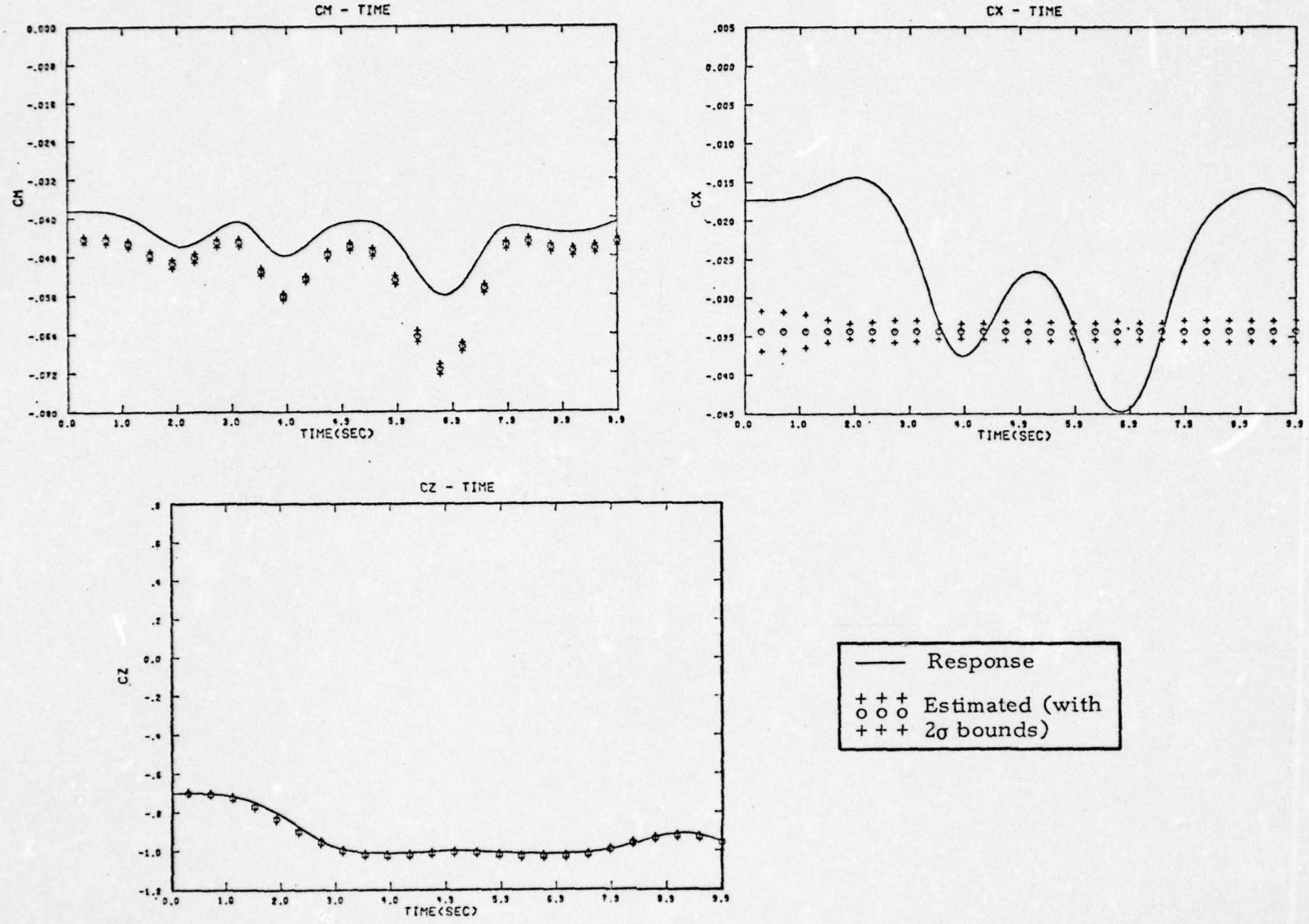

Figure 6.16 Longitudinal Static Coefficient Response (Simulated and Estimated) to Reduced Amplitude Sinusoidal Stabilator Input (Longitudinal Case 2, Ref. Fig. 6.2b).

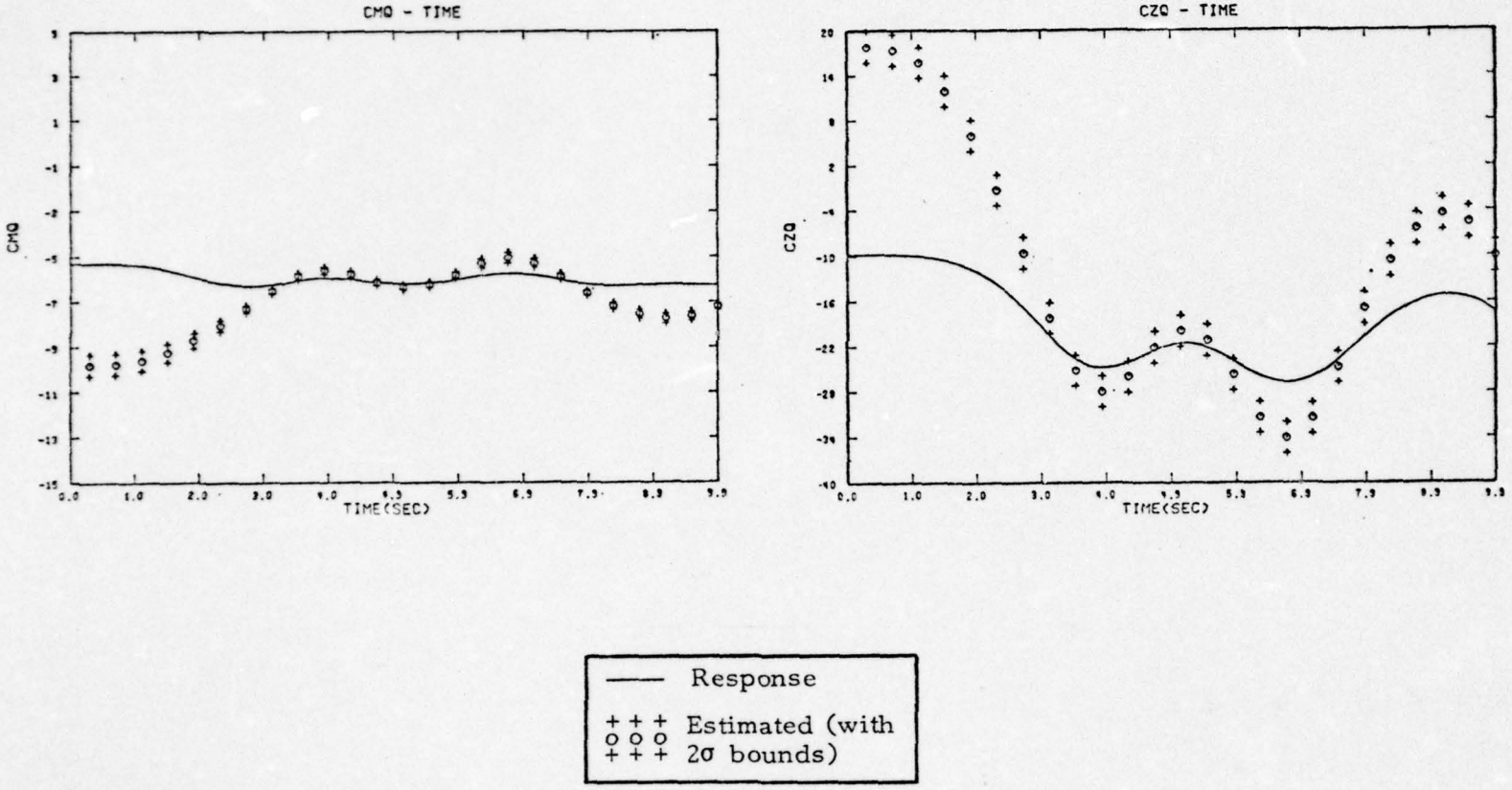

Figure 6.17 Longitudinal Dynamic Coefficient Response (Simulated and Estimated) to Reduced Amplitude Sinusoidal Stabilator Input (Longitudinal Case 2, Ref. Fig. 6.2b).

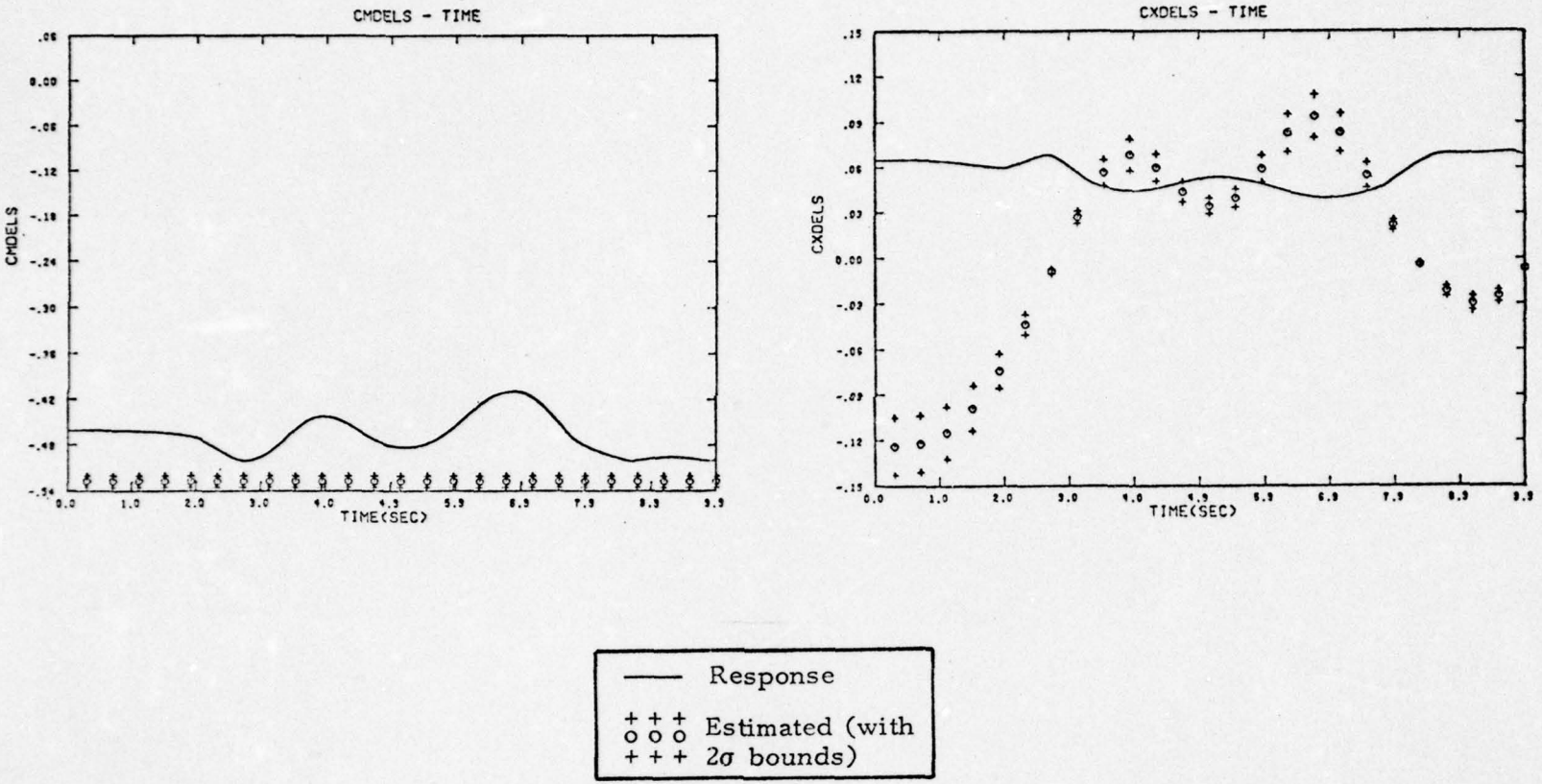

Figure 6.18 Longitudinal Control Effectiveness Response (Simulated and Estimated) to Reduced Amplitude Sinusoidal Stabilator Input (Longitudinal Case 2, Ref. Fig. 6.2b).

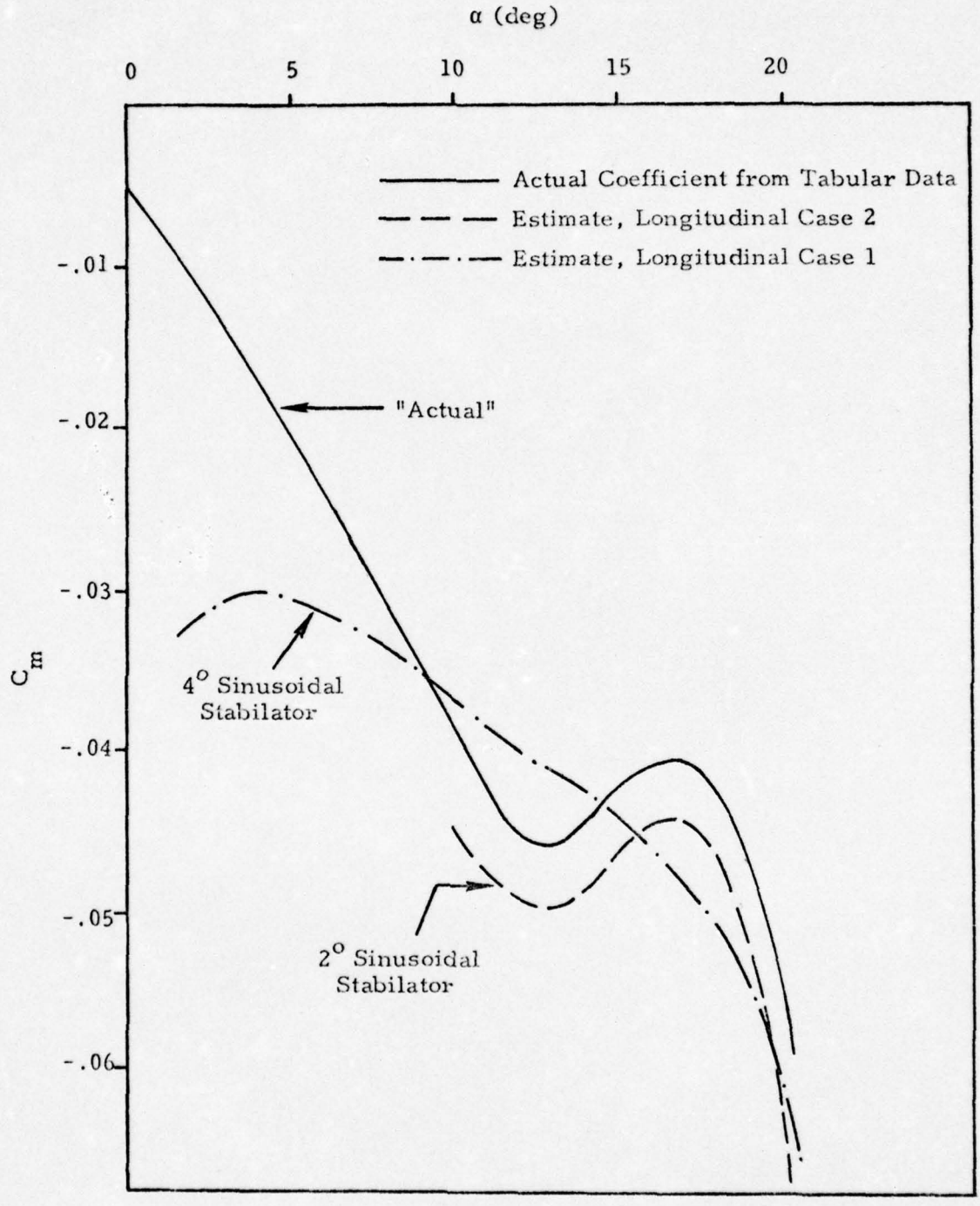

Figure 6.19 Estimate of C_m vs. α for Different Inputs

6.4.2 Information Aggregation

Combining parameter estimates to aggregate information from two experiments is a fairly straightforward procedure which involves both parameter estimates and information matrices (see Chapter IV). A difficulty can arise, however, when nonlinear aerodynamic coefficient expansions are identified. The expansions are really only valid for the operating range of the experiment from which they are estimated. Validity of the expansion fit outside of that operating range is very questionable since significant and unpredictable curvature variations in the actual coefficient function are likely.

It is recommended at present that aerodynamic coefficient estimates be combined from various experiments of different operating ranges in order to develop an overall coefficient function estimate. Coefficient estimates should be combined, on a point-by-point basis, only in those regions where estimate operating ranges overlap.

Ultimately, it would be desirable to accumulate previous estimate information and use it in the form of a priori information matrix values for each successive maximum likelihood processing of new data. This would result in continuing improvement of the estimates since each new set of estimates would automatically incorporate information from all previous experiments. However, a major difficulty of implementing this procedure for the estimation of nonlinear aerodynamic coefficients lies in the problem of combining previous parameter estimates which are only valid over part of the operating range of a new experiment. One possible technique is to weight the information matrix as a function of the distribution of the measurements for the experiment. This is equivalent to developing a chi-square distribution of variances for various measurement samples. The value of the information matrix would then go to zero at the limits of measurement excursions, reflecting the complete uncertainty about extrapolated aerodynamic coefficient values.

As an example of the present technique of a posteriori combination of aerodynamic coefficient estimates from different experiments over different operating ranges, lateral response case 4 results for $\frac{\partial C_n}{\partial \beta}$ are combined with those of lateral response case 1. Tables 6.13, 6.14 and Figures 6.20 and 6.21 describe

TABLE 6.13

Regression Results for Lateral Motion Case 4

EQUATION	OVERALL FIT F-RATIO	PARAMETER	PARAMETER ESTIMATE	PARAMETER F-VALUE	$F \geq 4\% F_{max}$
$\dot{v}$	1906.3	C_{y_β}	-5.01×10^{-1}	1.91×10^{3}	X
		C_{y_o}	1.21×10^{-3}	----	
$\dot{p}$	1361.1	C_{ℓ_β}	-7.35×10^{-1}	1.37×10^{3}	X
		$C_{\ell_{\alpha_\beta}}$	2.56	6.49×10^{2}	X
		$C_{\ell_{\beta^3}}$	2.58	1.80×10^{2}	X
		$C_{\ell_{\delta_a}}$	-4.92×10^{-2}	1.13×10^{2}	X
		$C_{\ell_{u^2 r^2}}$	2.00×10^{2}	1.12×10^{2}	X
		C_{ℓ_r}	5.79×10^{-1}	1.09×10^{2}	X
		$C_{\ell_{\alpha\delta_a}}$	-2.10	9.90×10^{1}	X
		C_{ℓ_α}	-4.25×10^{-1}	7.81×10^{1}	X
		$C_{\ell_{\delta_r}}$	5.99×10^{-3}	3.28×10^{1}	
		C_{ℓ_p}	3.72×10^{-2}	2.33×10^{1}	
		$C_{\ell_{\beta^4}}$	4.31	1.21×10^{1}	
		$C_{\ell_{u^3}}$	5.61	9.03	
		C_{ℓ_o}	8.99×10^{-4}	----	
$\dot{r}$	1079.3	$C_{n_{\delta_r}}$	-3.60×10^{-2}	9.50×10^{2}	X
		$C_{n_{\alpha_\beta}}$	-2.20	3.97×10^{2}	X
		C_{n_p}	-1.01×10^{-1}	1.61×10^{2}	X
		C_{n_α}	2.33×10^{-2}	1.58×10^{2}	X
		$C_{n_{\beta^5}}$	5.03×10^{1}	1.39×10^{2}	X
		C_{n_r}	-6.36×10^{-1}	9.38×10^{1}	X
		$C_{n_{\delta_a}}$	3.50×10^{-2}	8.88×10^{1}	X
		$C_{n_{\beta^2}}$	1.38×10^{-1}	5.45×10^{1}	X
		$C_{n_{\alpha^2\beta^2}}$	-1.66×10^{2}	5.41×10^{1}	X
		$C_{n_{p_\alpha}}$	-2.365	1.78×10^{1}	
		C_{n_o}	1.43×10^{-4}	----	

TABLE 6.14

Maximum Likelihood Results for Lateral Motion Case 4

$J_o = 10.401$

$J_f = 15.114$

$J_f - J_{f-1}/J_f = 2.83 \times 10^{-4}$

No. of Iterations = 10

Measurement Noise Variance Estimates:

β	9.76×10^{-3}	radians
$\dot{y}$	8.34×10^{-3}	g
p	4.28×10^{-2}	radians/sec
r	1.05×10^{-2}	radians/sec

PARAMETER	A PRIORI			FINAL	
	ESTIMATE	F-VALUE		ESTIMATE	F-VALUE
		REGRESSION	MAX. LIKELIHOOD		
$C_{n_{\delta_r}}$	-3.60×10^{-2}	9.50×10^{2}	1.18×10^{3}	-5.35×10^{-2}	1.69×10^{3}
C_{y_β}	-5.01×10^{-1}	1.91×10^{3}	1.26×10^{3}	-5.12×10^{-1}	1.41×10^{3}
C_{ℓ_β}	-7.35×10^{-1}	1.37×10^{3}	2.67×10^{2}	-7.58×10^{-2}	4.11×10^{2}
$C_{\ell_{\alpha_\beta}}$	2.56	6.49×10^{2}	3.79×10^{2}	2.00	2.64×10^{2}
$C_{n_{\beta^5}}$	5.03×10^{1}	1.39×10^{2}	3.65×10^{1}	8.86×10^{1}	2.43×10^{2}
C_{ℓ_o}	8.99×10^{-1}	----	1.77×10^{2}	5.27×10^{-4}	7.62×10^{1}
C_{n_p}	-1.01×10^{-1}	1.61×10^{2}	5.70×10^{1}	-6.85×10^{-2}	3.98×10^{1}
$C_{\ell_{r^3}}$	2.58	1.80×10^{2}	3.79×10^{1}	1.61	3.28×10^{1}
$C_{n_{\alpha_\beta}}$	-2.20	3.97×10^{2}	1.99×10^{1}	-1.35	2.92×10^{1}
C_{n_o}	1.43×10^{-4}	----	1.12	9.86×10^{-4}	2.02×10^{1}
C_{n_α}	2.33×10^{-2}	1.58×10^{2}	3.42×10^{1}	9.12×10^{-3}	6.51×10^{1}
C_{y_o}	1.21×10^{-3}	----	1.29	2.14×10^{-3}	4.54

lateral response case 4 results. Figure 6.22 shows the two estimates of $\frac{\partial C_n}{\partial \beta}$, the actual function and the combined estimate. The combined estimate is a better fit to the actual curve in the overlapping region than either estimate separately.

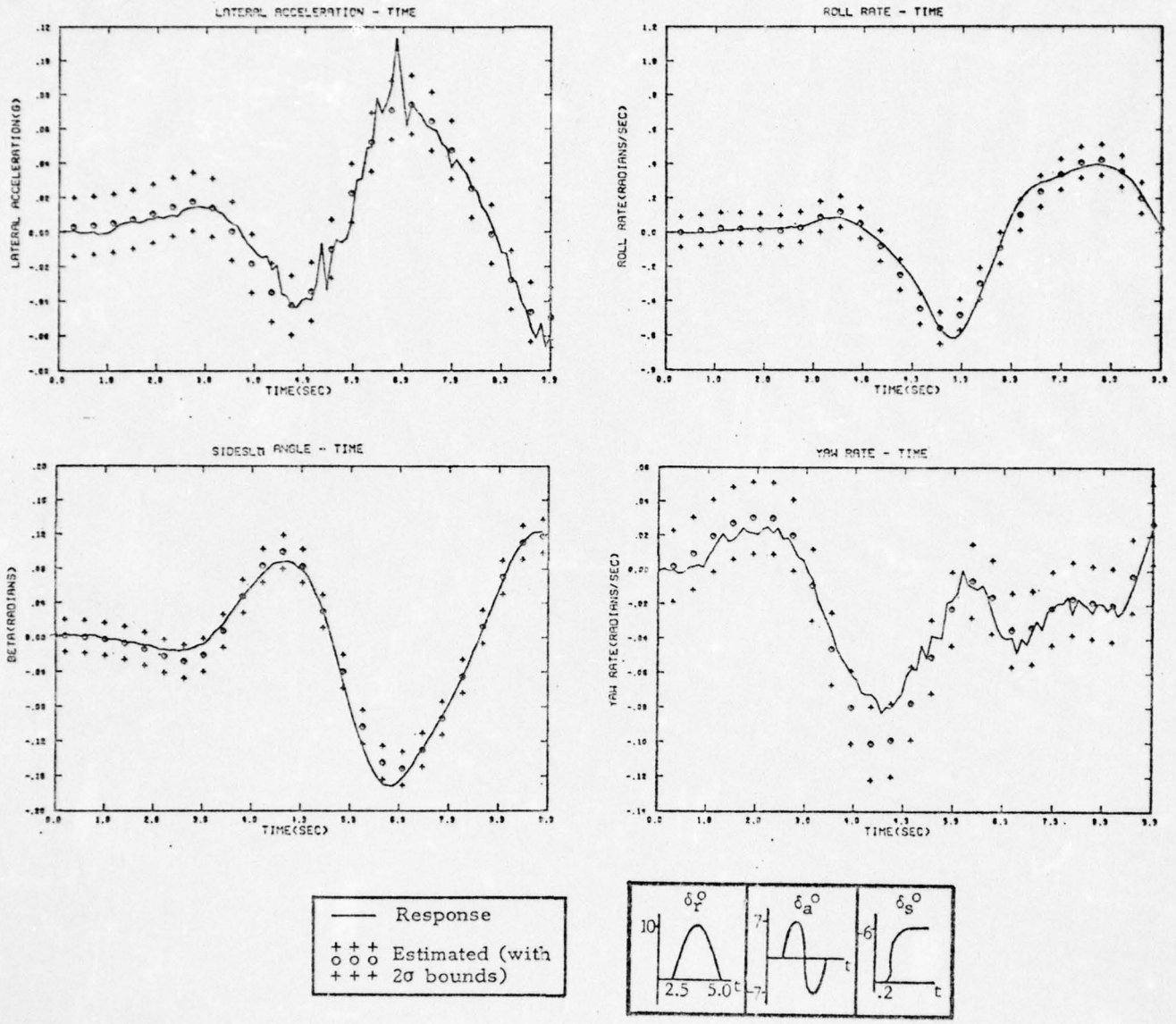

Figure 6.20 Lateral Measured and Estimated Response to a Combined Longitudinal/Lateral Input (Lateral Case 4, Ref. Fig. 6.2a).

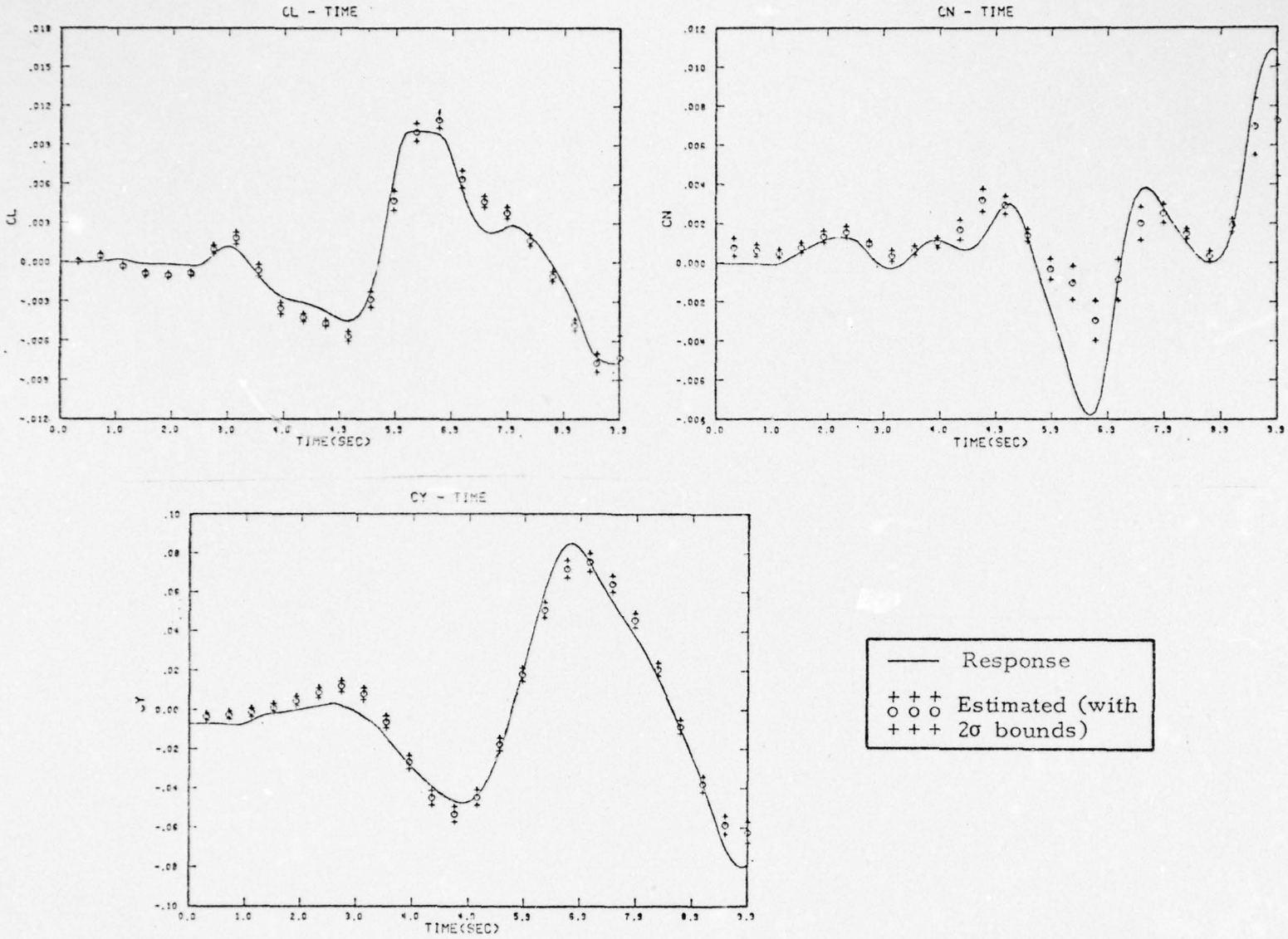

Figure 6.21 Lateral Static Coefficient Response (Simulated and Estimated) to a Combined Longitudinal/ Lateral Input (Lateral Case 4, Ref. Fig. 6.2a).

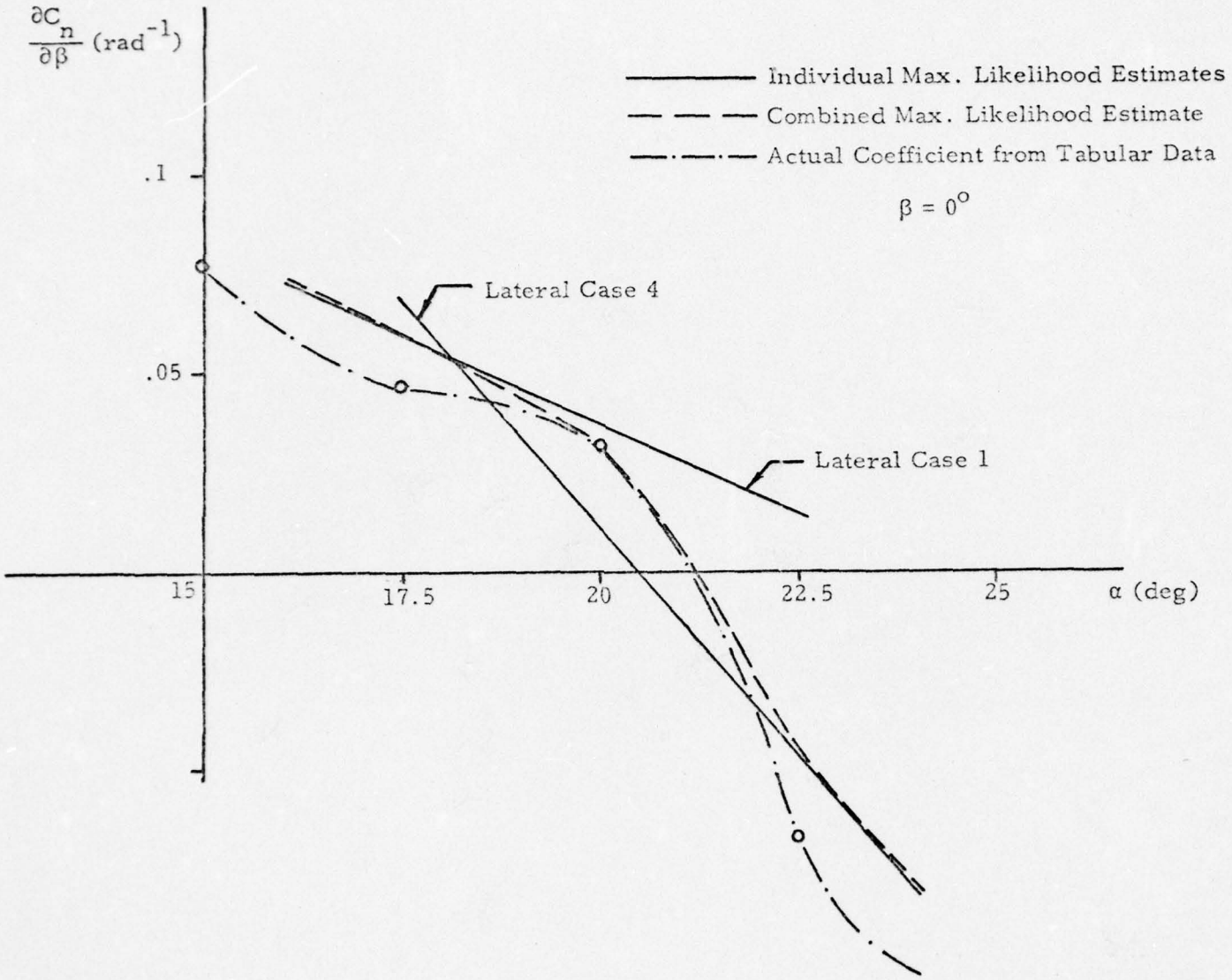

Figure 6.22 $\frac{\partial C_n}{\partial \beta}$ vs. α Development from Two Experiments

6.4.3 Increasing the Number of Parameters

A lack of sufficient parameters is frequently a cause of significant errors in an identification model time history, compared to the original system output. Thus, it is often erroneously concluded that increasing the number of parameters will improve the time history match and perhaps even improve the parameter estimates.

Over-parameterization is an attempt to derive more model parameter estimates from data than are actually identifiable from the useful information content of the data. In essence, the problem with over-parameterization is that the degree-of-freedom allowed the estimate or fit by adding parameters becomes too large relative to the quantity of the data. The result is that although there may be a monotonically improving fit to the actual data, the statistical significance of the fit improvement will eventually decrease (this situation is described by the F-ratio test in the regression program).

If the inclination to add parameters to improve the estimate fit to real data is continued beyond the point of maximal statistical significance, the overall confidence in estimates of parameters will also decline. A qualitative reason for this phenomenon is that the estimate model begins trying to account for noise in the real data in addition to modeling the underlying process of interest. In effect, the result is that a close to perfect fit of the available data may be obtained, but the predictive capability of the over-parameterized model is very poor.

Section 6.2 outlines the parameter set specification recommended for the identification procedure used in order to avoid the problem of over-parameterization. Advantage is taken of the readily available regression statistics related to overall fit and individual parameter significances in order to pick a realistic parameter set for maximum likelihood estimation.

As an illustration of the effects of an over-parameterized maximum likelihood estimation, the data from lateral case 1 is reprocessed with 22 parameters identified instead of the original 12. Results are given in Table 6.14 and Figures 6.23 through 6.25. Time history comparisons with the original 12 parameter

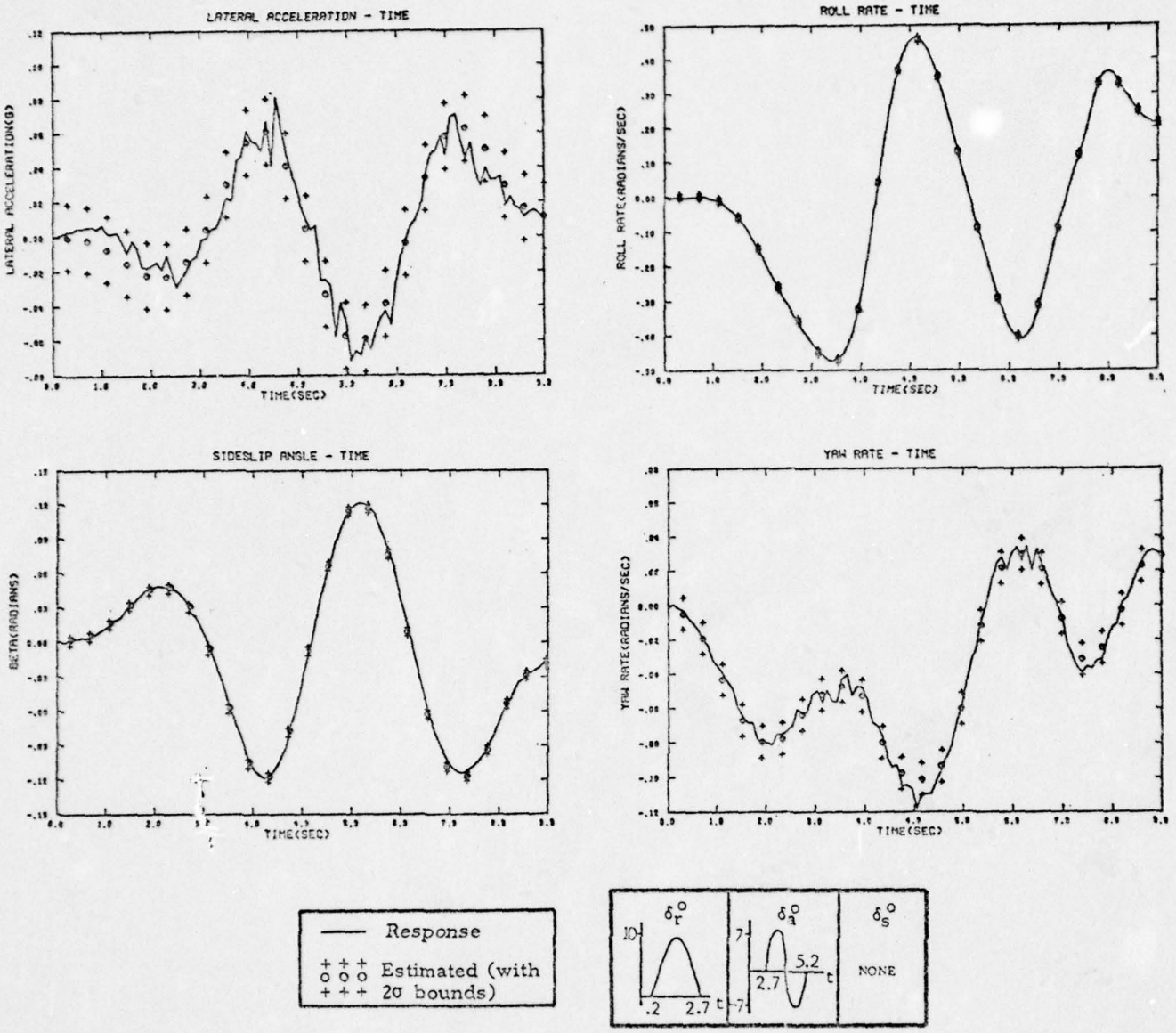

Figure 6.23 Lateral Measured and Estimated Response (Based on 22 Parameters) to an Aileron/Rudder Input (Lateral Case 1, Ref. Fig. 6.2a).

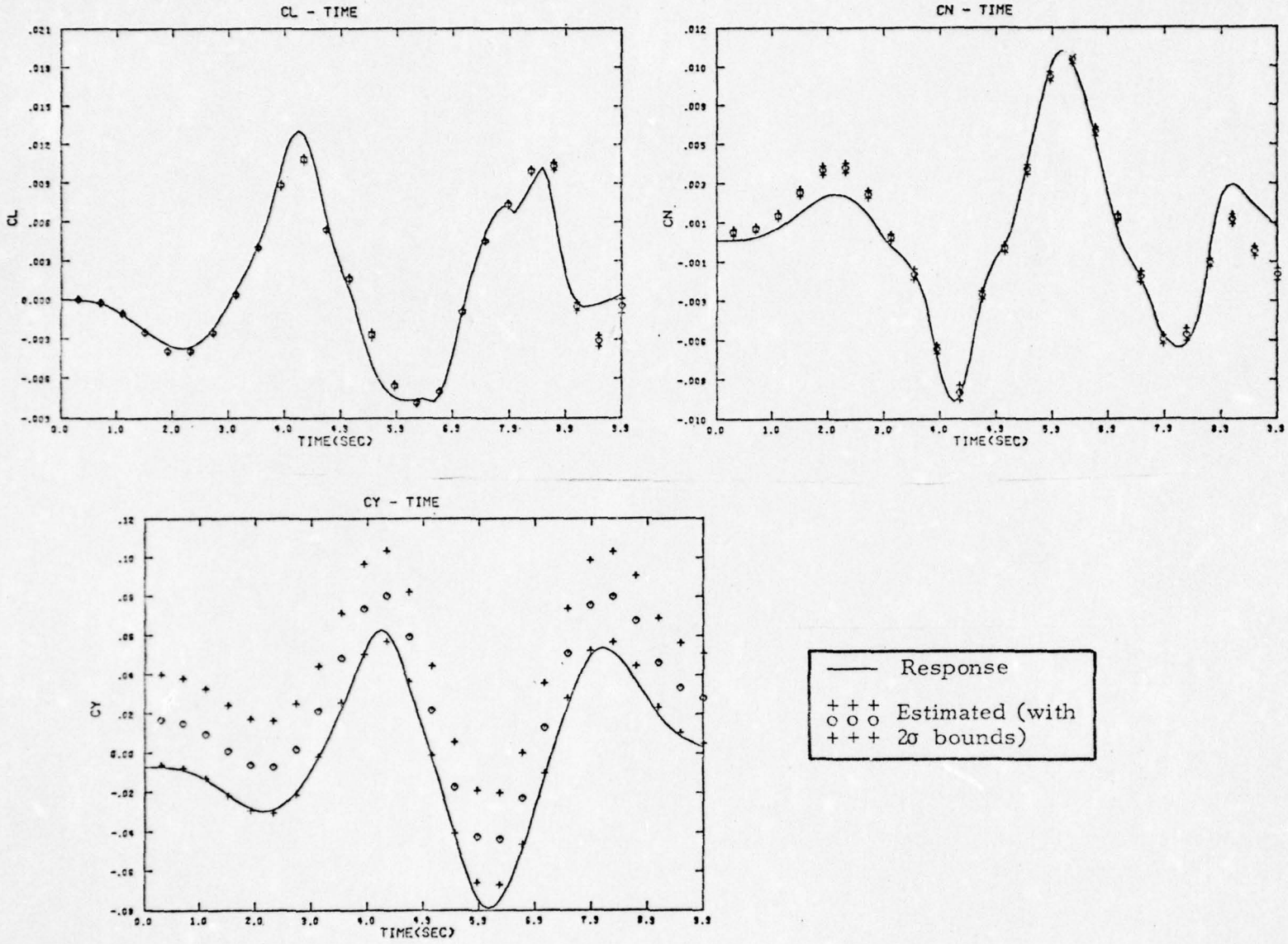

Figure 6.24 Lateral Static Coefficient Response (Simulated and Estimated Based on 22 Parameters) to an Aileron/Rudder Input (Lateral Case 2, Ref. Fig. 6.2a).

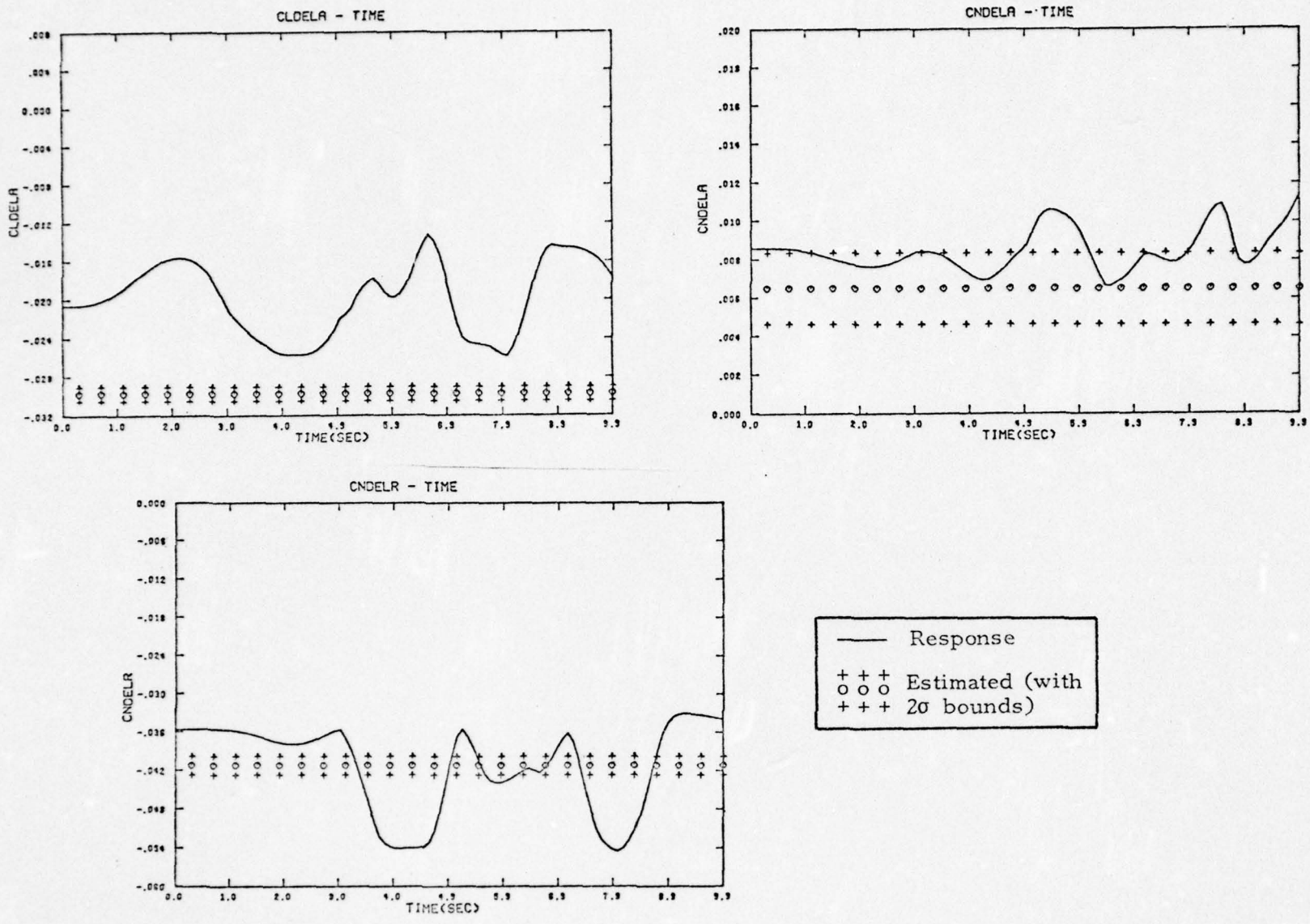

Figure 6.25 Lateral Control Effectiveness Coefficient Response (Simulated and Estimated Based on 22 Parameters) to an Aileron/Rudder Input (Lateral Case 1, Ref. Fig. 6.2a).

identification of lateral motion case 1 (Figures 6.3 to 6.5) demonstrate that the measurement estimates are improved. For coefficients, however, only $C_{n_{\delta r}}$ is significantly improved and C_n slightly improved. C_ℓ is about the same, while $C_{n_{\delta a}}$ is slightly worse and $C_{\ell_{\delta a}}$ and C_y are much worse. The net assessment is then that the 22 parameter identification produces slightly poorer parameter estimates than the 12 parameter identification. There may be a better optimum set size between 12 and 22 parameters, or even below 12; but the gain to be had is probably small since the change from 12 to 22 is so slight. The figure of 12, however, has the distinct advantage of having been found by a single pass, repeatable procedure, while the unknown "better" optimum set size must be found by maximum likelihood processing with several iterative choices of set size.

6.4.4 Example of Results for an Increased Data Length and Coupled Mode Models

In general, identification of more parameters is feasible without over-parameterizing the problem only if more information about the parameters is available. Previous discussions of Section 6.3 describe the impact of information quality in a given quantity of data. In this section, an example is presented where the data quality is comparable to earlier base results (i.e., approximately the same inputs are employed as in lateral response case 1 and longitudinal response case 1), but the quantity of data is increased because the experiment is simulated for 15.0 seconds rather than 10.0 seconds.

Details of this experiment are given in Figure 6.2c under lateral/longitudinal response case 1. Both lateral and longitudinal plane inputs are used and parameter estimates are obtained for all five degrees-of-freedom. Results are in the standard format of Table 6.15 and Figures 6.26 through 6.29.

There are 24 parameters in the significant set identified plus the 7 diagonal elements of the R matrix (which are estimates of the measurement noise covariances), giving a total of 31 estimates. The total of estimates for the comparable longitudinal motion case 1 and lateral motion case 1, less the estimates related to the $\dot{u}$ equation, is 30. Thus, approximately the same number of parameters are singled out in the combined case to describe responses similar to the decoupled cases. Examina-

TABLE 6.15

Maximum Likelihood Results for Lateral Motion Case 1,
22 Parameters Identified

$J_o = 18.544$

$J_f = 19.801$

$J_f - J_{f-1}/J_f = 8.542 \times 10^{-4}$

No. of Iterations = 4

	A PRIORI (12 Parameter Estimate)		FINAL	
PARAMETER	ESTIMATE	F-VALUE	ESTIMATE	F-VALUE
C_{ℓ_β}	-6.73×10^{-2}	1.54×10^{4}	-6.86×10^{-2}	4.06×10^{4}
$C_{\ell_{\alpha^5}}$	-1.68×10^{4}	3.06×10^{3}	-1.73×10^{4}	8.44×10^{3}
$C_{\ell_{\delta_a}}$	-2.68×10^{-2}	2.30×10^{3}	-2.98×10^{-2}	6.55×10^{3}
$C_{n_{\delta_r}}$	-4.95×10^{-2}	2.21×10^{3}	-4.13×10^{-3}	3.12×10^{3}
C_{ℓ_o}	1.42×10^{-3}	4.98×10^{2}	1.72×10^{-3}	1.91×10^{3}
C_{ℓ_α}	1.05×10^{-1}	8.28×10^{2}	9.85×10^{-2}	1.53×10^{3}
C_{y_β}	-5.36×10^{-1}	1.48×10^{3}	-5.29×10^{-1}	1.48×10^{3}
C_{ℓ_p}	4.95×10^{-1}	3.35×10^{2}	5.38×10^{-1}	9.37×10^{2}
$C_{\ell_{r_\alpha}}$	2.25×10^{1}	2.70×10^{3}	2.63×10^{1}	7.91×10^{2}
$C_{n_{\beta^2}}$	4.19×10^{-1}	4.60×10^{3}	4.63×10^{-1}	6.66×10^{2}
$C_{n_{\alpha\beta}}$	-4.86×10^{-1}	1.95×10^{2}	-5.34×10^{-1}	6.12×10^{2}
$C_{\ell_{\alpha^2}}$	1.51	7.36×10^{1}	1.85	2.92×10^{2}
C_{n_β}	5.88×10^{-2}	1.86×10^{2}	4.87×10^{-2}	2.47×10^{2}
$C_{\ell_{\alpha^2\beta}}$	-1.69×10^{1}	1.28×10^{2}	-1.37×10^{1}	1.84×10^{2}
$C_{n_{\delta_a}}$	6.87×10^{-3}	2.81×10^{1}	6.47×10^{-3}	4.80×10^{1}
C_{n_o}	3.29×10^{-4}	7.87	-5.85×10^{-4}	4.35×10^{1}
$C_{n_{\beta^3}}$	1.09	6.82×10^{1}	1.92	3.79×10^{1}
b_r	0.0	0.0	-2.9×10^{-3}	8.98
b_β	6.89×10^{-3}	4.23×10^{1}	1.45×10^{-3}	4.87
$b_{\ddot{y}}$	0.0	0.0	-2.28×10^{-2}	4.15
C_{y_o}	-3.40×10^{-3}	4.23×10^{1}	2.30×10^{-2}	4.15
b_p	0.0	0.0	3.62×10^{-4}	7.24×10^{-1}

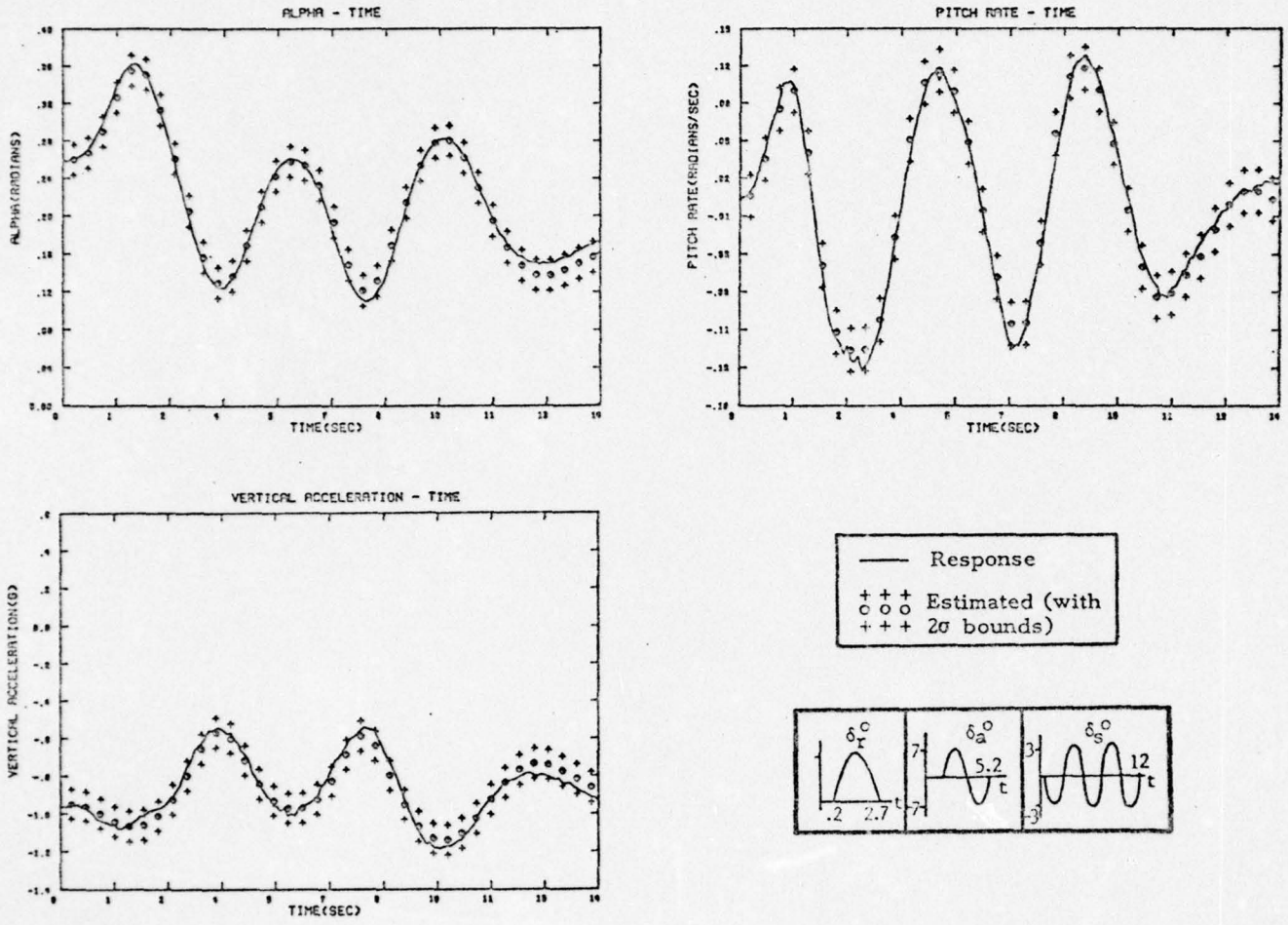

Figure 6.26 Longitudinal Measured and Estimated Response with Inclusion of Cross-Coupling of Equations and Increased Data Length (Longitudinal/Lateral Case 1, Ref. Fig. 6.2c).

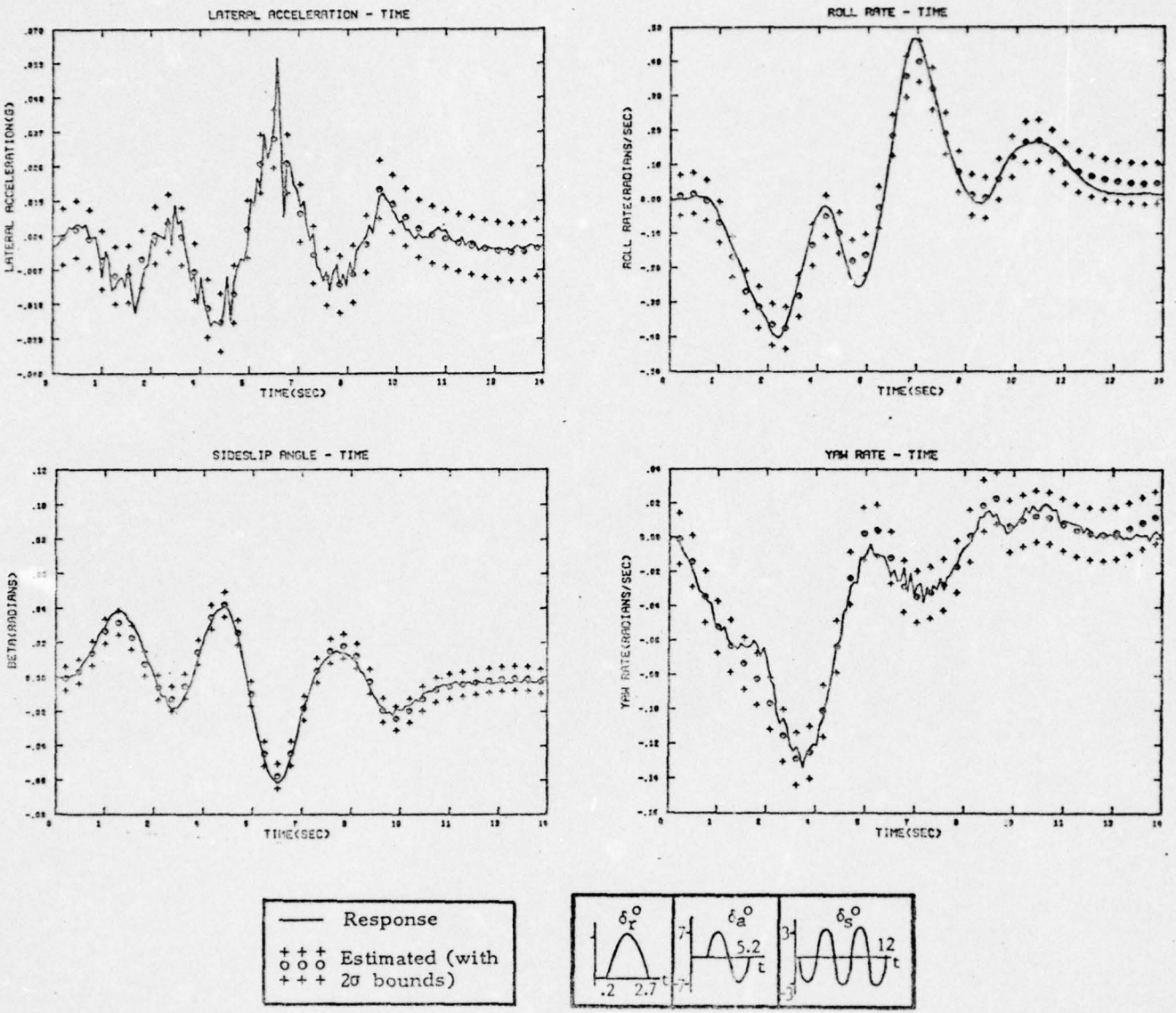

Figure 6.27 Lateral Measured and Estimated Response with Inclusion of Cross-Coupling of Equations and Increased Data Length (Longitudinal/Lateral Case 1, Ref. Fig. 6.2c).

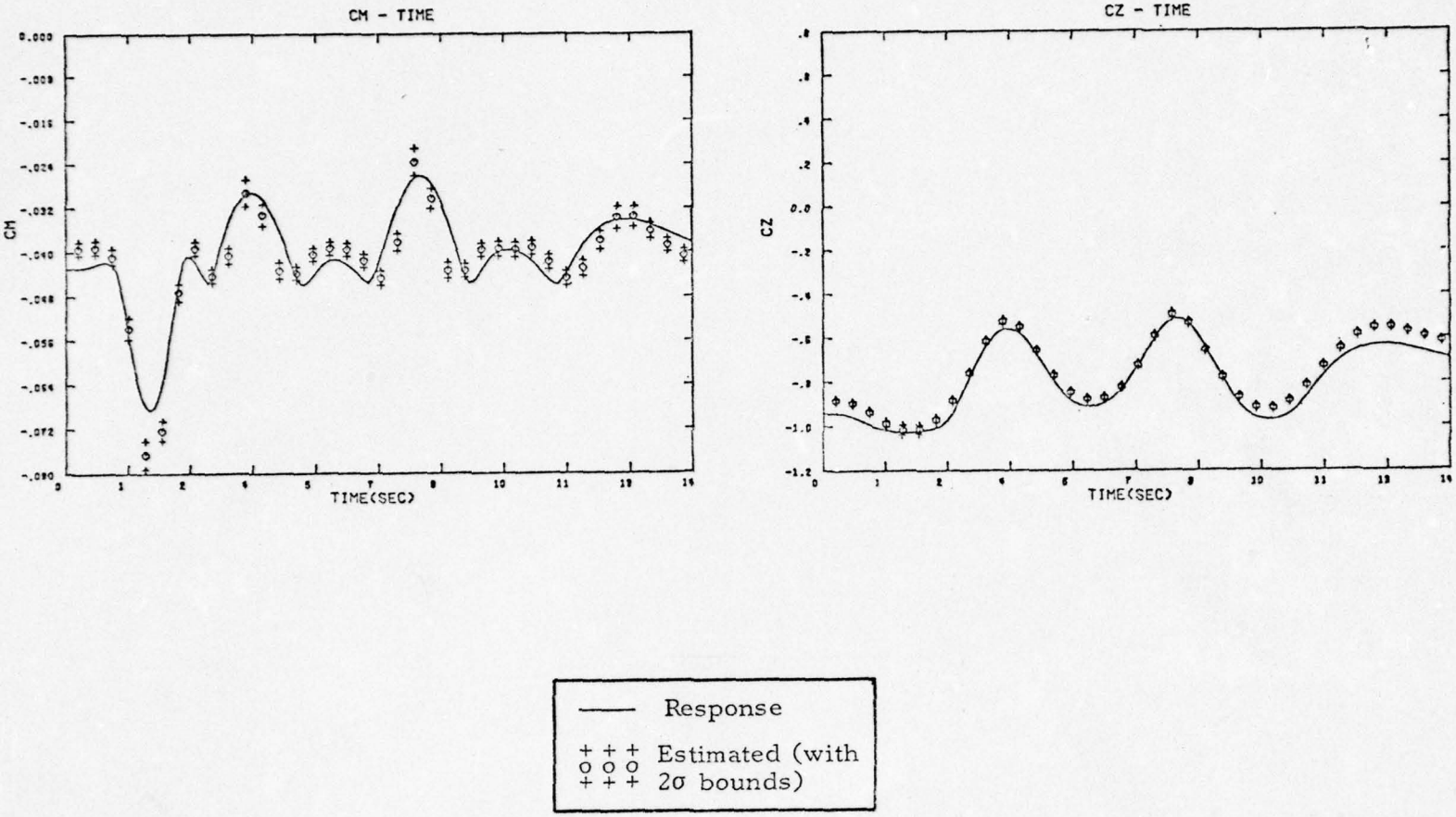

Figure 6.28 Longitudinal/Lateral Static Coefficient Response (Simulated and Estimated) with Inclusion of Equation Cross-Coupling and Increased Data Length (Longitudinal/Lateral Case 1, Ref. Fig. 6.2c).

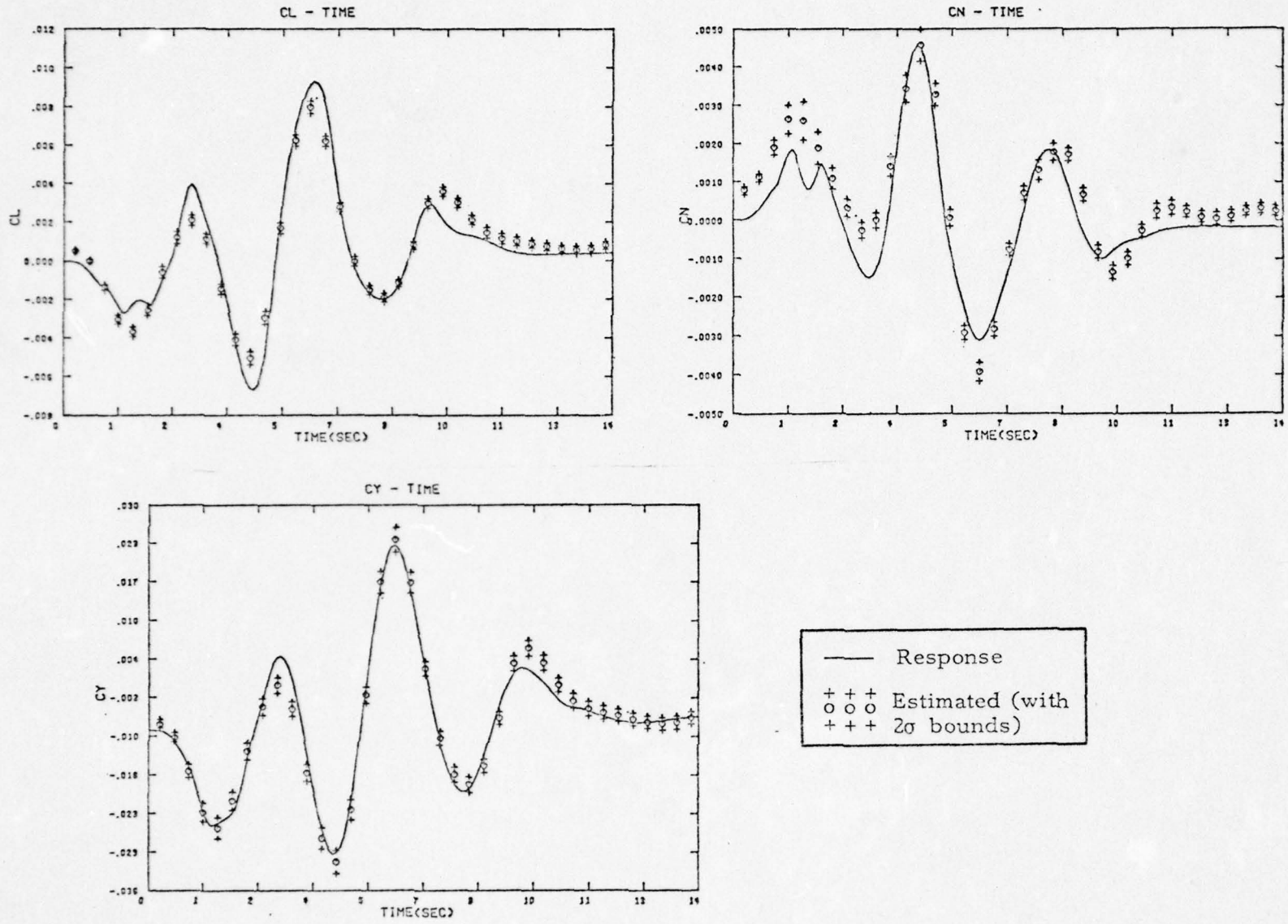

Figure 6.29 Lateral Static Coefficient Response (Simulated and Estimated) with Inclusion of Equation Cross-Coupling and Increased Data Length (Longitudinal/Lateral Case 1, Ref. Fig. 6.2c).

TABLE 6.16

Maximum Likelihood Results for Lateral/Longitudinal Motion Case 1

$J_o = 25.956$

$J_f = 28.720$

$J_f - J_{f-1}/J_f = 1.09 \times 10^{-3}$

No. of Iterations = 4

Measurement Noise Covariance Estimates

α	8.06×10^{-3}	radians
β	3.90×10^{-3}	radians
$\ddot{y}$	4.52×10^{-6}	g
$\ddot{z}$	3.91×10^{-2}	g
p	2.94×10^{-2}	radians/sec
q	9.32×10^{-3}	radians/sec
r	7.46×10^{-3}	radians/sec

PARAMETER	A PRIORI		FINAL	
	ESTIMATE	F-VALUE	ESTIMATE	F-VALUE
C_{z_o}	-8.24×10^{-1}	1.45×10^{4}	-8.06×10^{-1}	3.13×10^{4}
C_{m_o}	-3.85×10^{-2}	2.65×10^{3}	-4.26×10^{-2}	5.09×10^{3}
$C_{m_{\delta_s}}$	-4.24×10^{-1}	2.77×10^{3}	-4.60×10^{-1}	4.98×10^{3}
C_{ℓ_β}	-1.28×10^{-1}	1.33×10^{3}	-1.30×10^{-1}	3.91×10^{3}
C_{z_α}	-2.37	1.15×10^{3}	-2.40	2.67×10^{3}
C_{m_q}	-5.20	9.07×10^{2}	-6.22	2.08×10^{3}
$C_{n_{\delta_r}}$	-4.77×10^{-2}	8.33×10^{2}	-4.37×10^{-2}	1.75×10^{3}
C_{n_β}	1.08×10^{-1}	6.47×10^{2}	8.96×10^{-2}	1.28×10^{3}
C_{ℓ_p}	-1.59×10^{-1}	3.95×10^{2}	-1.76×10^{-1}	1.06×10^{3}
C_{y_β}	-5.51×10^{-1}	6.09×10^{2}	-5.50×10^{-1}	9.06×10^{2}
$C_{\ell_{\delta_a}}$	-4.51×10^{-2}	4.92×10^{2}	-4.01×10^{-2}	8.95×10^{2}
$C_{m_{\dot{\alpha}}}$	-1.90×10^{1}	2.48×10^{2}	-2.39×10^{1}	8.28×10^{2}
C_{y_o}	-9.60×10^{-3}	4.12×10^{2}	-8.89×10^{-3}	5.46×10^{2}
C_{n_o}	1.07×10^{-3}	1.26×10^{2}	1.07×10^{-3}	3.61×10^{2}
C_{m_α}	5.58×10^{-2}	2.54×10^{1}	1.07×10^{-1}	3.53×10^{2}
C_{ℓ_r}	-2.77×10^{-1}	1.07×10^{2}	-3.10×10^{-1}	3.09×10^{2}
$C_{\ell_{p_\alpha}}$	9.59×10^{-1}	3.06×10^{1}	1.48	2.53×10^{2}
$C_{z_{\alpha^2}}$	7.68	5.21×10^{1}	5.97	7.15×10^{1}
$C_{y_{\delta_r}}$	-4.70×10^{-2}	2.65×10^{1}	5.99×10^{-2}	6.16×10^{1}
$C_{n_{\alpha^2}}$	----	----	-8.12×10^{-2}	5.21×10^{1}
$C_{m_{\dot{\alpha}^2}}$	----	----	3.73×10^{-1}	3.57×10^{1}
C_{ℓ_o}	2.80×10^{-5}	2.67×10^{-1}	-1.97×10^{-4}	2.79×10^{1}
$C_{n_{\beta^3}}$	3.56×10^{-1}	2.09×10^{1}	1.07×10^{-1}	5.19
$C_{n_{\dot{\alpha}}}$	----	----	1.19×10^{-3}	4.03

tion of the aerodynamic coefficient time history estimates reveals, however, that the estimate fit is better in the longer data length case. C_m especially exhibits the best fit (Figure 6.30) for actual time history data that has significantly less well behaved variations. The coefficient estimates are also that much more remarkable because they represent estimates of two dimensional expansions in both α and β with simultaneous variations in both those variables. Two affects account for the improved parameter estimates:

a. A 50% increase in data length represents approximately a similar increase in useful information for identification of parameter values.

b. Simultaneous use of 7 measurements enables use of what information is available in cross mode measurements. This effect, although secondary, does contribute to the total information something not available in the separated lateral and longitudinal mode processing.

6.5 PREDICTION

The ultimate objective of all parameter identification techniques is the ability to use model parameter values estimated from one set of data to predict the responses of a different set of data. Of course, the operating range of the data to be predicted should not extend beyond the valid limits of the parameter estimates; within this constraint, the predicted response should closely approximate the measured response. For the model to be of engineering utility, it must not only be able to reproduce the data upon which it is based, but also be able to closely match responses to different inputs.

Figures 6.31 through 6.34 show the predicted and actual responses of the aircraft using parameter estimates from lateral/longitudinal response case 1 for lateral/longitudinal mode case 2 (described in Figure 6.2). The inputs are considerably different in form and amplitude between cases 1 and 2, which can be seen by comparing the time histories for both cases.

Orig. Tech Rep #2
5984

Smt fm glossy

Figure 6.30 Estimate of C_m vs. α for Different Inputs

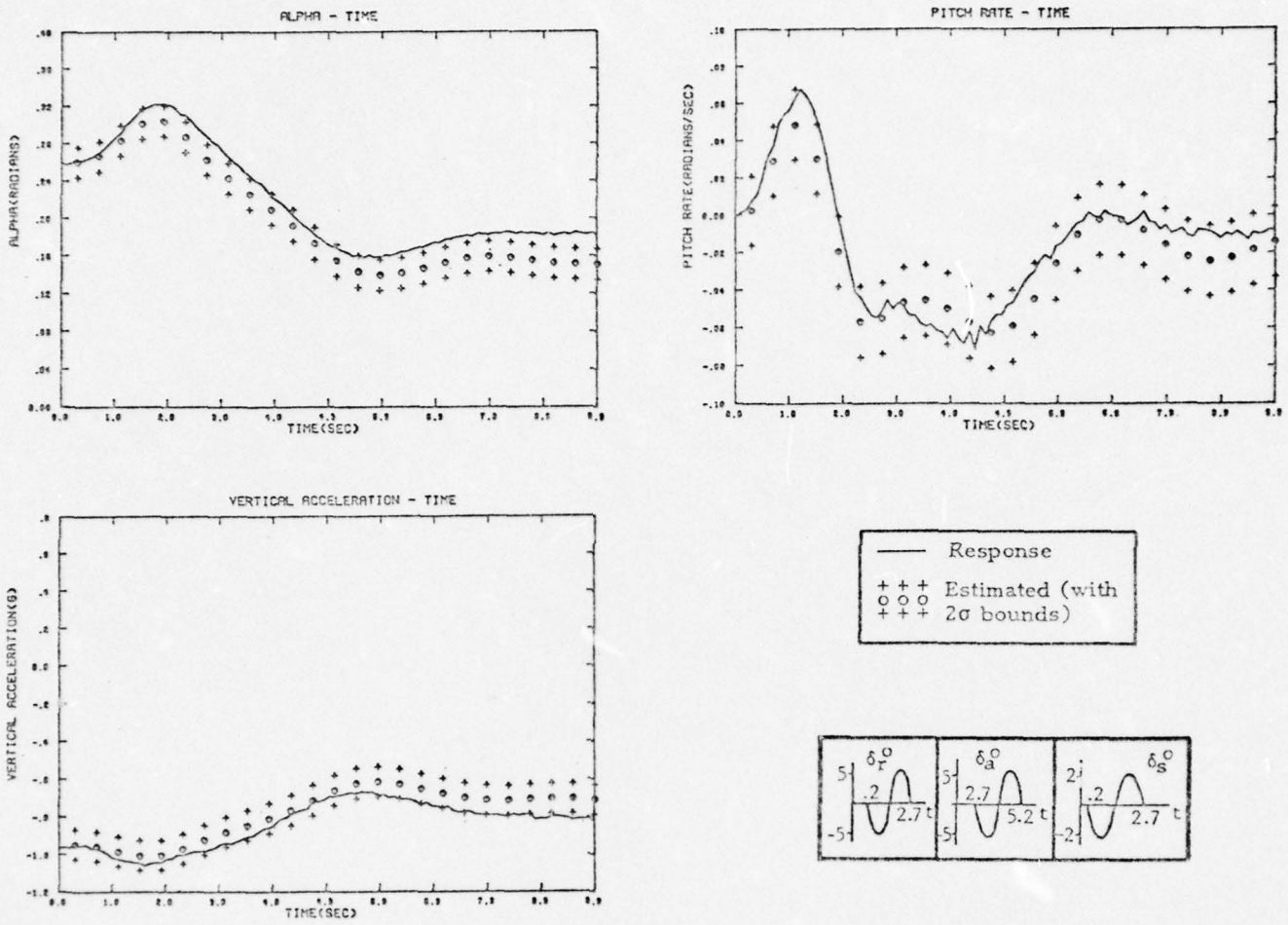

Figure 6.31 Longitudinal Predicted and Simulated Response to a Combined Stabilator/Aileron/Rudder Input (Longitudinal/Lateral Case 1, Ref. Fig. 6.2c).

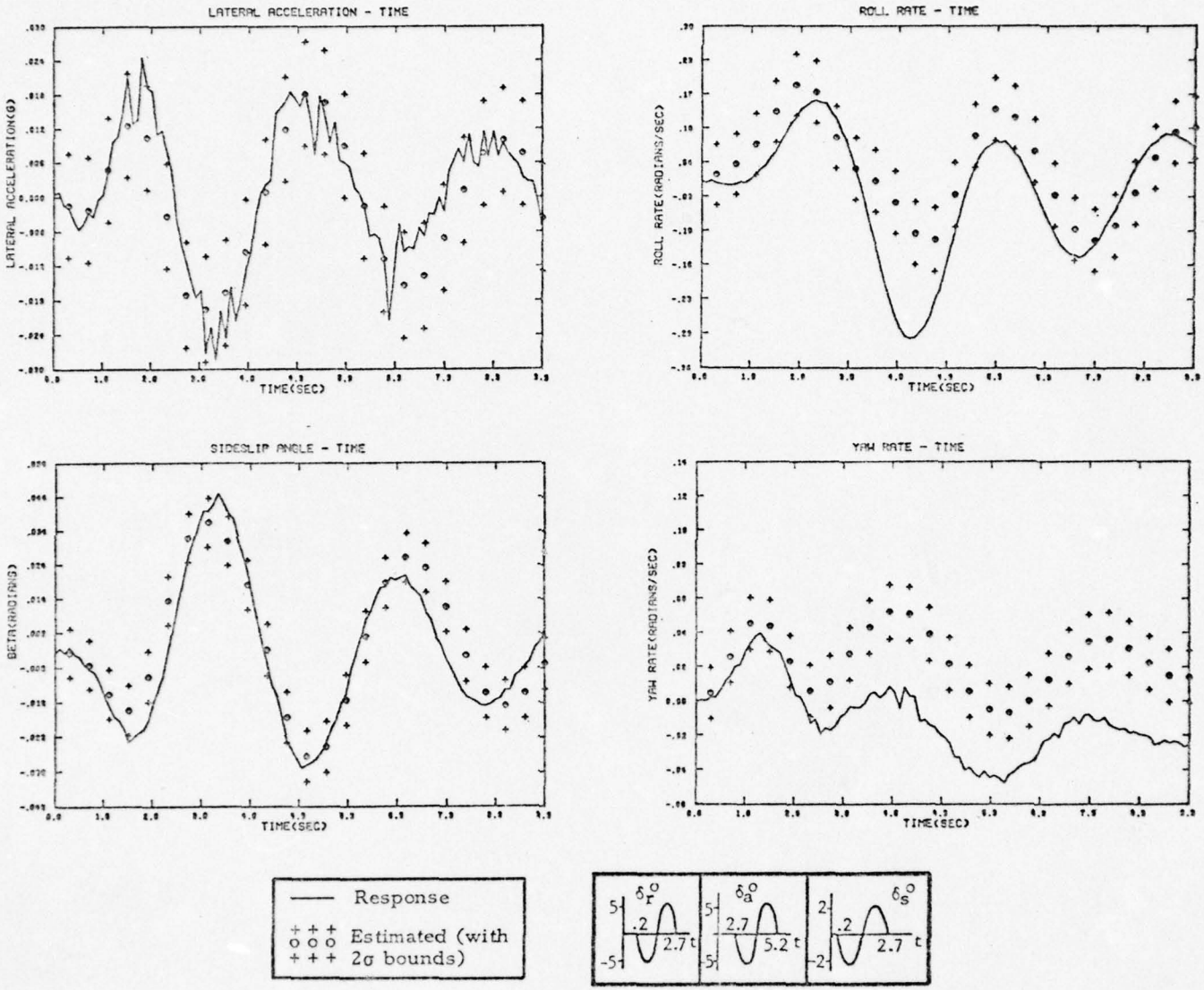

Figure 6.32 Lateral Predicted and Simulated Response to a Combined Stabilator/Aileron/Rudder Input (Longitudinal/Lateral Case 1 Estimated Parameters for Longitudinal/Lateral Case 2, Ref. Fig. 6.2c).

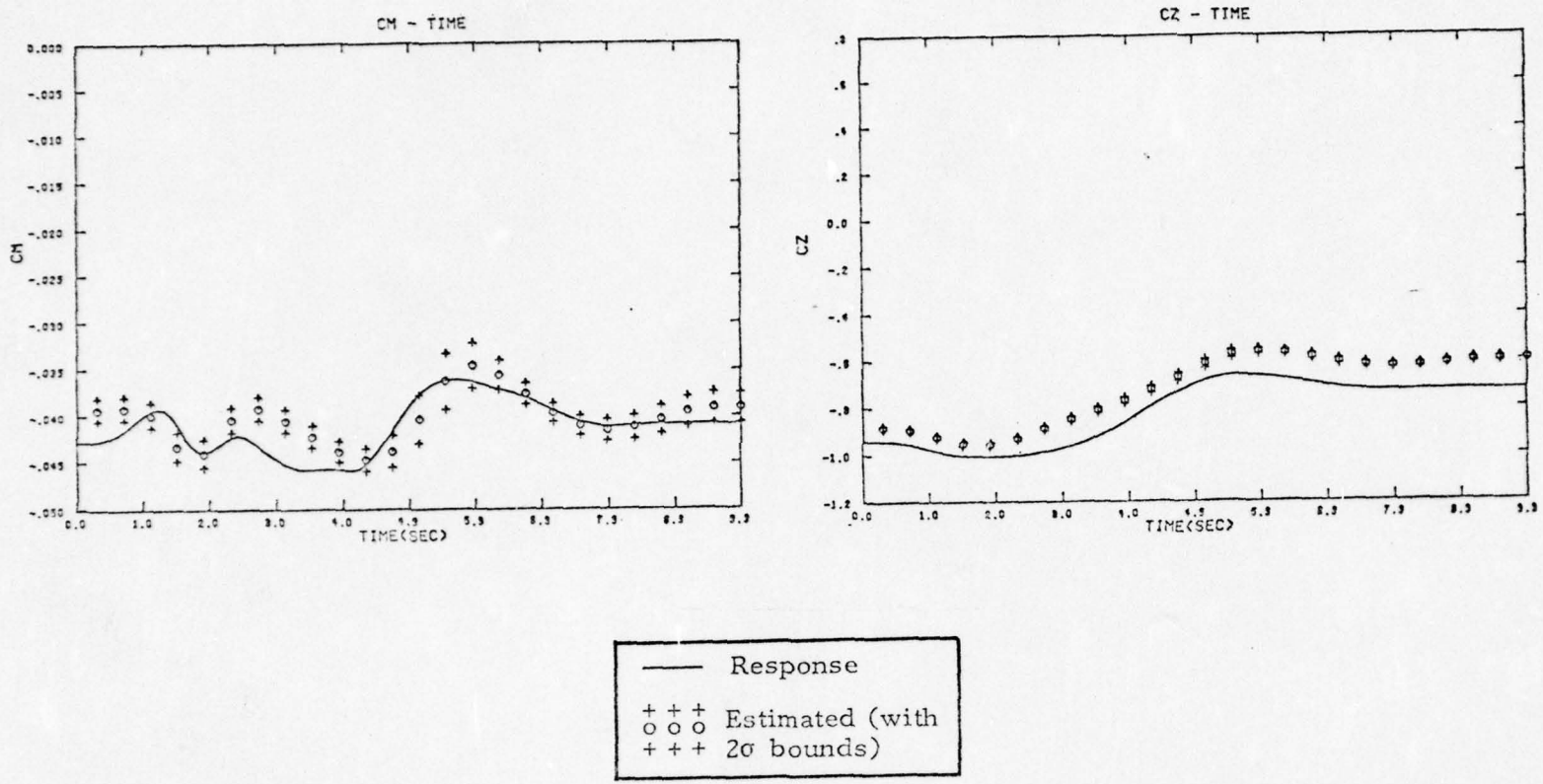

Figure 6.33 Longitudinal Predicted and Simulated Static Coefficient Response to a Combined Stabilator/Aileron/Rudder Input (Longitudinal/Lateral Case 1 Estimated Parameters for Longitudinal/Lateral Case 2 Prediction, Ref. Fig. 6.2c).

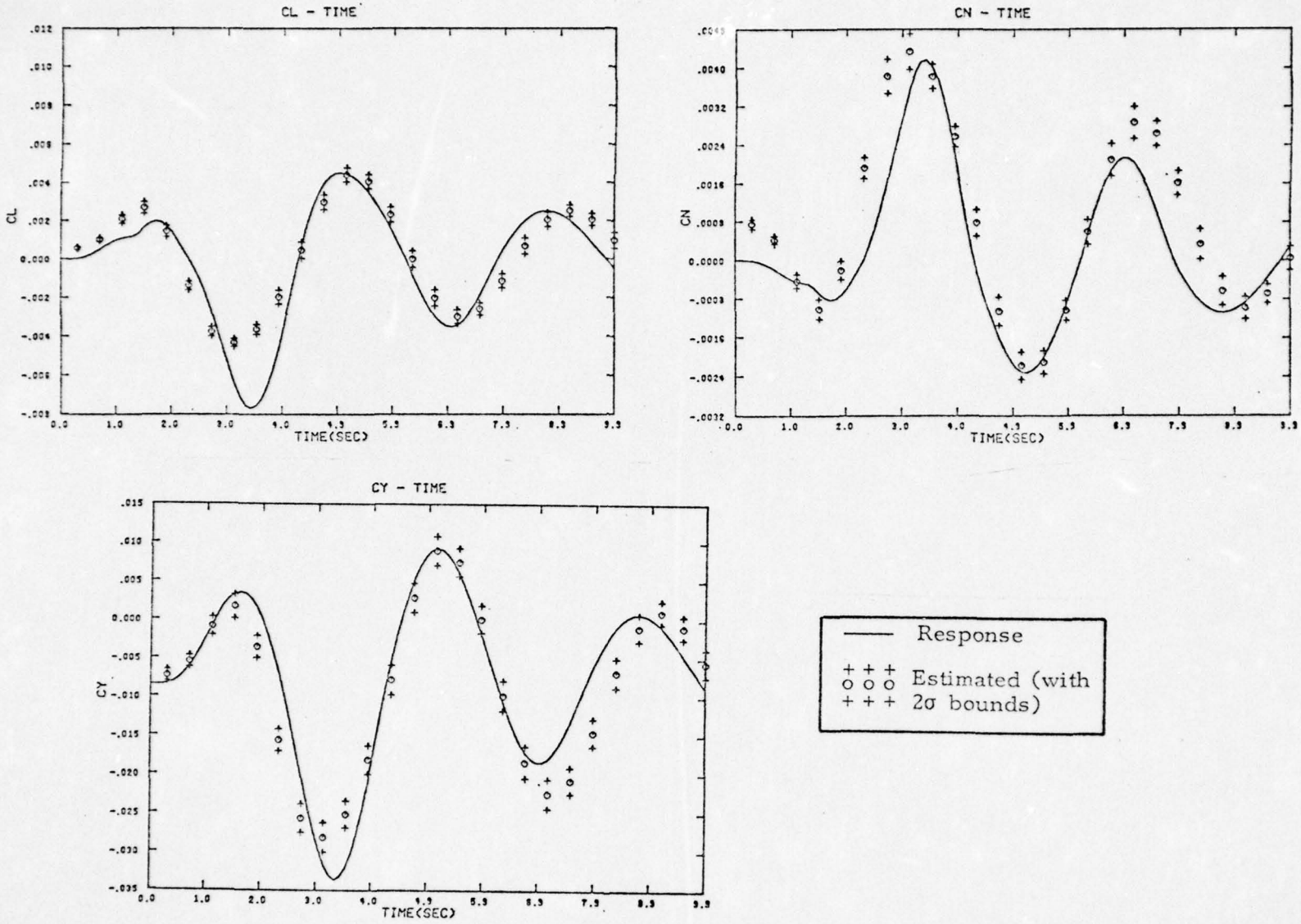

Figure 6.34 Lateral Predicted and Simulated Static Coefficient Response to a Combined Stabilator/Aileron/Rudder Input (Longitudinal/Lateral Case 1 Estimated Parameters for Longitudinal/Lateral Case 2 Prediction, Ref. Fig. 6.2c).

Although the measurement estimate fits for the prediction are not quite as good as the original parameter estimation data fit, the correspondence is, nevertheless, more than satisfactory. Even the aerodynamic coefficient time histories reveal remarkably good fits. An overall assessment of this relatively simple 31 parameter estimate model must be that it is successful in reproducing the far more complex simulation of real aircraft flight characteristics.

6.6 SUMMARY

This chapter demonstrates the use of a new procedure for the identification of stability and control parameters in the high angle-of-attack regime. The basis for development and verification of this procedure has been noisy data generated by a detailed nonlinear six degree-of-freedom simulator for the F-4 aircraft. This simulation has provided a "controlled" data capability which allows the flexibility to experiment with various identification problem solutions.

The method has been applied to various types of data noise, control inputs, flight conditions, and data lengths. Computation has been directed toward expansion and verification of the capability of the method, and detailed quantitative assessments of various trends have not, within the scope of this project, been possible.

a. The technique for isolating and estimating values of significant linear and nonlinear aircraft model parameters from realistic flight test data has been developed and demonstrated. The subset regression step gives the overall identification procedure the unique capability of being able to develop parameter estimates without any a priori knowledge of the model parameter values to be determined. Although some further development of this regression technique may be useful to improve structure estimation accuracy, the basic principal is found to significantly improve identification estimates.

b. The procedure is robust enough to yield reliable results in the presence of high levels of noise, both measurement and process.

c. Only significant parameters identifiable from the given data are estimated. Over-parameterization is thereby avoided, thus producing

more statistically reliable estimates, as well as eliminating much extra computation that would produce marginal benefit at best.

d. Effects of input design, estimate information aggregation, and data length are shown to be extremely important in determining the information available for parameter identification in a quantity of data. For example, input design results indicate that small amplitude sinusoidal stabilator deflections give good C_m vs. α nonlinear estimates. These estimates are further improved by increased data length.

e. In the most important test of any identification technique, the ability of the procedure to develop parameter estimates of a quality for excellent model predictions is demonstrated.

VII. CONCLUSIONS AND RECOMMENDATIONS

7.1 CONCLUSIONS

7.1.1 Summary of the Parameter Identification Procedure

The basic objective of this project has been the development and verification of techniques for identification of the stability and control coefficients of high performance aircraft in high angle-of-attack flight regimes. To meet this objective, the following three tasks have been completed:

1. Development of a detailed digital simulation of the dynamic response of an F-4 aircraft, including gust and instrumentation noise effects.

2. Application of an advanced regression program to determine the significant aerodynamic contributions to high angle-of-attack responses.

3. Implementation of a highly versatile version of the maximum likelihood parameter identification algorithm which estimates the values of significant stability and control coefficients for the high angle-of-attack flight regime.

The accomplishment of these tasks has demonstrated that significant aerodynamic contributions to complicated aircraft responses can be estimated by the sequential process of: (a) determining which effects are important (e.g., the regression phase), and (b) determining highly accurate parameter estimates of these effects (e.g., the identification phase). The importance of this new combined approach is that the source of many obstacles to identifying high angle-of-attack coefficients from flight data is avoided--namely, problems of identifiability and over-parameterization. This approach is not only useful for producing rapid determination of significant causes of complicated aircraft response, but also for identifying the parameters of a wider class of nonlinear systems than has previously been reported.

7.1.2 Specific Characteristics of the Integrated Process

Application of the model estimation program demonstrates a significant improvement in maximum likelihood efficiency, both in required computation and in accuracy of the results. The improvement in performance of the entire identification process is based on the following characteristics of the regression method:

1. The subset regression method selects parameters on their ability to match the measured response. By selecting the minimum number of variables to accomplish this match, the most significant variables are isolated.

2. The method yields a priori estimates from the data above, and does not itself require initial estimates. Though usually biased, the estimates given by the program are frequently better than a priori estimates from other sources.

3. The method gives significant evaluation of the estimated parameters, which serves an essential role in the final selection of a model structure to be used in the maximum likelihood algorithm.

4. The computational requirements of the regression algorithm are modest, and the algorithm can be used quickly to not only evaluate input designs, but also effects of measurement errors.

Subsequent applications of the maximum likelihood algorithm are optimized by introduction of the regression "pre-processing". The implementation of the maximum likelihood for this work can accept either linear or nonlinear aerodynamic expansions of the force and moment coefficients. Further, this algorithm can process parameters for only one dynamic equation or all six. The program includes calculations of parameter significance level.

7.1.3 Application to Simulated Data for the High Angle-of-Attack Stall/Post-Stall Regime

The evaluation of the integrated parameter identification process has been conducted with simulated data. The simulation is highly nonlinear and of much higher order than the identification models used. The measurement model is also highly nonlinear and not readily describable by linear error models for the entire flight regimes tested. Behavior of its modeling detail output of the simulation is regarded as equivalent to that obtained from actual flight test data, at least for the purposes of the identification evaluation.

The main conclusion of applying the identification procedure to the data is the predominant requirement for linear aerodynamic models, even for "nonlinear" regimes. Recognizing that such conditions may not be attainable, nonlinear models are required for large inputs where angle-of-attack and sideslip are simultaneously excited, such as would be obtained for large amplitude sinusoidal inputs or special maneuvers. The regression step is essential since it indicates whether or not nonlinear contributions are required. The ability to recognize and identify such nonlinear terms is requisite for determination of coefficients such as C_m and C_n.

Primary emphasis has been placed on the identification of static force and moment coefficients. Greatest errors have been found in estimates of the dynamic rate derivatives and control effectiveness derivatives. These errors are attributed to the relatively low rates which were obtained for inputs to identify the important static derivatives. Inputs may be modified, using input design algorithms discussed in the report, to improve the estimation of these derivatives. It must be noted that the errors of the dynamic derivatives which were obtained could not be found by comparing time history matches of the measurement of rate, as these were excellent in all cases. Only with comparison of the actual parameter time histories were these errors observed.

Techniques for improving parameter estimates include input design, increased data length (where possible), and data aggregation (e.g., statistically combining results of several tests). Such modifications have a significant effect

on flight test planning and should be available for identification of important but difficult to excite parameters. The integrated parameter identification process as developed in this work is amenable to such flight test design, using procedures detailed in the previous chapters.

The identification procedure is robust with respect to process and measurement noise. For this reason, the option of identifying process noise statistics was not included in the maximum likelihood implementation (and, hence, a substantial reduction in computer time).

The confidence established in the procedure led to evaluation of the identification results by a prediction criterion. Specifically, the parameter estimates from a specific lateral maneuver with one input are used to predict the response of the simulation to another input (for roughly the same flight regime). This prediction capability was verified with excellent results.

In summary, it is concluded that the application of the integrated parameter identification process developed for the high angle-of-attack stall/post-stall regime offers significant improvements in the ability to identify not only parameters, but also the entire system structure and parameters.

7.2 RECOMMENDATIONS

The method developed under this contract promises to be a valuable tool for Navy flight test data reduction requirements. As discussed, the procedure is highly oriented toward user needs and applicable to both linear and nonlinear models of typical Navy aircraft. This versatility is essential for many operations, tests, and evaluation requirements for high performance aircraft. Typical applications, for example, include:

1. Documentation of aircraft stability and control characteristics for critical flight regimes (e.g., high angle-of-attack) or operations (e.g., carrier landing). Such documentation is required for design evaluation, transfer function formulation (useful in handling quality evaluation), and maneuver envelope expansion.

2. Determination of effects of special design modifications such as leading edge slats, advanced avionics control systems, or modified aircraft instrumentation. The method developed for this project will be applicable for investigating and evaluating such modifications which are incorporated to improve maneuverability or handling qualities.

The method and analysis discussed in this report is also capable of being expanded to particular objectives. Such objectives include:

1. Combination of the regression algorithm with the maximum likelihood program to give one single program. The requirement here is to design the interface between the two techniques such that the amount of "tuning" the two methods to each other is included automatically.

2. Approximation analysis to the maximum likelihood algorithm to allow on-line and/or real time capability to provide faster acquisition of parameters. The requirement is to more completely model the data links of on-board or ground-based measurement systems and to modify the maximum likelihood algorithm to require less computer capacity while operating in real time.

3. Continuation of input design development for nonlinear systems to reduce flight test time as well as improve parameter estimates. The requirement is to relate the orthogonal polynomial representation to meaningful aerodynamic flight test terms.

4. Implementation of maximum likelihood techniques for fault detection of multivariable systems. The requirement is classification of faults and their relationship to parameters of the system.

5. Optimization of control surface and instrument location. The maximum likelihood technique uses several functions which depend on control surface locations and instrument location. Optimization of these functions will lead to strategies for not only improving the iden-

tification process, but also for the general control synthesis problem of light weight fighters, for example. Such aircraft must make optimum use of control surfaces for satisfactory maneuverability.

6. Modification of the models for aircraft could easily be made to extend the integrated parameter identification to missiles, RPV, or VTOL aircraft.

7. Other vehicles which can be treated, without extensive development, are surface ships (conventional, surface effect ships, semi-submerged hull designs, and hydrofoils) as well as submarines. Such systems are well known to be susceptible to significant nonlinear hydrodynamic nonlinear forces and moments.

8. One promising application of identification is the determination of aircraft engine parameters. The high performance requirements of such engines is placing stringent accuracy requirements on their design and test. The potentials of engine multi-variable control augment these accuracy goals. Modeling and identification of turbine dynamics, aerodynamics, and thermodynamics could greatly aid in achieving these requirements.

APPENDIX A
MAXIMUM LIKELIHOOD IDENTIFICATION OF PARAMETERS

A.1 INTRODUCTION

The maximum likelihood method is one of the most flexible techniques in statistics for identification of parameters from input-output data. Suppose it is possible to make a set of observations on a system, whose model has p unknown parameters θ. For any given set of values of the parameters θ from the feasible set Θ, we can assign a probability $p(Z|\theta)$ to each outcome Z. If the outcome of an actual experiment is z, it is of interest to know which sets of values of θ might have led to these observations. This concept is embedded in the likelihood function $\mathscr{L}(\theta|z)$. This function is of fundamental importance in estimation theory because of the likelihood principle of Fisher and others [40-42] which states that if the system model is correct, all information about unknown parameters is contained in the likelihood function. The maximum likelihood method finds a set of parameters $\hat{\theta}$ to maximize this likelihood function

$$\hat{\theta} = \max_{\theta \varepsilon \Theta} \mathscr{L}(\theta/z) \tag{A.1}$$

In other words, the probability of the outcome z is higher with parameters $\hat{\theta}$ in the model than with any other values of parameters from the feasible set. Usually it is more convenient to work with the logarithm of the likelihood function (it is possible to do so because the logarithm is a strictly monotonic function).

The great asset of the maximum likelihood method is that it can be used with linear or nonlinear models in the presence of process and measurement noise. The maximum likelihood estimates are asymptotically unbiased, consistent and efficient.

A.2 GENERAL NONLINEAR SYSTEMS

Consider the general nonlinear aircraft equations of motion

$$\dot{x} = f(x,u,\theta,t) + \Gamma(\theta,t)w \qquad 0 \leq t \leq T$$

$$E(x(0)) = x_o(\theta)$$

$$E\{(x(0) - x_o(\theta))(x(0) - x_o(\theta))^T\} = P_o(\theta) \qquad (A.2)$$

where

$x(t)$ is n x 1 state vector

$u(t)$ is ℓ x 1 input vector

θ is p x 1 vector of unknown parameters

Γ is n x q process noise distribution matrix

$w(t)$ is q x 1 random process noise vector

Sets of m measurements $y(t_k)$ are taken at discrete times t_k

$$y(t_k) = h(x(t_k),u(t_k),\theta,t_k) + v(t_k)$$

$$k = 1,2,3,\ldots,N \qquad (A.3)$$

$w(t)$ and $v(t_k)$ are Gaussian random noises with the following properties

$$E(w(t)) = 0 \qquad E(v(t_k)) = 0 \qquad E(w(t)\ v^T(t_k)) = 0$$

$$E(w(t)\ w^T(\tau)) = Q(\theta,t)\ \delta(t-\tau),\ E(v(t_j)\ v^T(t_k)) = R(\theta,t_j)\delta_{jk} \qquad (A.4)$$

The unknown parameters are supposed to occur in the functions f and h and in matrices Γ, Q, R, P_o and x_o. In the analysis to follow, the model and the functional form of f and h is assumed known correctly.

The set of observations $y(t_1),y(t_2),\ldots,y(t_N)$ constitutes the outcome Z in this case. The likelihood function for θ, which has the same form as the probability of the outcome z for a certain value of parameters θ, is given by

$$\mathcal{L}(\theta|z) \triangleq p(z|\theta)$$

$$= p(y(t_1),\ y(t_2),\ldots,y(t_N)|\theta)$$

$$= p(Y_N|\theta) \qquad (A.5)$$

where

$$Y_k = \{y(t_1),\ldots,y(t_k)\},\ k = 1,2,\ldots,N$$

$$p(Y_N|\theta) = p(y(t_N)|Y_{N-1},\theta)\cdot p(Y_{N-1}|\theta)$$

$$= p(y(t_N)|Y_{N-1},\theta)\ p(y(t_{N-1})|Y_{N-2},\theta)\ p(Y_{N-2}|\theta)$$

$$= \prod_{i=1}^{N} p(y(t_i)|Y_{i-1},\theta) \qquad (A.6)$$

The log-likelihood function is

$$\log(\mathcal{L}(\theta|z)) = \sum_{i=1}^{N} \log\{p(y(t_i)|Y_{i-1},\theta)\} + \text{constant} \qquad (A.7)$$

To find the probability distribution of $y(t_i)$ given Y_{i-1} and θ, the mean value and covariance are determined first.

$$E(y(t_i)|Y_{i-1},\theta) \triangleq \hat{y}(i/i-1) \qquad (A.8)$$

The expected value or the mean is the best possible estimate of measurements at a point given the measurements until the previous point.

$$\text{cov}(y(t_i)|Y_{i-1},\theta) = E\{(y(t_i)-\hat{y}(i/i-1))(y(t_i)-\hat{y}(i/i-1))^T\}$$

$$\triangleq E\{\nu(i)\ \nu(i)^T\}$$

$$\triangleq B(i) \qquad (A.9)$$

$\nu(i)$ are the innovations at point i and $B(i)$ is the innovations covariance. Since

$$y(t_i) - E(y(t_i)|Y_{i-1},\theta) = \nu(i) \tag{A.10}$$

it follows that $y(t_i)$ given Y_{i-1} and θ have the same distribution as $\nu(i)$. Kailath [44] has shown that as the sampling rate is increased, the innovations $\nu(i)$ tend towards having a Gaussian density. Assuming a sufficiently high sampling rate, the distribution of $\nu(i)$ and, therefore, $y(t_i)$ given Y_{i-1} and θ is Gaussian, i.e.,

$$p(y(t_i)|Y_{i-1},\theta) \cong \frac{\exp\left\{-\frac{1}{2}\nu(i)^T B^{-1}(i)\ \nu(i)\right\}}{(2\pi)^{m/2}|B(i)|^{1/2}} \tag{A.11}$$

$$\log\{p(y(t_i)|Y_{i-1},\theta)\} = -\frac{1}{2}\nu(i)^T B^{-1}(i)\nu(i) - \frac{1}{2}\log|B(i)| + \text{constant} \tag{A.12}$$

The log-likelihood function of Equation (A.7) *can be written as*

$$\log(\mathscr{L}(\theta|z)) = -\frac{1}{2}\sum_{i=1}^{N}\{\nu^T(i)\ B^{-1}(i)\ \nu(i) + \log|B(i)|\} \tag{A.13}$$

An estimate of the unknown parameters is obtained by maximizing the likelihood function or the log-likelihood function from the feasible set of parameter values.

$$\hat{\theta} = \max_{\theta\in\Theta} \log(\mathscr{L}(\theta|z)) \tag{A.14}$$

$$= \max_{\theta\in\Theta}\left[-\frac{1}{2}\sum_{i=1}^{N}\{\nu^T(i)B^{-1}(i)\nu(i) + \log|B(i)|\}\right] \tag{A.15}$$

The log-likelihood function depends on the innovations and their covariance. To optimize the likelihood function, a way must be found for determining these quantities. Both innovations and their covariance are outputs of an

extended Kalman filter. This required Kalman filter is developed now.

The extended Kalman filter is conventionally divided into two parts. In the first part, called the prediction equations, the state equations and state estimate covariance equations are propagated in time from one measurement point to the next. In the second part, called the measurement update equations, the measurements and associated measurement noise covariances are used to improve state estimates. The covariance matrix is also updated at this point to reflect the additional information obtained from the measurements.

Prediction Equations

The state prediction is done using the equations of motion (A.2). Starting at time t_{i-1} with current estimate $\hat{x}(i-1|i-1)$ of the state $x(t_i)$ and the covariance $P(i-1|i-1)$, the following equations are used to find the predicted state $\hat{x}(i|i-1)$ and the associated covariance $P(i|i-1)$; see Bryson and Ho [45].

$$\frac{d}{dt}\,\hat{x}(t|t_{i-1}) = f(\hat{x}(t|t_{i-1}),u(t),\theta,t) \tag{A.16}$$

$$\dot{P}(t|t_{i-1}) = F(t)\,P(t|t_{i-1}) + P(t|t_{i-1})\,F^{T}(t) + \Gamma Q \Gamma^{T} \tag{A.17}$$

$$t_{i-1} \leq t \leq t_i$$

The nxn matrix F is obtained by linearizing f about the best current estimate

$$F(t) = \frac{\partial f(\hat{x}(t|t_{i-1}),u(t),\theta,t)}{\partial \hat{x}(t|t_{i-1})} \tag{A.18}$$

Using (A.16) to (A.18), we can obtain

$$\hat{x}(t_i|t_{i-1}) \triangleq \hat{x}(i|i-1)$$

$$\text{and} \quad P(t_i|t_{i-1}) \triangleq P(i|i-1) \tag{A.19}$$

Thereafter, the measurement update equations are used.

Measurement Update Equations

The covariance and state estimate are updated using the measurements. The necessary relations are derived by Bryson and Ho [45] and are presented here without proof. The innovation and its covariance are

$$\nu(i) = y(i) - h(\hat{x}(i|i-1),\ u(t_i),\ \theta,\ t_i) \tag{A.20}$$

$$B(i) = H(i)\ P(i|i-1)\ H^T(i) + R \tag{A.21}$$

where H is obtained by linearizing h,

$$H(i) = \frac{\partial h(\hat{x}(i|i-1), u(t_i, \theta, t_i)}{\partial \hat{x}(i|i-1)} \tag{A.22}$$

The Kalman gain and the state update equations are

$$K(i) = P(i|i-1)\ H^T(i)\ B^{-1}(i) \tag{A.23}$$

$$\hat{x}(i|i) = \hat{x}(i|i-1) + K(i)\ \nu(i) \tag{A.24}$$

Finally, P(i|i), the covariance of error in updated state, is obtained by

$$P(i|i) = (I-K(i)\ H(i))\ P(i|i-1) \tag{A.25}$$

One can now return to the time update or prediction equations.

A.3 OPTIMIZATION PROCEDURE

Many possible numerical procedures can be used for this optimization problem. Modified Newton-Raphson [20] or Quasilinearization [21] have been found by experience to give quicker convergence than most procedures like the conjugate gradient or the Davison method. The modified Newton-Raphson is a

second order gradient procedure requiring computation of first and second order partials of the log-likelihood function.

$$\frac{\partial \log (\mathscr{P}(\theta|z))}{\partial \theta_j} = -\sum_{i=1}^{N} \left\{ \nu^T(i) B^{-1}(i) \frac{\partial \nu(i)}{\partial \theta_j} - \frac{1}{2} \nu^T(i) B^{-1}(i) \frac{\partial B(i)}{\partial \theta_j} B^{-1}(i) \nu(i) \right.$$

$$\left. + \frac{1}{2} \mathrm{Tr}\left(B^{-1}(i) \frac{\partial B(i)}{\partial \theta_j} \right) \right\} \qquad (A.26)$$

Also

$$\frac{\partial^2 \log (\mathscr{P}(\theta|z)}{\partial \theta_j \partial \theta_k} = -\sum_{i=1}^{N} \left\{ \frac{\partial \nu^T(i)}{\partial \theta_k} B^{-1}(i) \frac{\partial \nu(i)}{\partial \theta_j} - \frac{\partial \nu^T(i)}{\partial \theta_k} B^{-1}(i) \frac{\partial B(i)}{\partial \theta_j} B^{-1}(i) \nu(i) \right.$$

$$- \frac{\partial \nu(i)}{\partial \theta_j} B^{-1}(i) \frac{\partial B(i)}{\partial \theta_k} B^{-1}(i) \nu(i)$$

$$+ \nu^T(i) B^{-1}(i) \frac{\partial B(i)}{\partial \theta_j} B^{-1}(i) \frac{\partial B(i)}{\partial \theta_k} B^{-1}(i) \nu(i)$$

$$- \frac{1}{2} \mathrm{Tr}\left[B^{-1}(i) \frac{\partial B(i)}{\partial \theta_j} B^{-1}(i) \frac{\partial B(i)}{\partial \theta_k} \right] + \frac{\partial^2 \nu(i)}{\partial \theta_j \partial \theta_k} B^{-1}(i) \nu(i)$$

$$- \nu^T(i) B^{-1}(i) \frac{\partial^2 B(i)}{\partial \theta_j \partial \theta_k} B^{-1}(i) \nu(i)$$

$$\left. + \frac{1}{2} \mathrm{Tr}\left(B^{-1}(i) \frac{\partial^2 B(i)}{\partial \theta_j \partial \theta_k} \right) \right\} \quad j,k = 1,2,\ldots,p \qquad (A.27)$$

The last three terms in the equation for second partial of the log-likelihood function involve second partials of innovation and its covariance. Those terms are usually dropped. So the second partial is approximated by

$$\frac{\partial^2 \log(\mathcal{L}(\theta|z))}{\partial\theta_j\,\partial\theta_k} \cong -\sum_{i=1}^{N}\left\{\frac{\partial\nu^T(i)}{\partial\theta_j}B^{-1}(i)\frac{\partial\nu(i)}{\partial\theta_k} - \frac{\partial\nu^T(i)}{\partial\theta_k}B^{-1}(i)\frac{\partial B(i)}{\partial\theta_j}B^{-1}(i)\nu(i)\right.$$

$$-\frac{\partial\nu(i)}{\partial\theta_j}B^{-1}(i)\frac{\partial B(i)}{\partial\theta_k}B^{-1}(i)\nu(i)$$

$$+\nu^T(i)B^{-1}(i)\frac{\partial B(i)}{\partial\theta_j}B^{-1}(i)\frac{\partial B(i)}{\partial\theta_k}B^{-1}(i)\nu(i)$$

$$\left.-\frac{1}{2}\,\mathrm{Tr}\left[B^{-1}(i)\frac{\partial B(i)}{\partial\theta_j}B^{-1}(i)\frac{\partial B(i)}{\partial\theta_k}\right]\right\} \qquad (A.28)$$

The gradients of innovation and its covariance for parameter θ_j are (Equations (A.20) and (A.21))

$$\frac{\partial\nu(i)}{\partial\theta_j} = -\left.\frac{\partial h}{\partial x}\right|_{x=\hat{x}(i|i-1)}\frac{\partial\hat{x}(i|i-1)}{\partial\theta} - \frac{\partial h}{\partial\theta} \qquad (A.29)$$

$$j = 1,2,\ldots,p\ ;\ i = 1,2,\ldots,N$$

$$\frac{\partial B(i)}{\partial\theta_j} = \frac{\partial H(i)}{\partial\theta_j}P(i|i-1)H^T(i) + H(i)\frac{\partial P(i|i-1)}{\partial\theta_j}H^T(i)$$

$$+H(i)\,P(i|i-1)\frac{\partial H^T(i)}{\partial\theta_j} + \frac{\partial R}{\partial\theta_j} \qquad (A.30)$$

$$j = 1,2,\ldots,p$$

$$i = 1,2,\ldots,N$$

Recursive equations can be obtained for gradients of the predicted state and its covariance. This is done in stages by using the prediction and measurement update equations of Kalman filter. Differentiating (A.16) to (A.18) with respect to θ_j

$$\frac{d}{dt}\frac{\partial \hat{x}(t|t_{i-1})}{\partial \theta_j} = \frac{\partial f(\hat{x}(t|t_{i-1}),u(t),t,\theta)}{\partial \theta_j} + \frac{\partial f(\hat{x}(t|t_{i-1}),u(t),t,\theta)}{\partial \hat{x}(t|t_{i-1})} \times \frac{\partial \hat{x}(t|t_{i-1})}{\partial \theta_j}$$

$$\frac{\partial \hat{x}(0|0)}{\partial \theta_j} = \frac{\partial x_o(\theta)}{\partial \theta_j} \tag{A.31}$$

$$\frac{d}{dt}\frac{\partial P(t|t_{i-1})}{\partial \theta_j} = \frac{\partial F(t)}{\partial \theta_j} P(t|t_{i-1}) + F(t)\frac{\partial P(t|t_{i-1})}{\partial \theta_j} + \frac{\partial P(t|t_{i-1})}{\partial \theta_j} F^T(t) + P(t|t_{i-1})\frac{\partial F^T(t)}{\partial \theta_j} + \frac{\partial \Gamma}{\partial \theta_j} Q\Gamma^T + \Gamma\frac{\partial Q}{\partial \theta_j}\Gamma^T + \Gamma Q\frac{\partial \Gamma^T}{\partial \theta_j}$$

$$\frac{\partial P(0|0)}{\partial \theta_j} = \frac{\partial P_o(\theta)}{\partial \theta_j} \qquad t_{i-1} \le t \le t \tag{A.32}$$

$$\frac{\partial F(t)}{\partial \theta_j} = \frac{\partial^2 f(\hat{x}(t|t_{i-1}),u(t),\theta,t)}{\partial \theta_j\, \partial \hat{x}(t|t_{i-1})} \qquad j = 1,2,\ldots,p \tag{A.33}$$

The sensitivity functions are updated at measurement points by differentiating (A.22) to (A.25) with respect to θ_j.

$$\frac{\partial H(i)}{\partial \theta_j} = \frac{\partial^2 h(\hat{x}(i|i-1),u(t_i),\theta,t_i)}{\partial \theta_j\, \partial \hat{x}(i|i-1)} \tag{A.34}$$

$$\frac{\partial K(i)}{\partial \theta_j} = \frac{\partial P(i|i-1)}{\partial \theta_j} H^T(i)\, B^{-1}(i) + P(i|i-1)\frac{\partial H^T(i)}{\partial \theta_j} B^{-1}(i) - P(i|i-1)\, H^T(i)\, B^{-1}(i)\frac{\partial B(i)}{\partial \theta_j} B^{-1}(i) \tag{A.35}$$

$$\frac{\partial \hat{x}(i|i)}{\partial \theta_j} = \frac{\partial \hat{x}(i|i-1)}{\partial \theta_j} + \frac{\partial K(i)}{\partial \theta_j} \nu(i) + K(i) \frac{\partial \nu(i)}{\partial \theta_j} \tag{A.36}$$

$$\frac{\partial P(i|i)}{\partial \theta_j} = (I-K(i)\ H(i))\ \frac{\partial P(i|i-1)}{\partial \theta_j} - \frac{\partial K(i)}{\partial \theta_j} H(i)\ P(i|i-1)$$

$$- K(i)\ \frac{\partial H(i)}{\partial \theta_j} P(i|i-1) \tag{A.37}$$

$$j = 1,2,3,\ldots,p$$

The negative of the matrix of second partials of the log-likelihood function is called the information matrix M. The step size $\Delta\theta$ for parameter estimates is given by

$$\Delta\theta = M^{-1} \frac{\partial \log (\mathscr{L}(\theta|z)}{\partial \theta} \tag{A.38}$$

The information matrix provides a lower bound on parameter estimate covariances, i.e.,

$$E(\theta-\hat{\theta})\ (\theta-\hat{\theta})^T \geq M^{-1} \tag{A.39}$$

This is called the Cramer-Rao lower bound. [46,47] The maximum likelihood estimates approach this bound asymptotically.

A.4 LINEAR SYSTEMS

In a linear system, the functions f and h are defined as

$$f(x,u,\theta,t) \triangleq F(\theta,t)x + G(\theta,t)u$$

$$\text{and} \quad h(x,u,\theta,t) \triangleq H(\theta,t)x + D(\theta,t)u \tag{A.40}$$

In this case, it has been shown that if the model is correct, the innovations are white and have Gaussian density at the true values of the parameters. Therefore, the assumption of fast sampling rate is not necessary.

The basic algorithm is the same. However, some of the equations can now be simplified. The equivalence between F(t) and H(i) of (A.18) and (A.22) and F(θ,t) and H(θ,t_i) of (A.40) is obvious. Equations (A.16) and (A.20) now become

$$\frac{d}{dt}\hat{x}(t|t_{i-1}) = F(\theta,t)\,\hat{x}(t|t_{i-1}) + G(\theta,t)\,u(t) \tag{A.41}$$

and

$$\nu(i) = y(i) - H(\theta,t_i)\,\hat{x}(i|i-1) - D(\theta,t_i)\,u(t_i) \tag{A.42}$$

Equations (A.29) and (A.31) can be written as

$$\frac{\partial \nu(i)}{\partial \theta_j} = - H(\theta,t_i)\,\frac{\partial \hat{x}(i|i-1)}{\partial \theta_j} - \frac{\partial H(\theta,t_i)}{\partial \theta_j}\,\hat{x}(i|i-1)$$

$$- \frac{\partial D(\theta,t_i)}{\partial \theta_j}\,u(t_i) \tag{A.43}$$

and

$$\frac{d}{dt}\frac{\partial \hat{x}(t|t_{i-1})}{\partial \theta_j} = F(\theta,t)\,\frac{\partial \hat{x}(t|t_{i-1})}{\partial \theta_j} + \frac{\partial F(\theta,t)}{\partial \theta_j}\,\hat{x}(t|t_{i-1})$$

$$+ \frac{\partial G(\theta,t)}{\partial \theta_j}\,u(t) \tag{A.44}$$

All other equations remain the same.

There is considerable reduction in computation requirement for time-invariant linear system. In this case, matrices F, G, H, D, Γ, Q and R and

their derivatives with respect to parameters are constant. Gupta [48] has shown that the computation of state sensitivities can be reduced to many fewer equations. Similar reductions are possible in the computation of covariance sensitivities.

A.5 TIME INVARIANT LINEAR SYSTEMS IN STATISTICAL STEADY STATE

In many aircraft applications, the Kalman filter is in steady state for the duration of the experiment. This occurs when the Kalman filter is in operation for a sufficiently long time and the process and measurement noise covariances do not change. The Kalman gain and the innovations and the state covariances approach constant values. The time update and measurement update equations for the covariances are

$$\frac{d}{dt} P(t|t_{i-1}) = FP(t|t_{i-1}) + P(t|t_{i-1})F^T + \Gamma Q \Gamma^T \tag{A.45}$$

$$K = P(i|i-1)H^T B^{-1} \tag{A.46}$$

$$B = HP(i|i-1)H^T + R \tag{A.47}$$

$$P(i|i) = (I-KH)\, P(i|i-1) \tag{A.48}$$

By definition of the steady state

$$P(i-1|i-1) = P(i|i)$$

Therefore, from (A.45)

$$P(i|i-1) = e^{F\Delta t}\, P(i-1|i-1)\, e^{F^T\Delta t} + \int_{t_{i-1}}^{t_i} e^{F(t_i-\tau)}\, \Gamma Q \Gamma^T e^{F^T(t_i-\tau)} d\tau \tag{A.49}$$

$$= e^{F\Delta t}\, (I-KH)\, P(i|i-1) e^{F^T\Delta t} + \int_{t_{i-1}}^{t_i} e^{F(t_i-\tau)} \Gamma Q \Gamma^T\, e^{F^T(t_i-\tau)} d\tau$$

$$\triangleq \varphi(\Delta t)\ (I-KH)\ P(i|i-1)\ \varphi(\Delta t) + Q' \qquad (A.49)$$

$$= \varphi(\Delta t)\ (P(i|i-1) - KBK^T)\ \varphi(\Delta t) + Q'$$

Using (A.46), (A.47) and (A.49), we can solve for P(i|i-1) and then find K and B. Also, it can be shown that

$$\frac{\partial P}{\partial \theta_j} = A_1 \frac{\partial P}{\partial \theta_j} A_1^T + A_2 - \varphi P A_3 P \varphi^T \qquad (A.50)$$

$$\frac{\partial K}{\partial \theta_j} = (I-KH) \frac{\partial P}{\partial \theta_j} H^T (HPH^T + R)^{-1} + A_2 \qquad (A.51)$$

$$\frac{\partial B}{\partial \theta_j} = \frac{\partial H}{\partial \theta_j} PH^T + H \frac{\partial P}{\partial \theta_j} H^T + HP \frac{\partial H^T}{\partial \theta_j} + \frac{\partial R}{\partial \theta_j} \qquad (A.52)$$

where

$$A_1 = \varphi(I-KH)$$

$$A_2 = \frac{\partial \varphi}{\partial \theta_j} (I-KH) P \varphi^T + \varphi (I-KH) P \frac{\partial \varphi^T}{\partial \theta_j} - \varphi K \frac{\partial H}{\partial \theta_j} P \varphi^T + \frac{\partial Q'}{\partial \theta_j}$$

$$A_3 = \frac{\partial H^T}{\partial \theta_j} B^{-1} H + H^T B^{-1} \frac{\partial H}{\partial \theta_j} PH^T + HP \frac{\partial H^T}{\partial \theta_j} + \frac{\partial R}{\partial \theta_j} B^{-1} H \qquad (A.53)$$

$$P \triangleq P(i|i-1)$$

Thus, it is possible to solve for $\frac{\partial P}{\partial \theta_j}$ using (A.50) and then find $\frac{\partial K}{\partial \theta_j}$ and $\frac{\partial B}{\partial \theta_j}$ from (A.51) and (A.52). (A.50) is a linear equation in $\frac{\partial P}{\partial \theta_j}$ and the coefficient of the unknown matrix does not depend on the parameter θ_j. Thus, the sensitivity of state covariance matrix can be determined very quickly for all parameters. Once the sensitivity of P, K and B for unknown parameters

is determined, only state sensitivity equations need to be updated. The computation of state sensitivity functions can be reduced to many fewer equations as pointed out in Section A.4.

An approximation suggested by Mehra [34] simplifies the problem further. The unknown parameters are defined to include elements in K and B matrices instead of Q and R. Optimizing the log-likelihood function for parameters in B gives

$$\hat{B} = \frac{1}{N} \sum_{i=1}^{N} \nu(i)\ \nu^T(i) \tag{A.54}$$

The gradient of the log-likelihood function with respect to other unknown parameters is

$$\frac{\partial\ \mathrm{Log}(\mathcal{L}(\theta|z))}{\partial\theta_j} = -\sum_{i=1}^{N} \nu^T(i)\ \hat{B}^{-1}\ \frac{\partial\nu(i)}{\partial\theta_j} \tag{A.55}$$

The sensitivity of innovations to parameters is determined using the following recursive equations

$$\frac{d}{dt}\,\hat{x}(t|t_{i-1}) = F\hat{x}(t|t_{i-1}) + Gu(t)$$

$$\frac{d}{dt}\ \frac{\partial\hat{x}(t|t_{i-1})}{\partial\theta_j} = \frac{\partial F}{\partial\theta_j}\,\hat{x}(t|t_{i-1}) + F\ \frac{\partial\hat{x}(t|t_{i-1})}{\partial\theta_j} + \frac{\partial G}{\partial\theta_j}\,u(t)$$

$$j = 1,2,\ldots,p \qquad t_{i-1} \le t \le t_i \tag{A.56}$$

$$\nu(i) = y(i) - H\hat{x}(i|i-1) - Du(t_i)$$

$$\hat{x}(i|i) = \hat{x}(i|i-1) + K\nu(i) \tag{A.57}$$

$$\frac{\partial \nu(i)}{\partial \theta_j} = - \frac{\partial H}{\partial \theta_j} \hat{x}(i|i-1) - H \frac{\partial \hat{x}(i|i-1)}{\partial \theta_j} - \frac{\partial D}{\partial \theta_j} u(t_i)$$

(A.58)

$$\frac{\partial \hat{x}(i|i)}{\partial \theta_j} = \frac{\partial \hat{x}(i|i-1)}{\partial \theta_j} + \frac{\partial K}{\partial \theta_j} \nu(i) + K \frac{\partial \nu(i)}{\partial \theta_j}$$

$$j = 1,2,\ldots,p$$

Note that

$$\frac{\partial K}{\partial \theta_j} = 0 \quad \text{if } \theta_j \text{ is not an element of K matrix}$$

$$= I_{j',k'} \text{ if } \theta_j \triangleq K_{j',k'} \qquad \text{(A.59)}$$

where $I_{j',k'}$ is a matrix of all zeroes except a 1 at the j',k' position.

This approximation simplifies the optimization considerably. However, this usually leads to an overparameterized model. In other words, once K and B are determined, it is not possible to find any corresponding Γ, Q and R which have the desired (known a priori) structure. A good estimate of elements in Γ, Q and R matrices can be obtained by a least-squares type approach. The fit to the observed data is better than with true values of parameters but the parameter estimates do not have minimum variance. This approximation is not good in aircraft application where the structure of Q and R is known fairly well, but is excellent where there are many process noise sources and the characteristics of both Q and R are relatively unknown (e.g., economic systems).

A.6 MAXIMUM LIKELIHOOD WITH NO PROCESS OR MEASUREMENT NOISE

The maximum likelihood method can be simplified when either process noise or measurement noise are absent.

AD-A032 800 SYSTEMS CONTROL INC PALO ALTO CALIF F/G 1/1
IDENTIFICATION OF AIRCRAFT STABILITY AND CONTROL COEFFICIENTS F--ETC(U)
MAR 74 W E HALL, N K GUPTA, R G SMITH N00014-72-C-0328
UNCLASSIFIED TR-2 NL

3 OF 3
AD
A032800

END
DATE
FILMED
1-77

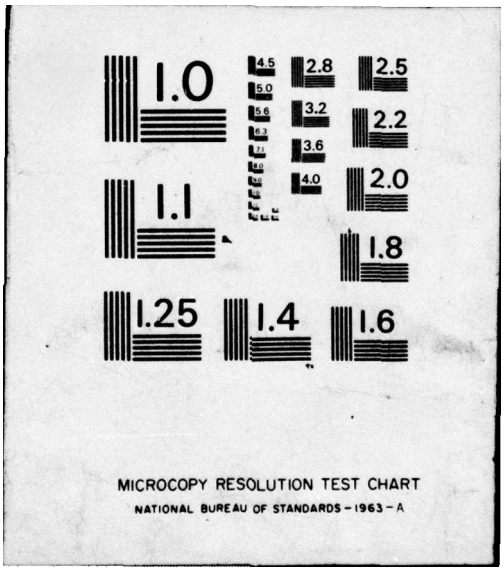
1.0
1.1
1.25
1.4
1.6
1.8
2.0
2.2
2.5
2.8
3.2
3.6
4.0
4.5
5.0
5.6
MICROCOPY RESOLUTION TEST CHART
NATIONAL BUREAU OF STANDARDS - 1963 - A

No Process Noise

If the process noise is zero and initial states are known perfectly, i.e., w(t) and P(0) are zero, the covariance of the error in the predicted state is also zero. It is clear from (A.23) that Kalman gains are zero. The innovations is the output error, i.e.,

$$\nu(i) = y(i) - h(x(t_i), u(t_i), \theta, t_i) \tag{A.60}$$

and the innovation covariance is (A.21)

$$B(i) = R \tag{A.61}$$

the log-likelihood function is,

$$\log\ (\mathscr{L}(\theta|z)) = -\frac{1}{2} \sum_{i=1}^{N} \nu^T(i)\ R^{-1} \nu(i) + \log\ |R| \tag{A.62}$$

which on optimizing for unknown parameters in R gives

$$\hat{R} = \frac{1}{N} \sum_{i=1}^{N} \nu(i)\ \nu^T(i) \tag{A.63}$$

The equality in (A.63) holds only for those elements of R which are not known a priori. For instance, even if R is known to be diagonal, the right hand side matrix will not be diagonal in general, but the off-diagonal terms should be ignored before they are equated to $\hat{R}$. Using (A.63) in (A.62)

$$\log\ (\mathscr{L}(\theta|z)) = -\frac{1}{2} \sum_{i=1}^{N} \nu^T(i)\ \hat{R}^{-1}\ \nu(i) + \text{constant} \tag{A.64}$$

The optimizing function is the same as that for the output error method except that the measurement noise covariance matrix is determined using (A.63) and is used as the weighting matrix in the criterion function. In the output

error method, the measurement noise is assumed known and the weighting function is arbitrary.

The first and second derivatives of the log-likelihood function with respect to unknown parameters are

$$\frac{\partial}{\partial\theta_j}\log(\mathscr{L}(\theta|z)) = -\sum_{i=1}^{N} \nu^T(i)\,\hat{R}^{-1}\,\frac{\partial\nu(i)}{\partial\theta_j} \tag{A.65}$$

$$\frac{\partial^2 \log(\mathscr{L}(\theta|z))}{\partial\theta_j\,\partial\theta_k} = -\sum_{i=1}^{N}\left\{\frac{\partial\nu^T(i)}{\partial\theta_k}\,\hat{R}^{-1}\,\frac{\partial\nu(i)}{\partial\theta_j} + \nu^T(i)\,\hat{R}^{-1}\,\frac{\partial^2\nu(i)}{\partial\theta_j\,\partial\theta_k}\right\} \tag{A.66}$$

The terms in the second derivative are approximated as

$$\frac{\partial^2 \log(\mathscr{L}(\theta|z))}{\partial\theta_j\,\partial\theta_k} = -\sum_{i=1}^{N}\left\{\frac{\partial\nu^T(i)}{\partial\theta_k}\,\hat{R}^{-1}\,\frac{\partial\nu(i)}{\partial\theta_j}\right\} \tag{A.67}$$

No Measurement Noise

If all states are measured with no noise, the covariance of the error in state estimates is zero at the beginning of any time update,

$$P(i-1|i-1) = 0$$

and $\hat{x}(i-1|i-1) = x(i-1)$ (A.68)

It is easy to show in this case that for fast sampling the log-likelihood function is quadratic in the difference between measured values of $\dot{x}$ and $f(x,u,\theta,t)$. The method reduces to the equation error method, the weight W being chosen as

$$W = \frac{1}{T} \int_{o}^{T} (\dot{x} - f(x,u,\theta,t))(\dot{x} - f(x,u,\theta,t))^{T} dt \qquad (A.69)$$

Thus, the maximum likelihood method and equation-error methods are equivalent except for the technique for choosing the weighting matrix.

APPENDIX B

MODEL STRUCTURE DETERMINATION BY MULTIPLE REGRESSION TECHNIQUES

This appendix provides an intuitive and mathematical basis for the multiple regression technique application to model building from data. The basic reference is Volume II of Kendall and Stuart [49].

B.1 LEAST SQUARES METHOD

The method of least squares (also known as regression method or equation error method) is based on the minimization of the scalar sum of squares

$$J = (y - X\theta)^T(y - X\theta) \tag{B.1}$$

with respect to the components of θ. The cost (B.1) is predicated on a linear model of the form

$$y = X\theta + \varepsilon \tag{B.2}$$

where y is an (mx1) vector of observations, X is an mxp matrix of known coefficients* ($m > p$) and θ is a px1 vector of parameters. ε is an (nx1) vector of disturbance or error random variables with $\mathcal{E}(\varepsilon) = 0$ (zero mean) and variance $\mathcal{E}(\varepsilon\varepsilon^T) = \sigma^2 I$ (components of ε are uncorrelated with the same variance σ^2).

Minimization of J with respect to θ yields the well-known least squares estimator

$$\hat{\theta} = (X^T X)^{-1} X^T y \tag{B.3}$$

---

* The discussions of this appendix assume the data and parameters are centered about their means.

where (X^TX) is nonsingular. Substituting Eq. (B.2) into Eq. (B.3), it is easily shown that

$$\mathcal{E}(\hat{\theta}) = \theta \tag{B.4}$$

$$\mathcal{E}\{(\hat{\theta}-\theta)(\hat{\theta}-\theta)^T\} = \sigma^2(X^TX)^{-1} \tag{B.5}$$

where X is fixed in repeated samples and assuming $\mathcal{E}(X^T\varepsilon) = 0$.

In actual experimentation, σ^2 is not known and must be estimated. This is due to the fact that $\varepsilon = y - X\theta$, the error, is a nonobservable, stochastic variable. However, estimates of the variance of $\hat{\varepsilon} = y - X\hat{\theta}$ (Fig. B.1), s^2, may be determined which estimate σ^2. The sum of squares of the residuals is found by solving Eqs. (B.1) and (B.2) for $\hat{\varepsilon}^T\hat{\varepsilon}$, i.e.,

$$\begin{aligned}\hat{\varepsilon}^T\hat{\varepsilon} = (y - X\hat{\theta})^T(y - X\hat{\theta}) &= \varepsilon^T\mathcal{M}\varepsilon \\ &= y^T\mathcal{M}y\end{aligned} \tag{B.6}$$

where $\mathcal{M} = (I_m - X(X^TX)^{-1}X^T)$. Note that $\mathcal{M}^2 = \mathcal{M} = \mathcal{M}^T$. Since $\mathcal{M}$ is thus idempotent and $\mathrm{tr}\mathcal{M} = m - p$,* taking the expectation of Eq. (B.6) yields

$$s^2 = \frac{1}{m-p}(y-X\hat{\theta})^T(y-X\hat{\theta}) = \frac{\hat{\varepsilon}^T\hat{\varepsilon}}{m-p} \tag{B.7}$$

which estimates σ^2. Equation (B.7) in Eq. (B.5) gives the sample estimate of the covariance of $\hat{\theta}$.

$$(\hat{\theta}-\theta)(\hat{\theta}-\theta)^T = s^2(X^TX)^{-1} \tag{B.8}$$

Note that Eq. (B.3) produces unbiased estimates of $\hat{\theta}$ only if the model is correct.

---

* The rank of $I-\mathcal{M} = X(X^TX)^{-1}X^T$ is p, and the rank of I_m is m. If the observations are not centered, then p is replaced by p+1.

B.2 DECOMPOSITION OF VARIANCE

Substituting the estimate $\hat{\theta}$ into J, it is found that

$$\hat{J} = \hat{\varepsilon}^T\hat{\varepsilon} = y^T y - \hat{y}^T\hat{y} \tag{B.9}$$

where

$$\hat{y} = (y|X) = X\hat{\theta} \tag{B.10}$$

Equation (B.9), a consequence of the orthogonality theorem of least squares, decomposes the sum of squares of the data variation ($y^T y$) into the contribution from the sum of squares of the regression equation ($\hat{y}^T\hat{y}$) and sum of squares of the residuals ($\hat{\varepsilon}^T\hat{\varepsilon}$), i.e.,

$$y^T y = \hat{y}^T\hat{y} + \hat{\varepsilon}^T\hat{\varepsilon} \tag{B.11}$$

The basic idea of subset regression is to compute the reduction in error sum of squares ($\hat{\varepsilon}^T\hat{\varepsilon}$) relative to the increase in regression sum of squares ($\hat{y}^T\hat{y}$) which is caused by adding (or subtracting) new variables θ_i in the regression. Ratios based on these incremental sum of squares may then be used to determine the significance of these added parameters. These ratios may be formulated as test statistics for which, under the assumption of normally distributed errors, ε, standard significance testing may be performed. That the errors are, in fact, normally distributed, is justified by the central limit theorem on the normality of the distribution of a large number of random disturbances.

B.2.1 Significance of the Regression Equation

The solution $\hat{\theta}$, Eq. (B.3), to the minimization of error sum of squares is unique when X has full column rank. Any coefficient vector which differs from the least squares vector $\hat{\theta}$ must lead to a larger sum of squares. That is, for any other coefficient vector, θ,

$$(y-X\theta) = (y-X\hat{\theta}) - X(\theta-\hat{\theta}) \tag{B.12}$$

has an error sum of squares

$$(y-X\theta)^T(y-X\theta) = y^T\mathcal{M}y + (\theta-\hat{\theta})X^TX(\theta-\hat{\theta}) \qquad (B.13)$$

The quantity $(\theta-\hat{\theta})$ is the "sampling error" of the regression.

Assume that it is desired to test the hypothesis that θ is some specific numerical value, say θ_o (e.g., $\theta_o = 0$ if there is not dependence of the data on θ). Then, if θ_o is the true value of θ,

$$\hat{\theta}-\theta_o = \hat{\theta}-\theta = (X^TX)^{-T}X^T(X\theta+\varepsilon) - \theta = (X^TX)^{-1}X^T\varepsilon \qquad (B.14)$$

Using Eqs. (B.6) and (B.14), Eq. (B.13) then becomes

$$(y-X\theta_o)^T(y-X\theta_o) = \varepsilon^T\mathcal{M}\varepsilon + \varepsilon^T(I-\mathcal{M})\varepsilon \qquad (B.15)$$

In order to fulfill the requirements for using statistical tests based on the sum of squares of Eq. (B.15), it is necessary to recall the fact that an indempotent quadratic form in independent standardized normal variates is a chi-squared variate with degrees of freedom given by the rank of the quadratic form* (Sec. 15.11, ref. [49]). Furthermore, if the two normalized sum of squares S_i/σ^2 and S_j/σ^2 are $\chi^2(\nu_i)$ and $\chi^2(\nu_j)$ distributed, and S_i and S_j are independent, then

$$F = \frac{S_i/\nu_i}{S_j/\nu_j} \qquad (B.16)$$

is a Fisher F ratio distributed with ν_i and ν_j degrees of freedom.

*A sum of squares S_i can be written as y^TAy where y is vector, A is a matrix of known constants. Then the number of degrees of freedom of S_i is defined to be the rank of A.

As discussed after Eq. (B.6), the rank of $\mathcal{M}$ is m-p and that of I-$\mathcal{M}$ is p. Thus, the ratio

$$\frac{\varepsilon^T(I-\mathcal{M})\ \varepsilon/p}{\varepsilon^T\mathcal{M}\ \varepsilon/m-p} \tag{B.17}$$

is distributed as F(p,m-p), if $\theta = \theta_o$. But from Eqs. (B.6) and (B.7), $\varepsilon^T\mathcal{M}\,\varepsilon = (m-p)s^2$ and it is easily shown that $\varepsilon^T(I-\mathcal{M})\varepsilon = (\hat{\theta}-\theta_o)X^TX(\hat{\theta}-\theta_o)$, if $\theta = \theta_o$. Hence,

$$\frac{(\hat{\theta}-\theta_o)X^TX(\hat{\theta}-\theta_o)}{ps^2} \sim F(p,m-p) \tag{B.18a}$$

Examination of Eq. (B.12) shows that the numerator of Eq. (B.14) is the difference between the sum of squares regressing on θ_o and the sum of squares of the actual parameters θ. High values of F(p,m-p) correspond to rejection of the hypothesis that $\theta = \theta_o$. In particular, to test whether the data depends on a specific parameter, θ_i of θ, the F(p,m-p) ratio is evaluated for $\theta_o = 0$.

A recursive form of Eq. (B.18a) is

$$F(q,m-p) = \frac{(\hat{\theta}-\theta_o)X^TX(\hat{\theta}-\theta_o)}{qs^2} \tag{B.18b}$$

where q is the number of parameters in the regression at any stage in adding (or deleting) parameters to improve fit.

The F ratio tests are based on quotients of regression "fit" to error "fit". The quantity,

$$\begin{aligned} R^2 &= \frac{(X\hat{\theta})^T(X\hat{\theta})}{y^Ty} \\ &= \hat{y}^T\hat{y}/y^Ty \end{aligned} \tag{B.19}$$

measures the regression sum of squares to observation sum of squares. The positive square root of Eq. (B.19), R, is the multiple correlation coefficient. The closer R is to unity, the better the performance of the subset of regression variables. Note that R is the cosine of the angle between the data vector and the p dimensional subspace spanned by the included subset of regression variables.

From the sum of squares decomposition (B.8), and Eq. (B.19), it may be shown that

$$F = \frac{R^2/p-1}{(1-R^2)/(m-p)} \tag{B.20}$$

which expresses the F ratio in terms of R^2.

The closer R to unity, the stronger the dependence of the data on the regression parameters and the higher the F value. If there is little dependence, R is "small", the hypothesis $\theta_i = 0$ is "correct", and F is "small". This test is dependent on choosing a critical value of F which specifies the cutoff levels. This critical F is chosen as a function of m (number of observations) and p (number of parameters) from tables of F statistical tables for a desired confidence level. The confidence level can be selected on the basis of a priori knowledge about level of noise in data.

B.2.2 Significance of Individual Conditions to the Regression Equations

The multiple correlation coefficient measures the dependence of the data on the complete set of regression variables. If several sets of parameters are to be evaluated with respect to their respective explanations of the data, the R coefficient would serve as one measure of relative performance. Unfortunately, it follows from the definition of R that increasing the number of explanatory variables always increases R, unless the added variables are linearly related to other included variables. Beyond a certain point, the added variables start fitting the random noise ε. For example, if the number

of variables is increased to m, a perfect fit can be obtained and R is one. In order to eliminate parameters not significant, only the most linearly independent variables are desired.

Stated in terms of the sum of squares principal, it is desired to incorporate those new variables into the regression which most reduce the error, given that the other variables are included in the regression. If the increase in regression sum of squares due to adding a new variable, say x_j, after variables x_i have been included in the regression, is denoted as $\Delta||\hat{y}||$, then the ratio

$$R^2_{yx_j \cdot x_1, x_2, \ldots, x_{j-1}, x_{j+1}, \ldots, x_p} = \frac{\Delta||\hat{y}||}{\hat{\varepsilon}^T\hat{\varepsilon} + \Delta||\hat{y}||} \tag{B.21}$$

measures the partial contribution of x_j to the regression. The square root of $R^2_{yx_j \cdot x_1, \ldots, x_p}$ is the partial correlation coefficient. Several forms of this definition may be written. One is defined by letting $\tilde{y}$ be the residuals from the regression of x_j on the same variables. It may then be shown

$$R^2_{\tilde{y}\tilde{x}_j} = \frac{(\Sigma\tilde{y}\tilde{x}_j)^2}{(\Sigma\tilde{x}_j^2)(\Sigma\tilde{y})^2} \tag{B.22}$$

Note that, in general, $\Sigma_j R^2_{\tilde{y}\tilde{x}_j} \neq R^2$.

Now, let the regression equation $y = X\theta + \varepsilon$ be partitioned as

$$y = X_1\theta_1 + X_2\theta_2 + \varepsilon \tag{B.23}$$

where X_1 includes q variables and X_2 contains p-q variables. Then

$$y - X_1\theta_1 = X_2\theta_2 + \varepsilon \tag{B.24}$$

which shows that an estimate of θ_2 could be obtained by regressing the residuals from the regression of y on X_1 (i.e., which estimates θ_1). Then the vector $y-X_1\theta_1$ is regarded as a new observation, say $y^{(1)}$, which may be regressed on X_2 to estimate θ_2. This decomposition can be applied to each possible subset of variables, X_i, "bringing in" new variables from the right to left hand side of Eq. (B.24). The requirement on "bringing in" new variables may be satisfied by examining the significance of each variable.

The F test may be used to determine the significance of a single parameter by noting the estimate of the variance σ^2, s^2, is distributed as $\sigma^2\chi^2_{m-p}$. Hence, $s^2/\sigma^2 \sim (\chi^2_{m-p})/(m-p)$ from Eq. (B.7). Then for the parameter θ_i,

$$\frac{\hat{\theta}_i-\theta_i}{s_{\theta_i}} = \frac{(\hat{\theta}_i-\theta_i)/\sigma_{\theta_i}}{s_{\theta_i}/\sigma_{\theta_i}} \tag{B.25}$$

where s_{θ_i} is the standard error of θ_i, which, from Eq. (B.8) is

$$s_{\theta_i} = s\sqrt{s_{ii}} \tag{B.26}$$

where s_{ii} is the square root of the i^{th} diagonal term of $(X^TX)^{-1}$.

Since $(\hat{\theta}_i-\theta_i)/\sigma_i \sim \eta(0,1)$, it follows that, by definition of Student's t distribution that

$$\frac{\hat{\theta}_i-\theta_i}{s_i} \sim t_{m-p}. \tag{B.27}$$

In particular, if it is desired to test the hypothesis $\theta_i = 0$ (i.e., y does not depend on θ), the statistic $t = \theta_i/s_{\theta_i}$ is used. It is shown in [49] that the F distribution with 1 and (m-p) degrees of freedom is equivalent to the t^2 distribution with m-p degrees of freedom. Hence, the significance of individual regression coefficients, θ, is determined from F ratios

$$F = \theta_i^2 / s_i^2 \tag{B.28}$$

If the ratio (B.28) indicates a variable is not significant, then the variable is deleted. To bring in another variable, the partial correlation coefficients of all other parameters are examined. To form the F ratio for these coefficients, Eq. (B.21) (with Eq. (B.26) may be manipulated to show

$$R^2_{\tilde{y}\tilde{x}_j} = \frac{(\theta_j / s_{\theta_j})}{(\theta_j / s_{\theta_i})^2 + (m-q)} \tag{B.29}$$

where q is the number of variables already in the regression. The corresponding F test is

$$F_j = \frac{r^2_{\tilde{y}\tilde{x}_j} (m-q)}{1 - r^2_{\tilde{y}\tilde{x}_j}} \tag{B.30}$$

The variable (F ratio with 1 and m-q degrees of freedom), is calculated for each of the remaining variables. The variable with the highest value is then brought into the regression.

B.2.3 Summary of the Subset Regression Method

The variables $x_1, x_2, \ldots, x_p$ are postulated as possible causative factors in determining the observed data, y (Eq. (B.23)). The variables $x_1, x_2, \ldots x_p$ are ranked according to the magnitude of their individual partial correlation coefficients with y (or F ratio, Eq. (B.38)).* The variables with the highest significance (F to enter) is added to the regression. The significance of the added parameter is then tested to determine if it is above the critical F value for deletion (Eq. (B.28). As variables are entered, new F ratios are computed from the remaining variables not in the regression since the degrees of free-

*The selection procedure described here is also known as univariate stepwise regression, for subset regression of order 1.

dom have been reduced. This process is terminated when no new variables satisfy the F ratio required to enter and when one are to be removed.

At each variable incorporation, the multiple correlation coefficient (R, Eq. (B.19)), the equation F ration (Eq. (B.20)), and the standard error of the entered parameter (Eq. (B.26)) are all included.

It is noted that, in general, the particular variables finally selected are not unique. Use of orthogonal variables would result in uniqueness.

B.3 COMPUTATIONAL CONSIDERATIONS

The previous sections have demonstrated that both classical and subset regression parameters are obtainable from steps in the solution of a set of linear equations (ref. Eq. (B.3)). In order to reinforce this connection, consider the augmented data-coefficient matrix (with rank p+1)

$$A = \begin{bmatrix} X^T X & X^T y \\ y^T X & y^T y \end{bmatrix}$$

Using the inversion of Eq. (B.3), it is found that the final element of A^{-1}, a^f, is

$$a^f = \frac{1}{y^T y - y^T X (X^T X)^{-1} X^T y} = \frac{1}{y^T y - \theta^T X^T X \theta}$$

$$= \frac{1}{(1-R^2)\, y^T y}$$

i.e., the multiple correlation coefficient (and the sum of squares $||\hat{\varepsilon}||$) are directly obtainable. Similarly, it is found that the diagonal element of $(X^T X)^{-1}$ corresponding to the i^{th} coefficient of x, is

$$(X^T X)^{-1}_{ii} = \frac{1}{(1 - P_i^2)\bar{x}_i^T \bar{x}_i}$$

where P_i^2 is the multiple correlation coefficient of the regression of x_k on $x_1, x_2, \ldots, x_{i-1}, x_{i+1}, \ldots, x_p$. It may be further shown that the variance of $\hat{\theta}_i$ is

$$\text{var } \hat{\theta}_i = \sigma^2 (X^T X)^{-1}_{ii} = \frac{\sigma^2}{(1-P_i^2) x^T x_i}$$

Computationally, the inversion of A is based on the Gauss-Jordan pivot algorithm. Let the k^{th} diagonal element of A be nonzero. Applying a Gauss-Jordan pivot on this element is a new matrix whose ij^{th} element is $\tilde{a}_{ij}$, i.e.,

$$\tilde{a}_{ij} = \begin{cases} a_{ij} - a_{ik}\, a_{kj}/a_{kk} & i \neq k \quad j \neq k \\ -a_{ik}/a_{kk} & i \neq k \quad j = k \\ a_{kj}/a_{kk} & i = k \quad j \neq k \\ 1/a_{kk} & i = k \quad j = k \end{cases}$$

The final result of this inversion is the matrix B,

$$B = \begin{bmatrix} (X^T X)^{-1} & \hat{\theta} \\ -\hat{\theta}^T & ||\hat{\varepsilon}|| \end{bmatrix}$$

The recursive algorithm of the Gauss-Jordan pivot sweeps through the A matrix, generating statistical parameters which guide the deletion and addition of new variables. Details of this selection for the Gauss-Jorden pivot are found in ref. [50] One further parameter of this method is the tolerance. This is a parameter of the computation algorithm itself and is a measure of the accuracy of the calculations and computer. If $\bar{a}_{ii}$ is the value of the i^{th} diagonal element of the non-negative matrix (a_{ij}) after pivoting on several elements, then $\bar{a}_{ii}/a_{ii}$ is the tolerance.

APPENDIX C
INPUT DESIGN

C.1 INTRODUCTION

Many new developments are being made in the field of input design. Recently, two efficient algorithms* were developed for linear systems. These techniques are capable of finding inputs which minimize a weighted sum of covariances of parameter estimates or any one of many other criteria related to estimation errors from the resulting experiment. They are referred to as Frequency Domain and Time Domain methods and are summarized in Section C.2. For details, see [50].

The input design techniques for linear systems are modified to work for certain nonlinear systems. However, a basically different approach is required to design optimal inputs which will identify the parameters of certain nonlinear systems accurately. These techniques are described in Sections C.3 and C.4.

C.2 INPUT DESIGN FOR LINEAR SYSTEMS

C.2.1 Frequency Domain Method [51,52]

Consider the state space representation of a discrete time system

$$x(k+1) = \Phi x(k) + Gu(k) \qquad k = 1,2,\ldots,N \tag{C.1}$$

and the noisy measurements

$$y(k) = Hx(k) + v(k) \tag{C.2}$$

where

---

* This work was performed with a support from the NASA Flight Research Center, Edwards, California, under Contract NAS 4-2068.

$x(\cdot)$ is a n x 1 state vector

$u(\cdot)$ is ℓ x 1 control vector

$y(\cdot)$ and $v(\cdot)$ are m x 1 measurement and noise vectors, respectively.

φ, G and H are matrices of appropriate dimensions and contain p unknown parameters θ. Fourier transform (C.1) and (C.2) to get

$$\tilde{y}(n) = H(e^{-j\frac{2\pi n}{N}} - \varphi)^{-1} G\tilde{u}(n) + \tilde{v}(n)$$

$$\underline{\Delta}\ T(n,\theta)\ \tilde{u}(n) + \tilde{v}(n) \qquad (C.3)$$

As the number of sample points increase, the average information matrix per sample approaches

$$M = \frac{1}{2\pi}\ \mathrm{Re}\int_{-\pi}^{\pi} \frac{\partial T^*}{\partial\theta}\ S_{vv}^{-1}(\omega)\ \frac{\partial T}{\partial\theta}\ dF_{uu}(\omega) \qquad (C.4)$$

where F_{uu} is the spectral distribution function of u and S_{vv} is the spectral density of v. The following algorithm converges to the optimal input (with energy constraint on input):

(a) Choose a nondegenerate input $f_o(\omega)$ (i.e., consisting of more than $\frac{b}{2m}$ frequencies, with a finite power in each frequency).

(b) Compute the function $\psi(\omega,f)$ and find the value of ω where it is maximum, call it ω_o, where

$$\psi(\omega,f) = \mathrm{Re}\left[\mathrm{Tr}\ S_{vv}^{-1}(\omega)\ \frac{\partial T}{\partial\theta}\ M^{-1}\ \frac{\partial T^*}{\partial\theta}\right] \qquad (C.5)$$

to minimize $|D|$, where $D \underline{\Delta} M^{-1}$

and

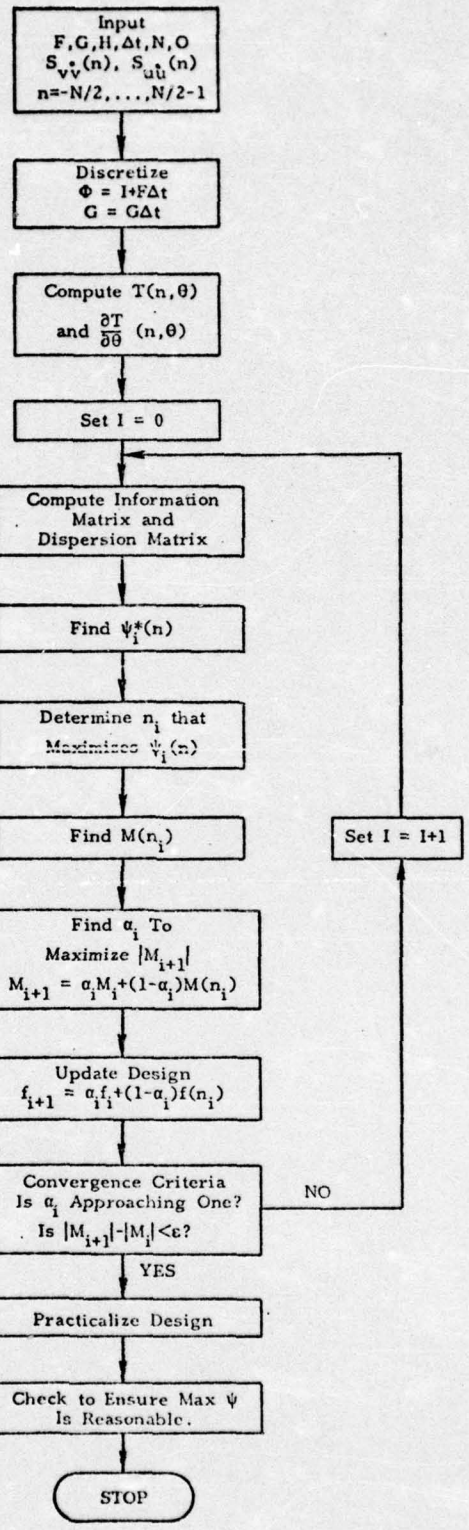

Figure C.1 Optimal Input Design Program in Frequency Domain (Maximize $|M|$)

$$\psi(\omega,f) = \mathscr{L}\left[D(f)\ \frac{\partial T^*(\omega)}{\partial\theta} S_{vv}^{-1}(\omega)\ \frac{\partial T(\omega)}{\partial\theta}\ D(f)\right] \qquad (C.6)$$

to minimize a linear functional R of D.

(c) Evaluate the normalized information matrix at ω_o.

(d) Update the design

$$f_1 = (1-\alpha_o)\ f_o + \alpha_o f(\omega_o) \qquad 0 < \alpha_o < 1 \qquad (C.7)$$

α_o is chosen to minimize $|D(f)|$ or $[\ \mathscr{L}(D(f_1))]$

where

$$M(f_1) = (1-\alpha_o)\ M(f_o) + \alpha_o M(\omega_o), \qquad 0 < \alpha_o < 1 \qquad (C.8)$$

It can be shown that such an α_o exists.

(e) Repeat steps (b) - (d) until desired accuracy is obtained.

Examples of application of this method to aircraft problems are given in reference [52].

C.2.2 Generalized Time Domain Method [53]

The continuous time representation of a linear system is

$$\dot{x} = Fx + Gu \qquad o \leq t \leq T$$
$$x(0) = 0 \qquad (C.9)$$

x(t) is a nx1 state vector, u(t) is a qx1 control vector and F and G are matrices with appropriate dimensions and depend on p unknown parameters θ. There are noisy measurements of m linear combinations of state.

$$y = Hx + v \tag{C.10}$$

H, an mxn matrix is a function of θ and v(t) is a white noise vector with zero mean and covariance R. There is an energy constraint on the input

$$\int_o^T u^T u = E \tag{C.11}$$

The information matrix for the unknown parameters θ is given as

$$M = \int_o^T \left(\frac{\partial (Hx)}{\partial \theta}\right)^T R^{-1} \frac{\partial (Hx)}{\partial \theta} \, dt \tag{C.12}$$

We explain without proof how different criterion can be optimized in this generalized time-domain approach. For details, see [53].

Trace of the Information Matrix*

The perfcrmance index in this case is

$$J = Tr \int_o^T \left(\frac{\partial (Hx)}{\partial \theta}\right)^T R^{-1} \frac{\partial (Hx)}{\partial \theta} \, dt$$

$$= \int_o^T \left(\frac{\partial H}{\partial \theta_i} x + H \frac{\partial x}{\partial \theta_i}\right)^T R^{-1} \left(\frac{\partial H}{\partial \theta_i} x + H \frac{\partial x}{\partial \theta_i}\right) dt \tag{C.13}$$

$$= \int_o^T X_\theta^T H_\theta^T R_\theta^{-1} H_\theta X_\theta \, dt \tag{C.14}$$

* A weighted trace of the information matrix can be maximized by a simple transformation of parameters; see ref. [50]. For multi-input, multi-output systems, this problem was first solved by Mehra [55].

and

$$\dot{x}_\theta = F_\theta x_\theta + G_\theta u \qquad x_\theta(0) = 0 \tag{C.15}$$

where

$$x_\theta \triangleq \begin{bmatrix} x \\ \hline \frac{\partial x}{\partial \theta_1} \\ \hline \frac{\partial x}{\partial \theta_2} \\ \hline \vdots \\ \frac{\partial x}{\partial \theta_m} \end{bmatrix} \tag{C.16}$$

$$H_\theta \triangleq \begin{bmatrix} \frac{\partial H}{\partial \theta_1} & H & 0 & \cdots & 0 \\ \frac{\partial H}{\partial \theta_2} & 0 & H & \cdots & 0 \\ \vdots & \vdots & & & \\ \frac{\partial H}{\partial \theta_m} & 0 & & \cdots & H \end{bmatrix} \tag{C.17}$$

$$R_\theta = \begin{bmatrix} R & & 0 \\ & \ddots & \\ & R & \\ & & \ddots \\ 0 & & R \end{bmatrix} \tag{C.18}$$

$$F_\theta = \begin{bmatrix} F & 0 & 0 \\ \dfrac{\partial F}{\partial \theta_1} & F & 0 \\ \vdots & \vdots & \vdots \\ \dfrac{\partial F}{\partial \theta_m} & C \cdots\cdots & F \end{bmatrix}, \quad G_\theta = \begin{bmatrix} G \\ \dfrac{\partial G}{\partial \theta_1} \\ \vdots \\ \dfrac{\partial G}{\partial \theta_m} \end{bmatrix} \tag{C.19}$$

Thus, we want to maximize (C.14) subject to state equations (C.15) and constraing (C.11). The necessary conditions for the optimum u involve solving the two-point boundary value problem

$$\frac{d}{dt}\begin{bmatrix} x_\theta \\ \lambda \end{bmatrix} = \begin{bmatrix} F_\theta & -\mu G_\theta G_\theta^T \\ H_\theta^T R_\theta^{-1} H_\theta & -F_\theta^T \end{bmatrix}\begin{bmatrix} x_\theta \\ \lambda \end{bmatrix} \triangleq \mathcal{H}\begin{bmatrix} x_\theta \\ \lambda \end{bmatrix}$$

$$x_\theta(0) = 0 \qquad \lambda(T) = 0 \tag{C.20}$$

and

$$u_{opt} = -\mu G_\theta{}^T \lambda \tag{C.21}$$

The smallest value of constant μ, for a nontrivial solution to the two-point boundary value problem gives the optimal solution. Constraint (C.11) is met by rescaling x_θ and λ This problem is solved by eigenvalue-eigenvector decomposition techniques [54].

Determinant or Linear Functional of Dispersion Matrix

The following algorithm converges to a stationary point.

(a) Choose any input $u_o(t)$, which gives nonsingular information matrix M_o.

(b) Find an input $u_m(t)$ to maximize $\varphi(u)$ where

$$\varphi = \mathrm{Tr}(M_o^{-1} M) \quad \text{to minimize the determinant of dispersion matrix}$$

$$= \mathscr{L}(M_o^{-1} M M_o^{-1}) \quad \text{to minimize a linear functional of the dispersion matrix} \qquad (C.22)$$

Both of these criteria can be recast as maximizing a weighted trace of the information matrix.

(c) The information matrix for input $\alpha u_o(t) + \beta u_m(t)$ is

$$M_1 = \alpha^2 M_o + \beta^2 M_m + 2\alpha\beta M_{om} \qquad (C.23)$$

where M_m is the information matrix for input $u_m(t)$ and M_{om} is a mixed information matrix defined in reference [53]. The energy constraint on the input requires

$$\alpha^2 + \beta^2 + 2\alpha\beta \int_o^T u_o^T(t)\, u_m(t)\, dt = 1 \qquad (C.24)$$

use (C.23) and (C.24) to find α between 0 and 1 which optimizes the criterion function for M_1. Such an α exists.

(d) Find M_1^{-1} and return to (b) if the error criterion is not met.

(e) Check if the solution is globally optimum.

C.3 NONLINEAR SYSTEMS

Methods for designing inputs to identify parameters of nonlinear dynamical system depend among other things on kind of nonlinearity, availability of computational optimization programs, and the way the input is applied during the flight test. Many techniques lead to complicated algorithms, which cannot be solved for real problems in a reasonable computation time. We start with

general nonlinear problem and will later discuss algorithms which can be used with specific nonlinearities.

C.3.1 General Nonlinear System

Consider a system with n states and m measurements, which follows the equations,

$$\dot{x} = f(x,u,\theta,t) \qquad 0 \leq t \leq T \tag{C.25}$$

$$y = h(x,u,t) + v \tag{C.26}$$

v is defined as in (C.11). For the sake of simplicity, h is assumed independent of θ. The information matrix for parameters θ is

$$M = \int_o^T \left(\frac{dh(x,u,t)}{d\theta}\right)^T R^{-1} \left(\frac{dh(x,u,t)}{d\theta}\right) dt \tag{C.27}$$

$$= \int_o^T \left(\frac{\partial x}{\partial \theta}\right)^T \left(\frac{\partial h}{\partial x}\right)^T R^{-1} \frac{\partial h}{\partial x} \frac{\partial x}{\partial \theta} dt \tag{C.28}$$

The equation governing the sensitivity of state to parameters is

$$\frac{d}{dt} \frac{\partial x}{\partial \theta} = \frac{\partial f}{\partial \theta} + \frac{\partial f}{\partial x} \frac{\partial x}{\partial \theta} \tag{C.29}$$

We, thus, wish to choose a bounded energy input to optimize a certain function of M of (C.28) subject to the state equations (C.25) and sensitivity equations (C.29). To maximize the trace of the information matrix, it is necessary to solve the following two point boundary value problem.

$$\dot{\lambda} = -\frac{\partial f_\theta(x_\theta, u, \theta, t)}{\partial x_\theta}\,\lambda + R_\theta^{-1}\,x_\theta \qquad \lambda(T) = 0$$

$$\dot{x}_\theta = f_\theta(x_\theta, u, \theta, t) \qquad x_\theta(0) = 0 \tag{C.30}$$

where x_θ is defined by (C.16) and

$$R_\theta^{-1} = \begin{bmatrix} \frac{\partial h}{\partial x}^T R^{-1} \frac{\partial h}{\partial x} & & 0 \\ & \ddots & \\ 0 & & \frac{\partial h}{\partial x}^T R^{-1} \frac{\partial h}{\partial x} \end{bmatrix} \tag{C.31}$$

$$f_\theta = \begin{bmatrix} f(x,u,\theta,t) \\ \hline \frac{\partial f}{\partial \theta_1} + \frac{\partial f}{\partial x}\frac{\partial x}{\partial \theta 1} \\ \hline \vdots \\ \hline \frac{\partial f}{\partial \theta_p} + \frac{\partial f}{\partial x}\frac{\partial x}{\partial \theta_p} \end{bmatrix} \tag{C.32}$$

The optimal input is,

$$u = -\left(\frac{\partial f_\theta}{\partial u}\right)^T \lambda \tag{C.33}$$

(C.30) is an extremely difficult problem to solve computationally. An approximation is to find states and controls to optimize the desired function of the information matrix, while satisfying the sensitivity equations only approximately. The ε-technique is a possible method. In this method, the following function is optimized.

$$\min_{x,u} J = \int_o^T \left\{ -x_\theta^T R_\theta^{-1} x_\theta + \varepsilon \| \dot{x}_\theta - f_\theta(x_\theta, u, \theta, t) \|_w^2 \right\} dt \qquad (C.34)$$

The constraint accruing from the sensitivity equations can be tightened by increasing ε. Gradient methods can be used to optimize J.

C.3.2 Application to Aircraft Problems

In flight tests of most aircraft, it is customary to measure all states and accelerations. If x_m is noisy measurements of state, with noise v_1 and a_m is the noisy measurements of accelerations with noise v_2,

$$a_m - v_2 = f(x_m - v_1, u, \theta, t) \qquad (C.35)$$

$$a_m - v_2 \cong \frac{\partial f}{\partial \theta}(x,u,\theta,t)\Delta\theta + \frac{\partial f}{\partial x}(x_m,u,\theta,t)v_1 + f(x_m,u,\theta,t) \qquad (C.36)$$

or

$$a_m - f(x_m,u,\theta,t) = \frac{\partial f}{\partial \theta}(x,u,\theta,t)\Delta\theta + v_2 + \frac{\partial f}{\partial x}(x_m,u,\theta,t)v_1 \qquad (C.37)$$

Assuming

$$\frac{\partial f}{\partial x}(x_m,u,\theta,t) \cong \frac{\partial f}{\partial x}(x,u,\theta,t) \qquad (C.38)$$

(C.37) becomes

$$y = \frac{\partial f}{\partial \theta}(x,u,\theta,t)\Delta\theta + v_2 + \frac{\partial f}{\partial x}(x,\theta,u,t)v_1$$

$$\triangleq h(x,u,\theta,t)\Delta\theta + g(x,u,\theta,t)v \qquad (C.39)$$

The information matrix for parameters θ (or $\Delta\theta$) is

$$M = \int_o^T h^T (gR_w g^T)^{-1} h \, dt \qquad (C.40)$$

The following procedure can be used to determine an input to approximately minimize the determinant or a linear functional of the dispersion matrix.

(a) Find functions h and g of (C.39).

(b) Choose an energy bounded input history $u_o(t)$ and state history $x_o(t)$ and find the corresponding information matrix M_o.

(c) Find input u(t) and state x(t), under same energy constraints as above to maximize $\varphi(u,x)$ defined in (C.22).

(d) Find α, optimal input and states as in step (c) of the algorithm for linear system (see page 199).

(e) Find M_1^{-1} and return to (b) if the error criterion is not met.

(f) $x^o(t)$ and $u^o(t)$ obtained this way will, in general, be incompatible. Find compatible input and state by minimizing

$$\int_o^T \left\{ \|x(t) - x^o(t)\|_{w_1} + \|u(t) - u^o(t)\|_{w_2} \right\} dt \qquad (C.41)$$

Subject to state equation constraints (C.25). This is a fairly simple optimization problem.

C.4 NONLINEAR SYSTEMS WITH SPECIFIC NONLINEARITIES

Some input design techniques can be used only with a particular class of nonlinearities. Two such techniques are presented here.

C.4.1 Describing Functions Method

This technique is a unique technique in that the nonlinear system is approximated by a linear system for design of input. This method works successfully only with very simple nonlinearities in low order systems. The nonlinear system is converted into its "frequency-domain" representation by one of the describing functions methods. The method described in Section C.2.1 is then used to determine the spectrum of optimal input in steady state.

C.4.2 Series Expansion of Nonlinear Functions

Every nonlinear function can be expanded in an infinite series of a set of complete functions. The truncated series is, usually, a good approximation for a finite range of the independent variables. In parameter identification technology, it is customary to express a nonlinear function as a polynomial in independent variables when the nature of nonlinearity is unknown or difficult to describe exactly. In the high angle-of-attack flight regime, the aerodynamic derivatives are functions of angle-of-attack, Mach number, altitude, etc. Each stability and control derivative is expanded into a suitable order polynomial in the independent variables (say angle-of-attack, α, and Mach number M), with unknown coefficients, viz.

$$C_{m_q}(\alpha,M) = P_o(M) + P_1(M)\alpha + P_2(M)\alpha^2,\ldots,P_k(M)\alpha^k \qquad (C.42)$$

and $P_i(M)$ are suitable polynomials in mach number.

$$P_i(M) = C_o^i + C_1^i M + C_2^i M^2 + \ldots + C_\ell^i M^\ell \qquad (C.43)$$

The problem of finding the nonlinear function of C_{m_q} is reduced to determination of the values of the polynomial coefficients. The order of the polynomial depends on the kind of nonlinearity and the range of the independent variables for which the function is to be defined.

Each different set of complete functions lead to a slightly different method for determining inputs which will accurately identify the coefficients of the terms in the expansion accurately. We discuss here various aspects of input design for systems which are linear except that some of the coefficients are expressed as polynomial expansions in some state variables.

The ultimate objective of any input is to determine the parameters of the expansion such that a good definition of the function is obtained over the range of interest. Let us see how it can be achieved. If $\tilde{C}_i^j$ be the error in estimating C_i^j, the error in the value of the aerodynamic coefficient would be (for example in C_{m_q})

$$\tilde{C}_{m_q}(\alpha,M) = \tilde{P}_o(M) + \tilde{P}_1(M)\alpha + \ldots + \tilde{P}_k(M)\alpha^k \tag{C.44}$$

and

$$\tilde{P}_i(M) = \tilde{C}_o^i + \tilde{C}_1^i M + \ldots + \tilde{C}_\ell^i M^\ell \tag{C.45}$$

Thus, to get minimum mean square error with weight $d(\alpha,M)$ in a certain range Ω of α and M, it is necessary to minimize

$$J = \int_{(\alpha,M)\ \varepsilon\Omega} d(\alpha,M) \left\{\tilde{C}_{m_q}(\alpha,M)\right\}^2 d\alpha dM$$

$$= Tr(WM^{-1}) \tag{C.46}$$

where M is the information matrix for the coefficients C_j^i (order $C_o^o, C_1^o, \ldots, C_o^o, C_o^1, C_1^1, C_2^1, \ldots, C_\ell^k$), and

$$W_{ki+j,ki'+j'} = \int_{(\alpha,M)\varepsilon\Omega} \alpha^{i+i'-2} M^{j+j'-2} d(\alpha,M) d\alpha\ dM \tag{C.47}$$

There are two basic methods for identifying the coefficients of polynomial expansions. In the first method, these polynomial coefficients are extracted from one input. This requires inputs with suitable amplitudes so that the independent variables of the polynomial expansions vary throughout the region of interest. The other important consideration in this method concerns the order of the polynomial which can be identified with enough confidence. This method is good where the variation in independent variable is small and can be achieved within a reasonable time.

The second method identified the value (and maybe slope) of the function at different values of the independent variable. This is done by exciting the aircraft modes at the desired trim value of the independent variable. A polynomial can then be passed through these points by a least squares type technique. Here it is necessary to select the values of the independent variables at which the experiment should be carried out and also the duration of the experiment at each point.

C.4.2.1 Input Amplitudes to Identify Polynomial Expansions

In linear systems, parameter estimate error covariances scales with input energy. If the energy is doubled, the variance in all parameter estimates decreases by a factor of two. In nonlinear systems, this is not true. In particular, the accuracy of the coefficients of high order terms in the expansion increases in much higher proportion with increasing state and input amplitudes. For very small amplitudes, the system "looks" like a linear system obtained by linearizing the nonlinear system around the average state.

To simplify the discussion, we assume that all states and acceleration are measured and that the system involves only one nonlinear derivative C which is expressed as a polynomial in some state variable α. If the measurements are substituted in state equation (C.25)

$$\dot{x}_m + \dot{v}_x = f(x_m + v_x,\ u,\ C(\alpha),t) \qquad (C.48)$$

where v_x is the measurement noise in x, etc. The above equation can be solved for $C(\alpha)$ to give

$$y(t) = C(\alpha(t)) + n(t) \tag{C.49}$$

let

$$C(\alpha) = C_1 + C_2\alpha + \ldots + C_m\alpha^{m-1} \tag{C.50}$$

and

$$C \triangleq \begin{bmatrix} C_1 \\ \vdots \\ C_m \end{bmatrix} \tag{C.51}$$

An estimate of C from this experiment is,

$$\hat{C} = \left[\int_o^T \frac{1}{r} \begin{bmatrix} 1 & \alpha & \cdots & \alpha^{m-1} \\ \alpha & \alpha^2 & & \alpha^m \\ \vdots & & & \\ \alpha^{m-1} & \cdots & & \alpha^{2m-2} \end{bmatrix} dt \right]^{-1} \int_o^T \frac{y(t)}{r} \begin{bmatrix} 1 \\ \alpha \\ \vdots \\ \alpha^{m-1} \end{bmatrix} dt \tag{C.52}$$

where r is the power spectral density of n. The covariance of $\hat{C}$ is lower bounded by

$$\mathrm{Cov}(\hat{C}) \geq \left[\int_o^T \frac{1}{r} \begin{bmatrix} 1 & \alpha & \cdots & \alpha^{m-1} \\ \alpha & \alpha^2 & & \alpha^m \\ \vdots & & & \vdots \\ \alpha^{m-1} & & & \alpha^{2m-2} \end{bmatrix} dt \right]^{-1} = M^{-1} \tag{C.54}$$

$$M = \int_{\alpha} \frac{1}{r\dot{\alpha}} \begin{bmatrix} 1 & \alpha & \cdots & \alpha^{m-1} \\ \alpha & \alpha^2 & & \alpha^m \\ \vdots & & & \vdots \\ \alpha^{m-1} & \cdots & & \alpha^{2m-2} \end{bmatrix} d\alpha \qquad (C.54)$$

$$= \int_{a}^{b} \frac{d(\alpha)}{r} \begin{bmatrix} 1 & \alpha & \cdots & \alpha^{m-1} \\ \alpha & \alpha^2 & & \alpha^m \\ \vdots & & & \vdots \\ \alpha^{m-1} & \cdots & & \alpha^{2m-2} \end{bmatrix} d\alpha \qquad (C.55)$$

where α varies between a and b and $d(\alpha)$ is

$$d(\alpha^*) = \sum_{\substack{\text{whenever} \\ \alpha=\alpha^*}} \frac{1}{\dot{\alpha}^*} \qquad (C.56)$$

$d(\alpha)$ is a measure of the fraction of time spent in the neighborhood of α during the experiment. To study the nature of estimation error, it is best to expand $C(\alpha)$ in polynomials which are orthogonal over the interval $a \leq \alpha \leq b$ with kernel $d(\alpha)$, i.e.,

$$C(\alpha) = C_1' P_1(\alpha) + C_2' P_2(\alpha) + \ldots + C_m' P_m(\alpha) \qquad (C.57)$$

where $P_i(\alpha)$ is a (i-1)st order polynomial in α. Then the information matrix for parameter vector C' is

$$M' = \int_{a}^{b} \frac{d(\alpha)}{r} \begin{bmatrix} P_1^2(\alpha) & P_1(\alpha)P_2(\alpha) & \cdots & P_1(\alpha)P_m(\alpha) \\ P_1(\alpha)P_2(\alpha) & P_2^2(\alpha) & & \vdots \\ \vdots & & & \vdots \\ P_1(\alpha)P_m(\alpha) & \cdots & & P_m^2(\alpha) \end{bmatrix} d\alpha \qquad (C.58)$$

$$= \text{diag} \left\{ \int_a^b \frac{d(\alpha)}{r} \; P_i^2(\alpha) d\alpha \right\} \tag{C.59}$$

Since from condition of orthogonality

$$\int_a^b \frac{d(\alpha)}{r} \; P_i(\alpha) \; P_j(\alpha) d\alpha = 0 \qquad i \neq j \tag{C.60}$$

$$M'^{-1} = \text{diag} \left\{ \int_a^b \frac{d(\alpha)}{r} \; P_i^2(\alpha) d\alpha \right\}^{-1} \tag{C.61}$$

Thus, the variance of $\hat{C}_i'$ is

$$\text{cov}(\hat{C}_i') \geq \left(\int_a^b \frac{d(\alpha) P_i^2(\alpha) d\alpha}{r} \right)^{-1} \tag{C.62}$$

The ratio of parameter value to its standard deviation is

$$t_i' \leq C_i' \left\{ \int_a^b \frac{d(\alpha) P_i^2(\alpha) \; d\alpha}{r} \right\}^{\frac{1}{2}} \tag{C.63}$$

A good $d(\alpha)$ can be established based on the system and the class of inputs. Then the t-ratio for each parameter is determined for the experiment duration. The t ratios usually decrease with increasing i and decreasing (b-a). A suitable (b-a) is chosen to obtain acceptable t-values for the coefficients of the polynomial. For the case where equal time is spent at all α ($a \leq \alpha \leq b$),

$$d(\alpha) = \frac{T}{b-a} \tag{C.64}$$

and $P_i(a)$ are (for a = -1, b = 1),

$$P_o(\alpha) = 1$$

$$P_1(\alpha) = x$$

$$P_2(\alpha) = x^2 - 1/3$$

$$P_3(\alpha) = x^3 + 5/3x^2 - 5/9 \qquad \text{(C.65)}$$

etc.

The expression on the RHS of (C.62) can be computed for all i with r as a parameter.

C.4.2.2 Selection of Experiment Points to Identify Polynomial Expansions

Consider the system

$$\dot{x} = F(x)\, x + G(x)\, u \qquad \text{(c.66)}$$

The matrices F and G contain aerodynamic derivatives which are expressed as polynomial expansions in some state variables. Suppose an experiment is carried out starting from a trim value x_o. It is assumed that the terms in F(x) and G(x) are slowly varying functions of x, so that during this experiment these matrices are almost constant. We can design optimal input for this linear systems so as to obtain "best estimates" of F(x) and G(x). The accuracy of these estimates depends on x_o and the time t_o spent during the experimentation. In particular for an aerodynamic coefficient C which is a function of some state, say α,

$$C(\alpha_o)_e = C_1 + C_2\alpha_o + \ldots + C_m\alpha_o^{m-1} + n(\alpha_o, t_o) \qquad \text{(C.67)}$$

where the noise $n(\alpha_o, t_o)$ has mean zero and covariance which depends on α_o and decreases linearly with t_o, i.e.,

$$E(n^2(\alpha_o, t_o)) = \frac{r(\alpha_o)}{t_o} \tag{C.68}$$

It is clear that if the experiment is carried out in the neighborhood of x_i $(i=1,2,3,\ldots\ell)$ for time t_i, the coefficients C_i's can be estimated using the formulae

$$\hat{C} \triangleq \begin{bmatrix} \hat{C}_1 \\ \hat{C}_2 \\ \vdots \\ \hat{C}_m \end{bmatrix} = M^{-1}Y \tag{C.69}$$

where

$$M = \sum_{i=1}^{\ell} \begin{bmatrix} 1 \\ \alpha_i \\ \alpha_i^2 \\ \vdots \\ \alpha_i^{m-1} \end{bmatrix} \frac{t_i}{r(\alpha_i)} \begin{bmatrix} 1 & \alpha_i & \alpha_i^2 & \cdots & \alpha_i^{m-1} \end{bmatrix} \tag{C.70}$$

and

$$Y = \sum_{i=1}^{\ell} \begin{bmatrix} 1 \\ \alpha_i \\ \alpha_i^2 \\ \vdots \\ \alpha_i^{m-1} \end{bmatrix} \frac{t_i}{r(\alpha_i)} C(\alpha_i)_e \tag{C.71}$$

The Cramer-Rao lower bound on parameter estimate covariance is

$$\mathrm{cov}(\hat{C}) \geq M^{-1} \tag{C.72}$$

The covariance of the estimates approached M^{-1} asymptotically. To obtain good estimates of the nonlinear function over the range of interest, it is necessary to minimize a weighted trace of M^{-1} with the constraint of fixed total experiment time.

$$\sum_{i=1}^{\ell} t_i = T \tag{C.73}$$

The information matrix has the following properties:

(a) It is a positive, semi-definite matrix as is clear from (C.70).

(b) The information matrix is sum of ℓ matrices each of rank one. Therefore, the rank of M cannot exceed ℓ. In other words, the information matrix is singular if the number of experiment points is fewer than m.

We now state and prove a theorem which leads to an algorithm for choosing ℓ, α_i and t_i $(i=1,2,3,\ldots,\ell)$. The set of ℓ, α_i and t_i is called a design .

Theorem C.1. The following are equivalent:

(a) A design α^* minimizes $\mathrm{Tr}(WM^{*-1})$

(b) A design α^* minimizes $\max_{\alpha} \{\varphi^*(\alpha)\}$

(c) A design α^* is such that

$$\max_{\alpha} \varphi^*(\alpha) = \mathrm{Tr}(WM^{*-1}) \tag{C.74}$$

where

$$\varphi(\alpha) = \frac{T}{r(\alpha)} \operatorname{Tr}\left\{ WM^{-1} \begin{bmatrix} 1 & \alpha & \cdots & \alpha^{m-1} \\ \alpha & \alpha^2 & & \alpha^m \\ \vdots & & & \vdots \\ \alpha^{m-1} & & & \alpha^{2m-2} \end{bmatrix} m^{-1} \right\} \tag{C.75}$$

Proof: Consider a design α^* which minimizes $\operatorname{Tr}(WM^{*-1})$. The information matrix for a design which a linear combination of L* and another design in which time T is spent at α is

$$M = \sum_{i=1}^{\ell} \begin{bmatrix} 1 \\ \alpha_i \\ \vdots \\ \alpha_i^{m-1} \end{bmatrix} \frac{t_i(1-\beta)}{r(\alpha_i)} \left(1, \alpha_i, \ldots, \alpha_i^{m-1}\right)$$

$$+ \begin{bmatrix} 1 \\ \alpha \\ \vdots \\ \alpha^{m-1} \end{bmatrix} \frac{T(\beta)}{r(\alpha)} \left(1, \alpha, \ldots, \alpha^{m-1}\right) \tag{C.76}$$

Since L* minimizes $\operatorname{Tr}(WM^{-1})$

$$\left.\frac{\partial \operatorname{Tr}(WM^{-1})}{\partial \beta}\right|_{\beta = 0} = -\left. \operatorname{Tr}\left(WM^{-1} \frac{\partial M}{\partial \beta} M^{-1}\right)\right|_{\beta = 0} \geq 0 \tag{C.77}$$

Also

$$\frac{\partial M}{\partial \beta} = - \sum_{i=1}^{\ell} \begin{bmatrix} 1 \\ \alpha_i \\ \vdots \\ \alpha_i^{m-1} \end{bmatrix} \frac{t_i}{r(\alpha_i)} \quad (1, \alpha_i, \ldots, \alpha_i^{m-1})$$

$$+ \frac{T}{r(\alpha)} \begin{bmatrix} 1 & \alpha & \cdots & \alpha^{m-1} \\ \alpha & \alpha^2 & & \alpha^m \\ \vdots & & & \vdots \\ \alpha^{m-1} & \cdots & & \alpha^{2m-2} \end{bmatrix} \tag{C.78}$$

From (C.77) and (C.78)

$$+ \mathrm{Tr}(WM^{*-1}) - \frac{T}{r(\alpha)} \mathrm{Tr}\, WM^{*-1} \begin{bmatrix} 1 & \alpha & \cdots & \alpha^{m-1} \\ \alpha & \alpha^2 & & \alpha^m \\ \vdots & & & \vdots \\ \alpha^{m-1} & \cdots & & \alpha^{2m-2} \end{bmatrix} M^{-1} \geq 0$$

or

$$\varphi^*(\alpha) \leq \mathrm{Tr}(WM^{*-1}) \tag{C.79}$$

Since we can choose any α from the range of interest, (C.79) holds for all α. Also for any design L

$$\sum_{\alpha=\alpha_1}^{\alpha_\ell} \varphi(\alpha) \frac{t_i}{T} = \mathrm{Tr}\, WM^{-1} \sum_{\alpha=\alpha_1}^{\alpha_\ell} \frac{t_i}{r(\alpha)} \begin{bmatrix} 1 & \alpha & \cdots & \alpha^{m-1} \\ \alpha & \alpha^2 & & \alpha^m \\ \vdots & & & \vdots \\ \alpha^{m-1} & \cdots & & \alpha^{2m-2} \end{bmatrix} M^{-1}$$

$$= \mathrm{Tr}(WM^{-1}MM^{-1}) = \mathrm{Tr}(WM^{-1}) \tag{C.80}$$

Since

$$\sum_{i=1}^{\ell} \frac{t_i}{T} = 1 \qquad \text{and } t_i \geq 0 \tag{C.81}$$

$$\max_{\alpha} \varphi(\alpha) \geq \mathrm{Tr}(WM^{-1}) \tag{C.82}$$

(C.79) and (C.80) are in contradiction unless

$$\max_{\alpha} \varphi(\alpha) = \mathrm{Tr}(WM^{*-1}) \tag{C.83}$$

which proves (c) and in the light of (C.82), proves (b). The assertion that (b) or (c) imply (a) is quite straightforward.

The following procedure can be used to find the optimal design L*.

(a) Evaluate $r(\alpha)$ based on design of linear experiments in the neighborhood of α. This function may also include "cost" of carrying out the experiment about state α.

(b) Choose a nondegenerate design L. It should have at least m experiment points where finite time is spent. Find M^{-1}.

(c) Find α where $\varphi(\alpha)$ is maximum. This $\varphi(\alpha)$ is more than $\mathrm{Tr}(WM^{-1})$.

(d) Find a β between 0 and 1 such that by spending time $(T1-\beta)$ in points of design L and $T\beta$ at α, the $\mathrm{Tr}(WM^{-1})$ is minimized.

(e) The new design has $\ell+1$ points at α_i $(i=1,2,\ldots,\ell)$, α with time $(1-\beta)t_i$ $(i=1,2,\ldots,\ell)$, $T\beta$ at these points respectively.

(f) Check if $\max_{\alpha} \varphi(\alpha)$ is close to $\mathrm{Tr}(WM^{-1})$. If not, return to (c).

The fact that $\max_{\alpha} \varphi(\alpha)$ is greater than $\mathrm{Tr}(WM^{-1})$ is clear from (C.82). Also, from (C.77) and (C.78), for small β

$$\mathrm{Tr}(WM^{-1})_{\beta} = \mathrm{Tr}(WM^{-1})_{\beta=0} - \beta(\varphi(\alpha) - \mathrm{Tr}(WM^{-1})_{\beta=0}) \qquad (C.84)$$

Since $\mathrm{Tr}(WM^{-1})$ decreases for small β, it is clear that β of step (d) exists. Also, as long as the design is not optimal, it is always possible to decrease $\mathrm{Tr}(WM^{-1})$. Since it is bounded from below, it must converge to the optimum.

It can also be shown that the number of points in the design cannot exceed $\frac{m(m+1)}{2}$. In many cases, it is m.

APPENDIX D
SIMULATION EQUATIONS

This appendix is drawn from reference [1] wherein the complete simulation used for generating the data is described. Because of the significance of the detail of these equations, and the need to refer to them in this report, this appendix is given.

A flow chart of the simulation is given in Figure D.1. The following features are notable:

1. The aerodynamic data are "table look-up" and valid for $-10^{o} \leq \alpha \leq 110^{o}$ and $-40^{o} \leq \beta \leq +40^{o}$. These data are reported in reference [ ].

2. Three types of controls are available--pilot stick (autopilot), pilot stick (read in) and stability augmentation system.

3. The time histories of responses and aerodynamic coefficients may be outputted. The time histories are either outputted as calculated (ideal) or they are passed through nonlinear, randomly disturbed, instruments.

Further program characteristics are listed in Table 2.1.

D.1 EQUATIONS OF MOTION IN BODY AXES

D.1.1 Translation Equations

$$\begin{bmatrix} \dot{u} \\ \dot{v} \\ \dot{w} \end{bmatrix} = \begin{bmatrix} F_x^I + F_x^a + F_x^e + F_x^g \\ F_y^I + F_y^a + F_y^e + F_y^g \\ F_z^I + F_z^a + F_z^e + F_z^g \end{bmatrix}$$

where

$$\begin{bmatrix} F_x^I \\ F_y^I \\ F_z^I \end{bmatrix} = \begin{bmatrix} vr - wq \\ wp - ur \\ uq - vp \end{bmatrix}$$

APPENDIX D
SIMULATION EQUATIONS

This appendix is drawn from reference [1] wherein the complete simulation used for generating the data is described. Because of the significance of the detail of these equations, and the need to refer to them in this report, this appendix is given.

A flow chart of the simulation is given in Figure D.1. The following features are notable:

1. The aerodynamic data are "table look-up" and valid for $-10^{\circ} \leq \alpha \leq 110^{\circ}$ and $-40^{\circ} \leq \beta \leq +40^{\circ}$. These data are reported in reference [ ].

2. Three types of controls are available--pilot stick (autopilot), pilot stick (read in) and stability augmentation system.

3. The time histories of responses and aerodynamic coefficients may be outputted. The time histories are either outputted as calculated (ideal) or they are passed through nonlinear, randomly disturbed, instruments.

Further program characteristics are listed in Table 2.1.

D.1 EQUATIONS OF MOTION IN BODY AXES

D.1.1 Translation Equations

$$\begin{bmatrix} \dot{u} \\ \dot{v} \\ \dot{w} \end{bmatrix} = \begin{bmatrix} F_x^I + F_x^a + F_x^e + F_x^g \\ F_y^I + F_y^a + F_y^e + F_y^g \\ F_z^I + F_z^a + F_z^e + F_z^g \end{bmatrix}$$

where

$$\begin{bmatrix} F_x^I \\ F_y^I \\ F_z^I \end{bmatrix} = \begin{bmatrix} vr - wq \\ wp - ur \\ uq - vp \end{bmatrix}$$

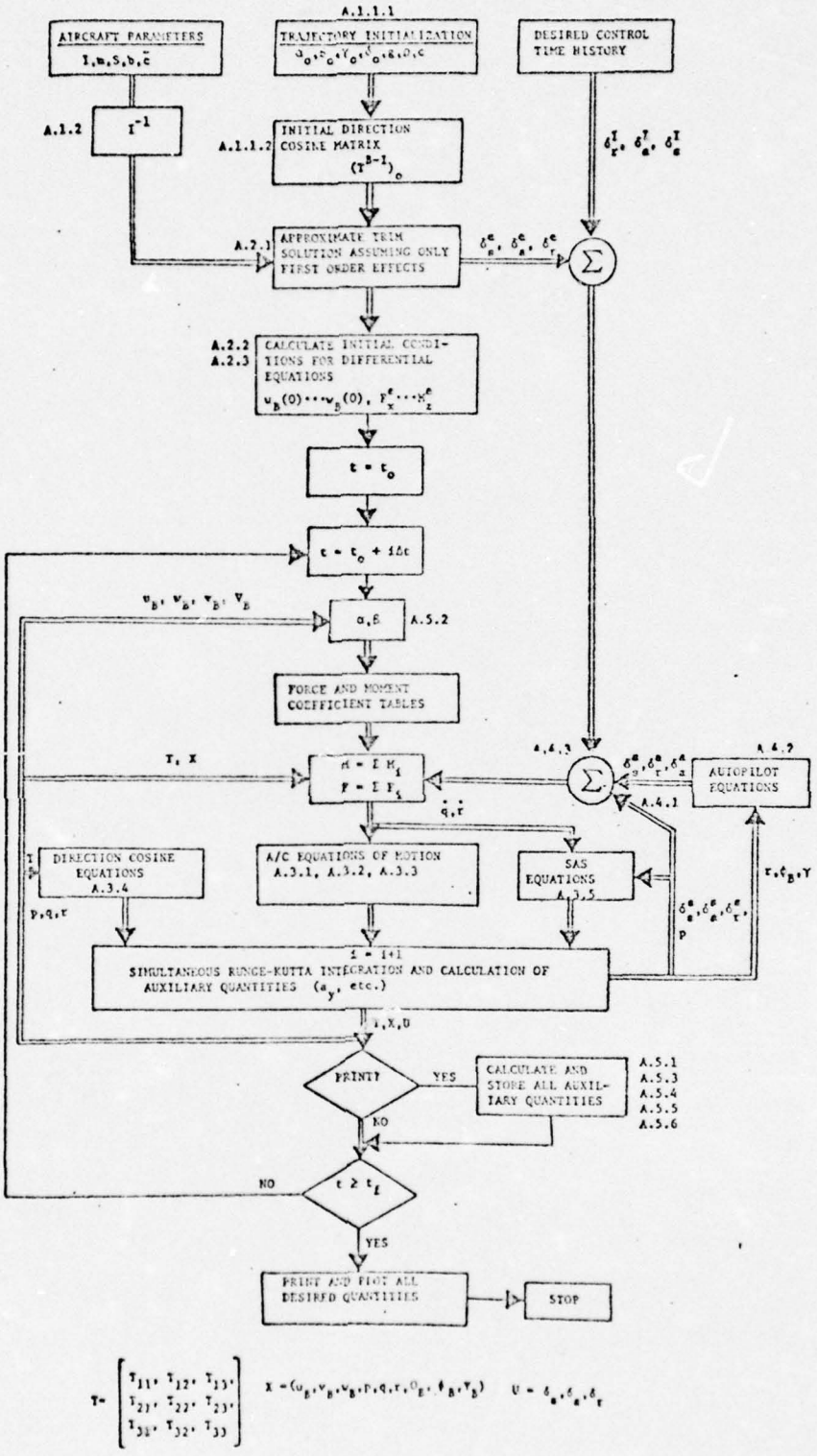

$$T = \begin{bmatrix} T_{11}, T_{12}, T_{13}, \\ T_{21}, T_{22}, T_{23}, \\ T_{31}, T_{32}, T_{33} \end{bmatrix} \qquad X = (u_B, v_B, w_B, p, q, r, \theta_E, \phi_B, \gamma_B) \qquad U = \delta_e, \delta_a, \delta_r$$

Figure D.1 Flow Chart of Six Degree-of-Freedom Simulation

$$\begin{bmatrix} F_x^a \\ F_y^a \\ F_z^a \end{bmatrix} = \frac{q_B S}{m} \begin{bmatrix} C_x + C_{x_{\delta s}} \delta s + \bar{c} q \, C_{x_q} / 2V_B \\ C_y + C_{y_{\delta r}} \delta r + C_{y_{\delta a}} \delta a + C_{y_{\delta s}} \delta s + b(rC_{y_r} + pC_{y_p})/2V_B \\ C_z + C_{z_{\delta s}} \delta s + \bar{c} q \, C_{z_q} / 2V_B \end{bmatrix}$$

$$\begin{bmatrix} F_x^g \\ F_y^g \\ F_z^g \end{bmatrix} = g \begin{bmatrix} T_{1,3} \\ T_{2,3} \\ T_{3,3} \end{bmatrix}$$

where $T_{1,3} = - \sin \Theta$

$T_{2,3} = \sin \Phi \cos \Theta$

$T_{3,3} = \cos \Phi \cos \Theta$

D.1.2 Rotational Equations

$$\begin{bmatrix} \dot{p} \\ \dot{q} \\ \dot{r} \end{bmatrix} = C \begin{bmatrix} M_x^I + M_x^a + M_x^e \\ M_y^I + M_y^a + M_y^e \\ M_z^I + M_z^a + M_z^e \end{bmatrix}$$

where

$$\begin{bmatrix} M_x^I \\ M_y^I \\ M_z^I \end{bmatrix} = \begin{bmatrix} \frac{1}{I_x} \left\{ p(qI_{xz} - rI_{xy}) + qr(I_y - I_z) + I_{yz}(q^2 - r^2) \right\} \\ \frac{1}{I_y} \left\{ q(rI_{xy} - pI_{yz}) + pr(I_z - I_x) + I_{xz}(r^2 - p^2) - rI_E \Omega_E \right\} \\ \frac{1}{I_z} \left\{ r(pI_{xy} - qI_{xz}) + pq(I_x - I_y) + I_{xy}(p^2 - q^2) + qI_E \Omega_E \right\} \end{bmatrix}$$

$$\begin{bmatrix} M_x^a \\ M_y^a \\ M_z^a \end{bmatrix} = q_B S \begin{bmatrix} \frac{b}{I_x}\left\{C_\ell + C_{\ell_{\delta r}}\delta r + C_{\ell_{\delta a}}\delta a + C_{\ell_{\delta s}}\delta s + b(rC_{\ell_r} + pC_{\ell_p})/2V_B\right\} \\ \frac{\bar{c}}{I_y}\left\{C_m + C_{m_{\delta s}}\delta s + \bar{c}q\, C_{m_q}/2V_B\right\} \\ \frac{b}{I_z}\left\{C_n + C_{n_{\delta r}}\delta r + C_{n_{\delta a}}\delta a + C_{n_{\delta s}}\delta s + b(rC_{n_r} + pC_{n_p})/2V_B\right\} \end{bmatrix}$$

and

$$C = \begin{bmatrix} 1 & -I_{xy}/I_x & -I_{xz}/I_x \\ -I_{xy}/I_y & 1 & -I_{yz}/I_y \\ -I_{xz}/I_z & -I_{yz}/I_z & 1 \end{bmatrix}^{-1}$$

$$= \frac{1}{\Delta}\begin{bmatrix} 1-I_{yz}^2/I_yI_z & (I_{xy}+I_{xz}I_{yz}/I_z)/I_x & (I_{xz}+I_{xy}I_{yz}/I_y)/I_x \\ (I_{xy}+I_{xz}I_{yz}/I_z)/I_y & 1-I_{xz}^2/I_xI_z & (I_{yz}+I_{xy}I_{xz}/I_x)/I_y \\ (I_{xz}+I_{xy}I_{yz}/I_y)/I_z & (I_{yz}+I_{xy}I_{xz}/I_x)/I_z & 1-I_{xy}^2/I_xI_y \end{bmatrix}$$

where

$$\Delta = 1 - \frac{I_{xy}^2}{I_xI_y} - \frac{I_{xz}^2}{I_xI_z} - \frac{I_{yz}^2}{I_yI_z} - \frac{2I_{xy}I_{xz}I_{yz}}{I_xI_yI_z}$$

D.1.3 Stability Augmentation System

$$\dot{\delta s}' = .15\dot{q} - \delta s' \qquad \text{pitch}$$

$$\dot{\delta r}' = 3\dot{r} - \frac{1}{2}\delta r_1' \qquad \text{yaw}$$

$\delta r' = \delta r_1' + .0168 a_y g$ if $|\delta r'| > 5^o$, set $\delta r' = (\text{sgn } \delta r') 5^o$

$\delta a' = .265 p$ if $|\delta a'| > 7.5^o$, set $\delta a' = (\text{sgn } \delta a') 7.5^o$

if $|\delta s'| > 0^\circ.5$, set $\delta s' = (\text{sgn } \delta s') 0^\circ.5$

D.1.4 Autopilot

$$\delta_r^a = 7r + \varphi_B$$

$$\delta_a^a = .3\varphi_B$$

$$\delta_s^a = + \gamma$$

D.1.5 Total Controls

$$\delta_r = \delta_{r_o} + \delta_r' + \delta_r^a + \delta_r^I \qquad |\delta r| \leq 30^o$$

$$\delta_a = \delta_{a_o} + \delta_a' + \delta_a^a + \delta_a^I \qquad |\delta a| \leq 30^o$$

$$\delta_s = \delta_{s_o} + \delta_s' + \delta_s^a + \delta_s^I \qquad -21^o \leq \delta s \leq 9^o$$

where

δ_r^I, δ_a^I, δ_s^I are input controls; δ_r^a, δ_a^a, δ_s^a are autopilot controls; δ_r', δ_a', δ_s' are SAS controls; δ_{r_o}, δ_{a_o}, δ_{s_o} are trim controls.

D.2 INSTRUMENTATION EQUATIONS

D.2.1 Attitude Gyros

$$\theta_m = (1 + k_\theta)\theta + b_\theta + w_\theta$$

$$\varphi_m = (1 + k_\varphi)\varphi + b_\varphi + w_\varphi$$

k_θ scale factor on pitch

b_θ bias on pitch

w_θ noise on pitch

D.2.2 Rate Gyros

D.2.2.1 Resolution

$$p_r = p + q\psi_p - r\theta_p$$

$$q_r = -p\psi_q + q - r\varphi_q$$

$$r_r = p\theta_r \quad q\varphi_r + r$$

where ψ_p, θ_p, ψ_q, φ_q, θ_r, φ_r are random variables of gyro Euler angle misalignment.

D.2.2.2 Measurements

$$p_m = (1 + k_p)\, p_r + b_p + w_p$$

$$q_m = (1 + k_q)\, q_r + b_q + w_q$$

$$r_m = (1 + k_r)\, r_r + b_r + w_r$$

D.2.3 Angular Accelerometers

D.2.3.1 Resolution

$$\dot{p}_r = \dot{p} + \dot{q}\psi_p - \dot{r}\theta_p$$

$$\dot{q}_r = -\dot{p}\psi_q + \dot{q} - \dot{r}\varphi_q$$

$$\dot{r}_r = \dot{p}\theta_r - \dot{q}\varphi_r + \dot{r}$$

D.3.3.2 Measurements

$$\dot{p}_m = (1 + k_{\dot{p}})\dot{p}_r + b_{\dot{p}} + w_{\dot{p}}$$

$$\dot{q}_m = (1 + k_{\dot{q}})\dot{q}_r + b_{\dot{q}} + w_{\dot{q}}$$

$$\dot{r}_m = (1 + k_{\dot{r}})\dot{r}_r + b_{\dot{r}} + w_{\dot{r}}$$

D.2.4 Velocity

$$V_i^2 = (1 + k_v)V_B^2 \sigma\, f_c(M) + b_v + w_v$$

where $\sigma = \rho/\rho_o$

$$f_c(M) = 1 + \frac{M^2}{4} + \frac{M^4}{40} + \ldots \qquad M = \text{Mach no.}$$

D.2.5 Angle-of-Attack

D.2.5.1 Indicated

$$\alpha_i = (1+k_\alpha)\, \tan^{-1} \frac{V_B \sin\alpha \cos\beta - q\,\ell_x + p\ell_y}{V_B \cos\alpha \cos\beta + q\ell_z - r\ell_y} + b_\alpha + w_\alpha$$

where ℓ_x, ℓ_y, ℓ_z are random variables

D.2.5.2 Corrected

$$\alpha_c = \alpha_i + \frac{\ell_x g}{V_i^2}(\bar{a}_n - \cos\varphi_m \cos\theta_m) + \frac{q_m \hat{\ell}_x}{V_i}\cos\alpha_i$$

where $\bar{a}_n = -\hat{a}_{Z_{cg}}$

$\hat{\ell}_x$ is a constant, estimated distance from the c.g. to vane

D.2.6 Sideslip Angle

D.2.6.1 Indicated

$$\beta_i = (1 + k_\beta) \tan^{-1} \frac{V_B \sin \beta + r\ell_x - p\ell_z}{V_B \cos \alpha \cos \beta + q\ell_z - r\ell_y} + b_\beta + w_\beta$$

D.2.6.2 Corrected

$$\beta_c = \beta_i |\cos \alpha_c| - \frac{r_m \hat{\ell}_x}{V_i} \cos \beta_i$$

D.2.7 Linear Accelerometer

D.2.7.1 CG Acceleration

$$\ddot{x}_{cg} = \frac{\dot{u} - vr + wq}{g} - T_{1,3}$$

$$\ddot{y}_{cg} = \frac{\dot{v} - wp + ur}{g} - T_{2,3}$$

$$\ddot{z}_{cg} = \frac{\dot{w} - uq + vp}{g} - T_{3,3}$$

D.2.7.2 Accelerometer Triad

$$\ddot{x}_A = \ddot{x}_{cg} + \frac{\dot{q}z_{cg_A} - \dot{r}y_{cg_A} - (r^2+q^2)x_{cg_A} + rpz_{cg_A} + pqy_{cg_A}}{g}$$

$$\ddot{y}_L = \ddot{y}_{cg} + \frac{\dot{r}x_{cg_L} - \dot{p}z_{cg_L} - (r^2+p^2)y_{cg_L} + rqz_{cg_A} + pqx_{cg_A}}{g}$$

$$\ddot{z}_v = \ddot{z}_{cg} + \frac{\dot{p}y_{cg_v} - \dot{q}x_{cg_v} - (q^2+p^2)z_{cg_v} + prx_{cg_v} + qry_{cg_v}}{g}$$

where $x_{cg_A}, y_{cg_A}, \ldots, z_{cg_v}$ are random variables

D.2.7.3 Axial Accelerometer

$$n_x = \ddot{x}_A + \frac{\psi_A \ddot{y}_A - \theta_A \ddot{z}_v}{g}$$

$$n_{x_m} = (1 + k_{n_x}) n_x + b_{n_x} + w_{n_x}$$

$$\hat{a}_{x_{cg}} = n_{x_m} + \frac{\dot{r}_m \hat{y}_{cg_A} - \dot{q}_m \hat{z}_{cg_A}}{g}$$

where ψ_A, θ_A are random variables; Euler angles of accelerometer misalignment

$\hat{y}_{cg_A}$, $\hat{z}_{cg_A}$ are constants, estimated position of the accelerometer

D.2.7.4 Lateral Accelerometer

$$n_y = \ddot{y}_L + \frac{\varphi_L \ddot{z}_v - \psi_L \ddot{x}_A}{g}$$

$$n_{y_m} = (1 + k_{n_y}) n_y + b_{n_y} + w_{n_y}$$

$$\hat{a}_{y_{cg}} = n_{y_m} + \frac{\dot{p}_m \hat{z}_{cg_L} - \dot{r}_m \hat{x}_{cg_L}}{g}$$

where φ_L, ψ_L are random variables, Euler angles of accelerometer misalignment

$\hat{x}_{cg_L}$, $\hat{z}_{cg_L}$ are constants, estimated position of the accelerometer

D.2.7.5 Vertical Accelerometer

$$n_z = \ddot{z}_v + \frac{\theta_v \ddot{x}_A - \varphi_v \ddot{y}_L}{g}$$

$$n_{z_m} = (1 + k_{n_z}) n_z + b_{n_z} + w_{n_z}$$

$$\hat{a}_{z_{cg}} = n_{z_m} + \frac{\dot{q}_m \hat{x}_{cg_v} - \dot{p}_m \hat{y}_{cg_v}}{g}$$

where θ_v, φ_v are random variables, Euler angles of accelerometer misalignment

$\hat{x}_{cg_v}$, $\hat{y}_{cg_v}$ are constants, estimates of the accelerometer position

D.2.7.6 Pilot Station Vertical Accelerometer

$$\ddot{x}_{ps} = \ddot{x}_{cg} + \frac{\dot{q} z_{ps} - \dot{r} y_{ps} - (r^2+q^2) x_{ps} + rpz_{ps} + pqy_{ps}}{g}$$

$$\ddot{y}_{ps} = \ddot{y}_{cg} + \frac{\dot{r} x_{ps} - \dot{p} z_{ps} - (r^2+p^2) y_{ps} + rqz_{ps} + pqx_{ps}}{g}$$

$$\ddot{z}_{ps} = \ddot{z}_{cg} + \frac{\dot{p} y_{ps} - \dot{p} x_{ps} - (q^2+p^2) z_{ps} + prx_{ps} + qry_{ps}}{g}$$

$$n_{ps} = \ddot{z}_{ps} + \frac{\theta_v \ddot{x}_{ps} - \varphi_v \ddot{y}_{ps}}{g}$$

$$n_{ps_m} = (1 + k_{n_z}) n_{ps} + b_{n_z} + w_{n_z}$$

where x_{ps}, y_{ps}, z_{ps} are random variables, the location of the pilot station relative to the c.g.

APPENDIX E
IDENTIFICATION MODEL EQUATIONS

E.1 INTRODUCTION

The equations of motion for the aircraft simulation are given in the preceding Appendix D. These equations are to provide the framework for data generation. For parameter identification, a less general, more approximated model representation is desired, which still retains the essential features of the known aircraft dynamics. Similar approximations must be applied to the instrumentation models. This appendix outlines the models used in the identification program.

E.2 DYNAMIC AND MEASUREMENT EQUATIONS

The state equations are:

$$\dot{\hat{u}} = \hat{v}\hat{r} - \hat{w}\hat{q} + \frac{\hat{q}_B S}{m}\left[\hat{C}_x + \hat{C}_{x_{\delta_s}}\hat{\delta}_s + \frac{\bar{c}}{2\hat{V}_B}\hat{C}_{x_q}\hat{q} + \frac{T_x}{m} - g\sin\hat{\theta}\right] \tag{E.1}$$

$$\dot{\hat{v}} = \hat{w}\hat{p} - \hat{u}\hat{r} + \frac{\hat{q}_B S}{m}\left[\hat{C}_y + \hat{C}_{y_{\delta_r}}\delta_r + \hat{C}_{y_{\delta_a}}\delta_a + \frac{b}{2\hat{V}_B}\left(\hat{C}_{y_r}\hat{r} + \hat{C}_{y_p}\hat{p}\right)\right]$$

$$+ \frac{T_y}{m} + g\cos\hat{\theta}\sin\hat{\varphi} \tag{E.2}$$

$$\dot{\hat{w}} = \hat{u}\hat{q} - \hat{v}\hat{p} + \frac{\hat{q}_B S}{m}\left[\hat{C}_z + \hat{C}_{z_{\delta_s}}\delta_s + \frac{\bar{c}}{2\hat{V}_B}\hat{C}_{z_q}\hat{q}\right] + \frac{T_z}{m} + g\cos\hat{\theta}\sin\hat{\varphi} \tag{E.3}$$

and, for

$$\hat{C}'_\ell = \hat{C}_\ell + \hat{C}_{\ell_{\delta_r}}\delta_r + \hat{C}_{\ell_{\delta_a}}\delta_a + \frac{b}{2\hat{V}_B}\left(\hat{C}_{\ell_r}\hat{r} + \hat{C}_{\ell_p}\hat{p}\right) \tag{E.4}$$

$$\hat{C}'_n = \hat{C}_n + \hat{C}_{n_{\delta_r}}\delta_r + \hat{C}_{n_{\delta_a}}\delta_a + \frac{b}{2\hat{V}_B}\left(\hat{C}_{n_r}\hat{r} + \hat{C}_{n_p}\hat{p}\right) \tag{E.5}$$

$$\dot{\hat{p}} = \frac{1}{F_5}\left\{\hat{q}_B Sb(I_x \hat{C}'_\ell + I_{xz}\hat{C}'_n) + \hat{p}\hat{q}F_1 + \hat{q}\hat{r}F_2 + \hat{q}F_3 + F_4\right\} \tag{E.6}$$

$$\dot{\hat{q}} = \frac{1}{I_y}\left\{\hat{q}_B S\bar{c}\left(\hat{C}_m + \hat{C}_{m_{\delta_s}}\delta_s + \frac{\bar{c}}{2\hat{V}_B}\hat{C}_{m_q}\hat{q}\right) - I_{xz}(\hat{p}^2 - \hat{r}^2)\right.$$

$$\left. - F_9\hat{p}\hat{r} - F_{10}\hat{r} + M_y\right\} \tag{E.7}$$

$$\dot{\hat{r}} = \frac{1}{F_5}\left\{\hat{q}_B Sb(I_z \hat{C}'_n + I_{xz}\hat{C}'_\ell) - \hat{q}\hat{r}F_1 + \hat{p}\hat{q}F_6 + \hat{q}F_7 + F_8\right\} \tag{E.8}$$

$$\dot{\hat{\varphi}} = \hat{p} + (\hat{q}\sin\hat{\varphi} + \hat{r}\cos\hat{\varphi})\tan\hat{\theta} \tag{E.9}$$

$$\dot{\hat{\theta}} = \hat{q}\cos\hat{\varphi} - \hat{r}\sin\hat{\varphi} \tag{E.10}$$

$$\dot{\hat{\psi}} = (\hat{q}\sin\hat{\varphi} + \hat{r}\cos\hat{\varphi})/\cos\hat{\theta} \tag{E.11}$$

$$F_1 = I_{xz}(I_x + I_z - I_y) \tag{a}$$

$$F_2 = I_{yz} - I_{xz}^2/(I_x I_z) \tag{b}$$

$$F_3 = I_{xz} I_e \Omega \tag{c}$$

$$F_4 = I_x M_x + I_{xz} M_z \tag{d}$$

$$F_5 = 1 - I_{xz}^2/(I_x I_z) \tag{e}$$

(E.12)

$$F_6 = I_{xy} + I_{xz}^2/(I_x I_z) \tag{f}$$

$$F_7 = I_z I_e \Omega \tag{g}$$

$$F_8 = I_z M_z + I_{xz} M_x \tag{h}$$

$$F_9 = I_x - I_y \tag{i}$$

$$F_{10} = I_e \Omega \tag{j}$$

$$\hat{V}_B = \hat{u}^2 + \hat{v}^2 + \hat{w}^2 \tag{k}$$

$$\hat{q}_B = \frac{\rho \hat{V}_B^2}{2} \tag{l}$$

(E.12)

The measurement equations are:

$$\hat{\alpha} = \tan^{-1}\left(\frac{\hat{u}}{\hat{w}}\right) + \hat{b}_\alpha \tag{E.13}$$

$$\hat{\beta} = \sin^{-1}\left(\frac{\hat{v}}{\hat{V}}\right) + \hat{b}_\beta \tag{E.14}$$

$$\ddot{\hat{x}} = (\dot{\hat{u}} - \hat{v}\hat{r} + \hat{w}\hat{q})/g + \sin\hat{\theta} + \hat{b}_{\ddot{x}} \tag{E.15}$$

$$\ddot{\hat{y}} = (\dot{\hat{v}} - \hat{w}\hat{p} + \hat{u}\hat{r})/g - \sin\hat{\varphi}\cos\hat{\theta} + \hat{b}_{\ddot{y}} \tag{E.16}$$

$$\ddot{\hat{z}} = (\dot{\hat{w}} - \hat{u}\hat{q} + \hat{v}\hat{p})/g - \cos\hat{\theta}\cos\hat{\varphi} + \hat{b}_{\ddot{z}} \tag{E.17}$$

$$\hat{p}_m = \hat{p} + \hat{b}_p \tag{E.18}$$

$$\hat{q}_m = \hat{q} + \hat{b}_q \tag{E.19}$$

$$\hat{r}_m = \hat{r} + \hat{b}_r \tag{E.20}$$

Comparison of Eqs. (E.13) - (E.12) with the detailed nonlinear instrumentation models of Appendix D indicates the degree of approximation of the measurements.

E.3 SENSITIVITY EQUATIONS

The dynamic equations, (E.1) - (E.11), may be functionally written

$$C\dot{x} = f_s + f_e + f_a \tag{E.21}$$

where C is a coefficient matrix of constants (which may or may not be known), f_s are inertial, engine gyroscopic and gravitational terms, f_e are engine thurst terms, and f_a are aerodynamic terms. Denoted θ_i as a particular parameter, the sensitivity of Eq. (E.21) to θ_i is

$$\frac{\partial \dot{x}}{\partial \theta_i} = C^{-1}\left[\frac{\partial f_s}{\partial \theta_i} + \frac{\partial f_a}{\partial \theta_i} - \frac{\partial C}{\partial \theta_i}(f_s + f_a + f_e)\right]$$

where $\partial f_e/\partial \theta_i$ is, in general, zero. Note that the assumption of $\partial f_e/\partial \theta_i = 0$ would not be used for cases where the engine thrust is highly dependent on state.

If the identification requirements include separation of $C_{x_{\dot{\alpha}}}$, $C_{y_{\dot{\beta}}}$, $C_{z_{\dot{\alpha}}}$, $\partial C/\partial \theta_i$ will be non-zero, otherwise $\partial C/\partial \theta_i = 0$.

The expression for $\partial f_a/\partial \theta_i$ is

$$\frac{\partial f_a}{\partial \theta_i} = \frac{\rho s}{m}\left\{\left[VC_S + \tfrac{1}{2}C_R\right]\frac{\partial V}{\partial \theta_i} + V\left[V\frac{\partial C_S}{\partial \theta_i} + \tfrac{1}{2}\frac{\partial C_R}{\partial \theta_i}\right]\right\}$$

where C_S are the static coefficients and C_R the dynamic rate coefficients with general expansions

$$C = C_o(\bar{\alpha},\bar{\beta}) + \sum_i C_{\alpha^{(i)}}\alpha^{(i)} + \sum_j C_{\beta^{(j)}}\beta^{(j)} + \sum_i \sum_j C_{\alpha^{(i)}\beta^{(j)}}\alpha^{(i)}\beta^{(j)}$$

and the coefficients θ are the coefficients of $\alpha^{(i)}$, $\beta^{(j)}$, or $\alpha^{(i)}\beta^{(j)}$.

Sensitivity equations for the measurements are obtained from Eqs. (E.13) - (E.20).

E.4 ALTERNATE IDENTIFICATION EQUATIONS FOR THE (α, β, V) FRAME

The identification equations of translational motion, for some applications, may be transformed to an α, β, V coordinate system. These are given in Table #.1. The corresponding linear accelerations are given in Table E.2.

TABLE E.1

Equations of Translational Motion in α, β, V System

$$\dot{V} = \frac{qS}{mV}\left\{\left[-C'_x - C_{x_{\delta_s}}\delta_s - \frac{\bar{c}}{2V}\left(C'_{x_{\dot{\alpha}}}\dot{\alpha} + C'_{z_q}q\right)\right]\cos\beta + \left[C_y + C_{y_{\delta_r}}\delta_r + \left(C_{y_{\dot{\beta}}}\dot{\beta} + C_{y_r}r + C_{y_p}p\right)\frac{b}{2V}\right]\sin\beta\right\}$$

$$+\frac{1}{V}\left\{\left(\frac{T_x}{m} - g\sin\theta\right)\cos\alpha\cos\beta + \left(\frac{T_z}{m} + g\cos\theta\sin\varphi\right)\sin\alpha\cos\beta + \left(\frac{T_y}{m} + g\cos\theta\sin\varphi\right)\sin\beta\right\}$$

where $(\cdot)' = (\cdot)\cos\alpha - (\cdot)\sin\alpha$

$$(\dot{\alpha} - q_b) = \frac{\left[\frac{qS}{mV\cos\beta}\left\{C'_z + C'_{z_{\delta_s}}\delta_s + \frac{\bar{c}}{2V}C'_{z_q}q\right\} - (p\cos\alpha + r\sin\alpha)\tan\beta + \frac{1}{V}\left\{\left(\frac{T_z}{m} + g\cos\theta\cos\varphi\right)\frac{\cos\alpha}{\cos\beta} - \left(\frac{T_x}{m} - g\sin\theta\right)\frac{\sin\alpha}{\cos\beta}\right\}\right]}{\left(1 - \frac{\bar{c}}{2V}C'_{z_{\dot{\alpha}}}\right)}$$

where $(\cdot)' = (\cdot)\cos\alpha - (\cdot)\sin\alpha$

$$\dot{\beta} = \frac{\left[\frac{qS}{mV}\left\{\left[C_y + C_{y_{\delta_r}}\delta_r + C_{y_{\delta_a}}\delta_a + \left(C_{y_r}r + C_{y_p}p\right)\frac{b}{2V}\right]\cos\beta + \left[\left(C'_{z_{\dot{\alpha}}}\dot{\alpha} + C_{z_q}q\right)\frac{\bar{c}}{2V} + C'_z + C'_{z_{\delta_s}}\delta_s\right]\sin\beta\right\}\right.}{\left.+(p\sin\alpha - r\cos\alpha) + \frac{1}{V}\left\{\left(\frac{T_y}{m} + g\cos\theta\sin\varphi\right)\cos\beta + \left(\frac{T_z}{m} + g\cos\theta\cos\varphi\right)\sin\beta\sin\alpha + \left(-\frac{T_x}{m} + g\sin\theta\right)\cos\alpha\sin\beta\right\}\right]}{\left(1 - C_{y_{\dot{\beta}}}\frac{b}{2V}\cos\beta\right)}$$

where $(\cdot)' = (\cdot)\cos - (\cdot)\sin\alpha$

TABLE E.2

Accelerometer Equations in α, β, V System

$$A_{x_{c.g.}} = \dot{V} \cos\beta \cos\alpha - V\left[(\dot{\beta}\cos\alpha + r)\sin\beta + (\dot{\alpha} - q)\sin\alpha\cos\beta\right] - g\sin\Theta$$

$$A_{y_{c.g.}} = \dot{V}\sin\beta + V\left[\cos\beta(\beta + r\cos\alpha - p\sin\alpha) + g\cos\Theta\sin\varphi\right]$$

$$A_{z_{c.g.}} = \dot{V}\cos\beta\sin\alpha + V\left[(p - \beta\sin\alpha)\sin\beta + (\dot{\alpha} - q)\cos\beta\cos\alpha - g\cos\Theta\cos\Phi\right]$$

REFERENCES

1. Hall, Jr., W.E., "Identification of Aircraft Stability and Control Derivatives for the High Angle-of-Attack Regime", Technical Report No. 1, prepared for the Office of Naval Research under Contract N00014-72-C-0328, June, 1973.

2. McElroy, C.E. and Sharp, P.S., "Stall/Near Stall Investigation of the F-4E Aircraft", Air Force Flight Test Center, Edwards Air Force Base, FIC-SD-70-20, October 1970.

3. Thelander, J.A., "Aircraft Motion Analysis", FDL-TDR-64-70, 1964.

4. Etkin, E., Dynamics of Atmospheric Flight, John Wiley and Sons (1971); (also Dynamics of Flight, John Wiley (1959)).

5. Grafton, S.B. and Libbey, C.E., "Dynamic Stability Derivatives of a Twin Jet Fighter for Angles-of-Attack From -10^{o} to 110^{o}", NASA TND-6091.

6. Anglin, E.L., "Static Force Tests of a Model of a Twin-Jet Fighter Airplane for Angles-of-Attack From -10^{o} to 110^{o} and Sideslip Angles From -40^{o} to $+40^{o}$", NASA TND-6425, August 1971.

7. Sorensen, J.A., "Analysis of Instrumentation Error Effects on the Identification Accuracy of Aircraft Parameters", NASA CR-112121, May, 1972.

8. Private Communication, Capt. David Carlton, Edwards Air Force Base, 7 July 1972.

9. Stepner, D.E. and Mehra, R.K., "Maximum Likelihood Identification and Optimal Input Design for Identifying Aircraft Stability and Control Derivatives", NASA CR-2200, March 1973.

10. Chen, R.T.N., Eulrich, B.J., and Lebacqz, J.V., "Development of Advanced Techniques for the Identification of V/STOL Aircraft Stability and Control Parameters", CAL Report No. BM-2820-F-1, August 1971.

11. Holmes, J.E., "Limitations in the Acquisition of Nonlinear Aerodynamic Coefficients from Free Oscillation Data by Means of the Chapman-Kirk Technique", presented at AIAA Guidance and Control Conference, August 1972.

12. Ross, A.J., "Investigation of Nonlinear Motion Experienced on a Slender-Wing Research Aircraft", Jour. of Aircraft, Vol. 9, No. 9, Sept. 1972, pp. 625-631.

13. Strutz, L.W., "Flight Determined Derivatives and Dynamic Characteristics for the HL-10 Lifting Body Vehicle at Subsonic and Transonic Mach Numbers", NASA TND-6934, Sept. 1972.

14. NASA Symposium, Parameter Estimation Techniques and Applications in Aircraft Flight Testing, Edwards Flight Research Center, April 24 & 25, 1973.

15. Astrom, K.J. and Eykhoff, P., "System Identification - A Survey", Automatica, Vol. 7, pp. 123-162, Pergamon Press, 1971.

16. Wolcowicz, C.H., Iliff, K.W., and Gilyard, G.B., "Flight Test Experience in Aircraft Parameter Identification", presented at AGARD Symposium on Stability and Control, Braunschweig, Germany, April 1972.

17. DiFranco, D., "In-Flight Parameter Identification by the Equation-of-Motion Technique--Application to the Variability Stability T-33 Airplane", Cornell Aeronautical Laboratory Report No. TC-1921-F-3, 15 December 1965.

18. Gerlach, O.H., "Determination of Performance and Stability Parameters from Non-Steady Flight Test Maneuvers, SAE National Business Aircraft Meeting, Wichita, Kansas, March 1970.

19. Goodwin, G.C., "Application of Curvature Methods to Parameter and State Estimation", Proc. IEEE, Vol. 16, No. 6, June 1969.

20. Taylor, L., et. al., "A Comparison of Newton-Raphson and Other Methods for Determining Stability Derivatives from Flight Data", Third Technical Workshop on Dynamic Stability Problems, Ames Research Center, 1968; also presented at AIAA Third Flight Test, Simulation and Support Conference, Houston, Texas, March 1969.

21. Bellman, R., et. al., "Quasilinearization, System Identification, and Prediction", RAND Corporation RM-3812, August 1963.

22. Kumar, K.S.P. and Shridhar, R., "On the Identification of Control Systems by the Quasilinearization Method", IEEE Trans., Vol. AC-10, pp. 151-154, April 1964.

23. Larson, D., "Identification of Parameters by Method of Quasilinarization", CAL Report 164, May 1968.

24. Denery, D.G., "An Identification Algorithm Which is Insensitive to Initial Parameter Estimates", AIAA Eighth Aerospace Science Conference, January 1970.

25. Young, P.C., "Process Parameter Estimation and Adaptive Control", In Theory of Self-Adaptive Control SystemsP. Hammond, ed., Plenum Press, New York, 1966.

26. Schalow, R.D., "Quasilinearization and Parameter Estimation Accuracy", Ph.D. Thesis, Syracuse University, 1967.

27. Dolbin, B., "A Differential Correction Method for the Identification of Airplane Parameters from Flight Test Data", University of Buffalo, Masters Thesis, December 1968.

28. Lason, L.S., et. al., "The Conjugate Gradient Method for Optimal Control Problems", IEEE Trans., G-AL, Vol. 12, No. 2, April 1967.

15. Astrom, K.J. and Eykhoff, P., "System Identification - A Survey", Automatica, Vol. 7, pp. 123-162, Pergamon Press, 1971.

16. Wolcowicz, C.H., Iliff, K.W., and Gilyard, G.B., "Flight Test Experience in Aircraft Parameter Identification", presented at AGARD Symposium on Stability and Control, Braunschweig, Germany, April 1972.

17. DiFranco, D., "In-Flight Parameter Identification by the Equation-of-Motion Technique--Application to the Variability Stability T-33 Airplane", Cornell Aeronautical Laboratory Report No. TC-1921-F-3, 15 December 1965.

18. Gerlach, O.H., "Determination of Performance and Stability Parameters from Non-Steady Flight Test Maneuvers, SAE National Business Aircraft Meeting, Wichita, Kansas, March 1970.

19. Goodwin, G.C., "Application of Curvature Methods to Parameter and State Estimation", Proc. IEEE, Vol. 16, No. 6, June 1969.

20. Taylor, L., et. al., "A Comparison of Newton-Raphson and Other Methods for Determining Stability Derivatives from Flight Data", Third Technical Workshop on Dynamic Stability Problems, Ames Research Center, 1968; also presented at AIAA Third Flight Test, Simulation and Support Conference, Houston, Texas, March 1969.

21. Bellman, R., et. al., "Quasilinearization, System Identification, and Prediction", RAND Corporation RM-3812, August 1963.

22. Kumar, K.S.P. and Shridhar, R., "On the Identification of Control Systems by the Quasilinearization Method", IEEE Trans., Vol. AC-10, pp. 151-154, April 1964.

23. Larson, D., "Identification of Parameters by Method of Quasilinarization", CAL Report 164, May 1968.

24. Denery, D.G., "An Identification Algorithm Which is Insensitive to Initial Parameter Estimates", AIAA Eighth Aerospace Science Conference, January 1970.

25. Young, P.C., "Process Parameter Estimation and Adaptive Control", In Theory of Self-Adaptive Control SystemsP. Hammond, ed., Plenum Press, New York, 1966.

26. Schalow, R.D., "Quasilinearization and Parameter Estimation Accuracy", Ph.D. Thesis, Syracuse University, 1967.

27. Dolbin, B., "A Differential Correction Method for the Identification of Airplane Parameters from Flight Test Data", University of Buffalo, Masters Thesis, December 1968.

28. Lason, L.S., et. al., "The Conjugate Gradient Method for Optimal Control Problems", IEEE Trans., G-AL, Vol. 12, No. 2, April 1967.

29. Suit, W.T., "Aerodynamic Parameters of the Navion Airplane Extracted from Flight Data", NASA TN D-6643, March 1972.

30. Steinmetz, G.S., Parrish, R.V., and Bowles, R.L., "Longitudinal Stability and Control Derivatives of a Jet Fighter Airplane Extracted from Flight Test Data by Utilizing Maximum Likelihood Estimation", NASA TN D-6532, March 1972.

31. Tyler, J.S., Powell, J.D., and Mehra, R.K., "The Use of Smoothing and Other Advanced Techniques for VTOL Aircraft Parameter Identification", Final Report to Cornell Aeronautical Laboratory under Naval Air Systems Command Contract No. N00019-69-C-0534, June 1970.

32. Astrom, K.J. and Wenmark, S., "Numerical Identification of Stationary Time Series", Sixth International Instruments and Measurements Congress, Stockholm, September 1964.

33. Kashyap, R.L., "Maximum Likelihood Identification of Stochastic Linear Dynamic Systems", IEEE Trans. AC, Feb. 1970.

34. Mehra, R.K., "Identification of Stochastic Linear Dynamic Systems Using Kalman Filter Representation", AIAA Journal, Vol. 9, No. 1, Jan. 1971.

35. Briggs, B.B. and Jones, A.L., "Techniques for Calculating Parameters of Nonlinear Dynamic Systems from Response Data", NASA TN 2977, July 1953.

36. Chapman, G.T. and Kirk, D.B., "A Method for Extracting Aerodynamic Coefficients from Free-Flight Data", AIAA Journal, Vol. 8, No. 4, April 1970, pp. 753-757.

37. Wells, W.R., "A Maximum Likelihood Method for the Extraction of Stability Derivatives from High Angle-of-Attack Flight Data, AFFDL/FGC-TM-72-16, Sept. 1972.

38. Goldberger, A.S., Econometric Theory, John Wiley & Sons, Inc., New York, 1964.

39. Akaike, H., "Statistical Predictor Identification", Ann. Inst. Statist. Math., Vol. 22, 1970.

40. Fisher, R.A., Statistical Methods and Scientific Inference, Oliver and Boyd, Edinburg, 1956.

41. Fisher, R.A., "Two New Properties of the Mathematical Likelihood", Proc. Roy. Soc., London, 144, 285; 1934.

42. Barnard, G.A., "Statistical Inference", Journal Royal Stat. Society, B11, 116, 1949.

43. Birnbaum, A., "On the Foundations of Statistical Inference", Journal American Statistical Association, 57, 269; 1962.

44. Kailath, T., "A General Likelihood-Ratio Formula for Random Signals in Gaussian Noise", IEEE Trans. Info. Theory, Vol. IT-15, May 1969.

45. Bryson, Jr., A.E. and Ho, Y.C., Applied Optimal Control, Girn Blaisdell, Waltham, 1969.

46. VanTrees, H.L., Detection Estimation and Modulation Theory, Vol. I, John Wiley & Sons, New York, 1968.

47. Rao, C.R., "Information and Accuracy Attainable in the Estimation of Statistical Parameters", Bull. Calcutta Math. Society, 37, pp. 81-91, 1945.

48. Gupta, N.K., "Practical Techniques for Sensitivity Functions Reductions in Linear Time-Invariant Systems", submitted to IEEE Control Society Special Issue on Time Series Analysis, December 1974.

49. Kendall, M.G. and Stuart, A., The Advanced Theory of Statistics, Vol. I and II, 2nd Edition, Charles Griffin & Co., Ltd., London, 1967.

50. Draper, M.R. and Smith, H., Applied Regression Analysis, John Wiley & Sons, Inc., New York, 1966.

51. Gupta, N.K. and Hall, Jr., W.E., "Input Design for Aircraft Parameter Identification", Final Report for Contract NAS 4-2068, February 1974, to appear as NASA CR.

52. Mehra, R.K., "Frequency Domain Synthesis of Optimal Inputs for Linear System Parameter Estimation", Technical Report No. 645, Division of Engineering and Applied Physics, Harvard University, Cambridge, 1973.

53. Gupta, N.K., Mehra, R.K. and Hall, Jr., W.E., "Frequency Domain Input Design for Aircraft Parameter Identification", proposed for presentation at A.S.M.E. Winter Annual Meeting, November 1974.

54. Gupta, N.K., "Time Domain Synthesis of Optimal Inputs for Linear System Parameter Estimation", Systems Control, Inc., Report No. 6991-02, November 1973.

55. Gupta, N.K. and Hall, Jr., W.E., "Eigenvalue-Eigenvector Decomposition to Solve Optimal Input Problem in Time Domain", SCI Technical Memo 6991-03, December 1973.

56. Mehra, R.K., "Optimal Inputs for Linear System Identification, Part I - Theory", JACC, Stanford, California, 1972.

Distribution List for Technical Report #2
to Contract N00014-72-C-0328

Office of Naval Research
Department of the Navy
Arlington, Virginia 22217
ATTN: Mr. D.S. Siegel, Code 461 (4)
Mr. M. Cooper, Code 430B (1)
Dr. S. Brodsky, Code 432 (1)

Director
Office of Naval Research Branch Office
1030 East Green Street
Pasadena, California 91106
ATTN: Mr. R.F. Lawson (1)
CDR R.L. Breckon (1)

San Francisco Area Office
Office of Naval Research
50 Fell Street
San Francisco, California 94102
ATTN: Mr. J. Froman (1)

Director
U.S. Naval Research Laboratory
Washington, D.C. 20390
ATTN: Technical Information Div. (3)
Library, Code 2029 (1)

Chief of Naval Development
Washington, D.C. 20360
ATTN: W.H. Young, NMAT-0334 (1)

Commander
Naval Air Systems Command
Washington, D.C. 20360
ATTN: R.F. Siewert, NAIR-3600 (1)
H. Andrews, NAIR-5301 (1)
R. A'Harrah, NAIR-53014 (1)
J.C. Taylor, NAIR-530141A (1)

Commanding Officer
Naval Air Development Center
Warminster, Pennsylvania 18974
ATTN: R. Fortenbaugh (1)
A. Piranian (1)

Commanding Officer
Naval Air Test Facility
Patuxent River, Maryland 20670
ATTN: Bob Traskos (1)
Roger Burton (1)

Commanding Officer
Naval Ship Research and
Development Center
Bethesda, Maryland 20034
ATTN: W.E. Smith, Code 1576 (1)

Air Force Flight Dynamics Laboratory
Air Force Systems Command
Wright Patterson Air Force Base
Ohio 45433
ATTN: D. Bowser, AFFDL/FGC (1)
F. Thomas, AFFDL/FGC (1)
P. Blatt, AFFDL/FGL (1)
D. Carltor, AFFDL/FGL (1)

National Aeronautics and Space Admin.
Langley Research Center
Hampton, Virginia 23365
ATTN: J.R. Chambers (1)
R.L. Bowles (1)
Dr. M.J. Queijo (1)
W. Reed III (1)
Dr. J. Creedon (1)

Director
U.S. Army Air Mobility Research
and Development Laboratory
Langley Directorate
Hampton, Virginia 23365
ATTN: Robert Tomain (1)

Director
U.S. Air Mobility Research and
Development Laboratory
Ames Directorate
Moffett Field, California 94303
ATTN: Dr. I. Statler (1)
Dr. R. Carlson

Calspan Corp.
P.O. Box 235
Buffalo, N.Y. 14221
ATTN: E.G. Rynaski (1)
R.T. Chen (1)

The Analytic Sciences Corp.
6 Jacob Way
Reading, Massachusetts 01867
ATTN: C. Price (1)

Nielsen Engineering and Research, Inc.
510 Clyde Ave.
Mountain View, Ca 94043
ATTN: Dr. Jack Nielsen (1)

Distribution List for Technical Report #2
to Contract N00014-72-C-0328

Office of Naval Research
Department of the Navy
Arlington, Virginia 22217
ATTN: Mr. D.S. Siegel, Code 461 (4)
Mr. M. Cooper, Code 430B (1)
Dr. S. Brodsky, Code 432 (1)

Director
Office of Naval Research Branch Office
1030 East Green Street
Pasadena, California 91106
ATTN: Mr. R.F. Lawson (1)
CDR R.L. Breckon (1)

San Francisco Area Office
Office of Naval Research
50 Fell Street
San Francisco, California 94102
ATTN: Mr. J. Froman (1)

Director
U.S. Naval Research Laboratory
Washington, D.C. 20390
ATTN: Technical Information Div. (3)
Library, Code 2029 (1)

Chief of Naval Development
Washington, D.C. 20360
ATTN: W.H. Young, NMAT-0334 (1)

Commander
Naval Air Systems Command
Washington, D.C. 20360
ATTN: R.F. Siewert, NAIR-3600 (1)
H. Andrews, NAIR-5301 (1)
R. A'Harrah, NAIR-53014 (1)
J.C. Taylor, NAIR-530141A (1)

Commanding Officer
Naval Air Development Center
Warminster, Pennsylvania 18974
ATTN: R. Fortenbaugh (1)
A. Piranian (1)

Commanding Officer
Naval Air Test Facility
Patuxent River, Maryland 20670
ATTN: Bob Traskos (1)
Roger Burton (1)

Commanding Officer
Naval Ship Research and
Development Center
Bethesda, Maryland 20034
ATTN: W.E. Smith, Code 1576 (1)

Air Force Flight Dynamics Laboratory
Air Force Systems Command
Wright Patterson Air Force Base
Ohio 45433
ATTN: D. Bowser, AFFDL/FGC (1)
F. Thomas, AFFDL/FGC (1)
P. Blatt, AFFDL/FGL (1)
D. Carltor, AFFDL/FGL (1)

National Aeronautics and Space Admin.
Langley Research Center
Hampton, Virginia 23365
ATTN: J.R. Chambers (1)
R.L. Bowles (1)
Dr. M.J. Queijo (1)
W. Reed III (1)
Dr. J. Creedon (1)

Director
U.S. Army Air Mobility Research
and Development Laboratory
Langley Directorate
Hampton, Virginia 23365
ATTN: Robert Tomain (1)

Director
U.S. Air Mobility Research and
Development Laboratory
Ames Directorate
Moffett Field, California 94303
ATTN: Dr. I. Statler (1)
Dr. R. Carlson

Calspan Corp.
P.O. Box 235
Buffalo, N.Y. 14221
ATTN: E.G. Rynaski (1)
R.T. Chen (1)

The Analytic Sciences Corp.
6 Jacob Way
Reading, Massachusetts 01867
ATTN: C. Price (1)

Nielsen Engineering and Research, Inc.
510 Clyde Ave.
Mountain View, Ca 94043
ATTN: Dr. Jack Nielsen (1)